

SYNTHESIS OF STARCH-BASED BIOPLASTICS  
REINFORCED WITH LIGNOCELLULOSIC FIBERS

YANG JIANLEI

FACULTY OF ENGINEERING  
UNIVERSITY OF MALAYA  
KUALA LUMPUR

2021

**SYNTHESIS OF STARCH-BASED BIOPLASTICS  
REINFORCED WITH LIGNOCELLULOSIC FIBERS**

**YANG JIANLEI**

**THESIS SUBMITTED IN FULFILMENT OF THE  
REQUIREMENTS FOR THE DEGREE OF DOCTOR OF  
PHILOSOPHY**

**FACULTY OF ENGINEERING  
UNIVERSITY OF MALAYA  
KUALA LUMPUR**

**2021**

**UNIVERSITY OF MALAYA**  
**ORIGINAL LITERARY WORK DECLARATION**

Name of Candidate: YANG JIANLEI

Matric No: KVA180040 / 17198807/1

Name of Degree: DOCTOR OF PHILOSOPHY

Title of Project Paper/Research Report/Dissertation/Thesis (“this Work”):  
SYNTHESIS OF STARCH-BASED BIOPLASTICS REINFORCED WITH  
LIGNOCELLULOSIC FIBERS

Field of Study: ADVANCED MATERIALS AND TECHNOLOGY

I do solemnly and sincerely declare that:

- (1) I am the sole author/writer of this Work;
- (2) This Work is original;
- (3) Any use of any work in which copyright exists was done by way of fair dealing and for permitted purposes and any excerpt or extract from, or reference to or reproduction of any copyright work has been disclosed expressly and sufficiently and the title of the Work and its authorship have been acknowledged in this Work;
- (4) I do not have any actual knowledge nor do I ought reasonably to know that the making of this work constitutes an infringement of any copyright work;
- (5) I hereby assign all and every rights in the copyright to this Work to the University of Malaya (“UM”), who henceforth shall be owner of the copyright in this Work and that any reproduction or use in any form or by any means whatsoever is prohibited without the written consent of UM having been first had and obtained;
- (6) I am fully aware that if in the course of making this Work I have infringed any copyright whether intentionally or otherwise, I may be subject to legal action or any other action as may be determined by UM.

Candidate’s Signature

Date:

Subscribed and solemnly declared before,

Witness’s Signature

Date:

Name:

Designation:

# SYNTHESIS OF STARCH-BASED BIOPLASTICS REINFORCED WITH LIGNOCELLULOSIC FIBERS

## ABSTRACT

Biodegradable starch-based bioplastics are environmentally friendly and have attracted considerable interest to replace the conventional petroleum-based plastics. As compared to synthetic plastics, starch-based bioplastics show low mechanical and water resistance properties that hamper their applications. Therefore, the current research work focused on synthesizing starch-based bioplastics with enhanced properties by incorporating lignocellulosic fiber reinforcements with crosslinking agents. In Malaysia, the abundant natural resources such as cassava starch, oil palm empty fruit bunch (EFB) fibers, and epoxidized palm oil (EPO) derived from palm oil enable us to synthesize these bioplastics. Lignin-containing lignocellulosic fibers were obtained by thermal and alkali treatments in order to improve their adhesion in the composites. The treatments removed spherical particles, fatty acid, and part of lignin or hemicellulose on the fiber surface. Thermal stability of fibers decreased after the treatment. The EFB fibers treated with 10 wt% NaOH (aq) at 180 °C demonstrated the best reinforcing effect on the physical properties of bioplastics. This was confirmed by more compact surface and higher thermal stability, higher tensile strength and increased water resistance as compared to the other bioplastics. These optimally treated fibers (TEFB) were applied to strengthen the bioplastics at varying loading levels. The contents of fibers had a positive effect on the tensile strength and water resistance of the bioplastics but reduced the melting behavior, thermal stability, and plasticization of the composites. Moreover, TEFB fibers above 10 wt% contents formed the aggregates in the bioplastics. The optimum addition level of fibers was 5 wt%. Due to the inherent hydrophilicity and possible incompatibility of starch and fibers, starch/TEFB-based bioplastics were further crosslinked by citric acid

(CA), EPO or epoxidized soybean oil (ESO). Low contents of the crosslinkers promoted the compatibility between fibers and starch effectively and led to a significant enhancement of tensile strength, while higher contents of crosslinkers showed a negative effect. The tensile strength increased from 0.83 MPa of the control sample to 1.62, 3.92 and 5.42 MPa for the bioplastics with the incorporation of CA, EPO and ESO, respectively. EPO was selected as the effective modifier of the bioplastics because EPO was the most abundant commodity oil in Malaysia and the bioplastics with ESO were very brittle. However, the compatibility and reactivity between EPO and starch were low. Further, starch/TEFB-based bioplastics were modified with CA-EPO prepolymer (CEPO) using melt blending to improve the compatibility. As evidenced by the Fourier transform infrared spectroscopy, CEPO generated strong interactions with starch/fibers through CA-inspired esterification reaction. The compatibility between starch and CEPO was obviously improved. As a result, the blending of CEPO in the composites has contributed to a higher evolution of the tensile strength than EPO. The tensile strength of the control sample increased from 3.67 to 6.90 MPa after the addition of 0.75 wt% CEPO. The water sensitivity of the composites was also moderately reduced upon the addition of both oils. This study indicated that the starch-based bioplastics with superior tensile strength and biodegradability can be used to replace part of commercial low-density polyethylene for packaging application.

**Keywords:** Starch, bioplastics, empty fruit bunch, citric acid, epoxidized palm oil

# **PENGHASILAN BIOPLASTIK BERASASKAN KANJI DIPERTINGKATKAN DENGAN SERAT LIGNOSELULOSA**

## **ABSTRAK**

Bioplastik berbiodegradasi bersifat mesra alam telah menarik minat pelbagai pihak bagi menggantikan plastik berasaskan petroleum. Dibandingkan dengan plastik sintetik, penggunaan bioplastik lebih terbatas kerana ia mempunyai sifat mekanikal dan ketahanan yang kurang. Dengan itu, kajian ini memfokuskan penghasilan bioplastik berasaskan kanji dengan peningkatan sifat melalui penggabungan serat lignoselulosa dan agen penghubung silang. Di Malaysia, kepelbagaian sumber semula jadi yang banyak seperti ubi kanji, serat tandan buah kelapa sawit kosong (EFB) dan minyak sawit epoksidasi (EPO) daripada kelapa sawit membolehkan kajian terhadap penghasilan bioplastik ini dijalankan. Serat lignoselulosa yang mengandungi lignin diperolehi melalui rawatan termal dan alkali untuk meningkatkan sifat kelekatan dalam komposit. Kedua-dua rawatan ini dapat mengeluarkan kekotoran berbentuk sfera, asid lemak dan sebahagian lignin dan hemiselulosa yang terdapat pada permukaan serat. Kestabilan termal serat berkurang selepas rawatan. Serat EFB yang dirawat dengan 10% berat NaOH pada suhu 180 °C menunjukkan kesan peningkatan serat yang terbaik pada sifat fizikal bioplastik. Ini dapat dipastikan lagi dengan permukaan serat yang lebih padat dan ketahanan yang lebih tinggi serta kekuatan tegangan dan sifat kalis air yang lebih baik dibandingkan dengan bioplastik yang lain. Serat yang dirawat pada tahap optimum digunakan untuk menguatkan sifat bioplastik pada tahap muatan yang berbeza. Kandungan serat mempunyai kesan positif terhadap kekuatan tegangan dan sifat kalis air bioplastik tetapi mengurangkan tingkah laku lebur, ketahanan termal dan sifat pemplastik komposit. Tambahan lagi, serat TEFB pada berat 10% keatas akan membentuk agregat dalam bioplastik. Maka, kadar optimum serat tambahan adalah 5% berat. Disebabkan oleh wujudnya sifat hidrofilik dan kemungkinan ketidaksesuaian kanji dan serat, bioplastik

berasaskan kanji/serat dihubung silangkan dengan asid sitrik (CA), EPO atau minyak kacang soya epoksidasi (ESO). Kandungan penghubung silang yang rendah meningkatkan kesesuaian di antara serat dan kanji dengan sangat berkesan dan menyebabkan kekuatan regangan meningkat secara mendadak. Sementara itu, kandungan penghubung silang yang tinggi (CA, EPO atau ESO) menunjukkan kesan yang negatif. Kekuatan tegangan meningkat daripada 0.83 MPa (sampel kawalan) kepada 1.62, 3.92 dan 5.42 MPa untuk bioplastik yang dihubung silang dengan CA, EPO dan ESO secara masing. EPO dipilih sebagai penggubah bioplastik yang berkesan kerana ia merupakan minyak komoditi yang banyak terdapat di Malaysia. Manakala, bioplastik bersama ESO adalah sangat rapuh. Walaupun begitu, kesesuaian dan reaktiviti antara EPO dan kanji adalah rendah. Dengan itu, bioplastik berasaskan kanji/serat TEFB diubah dengan CA-EPO pra polimer (CEPO) menggunakan teknik pencampuran lebur untuk meningkatkan kesesuaian antara kanji dan EPO. Ini dapat dibuktikan dengan spektroskopi inframerah transformasi, CEPO menghasilkan interaksi yang tinggi di antara kanji/serat melalui reaksi CA-esterifikasi terinspirasi. Kesesuaian antara kanji dan CEPO jelas menunjukkan peningkatan. Dalam pada itu, campuran EPO dalam komposit menyumbang kepada evolusi lebih tinggi terhadap kekuatan tegangan dibandingkan dengan EPO. Kekuatan tegangan untuk sampel kawalan meningkat daripada 3.67 kepada 6.90 MPa selepas tambahan berat CEPO sebanyak 0.75%. Sifat kepekaan air komposit juga berkurang secara sederhana setelah tambahan kedua-dua minyak. Kajian ini telah menunjukkan bioplastik berbiodegradasi berasaskan kanji dengan kekuatan tegangan yang unggul boleh digunakan bagi menggantikan sebahagian daripada plastik polietilena komersial berketumpatan rendah untuk kegunaan pembungkusan.

**Kata kunci:** Kanji, bioplastik, tandan buah kepala sawit kosong, asid sitrik, minyak sawit epoksidasi

## ACKNOWLEDGEMENTS

I would like to show my greatest gratitude to my supervisors Assoc. Prof. Ir. Dr. Ching Yern Chee and Prof. Dr. Chuah Cheng Hock for their insightful guidance in my PhD study and earnest help in my life. They advised me to choose the subject, carry out a series of relevant research, write the papers and submit papers to the journals. During the process of thesis writing, they provided many useful suggestions. This thesis would not be completed in time without their guidance, encouragement, and support.

My sincere thanks go to lab technicians Sarima and Taviq, my senior schoolmates (Dr Sampath, Dr Haniffa, Thaneisha), junior fellow (Shi wei, Sang, Farahin) and other fellow classmates. They shared their knowledge with me, provided me with the patient instruction and helped me out when my experiment was in trouble. I am deeply in debt to my beloved parents, wife, son, and sisters for their encouragement, understanding and love in my study. My study could not be possible without their persistent support and selfless sacrifice.

I appreciate the insightful comments from thesis defense committee members to improve my research work from various perspectives. I would like to show my sincere appreciation to University of Malaya for giving me such an opportunity to experience different research environment. I would like to thank officers and colleagues in Faculty of Engineering. All of you have been there to support me spiritually.

Sincerely yours,

Yang Jianlei, Jan 2021

## TABLE OF CONTENTS

Abstract .....	iii
Abstrak .....	v
Acknowledgements .....	vii
Table of Contents .....	viii
List of Figures .....	xiii
List of Tables.....	xx
List of Symbols and Abbreviations.....	xxi
<b>CHAPTER 1: INTRODUCTION.....</b>	<b>1</b>
1.1 Starch-based bioplastics .....	1
1.2 Problem statement.....	5
1.3 Research objectives.....	10
1.4 Scope of the research .....	10
1.5 Thesis outlines.....	11
<b>CHAPTER 2: LITERATURE REVIEW.....</b>	<b>13</b>
2.1 Structure and properties of starch and starch-based bioplastics.....	13
2.2 Ways to improve the properties of starch-based bioplastics.....	16
2.2.1 Blending with other polymers (mainly biodegradable).....	16
2.2.2 Adding the crosslinking agents .....	18
2.2.3 Chemical modification of starch .....	20
2.3 Structure and properties of lignocellulosic fibers and their application in the bioplastics .....	22
2.3.1 Structure and properties of lignocellulosic fibers.....	22
2.3.2 The bioplastics reinforced with lignocellulosic fibers .....	26

2.3.2.1	Cellulose-lignin incorporated bioplastics.....	29
2.3.2.2	Lignin-containing cellulosic fibers as reinforcements of bioplastics .....	31
2.3.2.3	Lignocellulosic fibers without delignification as reinforcements of the bioplastics.....	33
2.3.2.4	Comparison between lignocellulosic fiber and lignin in the bioplastics.....	38
2.3.3	Thermal treatment of fibers.....	39
2.3.4	Empty fruit bunch fibers and their application in the bioplastics.....	41
2.4	Starch/fiber-based bioplastics crosslinked with citric acid.....	43
2.5	Epoxidized plant oils as crosslinking agents in the bioplastics.....	46
2.5.1	The bioplastics crosslinked with epoxidized plant oils.....	46
2.5.2	The preparation method of starch/fiber-based bioplastics with epoxidized plant oils.....	48
2.6	Crosslinked epoxidized plant oils as crosslinking agents in the bioplastics.....	49
2.7	Summary .....	51
<b>CHAPTER 3: METHODOLOGY.....</b>		<b>54</b>
3.1	Materials .....	54
3.2	Methodology .....	55
3.2.1	Treatment of empty fruit bunch fibers .....	55
3.2.2	Epoxidation of palm oil and soybean oil.....	56
3.2.3	Modification of starch/fibers with epoxidized palm oil and citric acid- crosslinked epoxidized palm oil.....	56
3.2.4	Preparation of starch-based bioplastics by solution casting and compression molding .....	57

3.2.5	Preparation of starch-based bioplastics by melt blending.....	62
3.3	Characterization .....	64
3.3.1	Fourier transform infrared spectroscopy (FTIR).....	64
3.3.2	X-ray diffraction (XRD) of fibers, starch, and the bio-composites.....	64
3.3.3	Scanning electron microscopy (SEM).....	65
3.3.4	Diffraction scanning calorimetry (DSC) .....	65
3.3.5	Thermogravimetric analysis (TGA) .....	65
3.3.6	Mechanical properties .....	66
3.3.7	Moisture content.....	66
3.3.8	Water uptake.....	66
3.3.9	Water solubility .....	67
3.3.10	Opacity .....	67
3.3.11	Water vapor permeability (WVP).....	67
3.3.12	Biodegradability .....	68
3.3.13	Composition analysis of empty fruit bunch fibers .....	69
3.3.14	Statistical analysis .....	69
<b>CHAPTER 4: RESULTS AND DISCUSSION .....</b>		<b>70</b>
4.1	PART 1: Preparation and characterization of starch-based bioplastics reinforced with treated empty fruit bunch fibers .....	70
4.1.1	Characterization of treated empty fruit bunch fibers.....	70
4.1.1.1	Composition analysis and macroscopic observation of the fibers	70
4.1.1.2	Fourier transform infrared spectroscopy (FTIR).....	74
4.1.1.3	Scanning electron microscopy (SEM) .....	75
4.1.1.4	X-ray diffraction (XRD) .....	76
4.1.1.5	Thermogravimetric analysis (TGA).....	78

4.1.2	Preparation and characterization of starch-based bioplastics reinforced with treated empty fruit bunch fibers .....	80
4.1.2.1	Fourier transform infrared spectroscopy (FTIR).....	80
4.1.2.2	Scanning electron microscopy (SEM) .....	82
4.1.2.3	Diffraction scanning calorimetry (DSC).....	86
4.1.2.4	Thermogravimetric analysis (TGA).....	90
4.1.2.5	Mechanical properties .....	93
4.1.2.6	Water uptake and solubility .....	97
4.1.2.7	Opacity .....	99
4.1.2.8	Water vapor permeability (WVP) .....	101
4.2	PART 2: Preparation and characterization of crosslinked starch/fiber-based bioplastics with citric acid or epoxidized plant oils .....	103
4.2.1	Characterization of epoxidized plant oils .....	103
4.2.2	Preparation and characterization of crosslinked starch/fiber-based bioplastics with CA or EO .....	104
4.2.2.1	Fourier transform infrared spectroscopy (FTIR).....	104
4.2.2.2	Scanning electron microscopy (SEM) .....	107
4.2.2.3	Diffraction scanning calorimetry (DSC).....	110
4.2.2.4	Thermogravimetric analysis (TGA).....	114
4.2.2.5	Mechanical properties .....	117
4.2.2.6	Moisture content, water uptake and solubility .....	120
4.2.2.7	Water vapor permeability (WVP) .....	125
4.2.2.8	Opacity .....	127
4.2.2.9	Biodegradability .....	128
4.3	PART 3: Synthesis and characterization of starch/fiber-based bioplastics with citric acid-crosslinked epoxidized palm oil prepolymer (CEPO) .....	132

4.3.1 Fourier transform infrared spectroscopy (FTIR).....	132
4.3.2 X-Ray diffraction (XRD) .....	135
4.3.3 Scanning electron microscopy (SEM).....	137
4.3.4 Differential scanning calorimetry (DSC) .....	140
4.3.5 Thermogravimetric analysis (TGA).....	142
4.3.6 Mechanical properties .....	145
4.3.7 Water resistance properties .....	147
4.3.8 Opacity .....	149
4.3.9 Water vapor permeability (WVP) .....	151
4.3.10 Biodegradability .....	153
4.3.11 Comparison of the properties of starch-based bioplastics and low-density polyethylene (LDPE) .....	155
<b>CHAPTER 5: CONCLUSIONS AND RECOMMENDATIONS.....</b>	<b>157</b>
5.1 Conclusions .....	157
5.2 Recommendations.....	160
References.....	162
List of Publications and Papers Presented .....	191

## LIST OF FIGURES

Figure 1.1: Global bioplastic production capacity in 2019 by market application (European-bioplastics, 2020) .....	2
Figure 1.2: Global bioplastic production capacity in 2019 by material types (European-bioplastics, 2020) .....	3
Figure 2.1: Chemical structures of (a) amylose and (b) amylopectin (Xie et al., 2013). 14	
Figure 2.2: The schematic of the crosslinkers' mode of action in biopolymers (Garavand et al., 2017).....	20
Figure 2.3: Cellulose structure (Terzopoulou et al., 2015) .....	23
Figure 2.4: Representative hemicellulose structure (Terzopoulou et al., 2015) .....	24
Figure 2.5: Three lignin monomers (Duval & Lawoko, 2014).....	24
Figure 2.6: Global diagram of the uses of lignocellulosic fibers and lignin in the bioplastics.....	29
Figure 2.7: Potential production of biomass from oil palm in Malaysia in 2019 according to Malaysian Palm oil Board (2020) .....	42
Figure 2.8: Chemical structure of citric acid.....	44
Figure 2.9: Proposed reaction mechanism for crosslinked starch.....	44
Figure 2.10: Proposed reaction mechanism for starch/fiber-based bioplastics crosslinked with citric acid.....	46
Figure 2.11: Chemical structures of (a) epoxidized palm oil and (b) epoxidized soybean oil .....	48
Figure 2.12: Synthesis of bio-epoxy resin with epoxidized palm oil and citric acid .....	51
Figure 3.1: Flow diagram of the experiments in this study .....	55
Figure 3.2: Preparation method of starch-based bioplastics by solution casting and compression molding .....	58
Figure 4.1: Digital images for fibers. (a) raw EFB, (b) TEFB0, (c) TEFB5, (d) TEFB10, (e) TEFB20, (f) TEFB50, and (g) TMEFB fibers .....	73

Figure 4.2: FTIR spectra of raw and treated empty fruit bunch fibers including TEFB0, TEFB5, TEFB10, TEFB20, TEFB50, and TMEFB fibers. The solid lines indicate the bands at respective wavenumbers .....	75
Figure 4.3: SEM images of raw EFB (a and b), TEFB0 (c and d), TEFB10 (e and f) and TEFB50 (g and h), and TMEFB (i and j) fibers.....	76
Figure 4.4: X-ray diffraction patterns of the raw EFB and TEFB fibers .....	78
Figure 4.5: Thermogravimetric (TG) and derivative thermogravimetric (DTG) curves for raw EFB and TEFB fibers.....	79
Figure 4.6: Fourier transform infrared spectra of starch-based bioplastics incorporated with different types of fibers. The solid lines indicate the bands at respective wavenumbers.....	80
Figure 4.7: Fourier transform infrared spectra of starch-based bioplastics reinforced with different concentrations of TEFB10 fibers. The solid lines indicate the bands at respective wavenumbers.....	81
Figure 4.8: Scanning electron microscopy images of starch-based bioplastics. (a) ST, b) ST-EFB-2.5, (c) ST-TEFB0-2.5, (d) ST-TEFB10-2.5, (e) ST-TEFB50-2.5, and (f) ST-TMEFB-2.5 .....	84
Figure 4.9: Scanning electron microscopy images of starch-based bioplastics and native starch. (a) ST, (b) ST-TEFB10-2.5, (c) ST-TEFB10-5, (d) ST-TEFB10-10, (e) ST-TEFB10-20, and (f) starch granules.....	85
Figure 4.10: Diffraction scanning calorimetry thermograms of starch-based bioplastics reinforced with different types of treated fibers. The circle indicates the water evaporation peak .....	88
Figure 4.11: Diffraction scanning calorimetry thermograms of starch-based bioplastics reinforced with different contents of TEFB10 fibers .....	89
Figure 4.12: Thermogravimetric and derivative thermogravimetric curves of starch-based bioplastics reinforced with types of fibers .....	92
Figure 4.13: Thermogravimetric and derivative thermogravimetric curves of starch-based bioplastics reinforced with various loadings of TEFB10 fibers.....	93
Figure 4.14: Tensile strength and elongation at break of starch-based bioplastics reinforced with different types of treated empty fruit bunch fibers. a-c, A-C: Different letters with the uniform indicator show significant differences among the samples ( $p < 0.05$ ) .....	95

Figure 4.15: Tensile strength and elongation at break of different concentrations of TEFB10 fiber reinforced bioplastics. a-d, A-E: Different letters within the same symbol show significant differences among the samples ( $p < 0.05$ ) .....	97
Figure 4.16: Water uptake and solubility of starch-based bioplastics reinforced with different types of treated empty fruit bunch fibers. a, A-B: Various letters within the same indicator show remarkable differences among the samples ( $p < 0.05$ ).....	98
Figure 4.17: Water uptake and solubility of starch-based bioplastics reinforced with different contents of TEFB10 fibers. a-b, A-B: Different letters with the identical indicator show significant differences among the samples ( $p < 0.05$ ) .....	99
Figure 4.18: The opacity of starch-based bioplastics reinforced with types of fibers. a-c: Significant differences among the samples ( $p < 0.05$ ) are shown by different letters within the same indicator .....	100
Figure 4.19: The opacity of starch-based bioplastics reinforced with different contents of TEFB10 fibers. a-c: Significant differences among the samples ( $p < 0.05$ ) are demonstrated by different letters within the same indicator .....	101
Figure 4.20: Water vapor permeability of starch-based bioplastics reinforced with various contents of TEFB10 fibers. a-b: Significant differences among the samples ( $p < 0.05$ ) are illustrated by different letters within the same indicator.....	102
Figure 4.21: FTIR spectra of raw plant oils and epoxidized plant oils. The rectangles indicate the bands at respective wavenumbers.....	104
Figure 4.22: Fourier transform infrared spectra of crosslinked bioplastics with citric acid. The solid lines indicate the bands at respective wavenumbers .....	105
Figure 4.23: Fourier transform infrared spectra of starch/fiber-based bioplastics incorporated with epoxidized palm oil. The dashed lines indicate the bands at respective wavenumbers.....	106
Figure 4.24: Fourier transform infrared spectra of starch/fiber-based bioplastics incorporated with epoxidized soybean oil. The dashed lines indicate the bands at respective wavenumbers .....	107
Figure 4.25: Proposed interaction or reaction between epoxidized plant oils and starch/fibers.....	107
Figure 4.26: Surface images of the crosslinked bioplastics. (a) ST-TEFB10-5, (b) ST-TEFB10-5-CA0.75, (c) ST-TEFB10-5-CA3, (d) ST-TEFB10-5-EPO0.75, (e) ST-TEFB10-5-EPO3, (f) ST-TEFB10-5-ESO0.75, and (g) ST-TEFB10-5-ESO3 .....	109
Figure 4.27: Diffraction scanning calorimetry thermograms of the crosslinked bioplastics .....	114

Figure 4.28: Thermogravimetric and derivative thermogravimetric curves of starch/fiber-based bioplastics with citric acid.....	116
Figure 4.29: Thermogravimetric and derivative thermogravimetric curves of starch/fiber-based bioplastics with epoxidized palm oil.....	116
Figure 4.30: Thermogravimetric and derivative thermogravimetric curves of starch/fiber-based bioplastics with epoxidized soybean oil .....	117
Figure 4.31: Tensile strength of the crosslinked bioplastics. a-c, A-D, U-Y: Significant differences among the samples ( $p < 0.05$ ) are indicated by different letters within the same indicator. 1-3: Different numbers present significant differences among the formulations with different crosslinkers at the same concentration ( $p < 0.05$ ) .....	120
Figure 4.32: Elongation at break of the crosslinked bioplastics. a-d, A-C, U-Y: Different letters within the same indicator present significant differences among the samples ( $p < 0.05$ ). 1-3: Different numbers indicate significant differences among the samples with different crosslinkers at the same concentration ( $p < 0.05$ ) .....	120
Figure 4.33: Moisture content of the crosslinked bioplastics. a, A, U: Same letter within the same indicator indicates no significant difference among the samples ( $p > 0.05$ ). 1: Same number indicates no significant difference among the formulations with different crosslinkers at the same concentration ( $p > 0.05$ ).....	124
Figure 4.34: Water uptake of the crosslinked bioplastics. a, A-C, U-V: In the same indicator, different letters represent significant differences among the specimens ( $p < 0.05$ ). 1-2: Different numbers means significant differences among the formulations with different crosslinkers at the same concentration ( $p < 0.05$ ) .....	124
Figure 4.35: Water solubility of the crosslinked bioplastics. a-b, A, U-V: Diverse letters within the same indicator demonstrate significant differences among the samples ( $p < 0.05$ ). 1-2: Different numbers indicate significant differences among the formulations with different crosslinkers at the same concentration ( $p < 0.05$ ) .....	125
Figure 4.36: Water vapor permeability of the crosslinked bioplastics. a-d, A-B, U-W: Different letters within the same indicator represent significant differences among the samples ( $p < 0.05$ ). 1-2: Different numbers demonstrate significant differences among the formulations with different crosslinkers at the same concentration ( $p < 0.05$ ).....	126
Figure 4.37: The opacity of the crosslinked bioplastics. a-c, A-B, U-V: Different letters within the same indicator present significant differences among the samples ( $p < 0.05$ ). 1-2: Different numbers mean significant differences among the specimens with different crosslinkers at the same concentration ( $p < 0.05$ ) .....	128
Figure 4.38: The biodegradability of the crosslinked bioplastics with citric acid. a, A-C, U-W: Different letters within the same indicator present significant differences among the	

samples ( $p < 0.05$ ). 1-3: Different numbers mean significant differences among the specimens with different crosslinkers at the same concentration ( $p < 0.05$ ) ..... 130

Figure 4.39: The biodegradability of the crosslinked bioplastics with epoxidized palm oil. a-b, A, U-V: Different letters within the same indicator present significant differences among the samples ( $p < 0.05$ ). 1-3: Different numbers mean significant differences among the specimens with different crosslinkers at the same concentration ( $p < 0.05$ )..... 130

Figure 4.40: The biodegradability of the crosslinked bioplastics with epoxidized soybean oil. a-b, A-B, U-V: Different letters within the same indicator present significant differences among the samples ( $p < 0.05$ ). 1-2: Different numbers mean significant differences among the specimens with different crosslinkers at the same concentration ( $p < 0.05$ ) ..... 131

Figure 4.41: Fourier transform infrared spectra of the bioplastics incorporated with epoxidized palm oil. The dashed lines indicate the bands at respective wavenumbers 133

Figure 4.42: Fourier transform infrared spectra of the bioplastics incorporated with citric acid-crosslinked epoxidized palm oil. The dashed lines indicate the bands at respective wavenumbers..... 134

Figure 4.43: Fourier transform infrared spectra of modified starch/fiber powders with epoxidized palm oil and citric acid-crosslinked epoxidized palm oil ..... 134

Figure 4.44: Fourier transform infrared spectra of epoxidized palm oil and citric acid-crosslinked epoxidized palm oil. The red rectangle in the graph indicates the bands for epoxy group ( $838 \text{ cm}^{-1}$ )..... 135

Figure 4.45: Reaction mechanism between starch/fibers and citric acid-crosslinked epoxidized palm oil ..... 135

Figure 4.46: X-ray diffraction patterns of starch and the bioplastics..... 137

Figure 4.47: The surface photographs of all the bioplastics. (a) ST-TEFB10, 400 $\times$ , (b) ST-TEFB10, 1000 $\times$ , (c) ST-TEFB10-EPO0.75, 400 $\times$ , (d) ST-TEFB10-EPO0.75, 1000 $\times$ , (e) ST-TEFB10-EPO3, 400 $\times$ , (f) ST-TEFB10-EPO3, 1000 $\times$ , (g) ST-TEFB10-CEPO0.75, 400 $\times$ , (h) ST-TEFB10-CEPO0.75, 1000 $\times$ , (i) ST-TEFB10-CEPO3, 400 $\times$ , (j) ST-TEFB10-CEPO3, 1000 $\times$  ..... 139

Figure 4.48: Differential scanning calorimetry thermograms of the bioplastics incorporated with epoxidized palm oil..... 142

Figure 4.49: Differential scanning calorimetry thermograms of the bioplastics incorporated with citric acid-crosslinked epoxidized palm oil ..... 142

Figure 4.50: Thermal behaviors of the bioplastics with epoxidized palm oil ..... 144

Figure 4.51: Thermal behaviors of the bioplastics with citric acid-crosslinked epoxidized palm oil .....	145
Figure 4.52: Tensile strength of the prepared bioplastics. a-d, A-D: Significant differences among the specimens ( $p < 0.05$ ) are shown by diverse letters in the same indicator. 1-2: Different numbers demonstrate significant differences ( $p < 0.05$ ) between the samples with EPO and CEPO at the same loading .....	147
Figure 4.53: Elongation at break of the prepared bioplastics. a-c, A-D: Significant differences among the formulations ( $p < 0.05$ ) are shown by different letters in the same indicator. 1-2: Different numbers demonstrate significant differences ( $p < 0.05$ ) between the samples with EPO and CEPO at the same loading .....	147
Figure 4.54: Moisture content of starch-based bioplastics. a, A: Same letter within the same indicator indicates no significant difference among the samples ( $p > 0.05$ ). 1: Same number indicates no significant difference ( $p > 0.05$ ) between the formulations with EPO and CEPO at the same concentration .....	148
Figure 4.55: Water solubility of starch-based bioplastics. a, A: No significant difference among the formulations ( $p > 0.05$ ) is shown by same letter within the same indicator. 1: Same number demonstrates no significant difference ( $p > 0.05$ ) between the samples with EPO and CEPO at the same concentration .....	149
Figure 4.56: Water uptake of starch-based bioplastics. a-b, A-B: Different letters within the same indicator denote significant differences among the samples ( $p < 0.05$ ). 1-2: Different numbers mean significant differences ( $p < 0.05$ ) between the formulations with EPO and CEPO at the same concentration .....	149
Figure 4.57: The opacity of starch-based bioplastics. a-c, A-D: Significant differences among the samples ( $p < 0.05$ ) are indicated by different letters within the same indicator. 1-2: Different numbers present significant differences ( $p < 0.05$ ) between the formulations with EPO and CEPO at the same loading level.....	151
Figure 4.58: Water vapor permeability of starch-based bioplastics with epoxidized palm oil and citric acid-crosslinked epoxidized palm oil. a-b, A-C: Significant differences among the samples ( $p < 0.05$ ) are indicated by different letters within the same indicator. 1-2: Different numbers present significant differences ( $p < 0.05$ ) between the formulations with EPO and CEPO at the same loading level.....	153
Figure 4.59: The biodegradability of starch-based bioplastics with epoxidized palm oil. a, A, U-V: Significant differences among the samples ( $p < 0.05$ ) are indicated by different letters within the same indicator. 1-3: Different numbers present significant differences ( $p < 0.05$ ) of weight loss with time increasing at the same EPO level .....	154
Figure 4.60: The biodegradability of starch-based bioplastics with citric acid-crosslinked epoxidized palm oil. a, A, U-W: Significant differences among the samples ( $p < 0.05$ ) are indicated by different letters within the same indicator. 1-2: Different numbers present	

significant differences ( $p < 0.05$ ) of weight loss with time increasing at the same CEPO level..... 155

Universiti Malaya

## LIST OF TABLES

Table 2.1: Amylose and amylopectin ratios of different sources of starch (Muller et al., 2017) .....	14
Table 2.2: Various ways to improve the properties of starch-based bioplastics.....	16
Table 2.3: Chemical composition of some lignocellulosic fibers (John & Anandjiwala, 2008b; Li, Tabil, & Panigrahi, 2007; Mohammed, Ansari, Pua, Jawaaid, & Islam, 2015; Nurmi, 1993).....	23
Table 3.1: Formulation of each bioplastic reinforced with fibers based on dry weight..	59
Table 3.2: Formulations for crosslinked starch/fiber-based bioplastics based on dry weight .....	61
Table 3.3: Formulations of all the starch-based bioplastics prepared by melt blending based on dry weight .....	63
Table 4.1: Composition and properties of empty fruit bunch fibers before and after thermal and chemical treatments based on dry weight .....	72
Table 4.2: Crystallinity index and temperature at maximum decomposition rate ( $T_{max}$ ) of raw and treated fibers .....	78
Table 4.3: The melting temperature obtained from diffraction scanning calorimetry and thermal decomposition parameters from thermogravimetric analysis of the bioplastics incorporated with types of fibers.....	88
Table 4.4: The melting temperature and thermal decomposition parameters of the bio-composites reinforced with various contents of TEFB10 fibers.....	90
Table 4.5: The melting temperature and decomposition parameters of the bioplastics crosslinked with citric acid or epoxidized plant oils.....	113
Table 4.6: Thermal transition and decomposition parameters of all the prepared bioplastics crosslinked with epoxidized palm oil or citric acid-crosslinked epoxidized palm oil .....	140
Table 4.7: Properties of the bioplastics prepared in the study and commercial low-density polyethylene in the market.....	156

## LIST OF SYMBOLS AND ABBREVIATIONS

ANOVA	:	Analysis of variance
CA	:	Citric acid
CaCl <sub>2</sub>	:	Anhydrous calcium chloride
CEPO	:	Citric acid-epoxidized palm oil prepolymer
CH <sub>3</sub> COOH	:	Acetic acid
CI	:	Crystallinity index
CNW	:	Cellulose nanowhiskers
DP	:	Degree of polymerization
DSC	:	Differential scanning calorimetry
DTG	:	Derivative thermogravimetric curve
EFB	:	Empty fruit bunch
EO	:	Epoxidized plant oils
EPO	:	Epoxidized palm oil
ESO	:	Epoxidized soybean oil
FFB	:	Fresh fruit bunch
FTIR	:	Fourier transform infrared spectroscopy
HCl	:	Hydrochloric acid
H <sub>2</sub> O <sub>2</sub>	:	Hydrogen peroxide
H <sub>2</sub> SO <sub>4</sub>	:	Sulfuric acid
KBr	:	Potassium bromide
LCNF	:	Lignin-containing cellulosic nanofibrils
LDPE	:	Low-density polyethylene
NaCl	:	Sodium chloride
Na <sub>2</sub> CO <sub>3</sub>	:	Sodium carbonate

NaOH	:	Sodium hydroxide
Na <sub>2</sub> SO <sub>4</sub>	:	Anhydrous sodium sulfate
PBAT	:	Poly(butylene adipate-co-terephthalate)
PCL	:	Polycaprolactone
PE	:	Polyethylene
PET	:	Poly(ethylene terephthalate)
PHA	:	Polyhydroxyalkanoates
PHB	:	Poly-β-hydroxybutyrate
PHBV	:	Poly(3-hydroxybutyrate-co-3-hydroxyvalerate)
PLA	:	Poly(lactic acid)
PO	:	Palm oil
PP	:	Polypropylene
PVA	:	Poly(vinyl alcohol)
PVC	:	Poly(vinyl chloride)
RH	:	Relative humidity
SEM	:	Scanning electron microscopy
SO	:	Soybean oil
ST	:	Neat starch-based bioplastic
TEFB	:	Treated empty fruit bunch
TEFB10	:	Thermally treated fibers with 10 wt% NaOH
$T_g$	:	Glass transition temperature
TG	:	Thermogravimetric curve
TGA	:	Thermogravimetric analysis
$T_m$	:	Melting temperature
$T_{max}$	:	Temperature at maximum decomposition rate
TMEFB	:	Treated empty fruit bunch with traditional alkali method

$T_{onset}$	:	Onset melting temperature
$T_{5\%WL}$	:	Temperature at 5% weight loss
WVP	:	Water vapor permeability
XRD	:	X-ray diffraction

Universiti Malaya

## CHAPTER 1: INTRODUCTION

### 1.1 Starch-based bioplastics

Plastics are widely used in our daily life in various sectors such as packaging, food service, medical care, horticulture, agriculture, electronics, automotive, textile, and building & construction (Chaudhary, Torley, Halley, McCaffery, & Chaudhary, 2009; Nguyen Vu & Lumdubwong, 2016; Sagnelli et al., 2016). Most of these plastics such as poly(vinyl chloride) (PVC), polyethylene (PE), and polypropylene (PP) are synthesized from petroleum and are not biodegradable in nature, thus inducing seriously environmental problems (El Miri et al., 2015; Liu, Adhikari, Guo, & Adhikari, 2013; Taguet, Bureau, Huneault, & Favis, 2014). In addition, the reduction of usage of fossil fuels and costs involved in it require alternative and sustainable resources for future applications. Plastic manufacturing and processing may make up as much as 15% of the annual carbon emissions budget and 20% of petroleum consumed globally by year 2050 according to World Economic Forum (2016). Thus, the bioplastics, particularly those from renewable and biodegradable biomass feedstock, have been paid increased attention (Lebreton & Andrady, 2019; Lu, Xiao, & Xu, 2009).

Bioplastics mainly include three categories based on their origin and biodegradability: biobased biodegradable bioplastics (i.e. starch, protein, polyhydroxyalkanoates (PHA), or poly(lactic acid) (PLA)), biobased non-biodegradable bioplastics (i.e. poly(ethylene terephthalate) (PET)), and petroleum-based biodegradable bioplastics (i.e. polycaprolactone (PCL)) (Muller, Gonzalez-Martinez, & Chiralt, 2017). Currently, bioplastics only represent about 1% (2.11 million tons) of 359 million tons of plastics produced annually. Packaging accounts for the largest application (53%) for the total bioplastic market in 2019 according to European Bioplastics (2020) (Figure 1.1). As more biopolymer materials, products, and applications emerge, the market for global

bioplastic production capacity is promising (de Mesquita, Donnici, Teixeira, & Pereira, 2012; Fakhouri et al., 2013; Mukherjee et al., 2013; Sun et al., 2016; Wu et al., 2019).

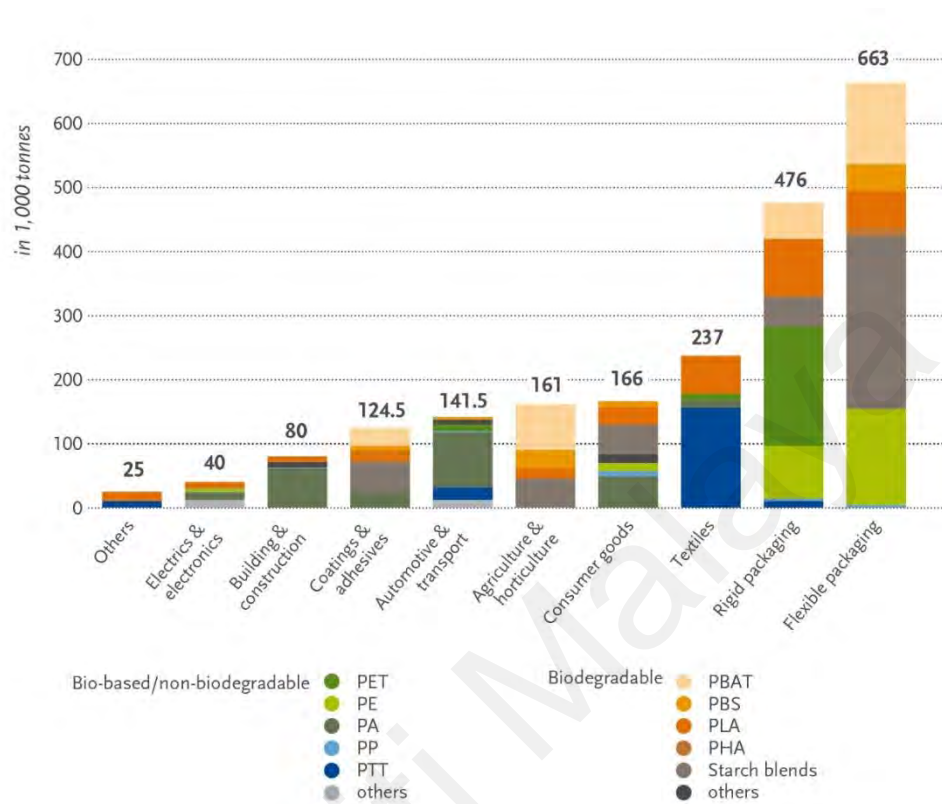


**Figure 1.1: Global bioplastic production capacity in 2019 by market application (European-bioplastics, 2020)**

Starch has attracted considerable interest due to the competitive advantages such as renewability, low cost, high abundance, biodegradability, and good film-forming property (Dai, Zhang, & Cheng, 2019; Shen, Haufe, & Patel, 2009). Starch-based bioplastics comprise the largest production capacity counting up to 21.3% in the bioplastic market while the remaining production is based on PLA, poly(butylene adipate-co-terephthalate) (PBAT), bio-based polyethylene (PE), and others (Figure 1.2) (European-bioplastics, 2020). Starch is an entirely biodegradable polysaccharide produced in photosynthesis process by green plants. It is one of the most abundant biopolymers in the world, along with chitin and cellulose (Montero, Rico, Rodriguez-Llamazares, Barral, & Bouza, 2017; Muller et al., 2017). Corn, rice, cassava, potato, and wheat are the main sources of

commercial starch in the market (Mohamad Yazid, Abdullah, Muhammad, & Matias-Peralta, 2018). Cassava is ranked the fifth most widely produced starch crop in the world, and the third among the food sources consumed in tropical regions (Edhirej, Sapuan, Jawaid, & Zahari, 2017). Sugarcane and corn are cultivated for animal feed and food purposes in Malaysia, while the main local sources of starch are cassava (Umar, Kamarudin, & Ramezani-Fard, 2013). Therefore, cassava starch would be used in the study.

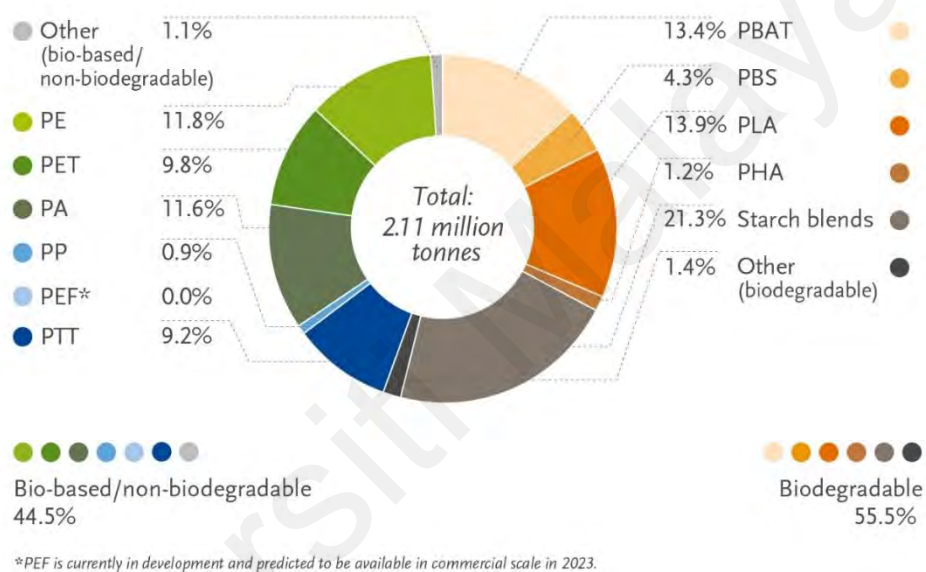


**Figure 1.2: Global bioplastic production capacity in 2019 by material types (European-bioplastics, 2020)**

Starch is composed of two primary forms: amylose and amylopectin, which occupy 98-99% of dry weight of starch. They are organized within the concentric rings by the formation of amorphous and semi-crystalline layers in granules (Montero et al., 2017). Normally, amylose is found to be 20-30%, while amylopectin accounts for 70-80%. The amylose to amylopectin ratio determines physicochemical properties of starch (Mohamad Yazid et al., 2018). The remainder comprises small amounts of phosphates, lipids, and minerals (Ghosh Dastidar & Netravali, 2012).

For pure starch, thermal degradation occurs before the melting owing to the strong inter- and intra- hydrogen bonds among the hydroxyl groups of the glucose units (Lim et al., 2020; Ma et al., 2017). In its native granular form, starch can be a reinforcing filler in other bioplastic materials such as PLA and PBAT (Sagnelli et al., 2017). Importantly, it forms a thermoplastic polymer when plasticized properly with glycerol, water, sorbitol, and other low-molecular weight polyhydroxy compounds (Teaca, Bodirlau, & Spiridon, 2013). The plasticizers can break hydrogen bonds between polymer molecules of starch and form hydrogen bonds with starch instead. Plasticizers are generally introduced to improve the flexibility of the composites because pure starch-based bioplastics are very brittle (Lim et al., 2020).

Plasticizers are characterized by their low molecular weight, allowing them to form interactions with starch molecules and replace the self-intramolecular and intermolecular hydrogen bonding, leading to increase of intermolecular spacing and molecular mobility of the starch chains (Gao et al., 2019). This transforms starch into a more amorphous material, resulting in the reduction of melting temperature ( $T_m$ ), glass transition temperature ( $T_g$ ) and degree of the crystallinity, such that starch can be fabricated using traditional methods such as solution casting, molding, and extrusion (Muscat, Adhikari, Adhikari, & Chaudhary, 2012). Upon addition of plasticizers, both flexibility and ductility of the bioplastics are improved at the expense of mechanical strength. Polyols (glycerol, sorbitol, xylitol, maltitol etc.), nitrogen-based compounds (ammonia, urea, amines, etc.), sucrose, inorganic salts, deep eutectic solvents, and citric acid (CA) are widely utilized as plasticizers (Adamus, Szychaj, Zdanowicz, & Jędrzejewski, 2018; Qiao, Tang, & Sun, 2011). The most common plasticizer for starch-based bioplastics is glycerol. Nowadays, there is also an increasing interest in using the bio-based plasticizers such as vegetable oils (e.g. linseed, soybean, sunflower, castor bean oil), epoxidized oils and fatty acid esters as secondary plasticizers (Awale et al., 2018; Sartori & Menegalli, 2016; Taghizadeh &

Favis, 2013).

To obtain starch-based bioplastics, starch and plasticizers can be processed by solution casting and thermal processing, which are also widely used for manufacturing common synthetic plastics (Fakhouri et al., 2013; Xie, Pollet, Halley, & Avérous, 2013). Solution casting is the most common method for bioplastic preparation on a laboratory scale, and involves solubilization, casting, and drying steps. Although it does not require specific equipment and consumes fewer raw materials, it is considered to be a highly energy-consuming procedure (Gironès et al., 2012). Thermal processing with designed equipment, such as extrusion, extrusion blow molding, injection molding, compression molding, and so forth, is currently a standard part of manufacturing the bioplastics due to the energy-efficiency and high productivity. It definitely has advantages over casting to produce the bioplastics concerning industrial scale-up (Montero et al., 2017; Mościcki et al., 2012).

## **1.2 Problem statement**

The hydrophilic character of starch and plasticizers generally results in poor mechanical and water resistance properties of the bioplastics in humid conditions, which hinder their extensive applications (Chung et al., 2010; Jiménez, Fabra, Talens, & Chiralt, 2012; Zhang, Zhang, Wang, Chen, & Wang, 2009). Adding the reinforcements is one of the most effective ways to improve these properties besides blending, chemical modification, and crosslinking (Cieśla & Sartowska, 2016; Liu, Sun, Hou, & Dong, 2016; Tongnuanchan, Benjakul, Prodpran, Pisuchpen, & Osako, 2016). The use of lignocellulosic fibers as reinforcing fillers in the composites has been proposed with the promising advantages in overcoming these shortcomings and also contributing to the waste management (El Halal et al., 2015; Rico, Rodriguez-Llamazares, Barral, Bouza, & Montero, 2016; Teaca et al., 2013).

Malaysia is one of the largest palm oil producers in the world with millions of tons of oil palm empty fruit bunch (EFB) fibers manufactured every year (Baharuddin et al., 2013; Ng, Yew, Basiron, & Sundram, 2011). The EFB fibers typically comprise of 17-33% hemicellulose, 43-65% cellulose and 13-37% lignin on a dry weight basis and have not been used optimally because they are bulky, wet (> 60% moisture content) and difficult to transport and handle (Haafiz et al., 2016; Nor Amalini, Noor Haida, Imran, & Mohamad Haafiz, 2019; Tan et al., 2013). The utilization of EFB fibers has attracted a large amount of interest as the reinforcing agents in the bioplastics (de Mesquita et al., 2012; Fahma, Hori, Iwata, & Takemura, 2017; Moshiul Alam, Beg, Reddy Prasad, Khan, & Mina, 2012).

The performance of fibers in the composites depends on the distribution of fibers in the bioplastics and interfacial adhesion between biopolymers and fibers. However, lignocellulosic fibers typically present low compatibility with starch, leading to low mechanical properties of the bioplastics (Abral, Putra, Asrofi, Park, & Kim, 2018; Ma et al., 2017). In order to enhance the interactions between fibers and starch, numbers of pretreatment methods have been explored such as physical, chemical, biological pretreatments, and combination of these pretreatments (Bhalla et al., 2018; Raman & Gnansounou, 2014). However, most of fiber pretreatment separates lignin and hemicellulose and generates some environmental problems (Agustin, Ahmmad, Alonzo, & Patriana, 2014; El Miri et al., 2015). Moreover, the application of lignin as reinforcements, plasticizers or compatibilizers in the bio-composites has witnessed varying success recently (Sun, Yang, Lu, & He, 2015; Yang, Ching, & Chuah, 2019). We might infer that fiber treatment methods which remove all the lignin are economically impractical.

Considerable efforts have focused on investigating thermal treatment of fibers with dry method in recent years which exhibits significant advantages (Niu et al., 2015;

Staroszczyk & Janas, 2010). The heat treatment can disrupt hydrogen bonding among the fibers and cause lignin to migrate to the fiber surface, which are likely to improve the compatibility within the matrix. Most of cellulose, hemicellulose and lignin of fibers would be kept after the treatment, which can make the most use of fibers to reinforce the bioplastics (Ghanbari, Tabarsa, Ashori, Shakeri, & Mashkour, 2018; Ma, Chang, & Yu, 2008a). In addition, this treatment is conducted in the solid state, can avoid significant fiber loss and separation and is energy-efficient and eco-friendly (Lee, Yang, Cheng, & Lee, 2018; Novo, Gurgel, Marabezi, & Curvelo, 2011).

With regard to the recalcitrant lignocellulosic fibers, multiple treatments can optimize the results by providing more flexibility for processing (Abdullah, Nazir, Raza, Wahjoedi, & Yussof, 2016; Berthet, Commandré, Rouau, Gontard, & Angellier-Coussy, 2016; Bhalla et al., 2018). NaOH treatment is a conventional method to strengthen the interfacial adhesion between the matrix and fibers (Vandenbossche et al., 2014; Yunus, Salleh, Abdullah, & Biak, 2010). Numerous studies have investigated thermal treatment of fibers in the presence of catalysts, especially various alkaline solutions (NaOH, Na<sub>2</sub>CO<sub>3</sub>, KOH, and K<sub>2</sub>CO<sub>3</sub>) (Berthet et al., 2016; Tan, Saritpongteeraka, Kungsanant, Charnnok, & Chaiprapat, 2018). However, reports regarding simultaneous thermal and alkaline modification of raw fibers with dry method and preparation of the bioplastics with these treated fibers are still rare. This enlightens us a simple and effective modification technique which can make the most use of fibers to fabricate starch-based bioplastics with favorable properties.

Though treated fibers could enhance the performance of starch-based bioplastics to a certain extent, both biopolymers along with plasticizers are hydrophilic and the resulted composites still show poor water resistance. Adding the crosslinking agents is one common approach to improve the water resistance of biopolymers besides lipids (Olivato, Grossmann, Yamashita, Eiras, & Pessan, 2012b; Wang, Zhang, Han, & Bai, 2009).

Crosslinking agents such as glutaraldehyde, boric acid, tri-metaphosphate, and epichlorohydrin always possess toxicity. Citric acid (CA) is a natural, non-toxic, and multi-carboxylic organic acid. Several studies have emphasized the crosslinking potential of CA to enhance the compatibility between starch and other polymers (S. Sun, Liu, Ji, Hou, & Dong, 2018; Wu et al., 2019). CA could weaken the interaction of starch molecules and provoke intermolecular ester linkages between the hydroxyl groups of starch and the carboxyl groups of CA (Olsson, Hedenqvist, Johansson, & Jarnstrom, 2013).

Currently, intensive studies are being conducted on the modification of bioplastics with epoxidized plant oils (EO) because of their hydrophobicity and functional epoxy groups (Basiak, Debeaufort, & Lenart, 2016; Thakur et al., 2017). EO represent one of the most commercially important materials because they are cheap, low-toxic, and can be produced in large scale (Ge et al., 2019). EO can undergo variety of reactions with many other functional compounds such as amines and carboxylic acids to develop crosslinked products by nucleophilic epoxy ring opening reactions (Belhassen, Vilaseca, Mutjé, & Boufi, 2014; Tan, Ahmad, & Chow, 2014). The application of EO provides the bio-composites with superior hydrophobic property and mechanical performance (Balart, Fombuena, Fenollar, Boronat, & Sánchez-Nacher, 2016; Li & Li, 2014).

Epoxidized soybean oil (ESO) is one of the most widely utilized EO throughout the world. It is exhibited that ESO can be used as the surface modifier for starch through the reaction of the epoxy groups with the hydroxyl groups (Belhassen et al., 2014). Palm oil (PO) is the cheapest and most abundant commodity oil in Malaysia (Goncalves, Sutili, Leite, de Souza, & Leal, 2012). The production of crude PO in Malaysia was approximately 19,858,367 tons in 2019 (Malaysian-Palm-Oil-Board, 2020). Developing new products from PO such as epoxidized palm oil (EPO) has attracted considerable interest (Uzoh, Onukwuli, Odera, & Ofochebe, 2013).

Epoxydized soybean oil has been established as the component in industrial production successfully, while EPO is just developed as a potential modifier recently (Awale et al., 2018). Oxirane oxygen contents of EO determine the number of reaction points and are suggested to be the key factor which affects the reaction efficiency of EO and their performance in the composites (Kim & Sharma, 2012; Orue, Eceiza, & Arbelaiz, 2018). ESO shows higher oxirane oxygen percent, thus a greater possibility of reaction compared to EPO (Tanrattanakul & Saithai, 2009). Therefore, it is meaningful to compare the effect of EPO on the properties of starch-based bioplastics with ESO and represent EPO as an alternative constituent for the bioplastics.

The fabricated bioplastics with EPO might still present water sensitivity because EPO has low oxirane oxygen content and might show low reactivity with starch. The epoxy groups in EPO molecules are positioned in the middle of fatty acid chains, which largely restricts their reactivity towards starch due to the steric effect (Meng et al., 2019; Xiong et al., 2013a). Additionally, EPO is immiscible with starch due to different polarity (Ge et al., 2019). Consequently, the interfacial adhesion between EPO and starch needs to be further improved (Shi et al., 2007).

Grafting multifunctional groups onto EO is a feasible strategy because the groups can serve as the crosslinkers to construct a strong crosslinking network with enhanced performance (Pawar, Kadam, Yemul, Thamke, & Kodam, 2016; Zhao et al., 2018). The epoxide rings of EO can be ring-opened by amines or poly(carboxylic acid)s to introduce other functionalities between EO and biopolymers (Li & Li, 2014). As CA can be used to crosslink with starch and act as the curing agent of EO, it might serve as a “bridge” between EO and starch (Garcia et al., 2014). Therefore, to create a new market avenue for oil palm industry, it is very interesting to use CA-crosslinked EPO (CEPO) prepolymer to modify the starch-based bioplastics. As a summary, the starch-based bioplastics fabricated with enhanced mechanical and water resistance properties might

show promising industrial applications.

### **1.3 Research objectives**

This work involves the fabrication of the bioplastics by materials that can be obtained widely in Malaysia such as native cassava starch, EFB fibers, PO, and CA. This study is intended to demonstrate that the bioplastics prepared by combining the widely available natural resources have the potential to become alternative sources in plastic industries, decrease the amount of discarded organic wastes and promote value-added industry development in Malaysia.

The objectives of the present study are as follows:

(a) To prepare and characterize thermal and alkali treated empty fruit bunch fibers and fabricate starch-based bioplastics with superior mechanical and water resistance properties with treated fibers.

(b) To study and compare the effect of crosslinkers such as citric acid, epoxidized palm oil, or epoxidized soybean oil on the properties of starch/fiber-based bioplastics, including structural, thermal, mechanical, water resistance, and biodegradable properties.

(c) To synthesize and characterize starch/fiber-based bioplastics modified by citric acid-crosslinked epoxidized palm oil via melt blending and obtain the formulation with the best mechanical and water resistance properties.

### **1.4 Scope of the research**

This research focuses on the preparation of starch-based bioplastics with superior mechanical and water resistance properties. Two approaches such as adding the reinforcements and crosslinking agents are attempted. Firstly, the EFB fibers are treated by heat and alkali treatments in order to improve their compatibility in starch-based bioplastics. Then, the reinforcing effect of treated EFB (TEFB) fibers on the properties of

the bioplastics is investigated. Next, the prepared starch/fiber-based bioplastics are crosslinked by CA, EPO and ESO to further improve the compatibility between starch and TEFB fibers. Finally, the starch/fiber-based bioplastics are modified by CEPO with reactive blending in order to enhance the reactivity between EPO and starch and assess the industrial application of EPO. This study explains the relationship between structure and physicochemical properties of the bio-composites.

## **1.5 Thesis outlines**

This thesis consists of five chapters as follows:

### **Chapter 1: Introduction**

This chapter introduces the prospect, material types and production capacity of the bioplastics. The sources and composition of starch and preparation method of starch-based bioplastics are described. Problem statement is also stated, as well as research objectives and scope of the study.

### **Chapter 2: Literature Review**

Chapter 2 initially reviews the structure and properties of starch and starch-based bioplastics, and the ways to improve the mechanical and water resistance properties of the composites. Then, structure and properties of lignocellulosic fibers, and their application in the reinforced bioplastics are introduced. The crosslinked bioplastics with CA and EO are illustrated critically. In the end, this chapter describes the ways to improve the bonding between EO and starch.

### **Chapter 3: Methodology**

The sources of materials used in the research are provided. The preparation methods for treated fibers, modified starch/fibers, EO and bioplastics are elucidated. These

prepared samples are further characterized by different characterization techniques.

#### **Chapter 4: Results and Discussion**

This chapter is comprised of three parts. The first part is to investigate the optimal thermal and alkali treatment of EFB fibers by observing their reinforcing effect on the properties of the bioplastics using solution casting. Then, the effect of different concentrations of optimally treated fibers on the properties of the composites is studied. The second part deals with the comparison of the properties of starch/fiber-based bioplastics crosslinked by CA, EPO, and ESO by the means of solution casting. The influence of various crosslinkers on the properties of the bio-composites is compared comprehensively. The third part synthesizes and characterizes starch/fiber-based bioplastics modified by CEPO by melt blending. The effect of EPO and CEPO on the properties of the composites is investigated and compared. Subsequently, the mechanical and physical properties of the prepared bioplastics are compared with that of traditional low-density polyethylene (LDPE).

#### **Chapter 5: Conclusions and Recommendations**

This chapter summarizes and concludes the main findings of the research. The recommendations for future study are put forward in the chapter.

## CHAPTER 2: LITERATURE REVIEW

### 2.1 Structure and properties of starch and starch-based bioplastics

Starch is a polysaccharide comprising two major components, i.e. amylose and amylopectin, which differ in branching and molecular size (Figure 2.1) (Ghosh Dastidar & Netravali, 2012). Amylose is a chiefly linear polymer composed of glucose units joined by  $\alpha(1-4)$ -glycosidic linkages. It has the molecular weight around  $10^5$ - $10^6$  g mol<sup>-1</sup> and degree of polymerization (DP) less than 600. Amylopectin is an extremely multiple-branched biopolymer with a high molecular weight of  $10^7$ - $10^9$  g mol<sup>-1</sup>. Amylopectin is based on  $\alpha(1-4)$ -linked linear glucose units (around 95%) and  $\alpha(1-6)$ -linked branch points (around 5%), with DP sometimes exceeding one million, which is primarily responsible for the materials' crystallinity (Blennow et al., 2013; Xie et al., 2013). There are many hydroxyl groups on the starch chains, one principal hydroxyl group at C-6, as well as two secondary hydroxyl groups at C-2 and C-3. These available hydroxyl groups might form the hydrogen bonds (Muscat et al., 2012).

Amylose content of starch varies depending on the botanical sources (Table 2.1). The amylose/amylopectin ratio is an important factor, influencing the mechanical, rheological, thermal, and processing properties of starch (Xie et al., 2013). Disruption and swelling of starch granules are facilitated in starch with high contents of amylopectin. High contents of amylose generate excellent film-forming ability and more rigid films (Montero et al., 2017; Nguyen Vu & Lumdubwong, 2016; Woggum, Sirivongpaisal, & Wittaya, 2015). The films of high-amylose starch are more stable during storage, lose little of the elongation at break and have no or a slight increase of tensile strength (Alves, Mali, Belía, & Grossmann, 2007; Hu, Chen, & Gao, 2009). Comparatively, bioplastics based on cassava starch showed the lowest tensile strength compared to those with other types of starch.

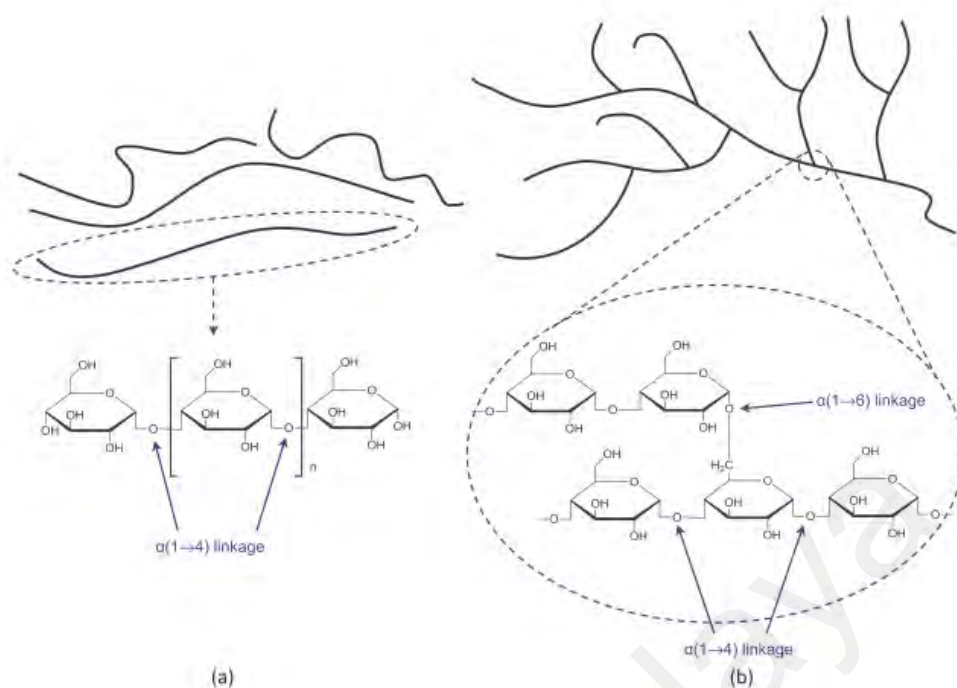


**Figure 2.1: Chemical structures of (a) amylose and (b) amylopectin (Xie et al., 2013)**

**Table 2.1: Amylose and amylopectin ratios of different sources of starch (Muller et al., 2017)**

Starch	Amylose (wt%)	Amylopectin (wt%)
Corn	28	72
Wheat	30	70
Potato	20	80
Cassava	16	84
Rice	20-30	70-80

Native starch is semicrystalline with different types of crystalline patterns (A-, B-, C- or V-type), attributed to the sources of starch. The A-, B-, and C-type conformations pack in a double helix, while V-type crystal shows a single helix structure deriving from amylose which is combined together with some materials such as butanol, iodine, water, and fatty acid (Krogars et al., 2003). During the process of making the bioplastics, the semicrystalline structure is destroyed by gelatinization or melting in the presence of plasticizers. However, the residual crystalline particles might serve as nucleus to trigger the recrystallization when water is lost and the temperature decreases with time, called retrogradation (C. Zhang et al., 2018). Specifically, the hydroxyl groups among the starch

chains are recombined by hydrogen bonds and rearranged into crystalline domains. Such recrystallization limits the practical use of starch-based bioplastics, as they become brittle and rigid during long term storage, which means their industrial value is reduced or lost (Chaudhary et al., 2009). Retrogradation is reflected by the XRD results as the intensity of crystalline peaks increases over time (Dai et al., 2019). Actually, it has been widely acknowledged that the recrystallization or retrogradation process is closely linked to the contents of amylose and amylopectin. In the starch with high amylose contents, the recrystallization is suppressed greatly due to the lack of the amylopectin branch structure (Liu et al., 2013).

Humidity is another considerable factor affecting the storage of the starch-based bioplastics. The previous studies signified that the films should not be kept in high humid circumstances (Hu et al., 2009). Their absorption of the surrounding moisture contributes to swelling of the samples and loss of the properties. Numerous authors have studied the relation between structure and properties of starch-based bioplastics in order to overcome these limitations, such as the amylose and amylopectin ratio in the raw starch and the structure they adopt. The granule organization and size in the starch and the presence of other components like proteins or lipids are also crucial (Montero et al., 2017).

Starch-based bioplastics reveal superior physical characteristics since they are colorless, tasteless, odorless, and have good oxygen barrier permeability (Yan, Hou, Guo, & Dong, 2012). However, starch-based bio-composites commonly present relatively low tensile strength, along with high moisture sensitivity, due to their high hydrophilic nature (Garavand, Rouhi, Razavi, Cacciotti, & Mohammadi, 2017; Muller et al., 2017). A broad range of elongation at break (1-129%) and tensile strength (0.4-38 MPa) is observed, depending on the types and levels of plasticizers. The water vapor permeability (WVP)

of starch-based bioplastics ranges from  $1.2 \times 10^{-7}$  to  $8.3 \times 10^{-5} \text{ g m}^{-1} \text{ s}^{-1} \text{ Pa}^{-1}$  according to different moisture contents or plasticizer levels (Muller et al., 2017).

## 2.2 Ways to improve the properties of starch-based bioplastics

Compared to the synthetic plastics, low tensile and water resistance properties of starch-based bioplastics limit their widespread applications. In order to improve these properties, various strategies have been developed, including blending with nanoparticles or other biodegradable polymers, adding the crosslinking agents to improve the compatibility of different polymers, and chemical modification of starch (Table 2.2) (Garavand et al., 2017; Sagnelli et al., 2017).

**Table 2.2: Various ways to improve the properties of starch-based bioplastics**

Methods	Instructions	Types of materials
Modification	Esterification	Maleic anhydride, octenyl succinate anhydride
	Oxidation	Hydrogen peroxide, sodium hypochlorite
	Acetylation	Acetic anhydride
	Graft copolymerization	PLA, PCL, Alkanols
Blending	Polymers	PLA, PCL, poly(3-hydroxyalkanoates) (PHA), protein, chitosan
	Reinforcements	Phyllosilicates, polysaccharide nanofillers, carbonaceous nanofillers, lignocellulosic fibers
	Lipids	Wax, fatty acid, plant oil, epoxidized plant oil
Crosslinkers/ Compatibilizers	Citric acid, butane-tetracarboxylic acid (BTCA), octanoic acid	

### 2.2.1 Blending with other polymers (mainly biodegradable)

Polymer blending is one of the most effective ways to develop new bio-composites with favorable properties as compared to the composites made from an individual component.

(a) The introduction of reinforcing fillers such as phyllosilicates (e.g. montmorillonite and clay) (Adamus et al., 2018; Chung et al., 2010), polysaccharide nanofillers (e.g. cellulose nanowhiskers or nanoparticles, chitin/chitosan nanowhiskers or nanoparticles) (El Miri et al., 2015), carbonaceous nanofillers (e.g. carbon black, graphite oxide, and carbon nanotubes) (Cheng, Zheng, Zhao, & Ma, 2013), and lignocellulosic fibers (e.g. sugar cane bagasse, wheat straw, forest wood, flax, hemp, and kenaf) (Adamus et al., 2018; Agustin et al., 2014; Campos et al., 2018; López, Mutjé, Carvalho, Curvelo, & Gironès, 2013).

(b) Mixing with lipids such as palmitic acid, stearic acid, beeswax, plant oils (Jiménez et al., 2012; Kowalczyk & Baraniak, 2014; Sartori & Menegalli, 2016; Volpe, De Feo, De Marco, & Pantani, 2018; Wang, Liu, Cui, Kang, & Yu, 2019) and epoxidized oils from palm oil, linseed oil, soybean oil, castor oil, sunflower oil, etc. so as to reduce the hygroscopic nature of the bio-composites and strengthen the WVP (Ge et al., 2019; Jiménez et al., 2012; Xiong et al., 2013b).

(c) Blending with other biodegradable polymers, such as gelatin, protein, carboxymethyl cellulose (Andreuccetti, Carvalho, & Grosso, 2010), chitosan (Ghanbarzadeh, Almasi, & Entezami, 2011), PLA (Teixeira et al., 2012), PCL, PBAT (Fialho et al., 2017), and poly(vinyl alcohol) (PVA) (J. P. López et al., 2013; Yao et al., 2011).

Specifically, bio-composites of oil palm mesocarp fibers and cassava starch were fabricated by extrusion. The composites containing 10 wt% raw fibers had stronger mechanical properties than those with alkali treated fibers, which recommended the use of fiber residues to reinforce the green bio-composites for various applications (Campos et al., 2018). The effects of different hydrophobic components-palmitic acid, oleic acid, stearic acid, lauric acid, butyric acid, and sucrose fatty acid ester on the properties of rice

starch- $\kappa$ -carrageenan-based bio-composites were evaluated. The addition of fatty acids enhanced tensile properties, transparency, and WVP of the films and could be utilized to prepare biodegradable edible films with desired properties for fruit packaging application (Thakur et al., 2017). Bio-nanocomposite films of starch/carboxymethyl cellulose reinforced with cellulose nanocrystals were developed by the solution casting method. The produced films showed enhanced tensile properties and optical transparency and reduced WVP, which meet the requirement for packaging application (El Miri et al., 2015).

Among green bioplastics, PLA is also considered as a prospective alternative to traditional petrochemical plastics because of its high strength and modulus (Tee et al., 2014). However, the most severe limitation of PLA is its notably high cost. Therefore, PLA is often mixed with cheaper biopolymers or bio-fillers. Blending thermoplastic starch with PLA not only results in the reduction of the overall cost of the final products, but also decreases the inherent rigidity and brittleness of PLA (Bocz et al., 2014). In another study, The PLA/starch composites were incorporated with various contents of EPO using the solution casting method. The thermal properties, such as crystallization temperature,  $T_m$ , and  $T_g$  decreased with growing amount of EPO, exhibiting that the addition of EPO enhanced the chain mobility of the composites (Awale et al., 2018).

### **2.2.2 Adding the crosslinking agents**

After blending with other polymers, the hydrophilic groups of starch still exist and are easy to move out to the air with time, then the long-term durability of hydrophobicity is uncertain (Ni, Zhang, Godwin, Dai, & Xiao, 2018). Fortunately, crosslinking effects have been considered to restrain the migration of hydrophilic groups by forming intra- or inter-molecular covalent or non-covalent bonds among different molecular chains in the stronger three-dimensional network (Figure 2.2) (Garavand et al., 2017). Crosslinking is extremely appropriate for biopolymers particularly those from proteins or carbohydrates,

overcoming the inherent limitations in mechanical and water sensitivity properties and making them more suitable for packaging application compared to petroleum-based materials (Wu et al., 2019). Typical crosslinkers include dichloroacetic acid, phosphorus oxychloride, sodium tri-metaphosphate,  $\text{Ca}^{2+}$ , epichlorohydrin, zirconium acetate, glutaraldehyde and various poly(carboxylic acid)s such as CA and 1,2,3,4-butane tetracarboxylic acid (Reddy & Yang, 2010; Sun, Liu, Ji, Hou, & Dong, 2018; Teixeira et al., 2012; Xiong et al., 2013a; Yildirim-Yalcin, Seker, & Sadikoglu, 2019).

Naturally occurred crosslinkers have attracted considerable interest considering environmental concerns, as well as the economic issues (Garavand et al., 2017). A novel biobased elastomer was developed using reactive extrusion from the mixture of starch, glycerol, and tartaric acid. Then the mixture was extruded with poly(butylene succinate) (30:70, wt%) to fabricate the bio-composites with superior strength (Zhang, He, Yin, & Jiang, 2019). Starch/PBAT films were extruded with CA and maleic anhydride as compatibilizers. The introduction of compatibilizers provided the materials with enhanced properties, revealing a potential replacement for non-biodegradable films (Olivato et al., 2012b). Potato starch/chitosan films crosslinked with different concentrations (5-20 wt%) of CA were obtained via a solution casting method. The films showed a denser structure along with improved mechanical, water resistance, and antimicrobial properties in comparison with un-crosslinked films (Wu et al., 2019).

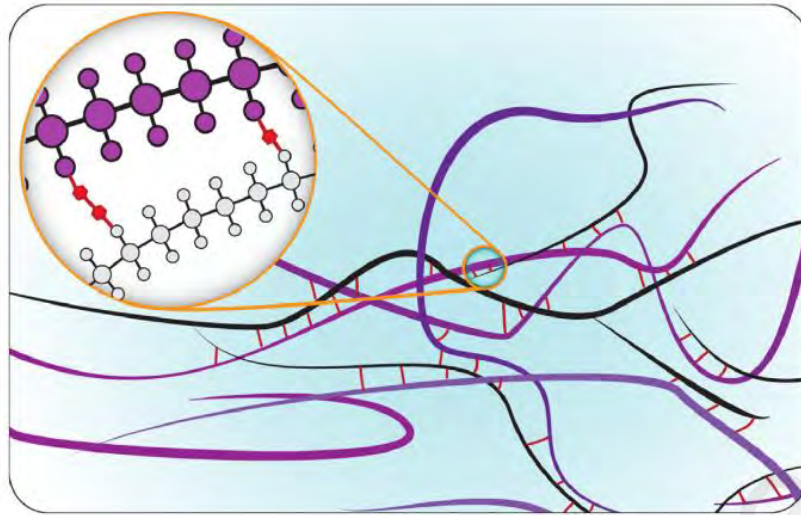


**Figure 2.2: The schematic of the crosslinkers' mode of action in biopolymers (Garavand et al., 2017)**

### 2.2.3 Chemical modification of starch

The hydrophilic character of native starch limits the development of starch-based products since the properties of the materials change in varying ambient humidity. Hence, numbers of studies have been performed to modify starch in order to obtain less hydrophilic materials (Cova, Sandoval, Balsamo, & Müller, 2010). Based on the modification methods, modified starch is subdivided into four categories: chemical modified starch, physical modified starch, enzymatic modified starch, and complex modified starch. According to previous studies, the water resistance, film-forming, mechanical and thermal properties of modified starch were superior to those of the native starch (Dai et al., 2019; Teaca et al., 2013).

Among them, chemical methods by substituting the hydroxyl groups of starch chains with hydrophobic groups have the most extensive use (Cova et al., 2010). Further, chemical modified starch is divided into esterified starch (e.g. carboxylic acid, acyl chloride and acid anhydride) (Cova et al., 2010), acetylated starch (e.g. acetic anhydride) (Bergel, Dias Osorio, da Luz, & Santana, 2018), oxidized starch (e.g.  $H_2O_2$  and  $NaClO$ ) (Hu et al., 2009), etherified starch (Woggum et al., 2015; L. Zhang et al., 2018), and

grafted starch (e.g. starch-g-polymer) (Yarahmadi et al., 2018) according to the reaction mechanism.

For example, the composite films based on octenyl-succinate/native sweet potato starch were obtained successfully and exhibited desired water-proof property (Li, Ye, Liu, & Zhao, 2015). Oxidized corn starch with sodium periodate significantly enhanced polymer crosslinking and compatibility of starch-based biodegradable active films, which promoted 40% and 33% reduction in oxygen and water vapor barrier capacity, and 40-92% increase of the films' strength, respectively (Moreno, Cardenas, Atares, & Chiralt, 2017). Thermoplastic starch was prepared from mixture of raw and acetylated corn starch. Despite of its low modification degree, the addition of acetylated starch improved the water resistance and reduced the WVP (López, Zaritzky, Grossmann, & García, 2013). After the hydroxypropylation of corn starch with propylene oxide (3-12 wt% of starch), only the minimal amount of plasticizer (20%) was required for obtaining the films with good flexibility. The obtained films also revealed appropriate tensile strength and WVP (Kim, Jane, & Lamsal, 2017).

Cassava starch was etherified with three different esters (i.e. dipropyl maleate, dibutyl maleate, and diethyl maleate). The modification of the starch surface added a hydrophobic character and thus amplified its potential applications (Clasen, Muller, Parize, & Pires, 2018). Bio-composites of PLA and starch, with ESO as the reactive compatibilizer, were melt-compounded by lab-scale co-extruder. Starch was coated with maleic anhydride to improve its compatibility and reactivity with ESO (Xiong et al., 2013a).

Chemical modification of starch is an effective method to enhance product properties (water resistance and mechanical properties, etc.) and the processing. However, chemical modification not only decreases the molecular weight of starch, but also gives rise to some toxic chemical byproducts and modifies the biodegradability, which might affect the

sustainable assessment of the final products adversely (García et al., 2012; Xie et al., 2013).

## **2.3 Structure and properties of lignocellulosic fibers and their application in the bioplastics**

### **2.3.1 Structure and properties of lignocellulosic fibers**

Lignocellulosic fibers are the largest source of renewable bioresources in the world. Generally, lignocellulosic materials are composed of cellulose, lignin and hemicellulose in addition to extracts (e.g. pectin, resins, waxes, etc.), ash and minerals (Lennartsson, Niklasson, & Taherzadeh, 2011; Thakur & Thakur, 2015). The compositions of cellulose, hemicellulose and lignin in a few lignocellulosic biomasses are shown in Table 2.3.

Cellulose is a linear biopolymer made up of 7000-15000 D-glucose monomers which are connected via  $\beta$ -1,4-glycosidic linkages (Figure 2.3) (Gibson, 2012). Cellulose chains are bonded by van der Waals forces and hydrogen bonds in the microfibrils. In the different cell walls, the arrangement of microfibrils is different. Microfibrils are combined to form the cellulose fibers (John & Anandjiwala, 2008a). Crystalline cellulose appears in the form of crystallinity (Béguin & P Aubert, 1994). Degree of polymerization (DP) of cellulose is between 1,510 and 5,500, which strengthens its crystallinity. Moreover, amorphous cellulose is non-organized, which takes up a small proportion. Crystalline cellulose is more resistant to degradation of enzyme compared to amorphous cellulose (Gibson, 2012; Perez, Munoz-Dorado, de la Rubia, & Martinez, 2002).

**Table 2.3: Chemical composition of some lignocellulosic fibers (John & Anandjiwala, 2008a; Li, Tabil, & Panigrahi, 2007; Mohammed, Ansari, Pua, Jawaid, & Islam, 2015; Nurmi, 1993)**

Fibers	Cellulose (wt%)	Hemicellulose (wt%)	Lignin (wt%)
Bagasse	55.2	16.8	25.3
Bamboo	26-43	30.0	21.0-31.0
Birch branches	33.3	23.4	20.8
Corn stalk	42.7	23.6	17.5
Flax	71.0	18.6-20.6	2.2
Kenaf	72.0	20.3	9.0
Hemp	68.0	15.0	10.0
Jute	41-48.0	21-24	18.0-22.0
Oil palm empty fruit bunch	44.2	33.5	20.4
Pine branches	32	32	21.5
Rice rusk	35.0-45.0	19.0-25.0	20.0
Rice straw	41.0-57.0	33.0	8.0-19.0
Sisal	65.0	12.0	9.9
Spruce branches	29	30	22.8
Switchgrass	34.0	27.0	17.0
Wheat straw	38.0-45.0	15.0-31.0	12.0-20.0

Hemicellulose is an amorphous and heterogeneously branched polymer of pentoses and hexoses, mainly D-galactose, D-xylose, D-mannose, L-arabinose, D-glucose, with 500-3,000 sugar monomers (John & Anandjiwala, 2008a).  $\beta$ -1,4- and occasionally  $\beta$ -1,3-glycosidic bonds are the main bonds between sugars. The representative structure of hemicellulose is shown in Figure 2.4. Hemicellulose has a lower molecular weight in contrast to cellulose (Gibson, 2012). Hemicellulose has a DP between 50 and 200, which makes it amorphous and easily hydrolysable (Li et al., 2007; Perez et al., 2002).

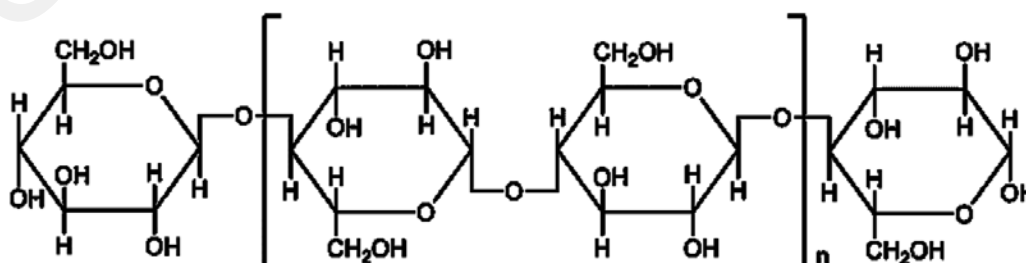


**Figure 2.3: Cellulose structure (Terzopoulou et al., 2015)**

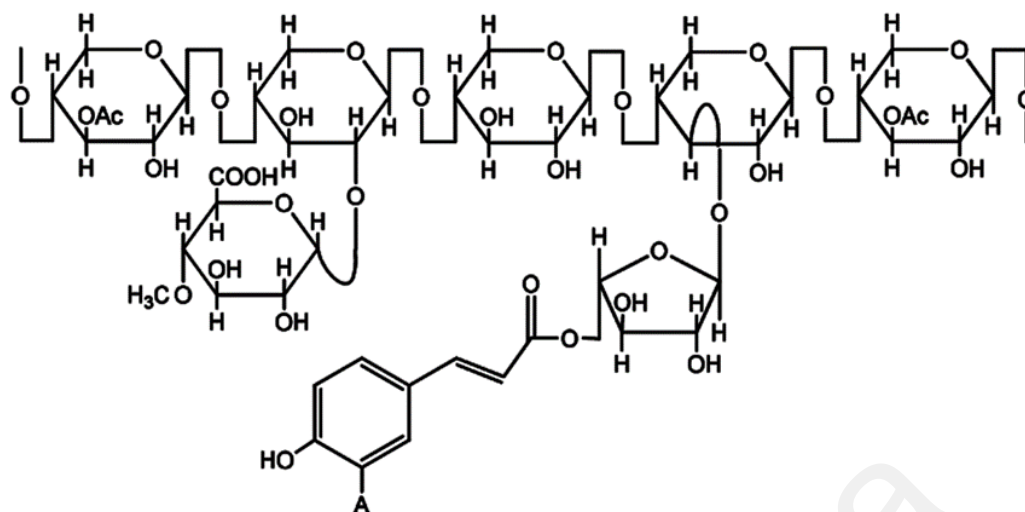


Figure 2.4: Representative hemicellulose structure (Terzopoulou et al., 2015)

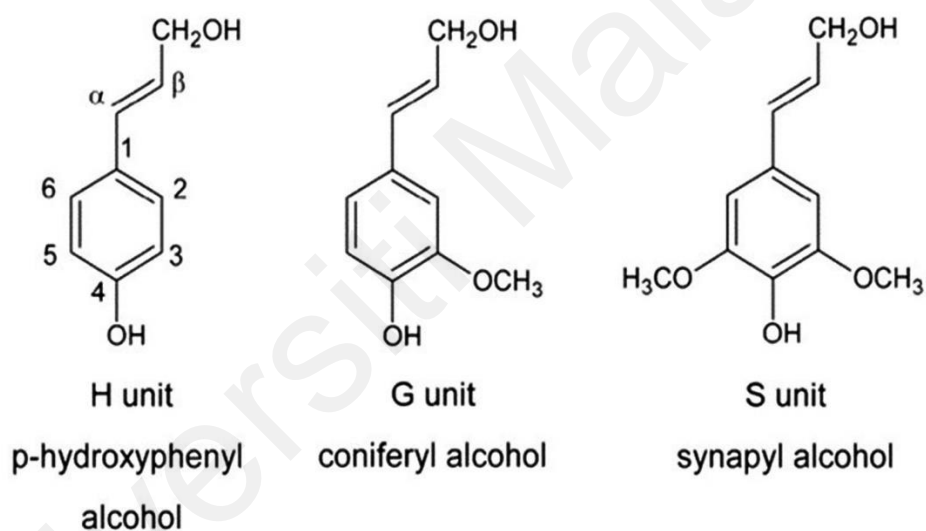


Figure 2.5: Three lignin monomers (Duval & Lawoko, 2014)

Lignin differs from cellulose and hemicellulose as it contains aromatic rings rather than long molecular chains. Depending on the different plants and extraction process, lignin is characterized by diverse chemical structures (Duval, Molina-Boisseau, & Chirat, 2013). The most essential differences are found in the monomer compositions, linkage types and functional groups in the lignin fragments (Yang et al., 2016). Lignin is a polyphenolic macromolecule, which consists of three phenylpropane monomeric units, coniferyl alcohol(G), p-hydroxyphenyl alcohol(H), and sinapyl alcohol(S) (Figure 2.5).

The coniferyl alcohol structure dominates in softwoods. Lignin in hardwood commonly contains both sinapyl alcohol and coniferyl alcohol structures with sinapyl alcohol dominant, while p-hydroxyphenyl alcohol structure predominates in lignin found in grasses (Glasser, 1999; Holmgren, Brunow, Henriksson, Zhang, & Ralph, 2006). Different types of carbon-oxygen (aryl-ether) and carbon-carbon bonds are formed in different subunits of lignin. The most frequent bonds are the carbon-oxygen links between  $\beta$ -end of the propenyl group ( $\beta$ -O-4) and p-hydroxy moiety (Agrawal, Kaushik, Nirmala, & Biswas, Soumitra, 2014; Perez et al., 2002). Different percentages of chemical groups in the lignin molecule structure such as methoxyl, hydroxyl, carbonyl, carboxyl et al. impart polarity to the lignin macromolecule. The dominant chemical groups are hydroxyl groups which are aliphatic or phenolic (Koda, Gaspar, Yu, & Argyropoulos, 2005; Yang et al., 2016). As the most recalcitrant component in lignocellulosic fibers, lignin is extremely resistant to enzymes and chemical impacts (Tolbert, Akinosho, Khunsapat, Naskar, & Ragauskas, 2014). Lignin does not dissolve in hot water, acids, and other solvents except alkalis (Feofilova & Mysyakina, 2016; John & Anandjiwala, 2008a; Rahimi, Ulbrich, Coon, & Stahl, 2014).

Because of the complicated structure, the molecular weight is an essential parameter of lignin (Baumberger et al., 2007; Tolbert et al., 2014). Molecular weight of lignin is from 1,000 to 20,000 g/mol. Lignin is widely fragmented in the extraction process and contains types of subunits which repeat randomly. Therefore, its DP is hard to analyze (Doherty, Mousavioun, & Fellows, 2011; Thakur, Thakur, Raghavan, & Kessler, 2014). Besides the molecular weight, another imperative parameter that affects the properties of lignin is the  $T_g$  (Thakur et al., 2014). In most of pulping process,  $T_g$  of lignin ranges from 100-170 °C. It is higher than the  $T_g$  of most synthetic materials (Irvine, 1985). Yoshida et al. found that the degree of association by hydrogen bonding from the phenolic hydroxyl groups primarily contributed to the high  $T_g$  of lignin (Yoshida, Mörck, Kringstad, &

Hatakeyama, 1987). The high  $T_g$  is also attributed to the chemical structure of lignin, particularly the aromatic ring of the main chain (Laurichesse & Avérous, 2014).  $T_g$  is considered as the most suitable parameter to assess miscibility of the polymers (Feldman, Banu, Campanelli, & Zhu, 2001). Complete compatibility in the polymeric blend can be implied by a single  $T_g$  which is an average  $T_g$  of each component. Two  $T_g$ s or above indicate low compatibility (Mousavioun, Doherty, & George, 2010).

Broadly speaking, lignocellulosic fibers are made up of cellulose fibers reinforced by a matrix of hemicellulose and either lignin or pectin in one or more layers, with the volume fraction and orientation of the cellulose fibers varying in each layer (Gibson, 2012). The cellulose molecules are hydrogen-bonded to hemicellulose. The cellulose-hemicellulose network is considered as the primary structural component of the fiber cell (Thakur & Thakur, 2015). Then, lignin covalently linked to hemicellulose strengthens the structure of cellulose-hemicellulose (Kulma et al., 2015; Sun, Lawther, & Banks, 1996). The hydrophobic lignin functions as a coupling agent filling in the voids that exist in cellulose-hemicellulose network. Lignin improves the stiffness of cellulose-hemicellulose network and protects cellulose fibers against biological attack and environmental pressure (Holmgren et al., 2006; Nanda, Maley, Kozinski, & Dalai, 2015; Thielemans, Can, Morye, & Wool, 2002). Different proportions and types of polysaccharides and lignin form lignin-carbohydrate complexes showing various compositions and structures. Lignin-carbohydrate complexes render cell walls recalcitrance for biorefining (Bhalla et al., 2018; Li, Pu, & Ragauskas, 2016; Tarasov, Leitch, & Fatehi, 2018).

### **2.3.2 The bioplastics reinforced with lignocellulosic fibers**

Numerous studies have demonstrated that synthetic fibers, such as glass and carbon fibers, are commonly used as the reinforcements in the bioplastics due to their strong mechanical properties. In spite of higher mechanical property of synthetic fibers,

lignocellulosic fibers are more promising because of rising concerns over environmental and resource impacts (Yatigala, Bajwa, & Bajwa, 2018). Recently, lignocellulosic fibers such as sugar cane bagasse, empty fruit bunch, wheat straw, rice straw, forest wood, flax, hemp, kenaf etc. have been widely used as the reinforcements in the bioplastics owing to their high strength, biodegradability, and low cost (J. P. López et al., 2013; Ochi, 2006; Thakur et al., 2014).

Although the studies on the application of lignocellulosic fibers in the bioplastics have been conducted for decades of years, the interfacial compatibility between matrix and fibers is still not addressed (John & Anandjiwala, 2008a; Li et al., 2007; Mahjoub, Bin Mohamad Yatim, & Mohd Sam, 2013). The addition level of lignocellulosic fibers in the bioplastics is seriously restricted by the low compatibility (Abral et al., 2018). The fact is that most of hydroxyl groups in the fibers and biopolymers have already formed either intra- or inter-molecular hydrogen bonds. As a consequence, it is difficult to form new hydrogen bonds between the two components by simple mixing, leading to low compatibility. Second, as free movement of fibers will be restricted by the high viscosity of biopolymers, agglomeration is possible to exist during drying and preparation processes because of their high hydrophilic character (Brodin, Vallejos, Opedal, Area, & Chinga-Carrasco, 2017). In most cases, only very low loadings (less than 5%) of fibers could be incorporated without leading to the agglomeration in the composites. Third, the amorphous components in the lignocellulosic fibers such as pectin, lignin, hemicellulose, and other waxy materials also destroy the interactions with the biopolymers (Faruk, Bledzki, Fink, & Sain, 2012).

Thus, pretreatment of fibers is imperative to improve the adhesion between matrix and fibers. Fiber-matrix interaction can be improved by pretreatment of the fibers using various chemical (alkali hydrolysis, acid hydrolysis, hydrogen peroxide, organic solvents, deep eutectic solvent and liquid hot water) (Medina et al., 2015; Sun, 2004; Tan et al.,

2013; Tan, Ngoh, & Chua, 2018), physical (milling, microwave, ultrasonic, plasma, dielectric barrier techniques and corona fall) (Maniglia & Tapia-Blacido, 2019; Remón, Matharu, & Clark, 2018; Yunus et al., 2010; Zianor Azrina et al., 2017), biological (enzyme hydrolysis), and physicochemical pretreatments (steam explosion, ammonia fiber explosion, and hydrothermal liquefaction) (Bhalla et al., 2018; Coral Medina et al., 2018; Miyata, Yamazaki, Hirano, & Kita, 2018; Parshetti, Kent Hoekman, & Balasubramanian, 2013; Raman & Gnansounou, 2014). Most of treatments are based on biomass biorefining and aim to remove amorphous materials from the fiber surface, disrupt hydrogen bonding in the network structure, and thus increase fiber aspect ratio and access of hydroxyl groups which can take part in bonding as well as chemical coupling. These treatments require considerable chemical, energy input or equipment requirement and produce many wastewaters of lignin. Moreover, lignin is second in plant biomass after cellulose and the most abundant natural aromatic resources. Recently, lignin has been incorporated into many biopolymers, such as starch, protein, cellulose, PLA and PBAT, to form the bioplastics, as shown in Figure 2.6. Some researchers have managed to use the cellulose fibers containing high content of lignin to develop green composites (Ghanbari et al., 2018; Ma et al., 2008a). The addition of lignin as reinforcements typically reduces cost and the water uptake and improves the strength (Sun et al., 2015). In addition, lignin plays an important part in antioxidant properties as a stabilizer because the phenolic hydroxyl groups can scavenge free radicals (Polat, Stojanovska, Negawo, Doner, & Kilic, 2017; Yang et al., 2016). Plasticizers can interact with the polymer by replacing polymer interactions (Kun & Pukánszky, 2017). This phenomenon improves the flexibility, mobility and workability of polymer by reducing intermolecular forces,  $T_g$  and the processing temperature of the blends (Villalobos et al., 2017). A plasticization effect has been observed when lignin is introduced into starch, protein and polycaprolactone (Baumberger, Lapierre, & Monties, 1998; Duval &

Lawoko, 2014; Duval et al., 2013; Thielemans et al., 2002; Wu, Wang, Li, Li, & Wang, 2009).

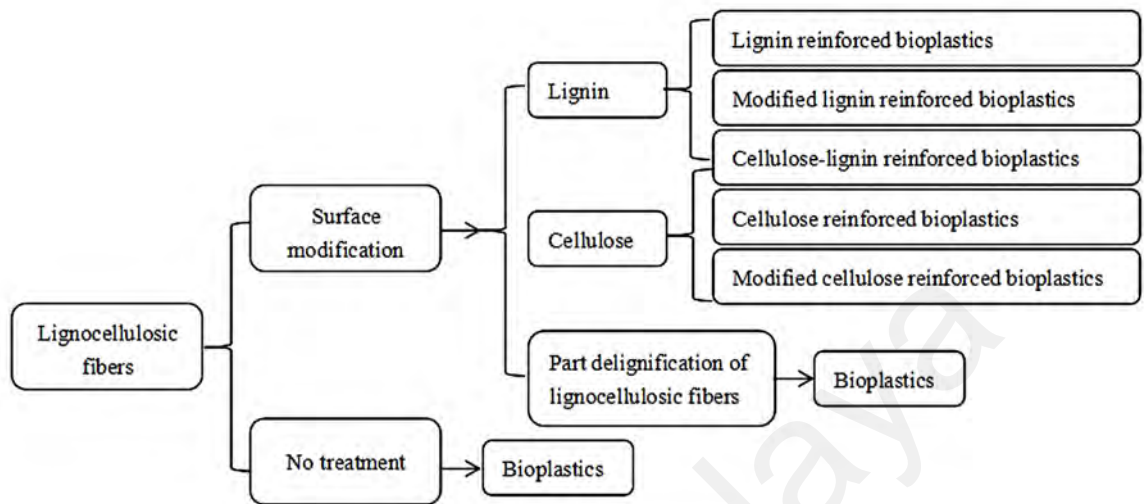


**Figure 2.6: Global diagram of the uses of lignocellulosic fibers and lignin in the bioplastics**

### 2.3.2.1 Cellulose-lignin incorporated bioplastics

Cellulose and lignin can be obtained separately by various treatments from lignocellulosic fibers and have been combined in the bioplastics. The compatibility between cellulose and other hydrophobic biopolymers could be remarkably enhanced by the amphiphilic lignin with polar phenolic OH and nonpolar hydrocarbon groups (Nair, Chen, Peng, Huang, & Yan, 2018). Therefore, lignin is a potential component for biocompatibilizer (Thakur et al., 2014; Thielemans et al., 2002). The addition of lignin could improve the compatibility between cellulose and matrix as shown by the SEM investigations. The impact properties are decreased, while Young's modulus and tensile strength could be improved significantly (Graupner, 2008).

Cellulose and lignin play different parts in cellulose-lignin bioplastics. In general, cellulose reinforces mechanical strength of the composites, while lignin reduces water uptake, improves thermal stability of the polymer matrix, and assures the good dispersion

of cellulose in biopolymers (Lin et al., 2013; Ma et al., 2015). They can generate mutual effects on the bioplastics (Liu, Peng, Cao, & Chen, 2014). A number of bio-based composites based on starch, lignin and cellulose were fabricated from an ionic liquid, 1-allyl-3-methylimidazolium chloride and coagulated in a system without solvent. The study found that the mechanical strength of the bio-composites was evidently depending on the contents of lignin, starch, and cellulose, resulting from the mutual supplement among different components. High gas barrier ability and great thermal stability were clearly observed in the bio-composites (Lewis, Waters, Stanton, Hess, & Salas-de la Cruz, 2016). Holo-cellulose and acid insoluble lignin of Pecan nutshell fiber were utilized as reinforcements of PLA based bioplastics. Flexural tests demonstrated that modulus of holo-cellulose bio-composites increased by 25% in comparison with the pure biopolymer. Conversely, high ductility and improved elongation at break were provided by the acid insoluble lignin in the PLA bioplastics. Plain PLA showed higher resilience than all the other bio-composites owing to the low compatibility between lignin and PLA (Agustin-Salazar et al., 2018). Moreover, isolated lignin and holo-cellulose components were blended with poly- $\beta$ -hydroxybutyrate (PHB). PHB melt crystallization was facilitated by holo-cellulose in cooling period as evidenced by the DSC investigation, while this phenomenon was not influenced by lignin. The rheological investigation of PHB and PHB-based blends indicated polymer viscoelastic properties improved remarkably. The high melt viscosity of PHB/lignin sample hampered chain mobility. The research provided a new point of view regarding the impact of cellulose and lignin on PHB (Angelini, Cerruti, Immirzi, Scarinzi, & Malinconico, 2016).

Plasticization properties and antibacterial activity of lignin are also observed in cellulose-lignin bioplastics. In addition, the addition content of nanoparticles is generally restricted below 3% due to strong inter-molecular hydrogen bonds. Miranda et al. (2015) evaluated the mechanical properties of corn starch bioplastics with lignin serving as a

plasticizer and cellulose nanocrystals acting as the reinforcing filler. The outcomes indicated that the incorporation of 1% cellulose nanocrystals and lignin significantly improved the modulus of elasticity and the maximum stress of about 1478% and 256%, respectively, compared to the group without lignin and cellulose (Miranda et al., 2015). Ternary PLA based bioplastics, with dispersed lignin nanoparticles and cellulose nanocrystals were produced by melt extrusion at contents of 1 and 3 wt%. The ternary systems presented higher modulus and strength values than those of binary PLA bioplastics and pure PLA. Furthermore, cellulose nanocrystals and lignin nanoparticles have shown antibacterial activity by reducing the bacterial pathogen multiplication because of the polyphenolic structure (Yang et al., 2016). In addition, cellulose-lignin nanocrystals can function as outstanding fillers for PLA to develop the bioplastics. To improve the thermo-mechanical and rheological properties of PLA bio-composites, cellulose nanocrystals coated with spray-dried lignin were combined. The results found that the lignin-coated cellulose nanocrystals enhanced their interfacial interaction with the PLA bio-composites and promoted the dispersion of cellulose nanocrystals, leading to a significantly improved thermo-mechanical and rheological properties. Nucleating sites at high density were induced by the super compatibility and dispersion of lignin-cellulose nanocrystals in PLA, generating an increase in PLA crystallinity. Adding 0.5 wt% lignin-cellulose nanocrystals to the PLA bio-composites induced a nearly 60% increase of storage modulus compared to pure PLA. This improvement of mechanical properties was derived from a remarkably improved crystallinity of PLA (Gupta, Simmons, Schueneman, Hylton, & Mintz, 2017).

### **2.3.2.2 Lignin-containing cellulosic fibers as reinforcements of bioplastics**

Lignin-containing cellulosic fibers indicate cellulose fibers with high contents of lignin after various treatments. Lignocellulosic residues containing a remarkable polysaccharide portion represent a very interesting source of fillers for bioplastics (Ago,

Ferrer, & Rojas, 2016). The interaction between lignin-containing cellulosic fibers and biopolymers are complex owing to the various composition of cellulosic fibers. The interaction between jute strands and PLA was evaluated. Five different lignin contents of strands were introduced into the PLA with the fiber ratio of 30 wt%. PLA matrix was prepared in a discontinuous extruder and characterized by tensile tests. Jute strands with a lignin content of 4% were the most suitable to be used as PLA filler as shown by macro and micromechanical analysis. The phenomenon was mainly attributed to their better interaction and dispersion within the PLA matrix and higher intrinsic mechanical properties. Lignocellulosic fillers obtained from bioethanol production were blended with PHB. Spectroscopic, thermal, and morphological characterization showed there was a high polysaccharide content in the filler. Lignocellulosic filler produced an active effect on the PHB physical aging by acting as a heterogeneous nucleating agent. Infrared spectroscopic data showed that a low interaction between the lignocellulosic filler and PHB was observed. Further, a deterioration of impact and tensile properties in the composites was attributed to this lack of connection. On the other hand, the biocomposites became more resistant to the degradation with concentrations of lignocellulosic fillers increasing, possibly because of the antibacterial activity of the lignin. Therefore, because lignocellulosic fillers improved the biopolymer properties in a cost-effective and environmentally friendly way, the utilization of these agro-industrial residues held great potential to widen the application of PHB (Angelini et al., 2014).

Lignin-containing cellulosic nanofibrils (LCNF) can produce enhanced properties when incorporated into bioplastics. Residual oil palm empty fruit bunches were extracted to obtain Lignin-containing cellulosic nanofibrils (LCNF) with a variety of separation methods. Different kinds of LCNF isolated were incorporated into starch bioplastics. The Young's modulus and yield stress achieved remarkable increases after the incorporation of LCNF. In addition, with LCNF loadings increasing, water uptake of the composite bio-

foams was reduced because of the low hydrophilicity of lignin residuals. The starch/LCNF nanocomposites displayed the same mechanical properties as those of polystyrene polymers. Therefore, they can be recognized as a potential and green alternative in insulation and packaging composites (Ago et al., 2016). In order to develop composite films by casting and hot press, PLA and different amounts of LCNF from 5 to 20 wt% were blended. A good interfacial adhesion between PLA and LCNF was indicated due to the existence of lignin and also evidenced by results of infrared spectroscopy and atomic force microscope characterization at the nanoscale. Water resistance, thermal and mechanical properties were confirmed to improve remarkably in the resultant bioplastics at 5-10 wt% LCNF addition (Nair et al., 2018).

Though the reports on lignin-containing cellulose reinforced bioplastics are scarce, they are adequate to indicate their promising application in the bioplastics in future. We might conclude that they might significantly affect and even determine whether direct use of lignocellulosic fibers in bioplastics will be achieved. They should be the hotspot in the future. Lignin-containing cellulosic nanofibrils would play a significant role in preparing the bioplastics with lignocellulosic fibers.

### **2.3.2.3 Lignocellulosic fibers without delignification as reinforcements of the bioplastics**

Lignocellulosic fibers without delignification mean that the lignocellulosic fibers are obtained without the process of removing the amorphous materials, which are mainly prepared via physical treatments. During the preparation of bioplastics, physical interactions between lignocellulosic fibers and biopolymers matrix are usually restricted and do not improve the performance of bio-composites significantly (Badia et al., 2014; Sun, Fridrich, de Santi, Elangovan, & Barta, 2018). Therefore, the ways attempted to improve the compatibility are mainly focused on increasing fiber-matrix interaction,

reducing degree of association, and improving the hydrophobic character of lignocellulosic fibers.

The interaction between matrix-fiber can be promoted with the compatibilizer or coupling agent interacting with both fibers and polymers (Liu, Misra, Askeland, Drzal, & Mohanty, 2005). González et al. (2011) reported the thermal and mechanical properties of fiber and PLA reinforced bio-composites. PLA-based composites were manufactured by injection molding. Both sisal and kraft fibers composites revealed higher impact strengths than that of neat PLA (24.61 J/m and 14.45 J/m, respectively). In addition, a good dispersion of reinforcements in the PLA composites was revealed by microscopic analysis (González, Santos, & Parajó, 2011). Both flexural strength and modulus of starch bio-composites were significantly increased by laccase treatment with the mediators including violuric acid and fibers. Water uptake of bio-composites was reduced considerably. This bio-composites represented promising means to produce non-food and disposable packaging materials based on above biopolymers (Narkchamnan & Sakdaronnarong, 2013). The effect of coupling agent and fibers on water uptake behavior was assessed in poly(3-hydrobutyrate-co-3-hydroxyvalerate) (PHBV)/sisal bio-composites, by analyzing the water absorption capability and water diffusion rate. It was found that more water would be incorporated when the bio-composites absorbed the water more quickly; as the content of sisal fibers increased in the bio-composites, the sample temperature became higher. In particular, saturated water absorption was more associated with the ratio of fibers, while temperature was primarily determined by water diffusion. Owing to chemical bonding between fiber and matrix, the interaction was affected by diffusion rate, but saturated water incorporation did not show significant impact on the interaction (Badia et al., 2014).

The effects of fiber properties such as fiber length or aspect ratio on increasing fiber-matrix interaction are also investigated. Fiber length is an important parameter to enhance

toughness and strength, while fiber dispersion mainly promotes strengths (Gallos, Paës, Allais, & Beaugrand, 2017; Hajiha & Sain, 2015; S. Bailey & Kraft, 1987). Soy and kenaf fiber bioplastics were manufactured by compression or injection molding. Mechanical properties and dynamic mechanical analysis characterized the effect of the processing method and fiber length on the performance of the bio-composites. The modulus and impact strength of the bioplastics rose with fiber orientation, fiber content and fiber length increasing. Microscopy observations revealed that fiber length could positively influenced the fracture surface as fiber content and fiber length increased. This suggested the predominant fiber bridging effects on impact strength of the bioplastics (Liu, Drzal, Mohanty, & Misra, 2007). A complex bio-composite by compounding and molding process was investigated with an aim of high impact strength. Low and high screw extrusion methods were involved. Fiber with 2.3 mm fiber length and 20 wt% fiber content indicated a good dispersion in the bio-composite whose impact strength was 130 J/m. It can be concluded that toughness was influenced by fiber dispersion, length and concentration (Hajiha & Sain, 2015). In order to investigate the effect of fiber amount and length, curaua fibers and poly(butylene succinate) were used to develop the bio-composites by compression molding. Mechanical strength, morphology and water uptake studies were performed to evaluate the characteristics of the bio-composites. It was found that the flexural and impact strengths increased as the fiber content increased. In addition, in the bio-composites with fiber content of 20 wt%, its impact strength was also affected by the fiber length ranging from 1 to 4 cm. However, the length of the fibers did not affect flexural strength significantly. Water uptake analysis confirmed the material was more sensitive to fiber content compared to fiber size. The resulting bioplastics could be applied to interior car parts or rigid packaging because they owned the same mechanical properties as poly(butylene succinate) (Frollini, Bartolucci, Sisti, & Celli, 2015).

Regarding lignocellulosic fiber reinforced bioplastics, it is typically acknowledged that stress transfer from the matrix to the fiber is enhanced by fibers having a high aspect ratio (length/width). A high aspect ratio is very crucial in lignocellulosic fiber reinforced bio-composites because it indicates possible strength performance (Faruk et al., 2012). Bio-composites were prepared using twin extrusion process with lignocellulosic hemp fiber as reinforcements and poly( $\epsilon$ -caprolactone) as matrix. Different aspect ratios (19-38) of fibers were prepared. Properties including low-velocity impact, flexural and tensile were enhanced in the poly( $\epsilon$ -caprolactone)/hemp fiber bio-composites. The best properties were revealed in the bio-composites with 26 aspect ratios, with modulus and flexural strength of 285% and 169%, respectively. However, mechanical properties presented a significant decrease in water immersed bio-composites; flexural moduli and tensile reduced by 62% and 90%, respectively. The results provided a green replacement of petroleum-based and conventional polymer matrix in potential applications (Dhakal et al., 2018). In addition, the adhesion between fibers and polymers and the dispersion of fiber in matrix are also vital to an effective stress transfer. The intense shearing forces can reduce the aspect ratio of cellulosic fibers in the mechanochemical process. The milling process can cause the degradation of the matters with lower molecular weight, which produces low mechanical properties. However, the negative effect from milling can be compensated by the crosslinked structure and effective fiber dispersion, providing the bioplastics with enhanced performance (Niu et al., 2015).

In addition, modification of lignocellulosic fibers is studied to improve hydrophobicity and compatibility of lignocellulosic fiber-matrix with thermal treatment or ultrasonic. To improve the properties and fiber/matrix adhesion of the bioplastics, wheat straw fibers/PHBV bioplastics were fabricated. Wheat straw fibers were treated by torrefaction treatment to increase their hydrophobicity. SEM observations revealed that an excellent fiber/matrix compatibility was achieved in the resulting bio-composites. Crystallinity and

molecular weight of bioplastics remained constant and the crystallization of PHBV was facilitated by the introduction of torrefied fibers compared to untreated fibers. Mechanical properties of wheat straw fiber/PHBV bio-composites were only affected by the 30 wt% of torrefied fibers. A 30% decrease in water vapor permeability was observed with 20 wt% torrefied fiber contents attributed to the hydrophobic nature of fibers and improvement of fiber/matrix adhesion (Berthet et al., 2016). The chemical composition of the fibers does not change significantly in physical treatments. Therefore, as mechanical bonding between the matrix and the fiber increased, the adhesion between them is improved (Faruk et al., 2012). Water hyacinth fiber with 10% volume fraction was employed to reinforce the bio-composites obtained from tapioca starch-based plastics. During gelatinization, the bio-composites were cast into a glass plate then placed in an ultrasonic bath. After vibrated with ultrasound for 30 min, the bio-composites with optimal properties can be produced. Tensile modulus and tensile strength increased by 108% and 83% after this vibration. At the same time, water resistance of the bioplastics increased by 25% and achieved a maximum (Asrofi, Abral, Putra, Sapuan, & Kim, 2018). The empty fruit bunch fibers and tapioca starch were blended to prepare the bioplastics. After the gelatinization of the bio-composites, the solution was cast into a glass plate and then vibrated in an ultrasonic bath with 250 watts and 40 kHz in different duration for 0, 15, 30, 60 min, respectively. The results demonstrated the characterization of the bio-composites has been influenced by the vibration during gelatinization. Different fracture surface of tensile sample was revealed by the SEM studies. For vibration duration of 60 min, strain was decreased to 35.1%, meanwhile tensile modulus and tensile strength increased to 277.4 and 64.4%, respectively, compared to untreated one. Water uptake of the untreated bio-composites was higher than that of the vibrated one. FTIR and XRD of the bio-composites have changed due to various vibration duration (Abral et al., 2018).

The number of research studies on lignocellulosic fibers and lignin reinforced bioplastics are much fewer compared to cellulose reinforced bioplastics. The difference can be explained by the complexity and difficulty to fully utilize lignocellulosic fibers and lignin. The development of processing technologies and innovative ways to enhance the properties of lignocellulosic fibers and lignin would further boost their potential applications in the bioplastics undoubtedly (Brodin et al., 2017; Kun & Pukánszky, 2017).

#### **2.3.2.4 Comparison between lignocellulosic fiber and lignin in the bioplastics**

The advantages of lignin over lignocellulosic fibers in the bioplastics are also reviewed and identified as follows. Firstly, lignocellulosic fibers and lignin play different roles when introduced into other biopolymers. Lignin can function as the reinforcement, plasticizer, stabilizer, or bio-compatible, which widens its application (Z. Sun et al., 2018; Yang et al., 2019). On the contrary, lignocellulosic fibers primarily act as the reinforcements in the bioplastics, which is ascribed to the more complex compositions and recalcitrant structures of lignocellulosic fibers compared to lignin (Sun et al., 2015). Secondly, chemical modifications of lignin such as functionalization of the hydroxyl groups are more widely studied than that of lignocellulosic fibers. In the end, the hydrophilic nature of lignocellulosic fibers is also a great challenge needed to be overcome in the bioplastics. Conversely, the lignin is hydrophobic (Kun & Pukánszky, 2017). As a consequence, lignin presents more advantages than lignocellulosic fibers in the bioplastics.

It seems to be unwise to remove all lignin when the researchers fabricate the bioplastics with lignocellulosic fibers (Elfehri Borchani, Carrot, & Jaziri, 2015). More focuses should be directed toward the use of lignocellulosic fibers in the bioplastics without removing lignin significantly. One way is to separate lignin by destroying the degree of association of lignin with other components and mix lignin with the residuals to produce

the bioplastics. Another way is to apply the lignocellulosic fibers directly or with simple modification in the bioplastics (Yang et al., 2019). This enlightens us a novel modification technique to make the most use of fibers to fabricate starch-based bioplastics with favorable properties.

### **2.3.3 Thermal treatment of fibers**

Hydro-thermal liquefaction and steam explosion have been extensively investigated for the pretreatment of fiber resources and their subsequent use as chemical feedstocks and fuels (Medina et al., 2016). The wet organic residues can be processed without preliminary separating and drying, and these processes involve low use of chemicals. Hou et al. (2014) developed a method of combined alkaline and steam flash-explosion treatment to extract cellulose fibers from bark of cotton stalks. Lightweight composites with superior properties were fabricated from polypropylene and the obtained fibers. However, these pretreatments require a high energy input and might enable the fibers to be hydrolyzed to some extent (Baharuddin et al., 2013; Miyata et al., 2018).

Thermal treatment of fibers with dry method has attracted considerable interests in recent years which exhibits significant advantages. Firstly, thermal treatment is one of the most economical processes conducted at the temperature range of 150-180 °C which can avoid noticeable fiber loss (C. Lee et al., 2018; Novo et al., 2011). Secondly, during the heat treatment, hydrogen bonding is disrupted and lignin migrates to the fiber surface, which is likely to improve the compatibility within the matrix (Berthet et al., 2016). Thirdly, thermal treatment conducted in solid state does not need many chemicals and is energy-efficient and eco-friendly (Niu et al., 2015; Staroszczyk & Janas, 2010).

For example, the influence of heat treatment on the chemical properties of bamboo fibers was investigated (C. Lee et al., 2018). The heat treatment was conducted in diverse conditions: four treatment temperatures (150-210 °C), three treatment media (i.e., air,

linseed oil, and nitrogen), and three durations (1-4 h). The outcomes showed that the treatment duration and temperature had a remarkable impact on the contact angle and surface color of the fibers. The heat treatment reduced the contents of  $\alpha$ -cellulose, holocellulose, and hemicellulose but increased the content of lignin of the bamboo. Urea formaldehyde-bonded oil palm trunk particleboard was exposed to temperature of 180-220 °C in palm oil for 2 h. Oil-covered particles exhibited lower water uptake as shown by the SEM. Modified samples possessed higher resistance against termites and thermal stability also (S. Lee et al., 2018).

The impact of the thermal treated *eucalyptus* fibers on the physical and mechanical properties of fiber-cements composites was evaluated. The fibers were heated at 140-230 °C for 1 h in the oven. The thermal treatments were efficient in removing the extractives. The improved contents of lignin led to the toughness decrease and apparent porosity increase in the reinforced composites (Silva et al., 2020). Wheat gluten bio-composites were produced by dip-coating of the flax-fiber-weaves into a wheat gluten/glycerol solution, followed by compression molding. Tensile tests showed that the flax yarn improved the crack-resistant properties significantly; the maximum stress increased from 2 to 29 MPa using 19 wt% flax fibers. This bio-composites can be shaped plastically under ambient conditions, while at the same time providing in-plane strength, stiffness, and crack-resistance (Wu et al., 2017). Polypropylene (PP) and *Eucalyptus camaldulensis* wood fibers plastic composites were developed by thermal treatment in order to enhance the dimensional stability. The fiber treatments were conducted at 120-180 °C for 20-40 min in a laboratory autoclave. Water uptake and swelling of the panels decreased significantly as the treatment time and temperature increased (Ayrilmis, Jarusombuti, Fueangvivat, & Bauchongkol, 2011).

Besides, NaOH treatment is a conventional method to improve interfacial adhesion between the matrix and fibers (Vandenbossche et al., 2014; Yunus et al., 2010). Numerous

studies investigated thermal treatments of fibers in the presence of catalysts, especially various alkaline solutions (NaOH, Na<sub>2</sub>CO<sub>3</sub>, KOH, and K<sub>2</sub>CO<sub>3</sub>) (Abdullah et al., 2016; Berthet et al., 2016; Bhalla et al., 2018). Cellulose fibers were extracted from bark of cotton stalks using a simultaneous alkaline and steam flash-explosion treatment (SFE-AT). The obtained fibers were combined with PP to make lightweight composites with favorable properties. Comparing three composites from SFE, AT, SFE-AT, the composites from SFE-AT exhibited the best stability to water resistance and mechanical properties. SFE detached bark of cotton stalks efficiently and subsequent AT (5 g/L NaOH solution) separated the non-cellulose impurities sufficiently (Hou et al., 2014). Rahman and Netravali (2018) fabricated advanced waxy maize starch-based bio-composites using cellulose fibers which were modified by a combination of 5% NaHSO<sub>3</sub> solution and thermal treatment at 140 °C. However, reports regarding simultaneous thermal and alkaline modification of raw fibers with dry method and their bioplastics are still rare. This suggests us a simple and effective thermal modification technique to improve interfacial adhesion between fibers and biopolymers.

#### **2.3.4 Empty fruit bunch fibers and their application in the bioplastics**

Oil palm, *Elaeis guineensis*, belongs to an important oil producing crop of many countries in southeast Asia (Medina et al., 2015). Malaysia is one of the biggest producers of oil palm in the world, including gross 5,900,157 hectares of oil palm plantations in 2019 (Figure 2.7). In the palm oil mills, a total of 101,423,699 tons of fresh fruit bunches (FFB) were gained. It was estimated that 19,858,367 tons of crude PO were produced according to Malaysian Palm oil Board (2020). After the PO extraction, the main solid biomass was oil palm EFB fibers (Hosseini & Wahid, 2014). It is estimated that for 1 ton of FFB processed, 220 kg of EFB fibers is generated which is around 32.2% of total solids generated during oil palm processing (Chiew & Shimada, 2013). Therefore, 22,313,213 tons of EFB fiber were produced in 2019.

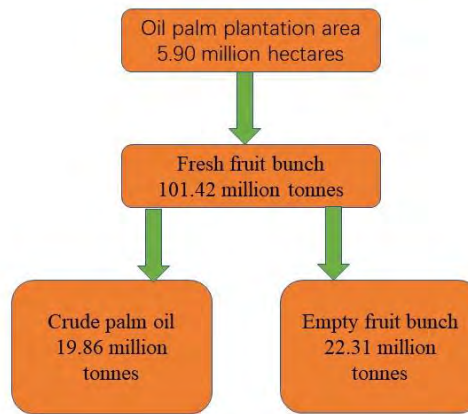


**Figure 2.7: Potential production of biomass from oil palm in Malaysia in 2019 according to Malaysian Palm oil Board (2020)**

EFB fibers are currently utilized as mulch for landscaping, raw materials for fertilizer manufacture, compost for plantation sites or burned in incinerators of palm oil mills (Bouza, Gu, & Evans, 2016; Chiew & Shimada, 2013; Fahma, Iwamoto, Hori, Iwata, & Takemura, 2010). Furthermore, EFB fibers can be chemically or biologically hydrolyzed to sugars to become a source of valuable carbon for the production of various chemicals such as bio-oils and ethanol (Tan et al., 2013). EFB fibers have recently been considered as potential reinforcements for the bioplastics. Generally, the contents of hemicellulose, lignin, and pectin are thought to interact adversely with polymers. Besides, silica bodies disperse uniformly on the fiber surface, which hampers the chemical penetration into the cellulose and hemicellulose (Yunus et al., 2010). Therefore, separation of these components from EFB fibers has attracted essential interest in scientific research when they are used as the reinforcements of the bio-composites (Moshiul Alam et al., 2012).

PLA-based bio-composites were reinforced with alkali and ultrasound treated EFB fibers by extrusion and injection molding. Interfacial and mechanical properties increased significantly due to the simultaneous fiber treatments (Moshiul Alam et al., 2012). Cellulose nanowhiskers (CNW) were isolated from EFB microcrystalline cellulose and used to reinforce PLA through solution casting. The tensile strength of the

nanocomposites increased with the addition of 3% CNW. The elongation at break decreased linearly with the CNW loading increasing due to polymer chain movement restriction (Haafiz et al., 2016). The cellulose/PP composites were fabricated by injection molding technique. Cellulose from EFB fibers were developed by autoclave and ultrasonication pretreatments. The composites with 25 wt% cellulose resulted in tensile strength as high as 27 MPa (Abdullah et al., 2016).

#### **2.4 Starch/fiber-based bioplastics crosslinked with citric acid**

Activated lignocellulosic fibers are miscible with starch potentially by forming hydrogen bond interactions with the hydroxyl groups. As these interactions are limited and both biopolymers along with plasticizers are hydrophilic, the resulting biocomposites still exhibit poor water resistance (Gironès et al., 2012). Therefore, to develop the bioplastics with enhanced water resistance properties, it has been customary through the use of crosslinking agents, which interact with both fibers and starch. The interaction creates a denser three-dimensional structure and decreases the swelling and accessible regions of starch, leading to an improvement in the water resistance and mechanical properties (Wu et al., 2019; Zhou, Tong, Su, & Ren, 2016).

Chemicals with multi-functional reactive groups, for example, glutaraldehyde, dialdehyde, di-isocyanate, glyoxal, epichlorohydrin, sodium tri-metaphosphate, boric acid and dicarboxylic acids, are commonly used for crosslinking purposes (Maier, Ensenberger, Irmischer, & Weiss, 2016; Wang et al., 2009). One of the most environmentally friendly crosslinking is through citric acid (CA). CA is a natural, low-cost, non-toxic, and multi-carboxylic organic acid (Figure 2.8). When CA is heated, it dehydrates and yields an anhydride, which could react with starch to provoke intermolecular ester bonds between the hydroxyl groups of starch and the carboxyl groups of CA (Figure 2.9). This creates a tight starch citrate for the composites (Chabrat, Abdillahi, Rouilly, & Rigal, 2012; Zhang et al., 2019). Moreover, it has been found that

CA could develop strong hydrogen bonds with starch. In addition, CA can act both as a crosslinker and a plasticizer in the starch-based bio-composites, which depends on the concentrations of CA added (Olivato, Grossmann, Bilck, & Yamashita, 2012a; S. Sun et al., 2018).

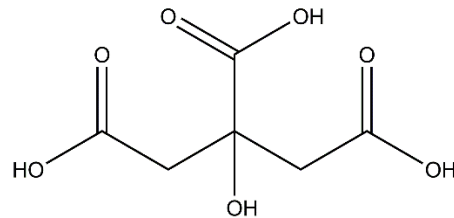


**Figure 2.8: Chemical structure of citric acid**

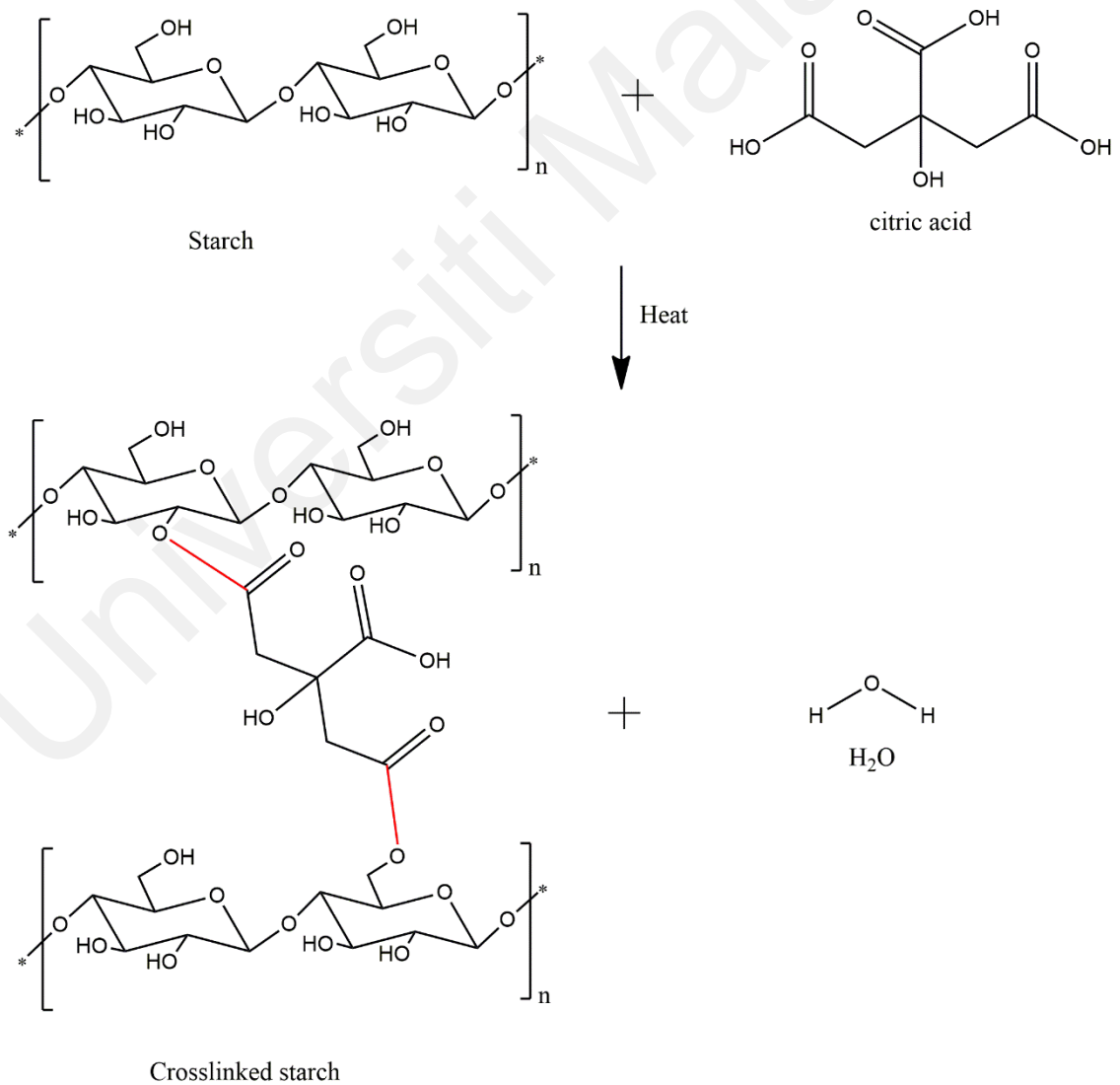


**Figure 2.9: Proposed reaction mechanism for crosslinked starch**

Several bio-composites based on starch, fillers and CA have been investigated. Owi et al. (2019) unveiled the physicochemical properties of starch/nanocellulose bio-nanocomposites crosslinked by *Citrus aurantifolia*. Harini, Chandra Mohan, Ramya, Karthikeyan, and Sukumar (2018) reported the effect of CA on performance of starch films reinforced by Walnut shell cellulose. Wang et al. (2009) surveyed the influence of CA and processing on the performance of thermoplastic starch/montmorillonite nanocomposites. Starch/cellulose-based composite foams were prepared via compression moulding at 220 °C with CA as a crosslinking agent (Hassan, Tucker, & Le Guen, 2020). The possible reaction mechanism between starch/fiber and CA is shown in Figure 2.10. These reports all demonstrated that the incorporation of fillers and CA in the appropriate contents enhanced the mechanical and water resistance properties of starch-based composites obviously. At the same time, CA increased the plasticization of starch and adhesion of fillers and starch in the composites efficiently. However, CA might cause the decomposition of starch. The effects of eggshell powder and CA on the properties of thermoplastic starch were investigated. All components were melt-blended using an internal mixer. CA led to the formation of crosslinking structures and caused accelerated biodegradation of starch due to hydrolysis. Conversely, addition of eggshell powder retarded the biodegradation (Praprudivongs & Wongpreedee, 2020). However, there is a paucity of information on the combined effect of lignin and hemicellulose-containing cellulose fibers and CA on the water-proof and tensile properties of starch-based bioplastics.

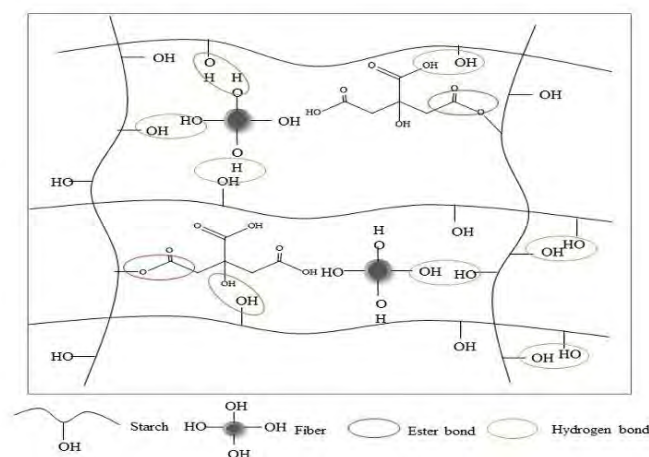


**Figure 2.10: Proposed reaction mechanism for starch/fiber-based bioplastics crosslinked with citric acid**

## 2.5 Epoxidized plant oils as crosslinking agents in the bioplastics

### 2.5.1 The bioplastics crosslinked with epoxidized plant oils

Plant oils are ideal replacement materials to petroleum-based polymers because they are renewable and low-cost (Liu, Chen, Xie, & Qiu, 2016). Another way to improve the filler-biopolymer adhesion and water resistance of the bioplastics is the addition of EO (Quiles-Carrillo, Montanes, Sammon, Balart, & Torres-Giner, 2018). EO can be obtained from plant oils by a C=C reaction with active oxygen, which involves the introduction of an oxygen atom and transforms the C=C into epoxy group (Zeng, Wu, Li, Wang, & Zeng, 2017; Zhao, Wu, Li, Wang, & Zeng, 2017). The structures of EPO and ESO are described in Figure 2.11.

The obtained epoxides can be used for several applications, such as plasticizers or stabilizers for plastics, starting materials for polyols, or thermosetting resins for composites (Carbonell-Verdu, Bernardi, Garcia-Garcia, Sanchez-Nacher, & Balart, 2015; Sarwono, Man, & Bustam, 2012; Suzuki, Botelho, Oliveira, & Franca, 2018; Tan et al., 2014). Epoxy resin from a m-xylylenediamine and diglycidyl ether of bisphenol was modified by 10 wt% of EPO (Sarwono et al., 2012). ESO containing octadecyl trimethyl ammonium functionalized montmorillonite (1-5 wt%) was thermally cured using

methylhexahydrophthalic anhydride with the catalyst of 2-ethyl-4-methylimidazole (Tan et al., 2014). Epoxidized cooking oil was synthesized and applied as the plasticizer for PVC (Suzuki et al., 2018). EO have also been recognized as reactive plasticizers or compatibilizers to biopolymers such as PLA due to the reactivity of epoxy groups (Mistri, Routh, Ray, Sahoo, & Misra, 2011; Xiong et al., 2013a).

Recently, numerous studies have applied EO to modify the properties of starch-incorporated or based composites. For example, Xiong et al. (2013a) fabricated a composite based on PLA and maleic anhydride grafted starch by melt compounding with ESO. Further, relevant studies have used ESO as the modifier for starch-based bio-composites by melt reactive blending (Belhassen et al., 2014). ESO has brought about a partial crosslinking of the epoxide ring with the hydroxyl groups of starch.

Only few researches were carried out on biopolymers, fillers and EO modifiers blended composites. Tanrattanakul and Saithai (2009) prepared bioplastic-organoclay nanocomposites with ESO of different epoxide contents. Balart et al. (2016) fabricated the bio-composites with PLA and hazelnut shell flour plasticized by epoxidized linseed oil. Meng et al. (2018) compounded cellulose nanofibrils and ESO into PLA to achieve high strength and toughness. In general terms, most of the studies were linked to PLA-based bio-composites reinforced with fibers. The interactions between biopolymers and EO occurred and led to the enhanced properties. However, as far as we know, no former study has proposed EO to modify starch/fiber-based bioplastics.

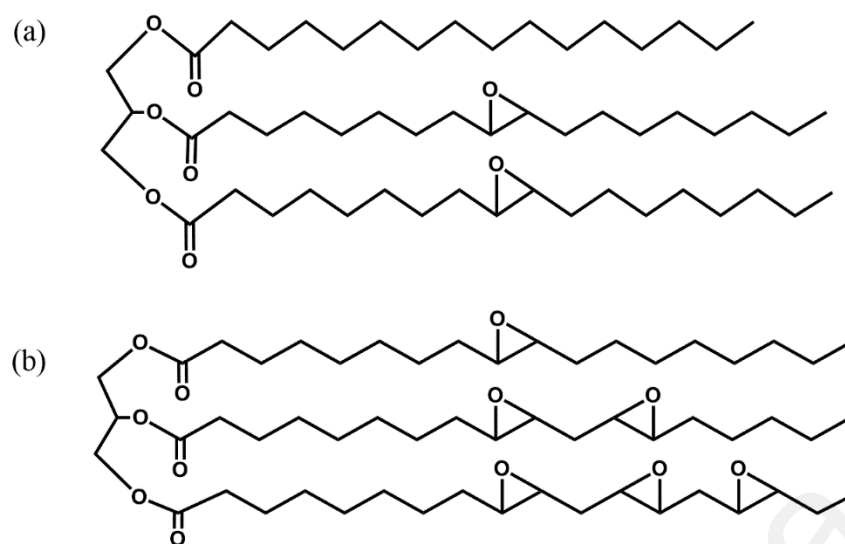


**Figure 2.11: Chemical structures of (a) epoxidized palm oil and (b) epoxidized soybean oil**

### 2.5.2 The preparation method of starch/fiber-based bioplastics with epoxidized plant oils

Lipids can be combined into starch-based films either by coating the surface of the formed films with lipid layers to obtain bilayer films or by incorporating lipids in the film-forming solution to obtain emulsified films (emulsion technique) (Jiménez et al., 2012; Thakur et al., 2017). Bilayer film preparation process requires two casting and drying steps, high temperature for lipid fusion or organic solvents for lipid dissolution. Bilayer films have better barrier efficiency against water transfer than emulsified films as the water molecules continue to permeate through the non-lipid phase. However, bilayer films are likely to develop cracks or pinholes, delaminate over time, and exhibit non-uniform surface. As concerns emulsified films, they only require one emulsion casting and one drying process. The emulsified films exhibit good structural cohesion and superior mechanical properties due to the water-resistance of the lipids. The emulsified films have the minimal use of organic solvents and appear to be more favorable in terms of simple and feasible preparation procedures (Galus & Kadzińska, 2015; Sartori & Menegalli, 2016).

As is well known, the introduction of polymer emulsion is also an important path to disperse and crosslink organic and/or inorganic fillers to further improve their reinforcing effect. The incorporated polymer emulsion could reduce the stress concentration caused by fillers, achieving synergistic reinforcement for the composites. In order to achieve high fiber content, it was decided to use an emulsion based on thermoplastic starch and PCL in combination with the basalt fibers (Wittek & Tanimoto, 2008).

The phase separation between starch and high contents of EO is possible to occur during drying process of emulsion even with the presence of emulsifiers (Saber, Chockchaisawasdee, Golding, Scarlett, & Stathopoulos, 2017). Also, many side reactions are supposed to occur for EO by emulsion technique (Zhou, Sain, & Oksman, 2016). The reaction is preferred to be conducted by melt reactive blending. According to the reported work that used EO as compatibilizers for the bio-composites, the reaction between the -OH groups of biopolymers and the epoxy groups of the compatibilizers could occur at high temperature (Belhassen et al., 2014).

## **2.6 Crosslinked epoxidized plant oils as crosslinking agents in the bioplastics**

In contrast to petroleum-based epoxies (typical of terminal epoxides), the epoxy groups in EO molecules are not positioned in the terminal of fatty acid chains, which largely restricts their reactivity with starch due to the steric effect (Meng et al., 2019; Xiong et al., 2013a). The low content of epoxy groups on EO can only provide low reactivity with starch. Additionally, EO is not easy to uniformly disperse in the composites because of the poor compatibility between EO and starch (Ge et al., 2019). Consequently, the interfacial adhesion between EO and starch needs to be further improved. Compatibilizers, such as poly-ethylenimine, maleic anhydride, tannic acid, stearic acid, and CA, have been evaluated to enhance the reactivity between hydrophilic starch and hydrophobic polyesters (Kadam, Pawar, Yemul, Thamke, & Kodam, 2015; Meng et al., 2019). For example, starch-based bioplastics were modified by ESO using reactive melt

blending with tetrabutylammonium bromide as a catalyst, which enhanced the strength and stiffness of the bio-composites significantly (Belhassen et al., 2014). In order to develop water-resistant coatings for starch-based bio-composites, poly-ethylenimine was applied to improve the interfacial adhesion between starch and acrylated epoxidized soybean oil (Meng et al., 2019).

Grafting multifunctional groups onto EO is a feasible strategy because the groups can serve as the crosslinkers to construct a strong crosslinking network with enhanced performance (Pawar et al., 2016; Zhao et al., 2018). For example, bamboo fibers-reinforced PLA bio-composites were toughened with tannic acid-crosslinked ESO prepolymer via reactive extrusion (Liu et al., 2019). Zhao et al. (2018) employed an epoxy and phosphate groups-containing soybean oil as a multifunctional crosslinker that reacted with soybean flour-based adhesive and kenaf fibers synergistically.

Reaction of carboxylic acids with non-terminal epoxy groups has also been proposed as attractive methods to improve the compatibility of biopolymers and EO by the acid-catalyzed ring-opening reaction between the carboxylic acid groups and epoxides, as shown in Figure 2.12 (Gogoi, Horo, Khannam, & Dolui, 2015b; Zeng et al., 2017). The carboxyl groups can generate transesterification reaction with  $\beta$ -hydroxyester links activated by the acid at high temperature without the incorporation of any external catalyst. Zhao et al. (2017) reported an efficient way of dynamic vulcanization of PLA and sebacic acid with ESO, exhibiting excellent thermal processability and tensile properties. A green bio-nanocomposite was prepared by the introduction of acid functionalized multiwalled carbon nanotubes into a CA-cured ESO prepolymer (Gogoi et al., 2015b). Lei, Liang, Feng, He, and Yang (2018) prepared lignocellulose bio-composites by modifying lignocellulosic fibers with CA-ESO resin, to obtain the bio-composites that exhibited high hydrophobicity and tensile strength. We might infer that the carboxyl groups of CA could act as a “bridge” between EO and starch/fibers by forming the interactions, which could

fully realize utilizing EO and CA in the composites.

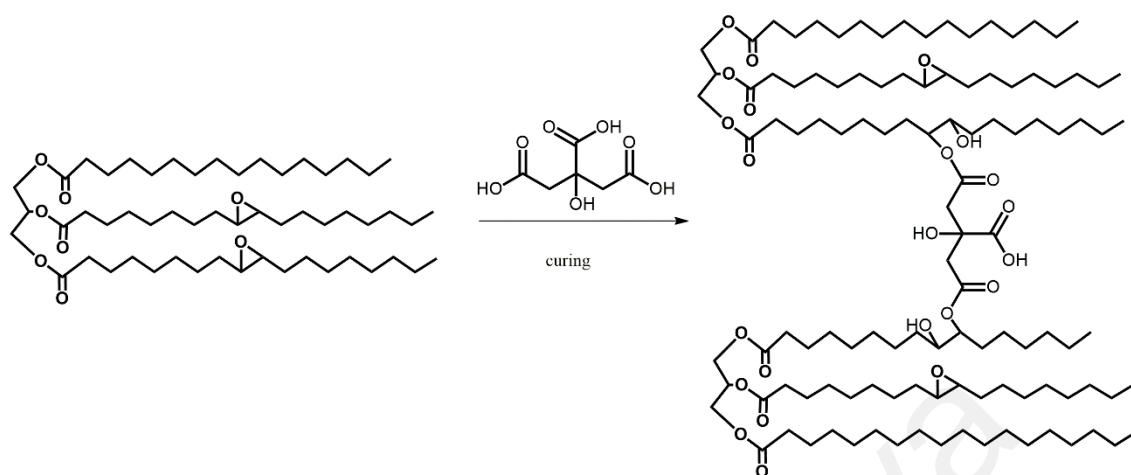


**Figure 2.12: Synthesis of bio-epoxy resin with epoxidized palm oil and citric acid**

In addition, CA may act as a compatibilizer between hydrophobic polymers and starch. Starch/PBAT films containing CA as the compatibilizer were produced by blown extrusion (Garcia et al., 2014). The presence of CA improved the plasticization and dispersion of starch in the starch/glycerol/linear low-density polyethylene blends (Ning, Jiugao, Xiaofei, & Ying, 2007). CA served as a compatibilizer and promoted depolymerization of both PLA and starch (Chabrat et al., 2012). Moreover, the crosslinking reaction of starch with CA has been widely known (Menzel et al., 2013; Seligra, Medina Jaramillo, Fama, & Goyanes, 2016).

## 2.7 Summary

The biodegradable bioplastics from renewable natural sources such as starch have attracted great interest due to the environmental problems of traditional petroleum-based plastics. Starch-based bioplastics comprise the largest production capacity in the bioplastic market due to the competitive advantages such as renewability, low cost, high abundance, and biodegradability. However, starch-based bioplastics generally exhibit poor mechanical and water resistance properties in humid conditions, which hinder their extensive applications. Ways to improve the properties of starch-based bioplastics have

been reviewed, which include blending with nanoparticles or other biodegradable polymers, adding the crosslinking agents, and chemical modification of starch. However, chemical modification not only decreases the molecular weight of starch, but also gives rise to some toxic chemical byproducts and modifies the biodegradability. Therefore, blending and crosslinking are attempted in the study.

Adding lignocellulosic fibers is one of the most effective ways to improve these properties due to their high strength and biodegradability. Most of the studies focus on purification of cellulose or nanocellulose by removing lignin and other impurities. However, lignin-containing cellulose fibers have been extensively used in the bioplastics as the additives. Through the literature review, it is confirmed that the pretreatment is involved to dissociate the interactions within the fibers without removing lignin significantly. Therefore, thermal and alkali treatment of fibers is recommended due to their competitive advantages.

The compatibility between starch and fibers is low. The problem can be overcome by adding the crosslinkers or compatibilizers. In order to reduce the environmental impact, only environmentally friendly crosslinkers such as CA, EPO, and ESO are reviewed comprehensively. CA is one of the most widely used crosslinkers for starch. The addition of CA can form ester bonds and hydrogen bonds with starch/fibers. This leads to the formation of crosslinked and compact structure with enhanced properties. EO are also promising crosslinkers due to their hydrophobicity and functional groups. Condensation reaction is likely to occur between starch and EO at high temperature, which would contribute to the crosslinked structure.

The low content of epoxy groups on EO can only provide low reactivity with starch. Grafting multifunctional groups onto EO is a feasible strategy because the groups can serve as the crosslinkers for starch to construct a strong crosslinking network. Carboxyl

groups of CA could act as a “bridge” between EO and starch/fibers by forming the interactions.

This novelty of the study is to demonstrate that the bioplastics prepared by combining the widely available natural resources have the potential to become alternative sources in plastic industries in Malaysia. The research also initially uses the citric acid-crosslinked epoxidized palm oil prepolymer as the modifier of the bioplastics. The starch-based bioplastics modified with fiber reinforcements and crosslinkers might possess superior mechanical, water resistance, and biodegradable properties and are expected to be alternatives to traditional plastics for various applications.

Universiti Malaysia

## CHAPTER 3: METHODOLOGY

### 3.1 Materials

Native cassava starch (moisture content 11.43%, amylose content around 21.20 %), oil palm empty fruit bunch (EFB) fibers (moisture content 9.30%), commercial refined palm oil (PO, minimum purity 99%, molecular weight 849 g/mol, 1.5 mol double bond per mol PO), and commercial soybean oil (SO, minimum purity 99%, molecular weight 872 g/mol, 4.6 mol double bond per mol SO) were provided by LGC Scientific SDN BHD located in the region of Selangor, Malaysia. The chemical composition and properties of EFB fibers are shown in Table 4.1. The molecular weight and epoxy equivalent weight of EPO were determined as 873 g/mol and 542 g/eq, respectively. Acetic acid ( $\text{CH}_3\text{COOH}$ ), acetone, anhydrous calcium chloride ( $\text{CaCl}_2$ ), anhydrous ethanol, anhydrous sodium sulfate ( $\text{Na}_2\text{SO}_4$ ), citric acid monohydrate (CA, > 99.5%), ethanol (95%), hydrochloric acid (HCl, 37%), hydrogen peroxide ( $\text{H}_2\text{O}_2$ , 30%), potassium bromide (KBr), sodium carbonate ( $\text{Na}_2\text{CO}_3$ ), sodium chloride (NaCl), sodium hydroxide (NaOH, pellet), sulfuric acid ( $\text{H}_2\text{SO}_4$ , 95-97%), and Tween 80 were obtained from Friendemann Schmidt Chemicals (Parkwood, Australia). Glycerol ( $\geq 99\%$ ) was obtained from Sigma-Aldrich and used as the plasticizer. Low-density polyethylene (LDPE) was purchased from The Polyolefin Company (Singapore). All the chemicals were analytical grade and used as received. The flow diagram of the experiments in this study is shown in Figure 3.1.

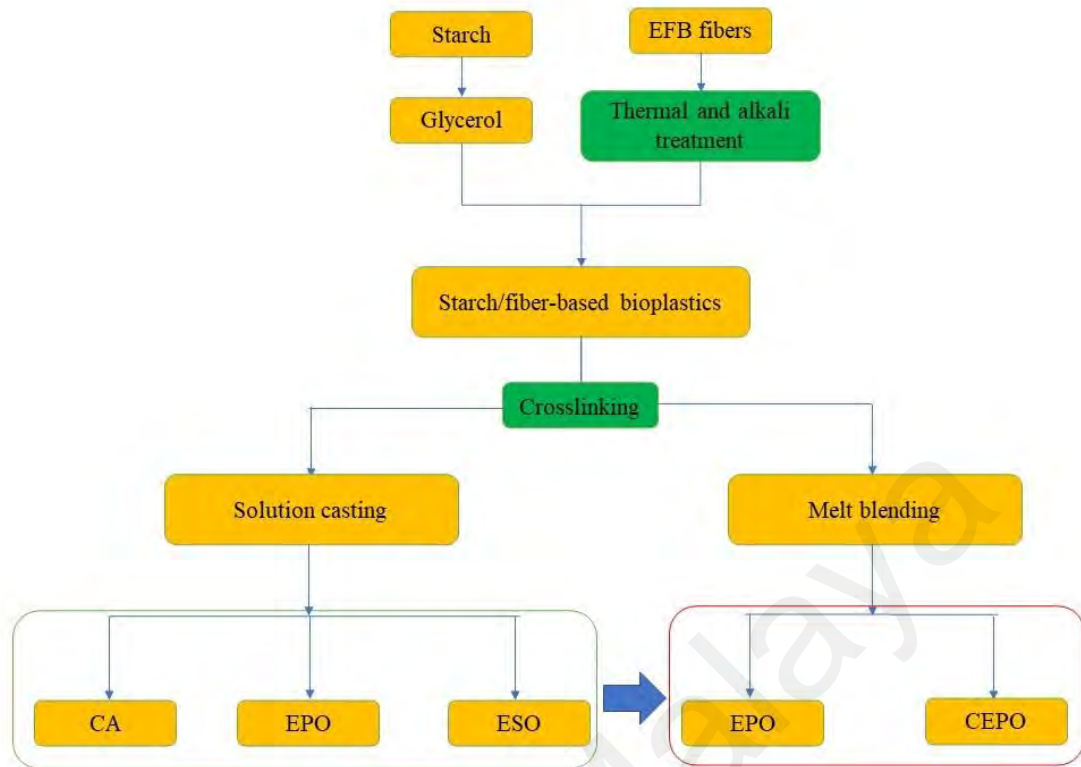


**Figure 3.1: Flow diagram of the experiments in this study**

## 3.2 Methodology

### 3.2.1 Treatment of empty fruit bunch fibers

EFB fibers were blended with different concentrations of NaOH (0-50 wt%) solution manually for 1 h at the weight ratio of 1:1. The mixtures were then dried at 60 °C for 12 h and heated at 180 °C for 30 min in the oven. Next, the samples were bleached by 5% H<sub>2</sub>O<sub>2</sub> at 60 °C for 4 h. Afterwards, the specimens were neutralized, filtered, rinsed three times with distilled water and oven-dried at 80 °C for 24 h. The solids were ground and sieved with 63 μm mesh size. The concentrations of NaOH for the fiber treatments were fixed at 0, 5, 10, 20 and 50 wt%. The resulted EFB fibers were coded as TEFB0, TEFB5, TEFB10, TEFB20, and TEFB50, respectively. For each code, the number indicated the weight proportion of NaOH to fibers (wt%).

EFB fibers were also treated by the traditionally alkali method (Campos et al., 2018). The alkali treatment of EFB fibers was performed in 2% (w/v) NaOH solution at 70 °C

under constant stirring for 60 min. The solution was bleached by 5% H<sub>2</sub>O<sub>2</sub> at 60 °C for 4 h. Then, the samples were neutralized with distilled water and filtered. The obtained fibers were heated in an oven (60 °C) until unchanging weight. The solids were ground and sieved with 63 µm mesh size and noted as TMEFB.

### **3.2.2 Epoxidation of palm oil and soybean oil**

EPO and ESO were synthesized by slightly modifying the procedures of Kim and Sharma (2012). A 500 mL four-neck reactor, equipped with a thermometer, a mechanical stirrer, an oil bath, a dropping funnel, and a cold-water condenser was used. For the epoxidation of PO, 200 g PO, 22.26 g CH<sub>3</sub>COOH and a required amount of H<sub>2</sub>SO<sub>4</sub> (2% of the H<sub>2</sub>O<sub>2</sub>-CH<sub>3</sub>COOH mixture) were blended and stirred for 30 min. For the epoxidation of SO, the mixture of 200 g SO, 50.40 g CH<sub>3</sub>COOH and H<sub>2</sub>SO<sub>4</sub> (2% of the H<sub>2</sub>O<sub>2</sub>-CH<sub>3</sub>COOH mixture) was prepared similarly. Afterwards, 84.09 g 30% H<sub>2</sub>O<sub>2</sub> (158.80 g for SO) were added at 2 mL/min, keeping the reaction at 60 °C for 8 h. Next, the solution was rinsed two times with 50 °C Na<sub>2</sub>CO<sub>3</sub> solution (5 wt%), followed by 50 °C distilled water. The oil layer was separated by decantation and dried overnight at 60 °C with Na<sub>2</sub>SO<sub>4</sub>. Na<sub>2</sub>SO<sub>4</sub> was separated by filtration with Whatman No. 4 filter paper. The oxirane oxygen contents of EPO and ESO were 2.95% and 6.23%, respectively, by following the AOCS Official Method Cd 9-57.

### **3.2.3 Modification of starch/fibers with epoxidized palm oil and citric acid-crosslinked epoxidized palm oil**

CEPO was prepared by following Gogoi, Boruah, Sharma, and Dolui (2015a) with a slight modification. The stoichiometric ratio of epoxy equivalent weight for EPO and acid equivalent weight for CA was 1:1. Firstly, a concentrated CA aqueous solution was prepared by mixing CA (0.3875 g) with distilled water by weight of 3:1, and then heated to 90 °C. After CA was dissolved completely, the mixture was blended with EPO (3 g) with continuous stirring in a 50 mL flask. The reaction was carried out at 90 °C for 30

min. The emulsion was converted into a transparent and homogeneous mixture as the reaction finished.

EPO or prepared CEPO was diluted with suitable amount of 95% ethanol, mixed with starch/fibers immediately and stirred for 1 h by hand. Then the mixture was dried at 60 °C for 24 h and 105 °C for 2 h to induce the crosslinking reaction.

### **3.2.4 Preparation of starch-based bioplastics by solution casting and compression molding**

The bioplastics were prepared by two methods in the study. Solution casting was the most common method for bioplastic preparation on a laboratory scale, while melt blending was used to produce the bioplastics concerning industrial scale-up. In the process of making the bioplastics by solution casting, it was difficult to peel the films off the glass plates in good condition even with the addition of 1% stearic acid (lubricant) due to the weak strength of the bioplastic films. Moreover, the films showed considerable measurement errors of mechanical properties. On the other hand, when we attempted to prepare the thermoplastic starch by melt blending with 1% stearic acid, the materials stuck to the screw rod of the mixer tightly and were hard to detach. Additionally, the thermocompression is the standard part of manufacturing the bioplastics in industries. Besides, high temperature is required for the crosslinking reaction between starch and CA or EO. Therefore, starch-based bioplastics were prepared using a combination of the solution casting and compression molding. The preparation method for all types of starch-based bioplastics involved gelatinization, casting and molding process as shown in Figure 3.2.

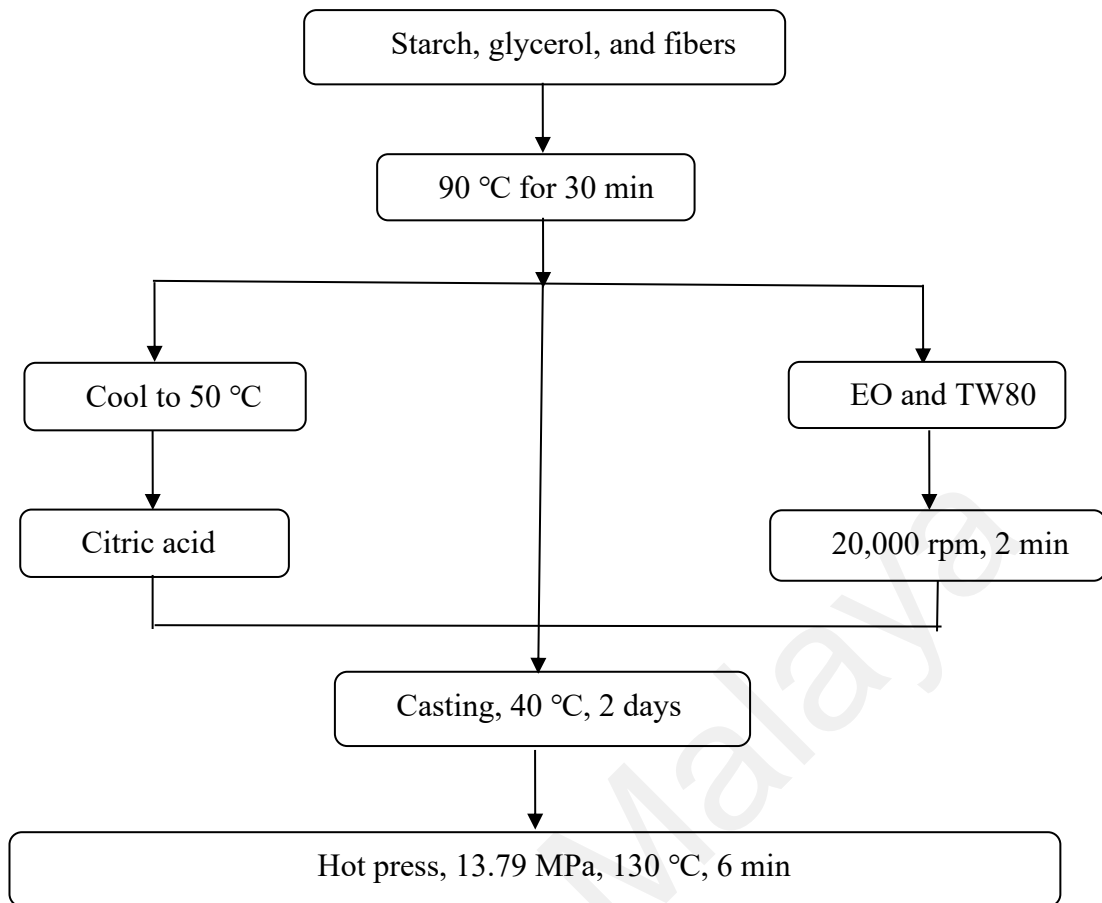


**Figure 3.2: Preparation method of starch-based bioplastics by solution casting and compression molding**

Firstly, 12.0000 g starch was suspended in 400 mL distilled water in a 1000 mL beaker. Treated EFB (TEFB) fibers and glycerol were slowly added to the starch solution. The mixtures were stirred at 40 °C for 10 min to reach homogeneous conditions and then heated at 90 °C for 30 min with continuous stirring until starch was completely gelatinized. Subsequently, the viscous solution was treated by sonification for 30 min and poured into the glass plates (diameter 15 cm). The plates were placed in the oven at 40 °C until dried (48 h).

The dry films (70.0000 g) were further processed by GT-7014-A30C Hydraulic Molding Test Press at 130 °C for 6 min with the load of 13.79 MPa. A mold of aluminum frame (200 mm × 200 mm × 1 mm) was used. Neat starch-based bioplastic (ST) and bioplastics with raw EFB fibers (ST-EFB-2.5) or TMEFB fibers (ST-TMEFB-2.5) were

fabricated using the same procedure mentioned above. The bioplastics reinforced with types of TEFB fibers were coded as ST-TEFB0-2.5, ST-TEFB5-2.5, ST-TEFB10-2.5, ST-TEFB20-2.5, and ST-TEFB50-2.5, respectively. As confirmed by the comprehensive discussion in the tensile strength section (Chapter 4), the TEFB10 fibers showed the best reinforcing effect on the properties of the bioplastics and were chosen for further optimization study for different contents of fibers. The bio-composites reinforced with different loading levels of TEFB10 fibers were coded as ST-TEFB10-2.5, ST-TEFB10-5, ST-TEFB10-10, and ST-TEFB10-20, respectively. The number at the end of each code indicated the weight percentage of fibers in the composites (wt%). The composition of each bioplastic is illustrated in Table 3.1.

**Table 3.1: Formulation of each bioplastic reinforced with fibers based on dry weight**

Bioplastic codes <sup>a</sup>	Starch (wt%)	Glycerol (wt%)	Fibers (wt%)
ST	70	30	0
ST-EFB-2.5	70	30	2.5
ST-TMEFB-2.5	70	30	2.5
ST-TEFB0-2.5	70	30	2.5
ST-TEFB5-2.5	70	30	2.5
ST-TEFB10-2.5	70	30	2.5
ST-TEFB20-2.5	70	30	2.5
ST-TEFB50-2.5	70	30	2.5
ST-TEFB10-5	70	30	5
ST-TEFB10-10	70	30	10
ST-TEFB10-20	70	30	20

<sup>a</sup>: ST represents neat starch-based bioplastic. TEFB10 indicates that the EFB fibers are treated with 10 wt% NaOH. The number at the end of each code indicates fiber weight percentage relative to the total weight of starch and glycerol in the composites.

For crosslinked bioplastics with CA, starch, glycerol and TEFB10 fibers were mixed and gelatinized following above procedures. In order to avoid the acidolysis, different amounts of CA (0.375, 0.75, 1.5, and 3 wt%) were added after the solution was cooled to 50 °C. The mixture was stirred for 30 min. The bioplastics were then prepared by casting and compression molding with above methods. These bioplastics were labeled as ST-TEFB10-5-CA0.375, ST-TEFB10-5-CA0.75, ST-TEFB10-5-CA1.5 and ST-TEFB10-5-CA3, respectively. Similarly, the number after CA indicated the loading level of CA in

the bioplastics.

Regarding EO-incorporated bioplastics, starch, TEFB10 fibers and glycerol were dispersed in the distilled water and stirred continuously at 90 °C for 30 min. Then, EO and Tween 80 (25 wt% of EO) were added. The blend was homogenized at 20,000 rpm for 2 min with a rotor-stator homogenizer. Afterwards, the emulsion solution was processed by casting and compression molding following above methods. The formulation for each bioplastic is shown in Table 3.2. All the fabricated specimens were maintained at 53% RH (relative humidity) for two days before further analysis.

Universiti Malaysia

**Table 3.2: Formulations for crosslinked starch/fiber-based bioplastics based on dry weight**

Sample names <sup>a</sup>	Starch (wt%)	Glycerol (wt%)	TEFB fibers (wt%)	CA (wt%)	EPO (wt%)	ESO (wt%)	Tween 80 (wt%)
ST-TEFB10-5	70	30	5	0	0	0	0
ST-TEFB10-5-CA0.375	70	30	5	0.375	0	0	0
ST-TEFB10-5-CA0.75	70	30	5	0.75	0	0	0
ST-TEFB10-5-CA1.5	70	30	5	1.5	0	0	0
ST-TEFB10-5-CA3	70	30	5	3	0	0	0
ST-TEFB10-5-EPO0.375	70	30	5	0	0.375	0	0.09375
ST-TEFB10-5-EPO0.75	70	30	5	0	0.75	0	0.1875
ST-TEFB10-5-EPO1.5	70	30	5	0	1.5	0	0.375
ST-TEFB10-5-EPO3	70	30	5	0	3	0	0.75
ST-TEFB10-5-ESO0.375	70	30	5	0	0	0.375	0.09375
ST-TEFB10-5-ESO0.75	70	30	5	0	0	0.75	0.1875
ST-TEFB10-5-ESO1.5	70	30	5	0	0	1.5	0.375
ST-TEFB10-5-ESO3	70	30	5	0	0	3	0.75

<sup>a</sup>: The number after each code represents its weight percentage relative to the total weight of starch and glycerol in the composites.

### 3.2.5 Preparation of starch-based bioplastics by melt blending

The components of modified starch/fibers, glycerol, stearic acid, and water were mixed for 1 h by hand, sealed and kept for 24 h at room temperature. Afterwards, the blends (35 g) were melt-blended in an internal mixer (Brabender, D-47055 Duisburg, Germany) with a capacity of 50 mL at 150 °C and 60 rpm for 10 min.

The obtained materials were ground to particles using a mill (HUEB-11K, TECO) equipped with a sieve size of 1 mm. The particles were dried at 60 °C in a drying oven for 24 h. The materials were processed by compression moulding (GT-7014-A30C Hydraulic Molding Test Press) with a stainless mold (200 mm × 200 mm × 1 mm) at a pressure of 13.79 MPa and 150 °C for 6 min. Before characterizing the bioplastics, the samples were equilibrated for two days in a chamber with 53% RH. The sample without oils was prepared as control. The formulation of each sample is described in Table 3.3.

For comparison, LDPE plastics were also prepared following above methods without adding any additives.

**Table 3.3: Formulations of all the starch-based bioplastics prepared by melt blending based on dry weight**

Samples codes <sup>a</sup>	Starch (wt%)	TEFB fibers (wt%)	EPO (wt%)	CA (wt%)	Glycerol (wt%)	Stearic acid (wt%)	Water (wt%)
ST-TEFB10	70	5	0	0	30	0.5	20
ST-TEFB10-EPO0.375	70	5	0.375	0	30	0.5	20
ST-TEFB10-EPO0.75	70	5	0.75	0	30	0.5	20
ST-TEFB10-EPO1.5	70	5	1.5	0	30	0.5	20
ST-TEFB10-EPO3	70	5	3	0	30	0.5	20
ST-TEFB10-CEPO0.375	70	5	0.375	0.0484	30	0.5	20
ST-TEFB10-CEPO.075	70	5	0.75	0.0969	30	0.5	20
ST-TEFB10-CEPO1.5	70	5	1.5	0.1938	30	0.5	20
ST-TEFB10-CEPO3	70	5	3	0.3875	30	0.5	20

<sup>a</sup>: TEFB10 indicates that the EFB fibers are treated with 10 wt% NaOH. The number at the end of each code represents weight percentage of oils relative to the total weight of starch and glycerol in the composites.

### 3.3 Characterization

#### 3.3.1 Fourier transform infrared spectroscopy (FTIR)

The FTIR spectra of the fibers, raw plant oils, EO and bioplastics were collected by Spectrum 400 FTIR/FT-FIR spectrometer with frequency ranges from 4,000 to 450  $\text{cm}^{-1}$ , an accumulation of 32 scans and a 4  $\text{cm}^{-1}$  resolution. The prepared samples except oils were cut and ground to obtain the powder. The specimens were pressed into pellets with KBr before the measurement. For comparison, the spectrum of CEPO after cured for 16 min at 150  $^{\circ}\text{C}$  in an oven was also measured.

To characterize the surface chemistry of modified starch/fibers, the modified starch/fiber particles were extracted by dissolving the powder (2.0000 g) in 95% ethanol (40 mL) for 24 h. Then, the particles were isolated by repeating the procedure for 3 times. The unreacted CA molecules were dissolved in ethanol. Then the particles were extracted with acetone (40 mL) for 24 h. The EPO or CEPO phase could dissolve in acetone, while the starch/fiber residues precipitated at the bottom. Thus, the residues were collected by repeating the procedure for 3 times. The washed starch/fibers were oven-dried (60  $^{\circ}\text{C}$ , 24 h). The unwashed starch/fibers and washed starch/fibers were all subjected to the FTIR analysis.

#### 3.3.2 X-ray diffraction (XRD) of fibers, starch, and the bio-composites

XRD patterns of fibers were recorded in a Panalytical Empyrean diffractometer in the  $2\theta$  range of 5-60 $^{\circ}$  with a scan rate of 2 $^{\circ}$ /min. The samples were exposed to Cu-K $\alpha$  radiation generated at 40 mA and 40 kV. The crystallinity index (CrI) was calculated with Equation (3.1) by Segal, Creely, Martin, and Conrad (1959):

$$\text{CrI (\%)} = \frac{I_{\text{cry}} - I_{\text{amp}}}{I_{\text{cry}}} \times 100 \quad (3.1)$$

where  $I_{cry}$  is the maximum intensity value for crystalline cellulose at  $2\theta$  angle of  $23^\circ$  and  $I_{amp}$  is the diffraction intensity for amorphous part (close to  $15^\circ$ ).

Diffraction patterns of native starch and the bio-composites were also collected.

### 3.3.3 Scanning electron microscopy (SEM)

The surface images of starch-based bioplastics and fibers were obtained using a scanning electron microscopy (SEM, Phenom Pro X). The samples were cut into small pieces and mounted vertically on the sample container. The specimens were sputter coated with gold using a sputter-coater (Polaron SC7640) and viewed at accelerating voltage of 5-15 kV.

### 3.3.4 Diffraction scanning calorimetry (DSC)

DSC thermograms of the bioplastics were measured by a DSC Q20 (TA Instrument). A bioplastic specimen of approximately 5-10 mg was cut and placed into an aluminum crucible. The reference was an empty crucible. The specimen was then scanned from  $-50$  to  $250^\circ\text{C}$  at a heating rate of  $10^\circ\text{C}/\text{min}$ . The nitrogen gas was used at a flow rate of  $10\text{ mL}/\text{min}$ . The melting temperature ( $T_m$ ) was calculated from the thermograms.

### 3.3.5 Thermogravimetric analysis (TGA)

TGA was performed to characterize the thermal stability and degradation behavior of the specimens. TGA was carried out from room temperature to  $600^\circ\text{C}$  under a nitrogen flow ( $10\text{ mL}/\text{min}$ ) with a PerkinElmer TGA 4000 at a heating rate of  $10^\circ\text{C}/\text{min}$ . The mass of the sample was approximately 5 mg. The thermogravimetric curves (TG) and derivative thermogravimetric curves (DTG) were continuously collected and represented as a function of temperature. A blank aluminum pan was used as a reference.

### 3.3.6 Mechanical properties

Mechanical properties were characterized by tensile strength and elongation at break, which indicate strength and flexibility of the bioplastics, respectively. The specimens were cut to dimensions of dumbbell shape and tested using AGS-X universal/tensile tester (Shimadzu, Japan) according to ASTM D638. The speed was fixed at 5 mm/min and the gauge length was 35 mm. At least 5 samples from separate bioplastic were tested and the average  $\pm$  standard deviation was reported.

### 3.3.7 Moisture content

The bioplastic specimens (1.0 cm  $\times$  1.5 cm) were weighed and oven-dried at 105 °C for 24 h. Moisture content of each sample was evaluated according to Equation (3.2):

$$\text{Moisture content (\%)} = \frac{(M_i - M_f)}{M_i} \times 100\% \quad (3.2)$$

where  $M_i$  and  $M_f$  are the initial weight and dry weight of the sample, respectively.

### 3.3.8 Water uptake

To determine the water uptake, the specimens were cut into dimensions of 1.0 cm  $\times$  1.5 cm and dried at 60 °C for 24 h. The dry bioplastics were conditioned in a desiccator with saturated NaCl solution at 25 °C until constant weight was achieved. The water uptake was measured with the following Equation:

$$\text{Water uptake (\%)} = \frac{W_t - W_0}{W_0} \times 100\% \quad (3.3)$$

where  $W_t$  and  $W_0$  represent the weight of the bioplastic after exposure to 75% RH and initial weight before exposure, respectively.

### 3.3.9 Water solubility

For water solubility, the dried specimens (1.0 cm × 1.5 cm) were immersed into 50 mL distilled water at 25 °C for 24 h. The solids were filtered and dried in an oven at 105 °C to reach constant weight. Water solubility was determined by the Equation (3.4):

$$\text{Solubility (\%)} = \frac{W_0 - W_1}{W_0} \times 100\% \quad (3.4)$$

where  $W_0$  is the weight of dry sample while  $W_1$  is the dry weight of sample after immersion in the water. The tests were carried out in triplicate.

### 3.3.10 Opacity

The opacity of starch-based bioplastics was analyzed according to the method reported by Li et al. (2015). For each sample, the light absorbance was observed at 600 nm using a UV-vis spectrophotometer (UV-2600, Shimadzu, Japan) against an empty cell. The opacity of each bioplastic was calculated with the following Equation:

$$\text{Opacity (mm}^{-1}\text{)} = \frac{A_{600}}{X} \quad (3.5)$$

where  $A_{600}$  shows the light absorbance at 600 nm and  $X$  represents the thickness (mm) of the bioplastics.

### 3.3.11 Water vapor permeability (WVP)

To measure the WVP of the bioplastics, the gravimetric method was employed. The cup with internal diameter of 6.60 cm was filled with 1.0000 g anhydrous  $\text{CaCl}_2$  to maintain 0% RH and then covered with the circular sample. The cup was weighed and placed in a desiccator containing saturated NaCl solution (75% RH) at 25 °C. The cup weight was measured every 24 h for 7 days. Water vapor transmission rate (WVTR) was defined as the line slope (g/h) divided by the cup mouth area ( $\text{m}^2$ ). The WVP ( $\text{g m/m}^2 \text{ h Pa}$ ) for each bioplastic was determined by the following Equations:

$$WVTR = \frac{w}{t \times A} \quad (3.6)$$

$$WVP = \frac{WVTR \times X}{P \times (R_1 - R_2)} \quad (3.7)$$

where  $w/t$  represents the weight increase per elapsed unit time,  $A$  means the exposed surface area of the composites,  $X$  means the bioplastic thickness (m),  $P$  indicates the water saturation vapor pressure (3.17 kPa at 25 °C), and  $R_1$  and  $R_2$  represent the RH in the desiccator and the cup, respectively.

### 3.3.12 Biodegradability

For soil burial test, garden pots with an approximate volume of 10 L were filled with soil taken from a culture field in University of Malaya, Malaysia. The dry bioplastic (2 cm × 2 cm) was enclosed in a nylon mesh netting (2 mm × 2 mm Mesh size), labeled, and buried in the soil at a depth of 10 cm. The pots were then placed in the laboratory at room temperature (~27 °C). The average pH value of the soil was 7.0. The soil was sprinkled with water regularly to maintain 50-60% humidity. The excess water was drained through a hole at the bottom of the pot. The test spanned for a total of 30 days. The samples were carefully collected from the soil every 15 days, placed in 50 mL water for 1 h, washed by deionized water to remove the soil, dried at 60 °C until the weight of the samples remain constant. The weight loss of the bioplastics was calculated by the Equation (3.8):

$$\text{Weight Loss (\%)} = \frac{W_i - W_f}{W_i} \times 100\% \quad (3.8)$$

where  $W_i$  indicates initial weight of the dry sample, and  $W_f$  means final weight of the dry sample.

### 3.3.13 Composition analysis of empty fruit bunch fibers

Composition analysis of raw EFB and TEFB fibers was carried out according to Zaini et al. (2017) with slight modifications. Specifically, dry EFB fibers ( $W_1$ ) were boiled in distilled water (100 mL) for 5 min on a magnetic stirrer and centrifuged after cooling. The solids were rinsed with hot water for 3 times, dried and weighted ( $W_2$ ). Then, above solids were boiled in 100 mL 2 mol/L HCl for 45 min with constant stirring. The mixtures were centrifuged and washed with 95% ethanol, anhydrous ethanol, and acetone for 2 times, respectively. The residues were dried to constant weight ( $W_3$ ) in the oven. Next, the particles were hydrolyzed with 10 mL refrigerated 75% H<sub>2</sub>SO<sub>4</sub> for 3 h at room temperature and further hydrolyzed for one night with additional 90 mL water. The solids were collected and washed with distilled water until the filtrate pH was 6.5~7.0. The samples were dried to constant weight ( $W_4$ ) in the oven. The fiber composition was calculated using the following Equations:

$$\text{Hemicellulose (\%)} = \frac{(W_2 - W_3)}{W_1} \times 100\% \quad (3.9)$$

$$\text{Cellulose (\%)} = \frac{W_3 - W_4}{W_1} \times 100\% \quad (3.10)$$

$$\text{Lignin (\%)} = \frac{W_4}{W_1} \times 100\% \quad (3.11)$$

where  $W_1$  is the initial weight of dry EFB fibers,  $W_2$  is the fiber weight after the removal of soluble matters in hot water,  $W_3$  is the residual weight of fibers after treated with HCl, and  $W_4$  is the final weight of fibers after hydrolyzed with H<sub>2</sub>SO<sub>4</sub>.

### 3.3.14 Statistical analysis

The results were subjected to an analysis of variance (ANOVA) and a Tukey test of multiple comparisons using SPSS 19.0 software (SPSS Inc., Chicago, USA). Differences were considered to be significant at  $p < 0.05$ .

## CHAPTER 4: RESULTS AND DISCUSSION

### 4.1 PART 1: Preparation and characterization of starch-based bioplastics reinforced with treated empty fruit bunch fibers

Firstly, this part investigated the thermal and alkali treatment of EFB fibers. Then, different types of treated EFB (TEFB) fibers were incorporated into starch-based bioplastics to evaluate their reinforcing performance. Subsequently, different concentrations of TEFB10 fibers were incorporated to investigate the most suitable loading level of TEFB10 fibers in the bioplastics. The physicochemical and structural properties of the resulted fibers and bioplastics were characterized and discussed.

#### 4.1.1 Characterization of treated empty fruit bunch fibers

##### 4.1.1.1 Composition analysis and macroscopic observation of the fibers

The composition and properties of EFB fibers before and after the treatments are shown in Table 4.1. Raw EFB fibers were comprised of higher content of hemicellulose (43.11%) than either cellulose (24.95%) or lignin (15.09%), which was different from the results of previous researchers who generally reported higher content of cellulose (Chiesa & Gnansounou, 2014). As the concentrations of NaOH increased, pH of the resulted fibers (before bleached) varied remarkably from 3.73 to 12.83 ( $p < 0.05$ ). Acid treatment aims at extracting hemicellulose while alkaline treatment ensures extraction of lignin and hemicellulose (Bhalla et al., 2018; Kovačević, Bischof, Vujasinović, & Fan, 2016). Therefore, these treatments are expected to change the composition of EFB fibers. With the loadings of NaOH increasing, the relative content of cellulose in the residues increased up to 54.51%, while the contents of hemicellulose and lignin decreased gradually to 20.72% and 9.58%, respectively. There were still 10-15% hot water-soluble matters in the residues.

As for the yields of TEFB fibers, two main weight loss conditions were observed. Firstly, the thermal treatment without the addition of NaOH caused significant weight loss of 43.51% ( $p < 0.05$ ). This was mainly related to the decomposition or removal of water-soluble matters, spherical particles, hemicellulose (62.09%) and lignin (32.58%), while the decomposition of cellulose was minor (5.40%). This was also confirmed by the FTIR and SEM below. The weight loss of fibers went up slightly ( $p > 0.05$ ) and only 4.05% fibers were decomposed when NaOH contents increased from 0 to 10 wt%. Then, remarkable weight loss occurred again when the concentration of NaOH surpassed 10 wt% ( $p < 0.05$ ). In this stage, the loss of fibers was primarily associated to cellulose, hemicellulose, and lignin. The decomposition percentages of cellulose, hemicellulose, and lignin in TEFB50 fibers were 40.97%, 87.01% and 82.85%, respectively.

For comparison, EFB fibers were also treated by the conventional method. The yield for TMEFB fibers was 34.38%, which was close to that of TEFB20 fibers. Cellulose dominated in TMEFB fibers (52.35%), while there were 30.57% of hemicellulose and 16.88% of lignin left. This confirmed that the traditional alkali treatment needed to be repeated for several times in order to obtain cellulose with higher purity. The hot water-soluble matter was only 0.2%.

**Table 4.1: Composition and properties of empty fruit bunch fibers before and after thermal and chemical treatments based on dry weight**

Samples	pH (before bleached)	Residues (%)	Cellulose (%)	Hemicellulose (%)	Lignin (%)	Water uptake (%)
EFB	3.96±0.03 <sup>a</sup>	100 <sup>a</sup>	24.95±1.22 <sup>c</sup>	43.11±1.63 <sup>a</sup>	15.09±0.56 <sup>cd</sup>	8.35±0.73 <sup>ab</sup>
TEFB0	3.73±0.02 <sup>b</sup>	56.49±2.22 <sup>b</sup>	41.78±2.18 <sup>b</sup>	28.93±0.46 <sup>bc</sup>	18.01±0.87 <sup>ab</sup>	7.03±0.31 <sup>abc</sup>
TEFB5	5.06±0.05 <sup>c</sup>	53.65±0.88 <sup>b</sup>	42.22±1.74 <sup>b</sup>	26.26±1.49 <sup>cd</sup>	18.47±0.67 <sup>a</sup>	6.42±0.60 <sup>c</sup>
TEFB10	10.04±0.04 <sup>d</sup>	52.44±1.29 <sup>b</sup>	44.70±1.30 <sup>b</sup>	24.55±0.73 <sup>de</sup>	15.45±0.74 <sup>bd</sup>	7.88±0.54 <sup>abc</sup>
TEFB20	10.24±0.04 <sup>e</sup>	39.82±0.74 <sup>c</sup>	45.54±2.72 <sup>b</sup>	25.74±0.52 <sup>cd</sup>	13.95±0.62 <sup>d</sup>	7.87±0.65 <sup>abc</sup>
TEFB50	12.83±0.03 <sup>f</sup>	27.02±1.86 <sup>e</sup>	54.51±1.69 <sup>a</sup>	20.72±0.90 <sup>e</sup>	9.58±0.38 <sup>e</sup>	8.19±0.17 <sup>b</sup>
TMEFB	-	34.38±0.56 <sup>d</sup>	52.35±0.77 <sup>a</sup>	30.57±2.00 <sup>b</sup>	16.88±1.40 <sup>abc</sup>	7.88±0.32 <sup>abc</sup>

Values were given as means ± standard deviations. <sup>a-f</sup>; mean values with diverse letters in the same column are significantly different ( $p < 0.05$ ).

The bleaching process aimed to obtain white TEFB fibers. Visually, the raw EFB fibers showed a yellow color (Figure 4.1a). The TEFB fibers whitened as the levels of NaOH changed from 0 to 5 wt% (Figure 4.1b-c). When higher NaOH contents were added, the pH of TEFB fibers before bleaching was around 10-12 where H<sub>2</sub>O<sub>2</sub> can maximize the bleaching effect (Abdullah et al., 2016; Rosa et al., 2009). However, TEFB fibers presented a yellow color again (Figure 4.1d-f). This revealed that appropriate NaOH level can promote the bleaching process. In addition, thermal degradation of lignin and hemicellulose at high alkali contents (10-50 wt%) produced more oxidation products such as quinones and chromophores on the fiber surface and resulted in dark or brown colors (C. Lee et al., 2018; T. Liu et al., 2014). Therefore, further bleaching process was required for these TEFB fibers. The obtained fibers using common alkali method showed a white color also (Figure 4.1g).

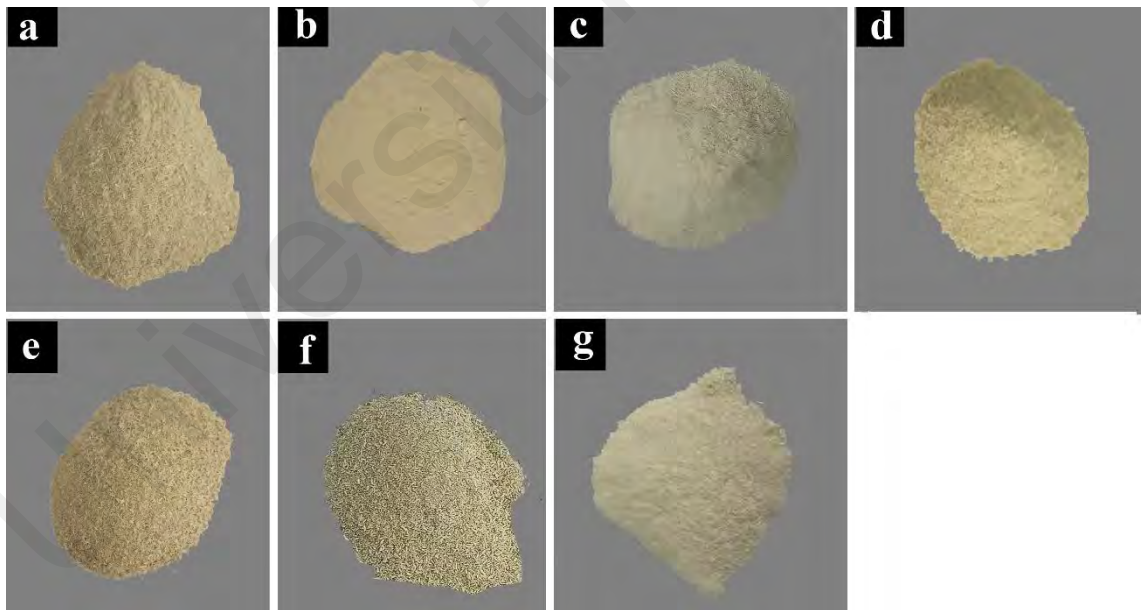


**Figure 4.1: Digital images for fibers. (a) raw EFB, (b) TEFB0, (c) TEFB5, (d) TEFB10, (e) TEFB20, (f) TEFB50, and (g) TMEFB fibers**

#### 4.1.1.2 Fourier transform infrared spectroscopy (FTIR)

The FTIR spectral bands representing the functional groups of cellulose, hemicellulose and lignin are shown in Figure 4.2. From the spectrum of raw EFB fibers, the bands in the  $3322\text{ cm}^{-1}$  and  $2923\text{ cm}^{-1}$  regions are attributed to O-H stretching vibration of cellulose and C-H stretching vibration of aliphatic moieties in cellulose and hemicellulose, respectively (Abral et al., 2018; Teaca et al., 2013). The bands for C-H were shifted to lower wavenumbers for the treated fibers. The bands at  $1705\text{-}1722\text{ cm}^{-1}$  are associated to C=O stretching of fatty acids, lignin, or hemicellulose present in the fibers. The bands in the  $1593\text{-}1607\text{ cm}^{-1}$  and  $1502\text{-}1505\text{ cm}^{-1}$  regions are assigned to aromatic skeletal vibrations in lignin. The bands at  $1423\text{ cm}^{-1}$ ,  $1370\text{ cm}^{-1}$  and  $1327\text{ cm}^{-1}$  are associated with stretching vibration of  $\text{-CH}_2$ , C-H and C-O of hemicellulose, respectively. The bands at  $1236\text{-}1241\text{ cm}^{-1}$  correspond to C-O-C of aryl-alkyl ether in lignin. The strong and broad absorbance bands at  $1023\text{-}1034\text{ cm}^{-1}$  are assigned as stretching vibration of C-O-C from hemicellulose and cellulose (Abral et al., 2018; Teaca et al., 2013). It was noted that the bands at  $1705\text{-}1722\text{ cm}^{-1}$ ,  $1593\text{-}1607\text{ cm}^{-1}$ ,  $1502\text{-}1505\text{ cm}^{-1}$  and  $1236\text{-}1241\text{ cm}^{-1}$  regions all diminished gradually as the alkaline contents increased. These changes indicated the increasing removal of fatty acid, hemicellulose, or lignin during the treatments. However, for the spectrum of TMEFB fibers, the bands at  $1593$  and  $1502\text{ cm}^{-1}$  remained, which indicated the presence of amounts of lignin in the fibers. This outcome was consistent with the composition analysis.

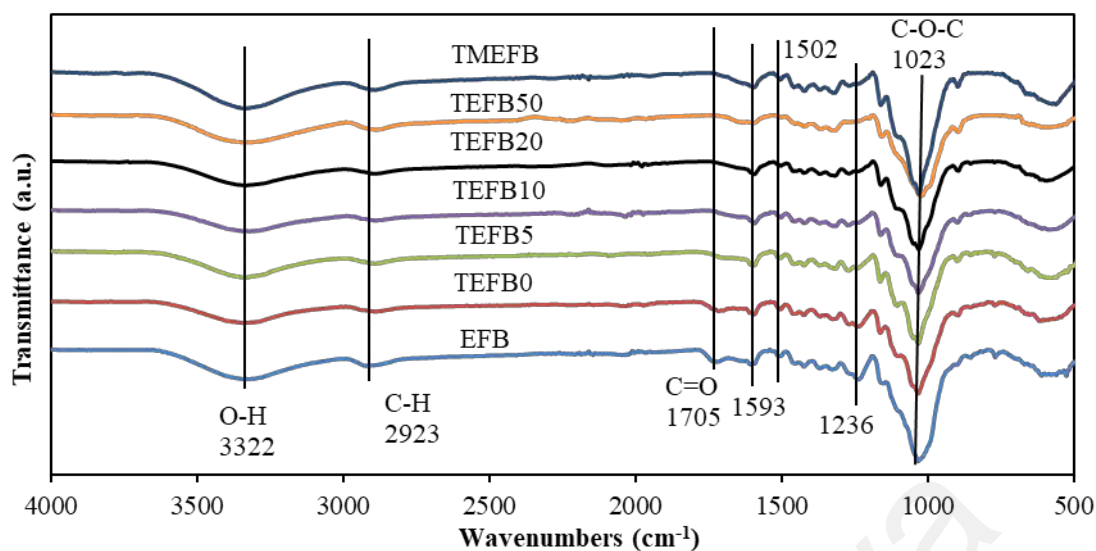


**Figure 4.2: FTIR spectra of raw and treated empty fruit bunch fibers including TEFB0, TEFB5, TEFB10, TEFB20, TEFB50, and TMEFB fibers. The solid lines indicate the bands at respective wavenumbers**

#### 4.1.1.3 Scanning electron microscopy (SEM)

Figure 4.3a-j depicts the surface morphology of EFB fibers before and after the treatments. The surface of untreated EFB fibers was attached with many small holes and spherical particles called “tyloses” (Figure 4.3a-b). In addition, a great number of waxes, fatty substances and silica deposition were expected to be present on the surface of EFB fibers and might act as a hindrance to the treatment (Norul Izani, Paridah, Anwar, Mohd Nor, & H’ng, 2013; Yunus et al., 2010). Significant surface changes of treated fibers were observed. The surface impurities such as tyloses, silica, oils and waxes were removed, which led to smoother and cleaner surfaces such as TEFB10 fibers (Figure 4.3e-f). The elimination of external materials can improve the surface area and make more fibrils exposed, especially in TEFB50 fibers (Figure 4.3g-h), which demonstrated the delignification process. These effects can promote better fiber-starch adhesion and provide higher strength to the bioplastics. However, the surface of TEFB50 fibers was seriously disrupted and changed rougher. It was reported that thermal treatment with elevated alkaline contents caused remarkable deterioration of the fiber stiffness (Norul

Izani et al., 2013). This was further verified by the mechanical properties of the bioplastics reinforced with TEFB fibers. The surface of TMEFB fibers also became cleaner but a little rougher after the alkali treatment, whose morphology might be between TEFB10 and TEFB50 fibers.

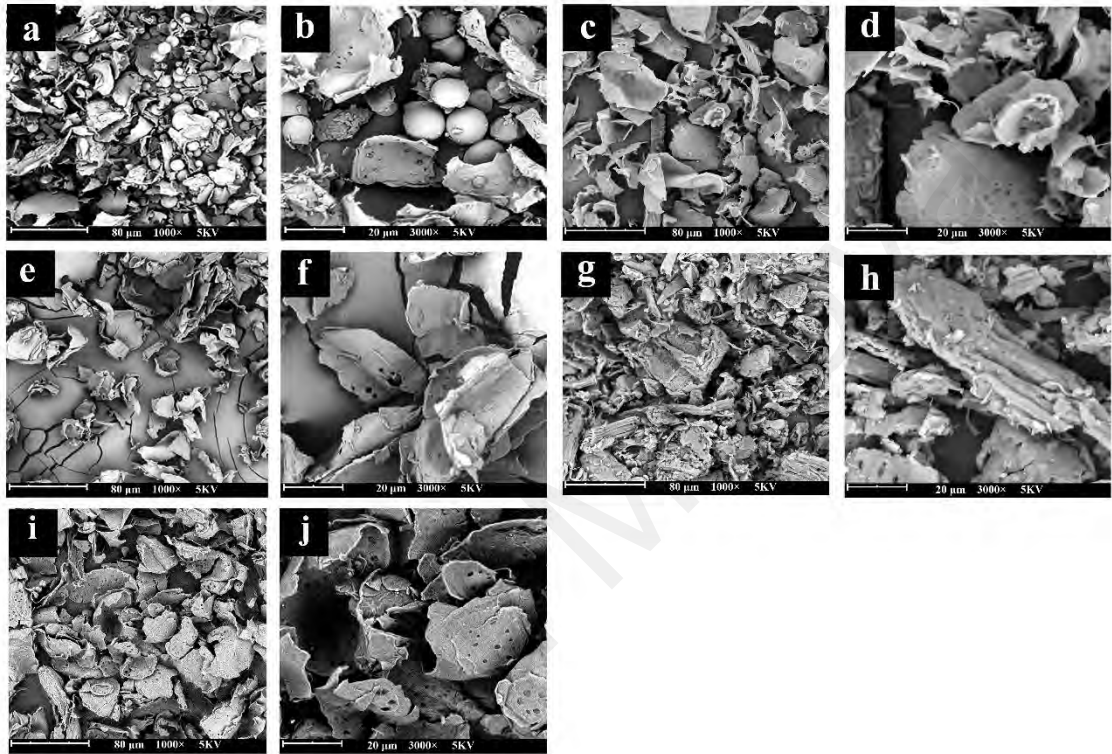


**Figure 4.3: SEM images of raw EFB (a and b), TEFB0 (c and d), TEFB10 (e and f) and TEFB50 (g and h), and TMEFB (i and j) fibers**

#### 4.1.1.4 X-ray diffraction (XRD)

The changes for XRD patterns of EFB fibers before and after the treatments are presented in Figure 4.4. The raw EFB fibers displayed the typical diffraction peak of cellulose I structure at  $2\theta = 23.0^\circ$ , attributed to diffraction from plane (200) (French, 2013). The diffraction peak at  $15.2^\circ$  derived from amorphous materials according to Goh, Ching, Chuah, Abdullah, and Liou (2015), Nurul Suraya Rosli, Shuhaida Harun, Jamaliah Md Jahim, and Othaman, (2017), and Sukiran et al. (2020). The peak intensity showed a diverse change depending on the contents of alkali for fiber treatment. The raw EFB

fibers showed the crystallinity index (CrI) of 28.68%, which was lower than the studies of Nurul Suraya Rosli et al. (2017) (40%) and Sohni et al. (2018) (41%) (Table 4.2). CrI of fibers was decreased to 16.73% for TEFB0. Goh et al. (2015) found that CrI of EFB fibers remained similar or lower after the ammonium persulfate or acid treatment. Li et al. (2017) also discovered that there was a slight decrease of the CrI of the raw materials due to torrefaction. However, CrI was increased to 78.12% for TEFB10 fibers. The rising CrI of TEFB fibers can be attributed to the removal of the amorphous materials such as lignin and hemicellulose via the treatments (Maniglia & Tapia-Blacido, 2019). Meanwhile, other chains of para-crystalline and amorphous cellulose may have realigned and were transformed to cellulose I during the treatments (Baharuddin et al., 2013). CrI might determine the reinforcing effect of fibers in the composites. This result was consistent with the respective tensile strength of the reinforced bioplastics as shown below.

Interestingly, the peak around  $15^\circ$  emerged as the extremely intense peak in TEFB50 fibers. The CrI of TEFB50 fibers cannot be calculated by the equation of Segal et al. (1959) because the result was lower than 0. Li et al. (2017) reported that the CrI of the fibers was decreased to 0 because the crystalline peaks disappeared completely after severe torrefaction. Alkaline treatment could consume the crystalline cellulose while increasing the amount of amorphous cellulose (Goh et al., 2015). Therefore, some crystalline cellulose might be transformed into amorphous materials in TEFB50 fibers. It was inferred that reduction in CrI of TEFB50 fibers might present better susceptibility for enzymatic digestibility or other potential applications (Hassan et al., 2013).

Two other diffraction peaks at  $2\theta = 17.2^\circ$  and  $17.9^\circ$  were also observed for raw EFB fibers in the present study. Both peaks might be assigned to the amorphous materials because their peak intensity all reduced gradually as the loadings of NaOH increased. In addition, TEFB50 fibers exhibited the typical diffraction patterns of cellulose II at  $2\theta = 20.2^\circ$ . Cellulose I can be converted to cellulose II by regeneration of dissolved cellulose

or strong alkaline treatment during kraft pulping (Haafiz et al., 2016; John & Anandjiwala, 2008b).

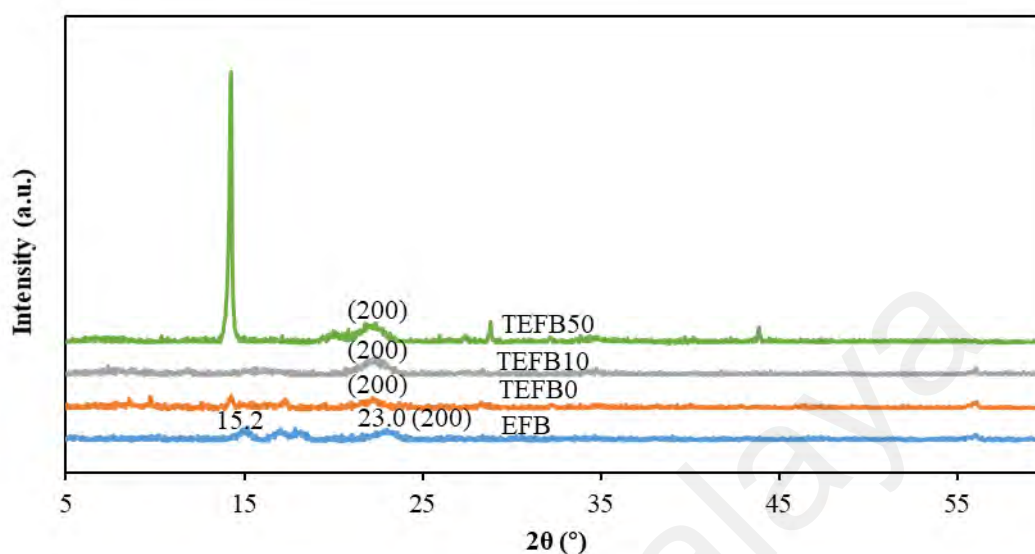


Figure 4.4: X-ray diffraction patterns of the raw EFB and TEFB fibers

Table 4.2: Crystallinity index and temperature at maximum decomposition rate ( $T_{max}$ ) of raw and treated fibers

Samples	Crystallinity index (%)	$T_{max}$ (°C)
EFB	28.68	361.89
TEFB0	16.73	341.16
TEFB5	-	355.34
TEFB10	78.12	341.84
TEFB20	-	336.93
TEFB50	-	351.75

#### 4.1.1.5 Thermogravimetric analysis (TGA)

Thermal stability of the fibers was explored by TGA where the weight loss and temperature at maximum decomposition rate ( $T_{max}$ ) were monitored as a function of temperature (Figure 4.5). All samples exhibited three-stage degradation curves. In the first stage from 50 to 110 °C, the weight loss is primarily attributed to water evaporation in the fibers. The second stage in the range of 240-410 °C corresponds to the degradation of hemicellulose, lignin, and cellulose, leaving a 20-35% content (Rosa et al., 2009). TEFB fibers suffered a decrease of the initial degradation temperature and a faster

decomposition process compared to EFB fibers. In addition, the DTG plots revealed that raw EFB fibers showed  $T_{max}$  at 361.89 °C (Table 4.2). Treatment of fibers shifted  $T_{max}$  to lower temperatures between 336.93 and 355.34 °C, indicative of decreasing thermal stability due to the treatments. These changes can be interpreted by the elimination of silica on the fiber surface which maintained higher thermal stability than fibers (Campos et al., 2018). TEFB5 fibers revealed higher  $T_{max}$  than the fibers treated by 10-50 wt% alkali. This might suggest that the thermal treatment with high contents of alkali might disrupt the thermal stability of fibers due to the decomposition of fibers, as shown by composition analysis and SEM. Interestingly, TEFB50 fibers presented higher  $T_{max}$  than TEFB20 fibers. This might be due to that 50 wt% alkali caused the significant decomposition of materials with low thermal stability, leading to the fibers with thermal resistance. At last, in the range of 410-600 °C the carbonaceous residues degraded. The residues were observed in the range of 4-9% at 600 °C for all the fibers.

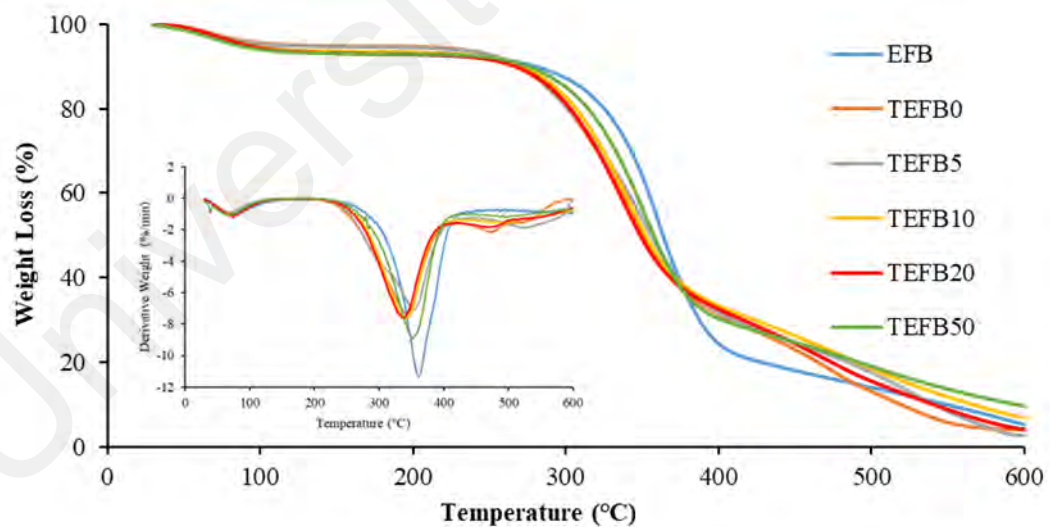


**Figure 4.5: Thermogravimetric (TG) and derivative thermogravimetric (DTG) curves for raw EFB and TEFB fibers**

## 4.1.2 Preparation and characterization of starch-based bioplastics reinforced with treated empty fruit bunch fibers

### 4.1.2.1 Fourier transform infrared spectroscopy (FTIR)

The FTIR spectra of starch-based bioplastics reinforced with raw fibers and types of treated fibers are shown in Figure 4.6. Owing to the low content of fibers (2.5 wt%) in the bio-composites, the FTIR spectra of all the bioplastics showed similar characteristics. The bands in the 3287-3293  $\text{cm}^{-1}$  regions are attributed to O-H stretching vibration (Sahari, Sapuan, Zainudin, & Maleque, 2013). The bands in the 2922-2930  $\text{cm}^{-1}$  regions are assigned to C-H stretching vibration. The bands at 1646-1649  $\text{cm}^{-1}$  are associated with the tightly bound water in the starch. The bands in the 1408-1413  $\text{cm}^{-1}$  and 1364-1368  $\text{cm}^{-1}$  regions are assigned to C-H bending and C-H deformation, respectively (Abral et al., 2019). The broad and strong absorbance bands at 993-996  $\text{cm}^{-1}$  are characteristic of the anhydro-glucose ring O-C stretching (Sahari et al., 2013).

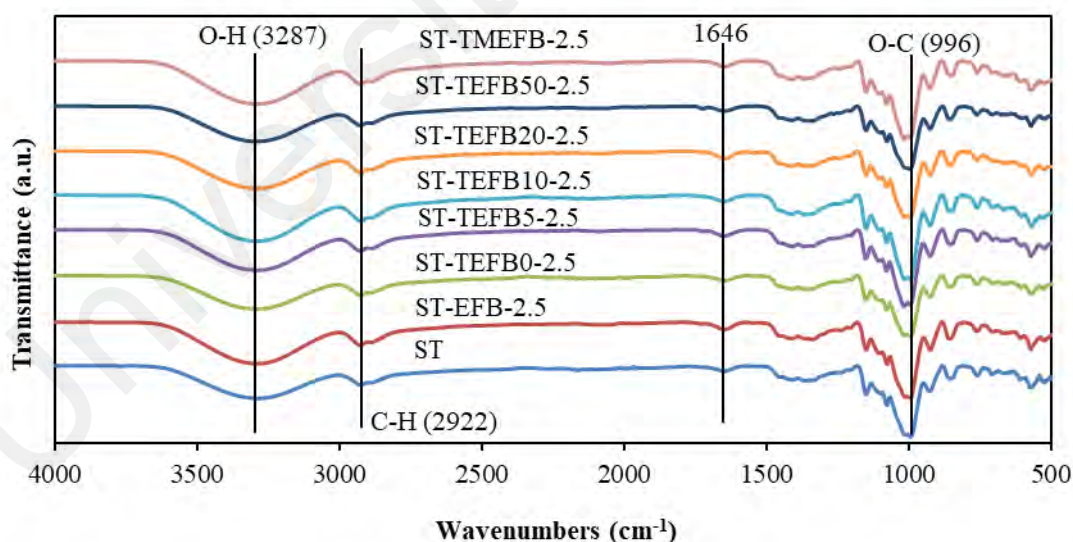


**Figure 4.6: Fourier transform infrared spectra of starch-based bioplastics incorporated with different types of fibers. The solid lines indicate the bands at respective wavenumbers**

As confirmed by the comprehensive discussion in the tensile strength section (Chapter 4), the TEFB10 fibers showed the best reinforcing effect on the properties of the

bioplastics and were chosen for further optimization study for different contents of fibers. The FTIR spectra of the bioplastics can monitor the molecular interaction by observing the band shifts of functional groups (El Miri et al., 2015; Ma et al., 2017). The typical O-H bands shifted to higher wavenumbers after the addition of different types of fibers, which can be ascribed to the reduction of hydrogen bonds within starch molecules and the formation of hydrogen bonds between starch/glycerol and fibers. Therefore, the addition of fibers might hamper the plasticization of starch. These trends have been observed previously in cellulose nanocrystal-filled starch-based bio-composites and nanocellulose-filled starch-based bioplastics (Balakrishnan et al., 2019; El Miri et al., 2015).

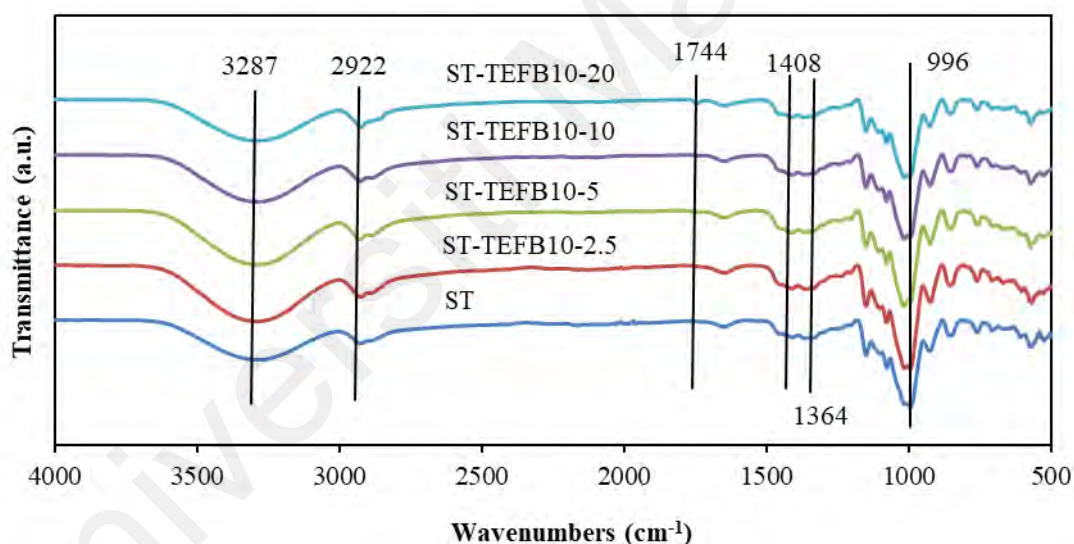


**Figure 4.7: Fourier transform infrared spectra of starch-based bioplastics reinforced with different concentrations of TEFB10 fibers. The solid lines indicate the bands at respective wavenumbers**

Similarly, the typical O-H bands of the spectra were all situated at higher wavenumbers after the addition of different concentrations of TEFB10 fibers (Figure 4.7). Another main spectrum difference for the bioplastics reinforced with different contents of TEFB10 fibers was related to the appearance of characteristic bands in the 1718-1744  $\text{cm}^{-1}$  regions, which are associated with C=O stretching (Abdullah et al., 2016; Essabir, Bensalah,

Rodrigue, Bouhfid, & Qaiss Ael, 2016). The band intensity became stronger as the fiber contents increased. Similar results were also observed by S. Lee et al. (2018). Starch might be responsible for the new bands because of the possible production of carboxylic acid, aldehydes or ketones compounds by thermal decomposition of starch (Miyata et al., 2018). The well-known mechanism of starch decomposition catalyzed by temperature ( $> 100\text{ }^{\circ}\text{C}$ ) is called ‘caramelization’, which might occur during the molding process (Lomeli-Ramirez et al., 2014). These results can be further confirmed by the lower thermal stability of the composites as the contents of fibers increased, as revealed by the TGA analysis. The decomposition product of starch might also result in the ester groups with residual lignin or hemicellulose of fibers during the compression molding. It was reported that the incorporation of EFB fibers with PLA led to the appearance of new ester groups due to chemical reaction (Moshiul Alam et al., 2012).

#### **4.1.2.2 Scanning electron microscopy (SEM)**

In order to assess the dispersion of fibers in the starch-based bioplastics, surface micrographs of the bioplastics were investigated by the SEM (Figure 4.8a-f). It was observed that the surface of unloaded ST bioplastics was homogeneous and continuous without any starch granule and void, which revealed a good gelatinization of starch. The individual fiber can be easily distinguished on the surface of the composites reinforced with fibers. Importantly, many white domains, which were supposed to be starch granules, were clearly observed in the bioplastics with fibers. The interactions between fibers and plasticizers would reduce the hydrogen bonding interactions between starch and plasticizers, thus hindering the plasticization of starch and resulting in starch granules in the network (El Miri et al., 2015). Only a few voids were formed in the contact surface between starch and some large fibers. These indicated a good adhesion between the matrix and fibers, which could be ascribed to the similarity of chemical structure between cellulose and starch and the formation of hydrogen bond interactions between the two

components (Gironès et al., 2012). Comparatively, ST-TEFB10 bioplastics showed the most compact and smoothest surface among all the bioplastics with fibers. The adhesion between fibers and starch was related to their effectiveness in enhancing the properties of the bioplastics (Cieśla & Sartowska, 2016).

Universiti Malaya

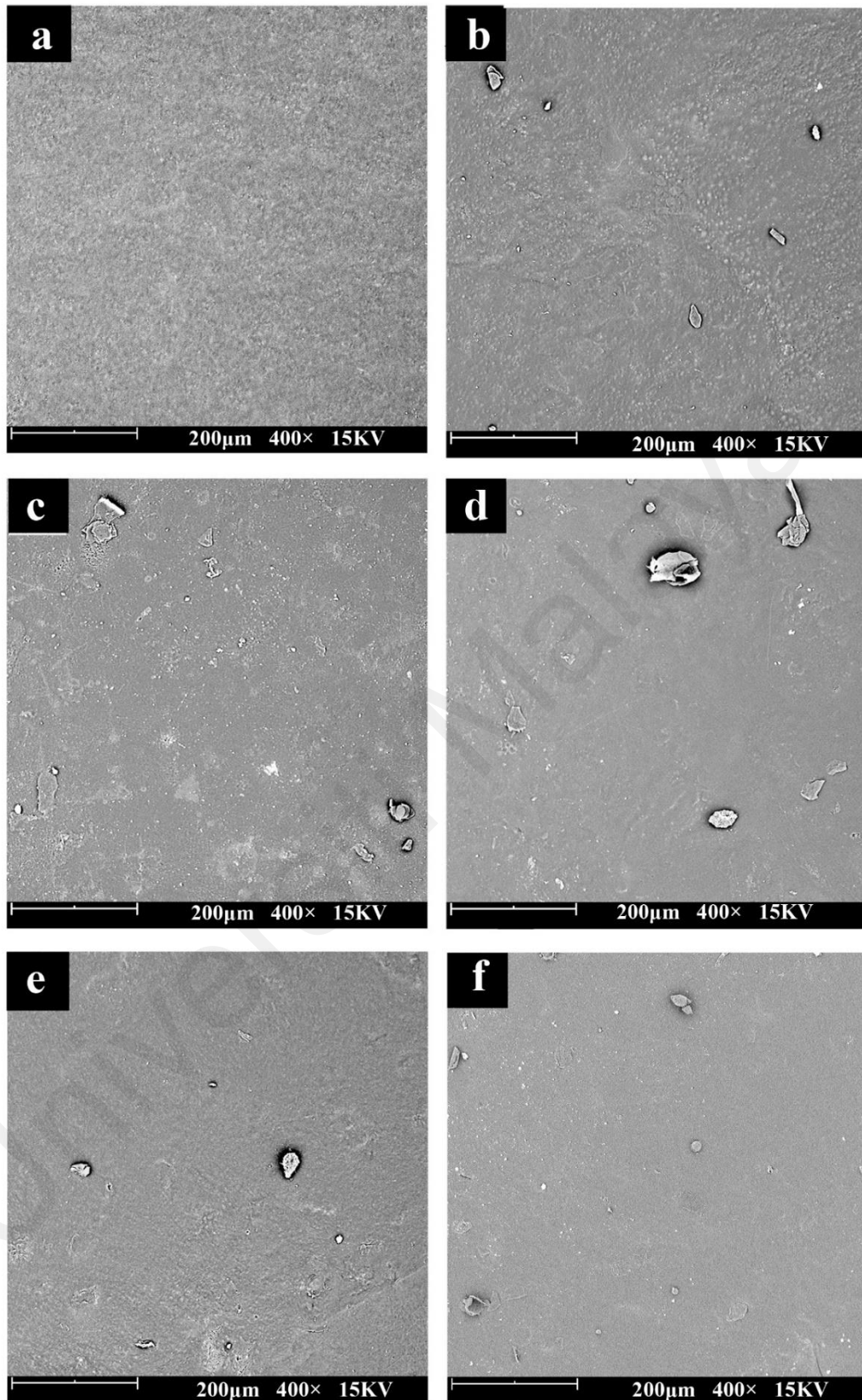


**Figure 4.8: Scanning electron microscopy images of starch-based bioplastics. (a) ST, (b) ST-EFB-2.5, (c) ST-TEFB0-2.5, (d) ST-TEFB10-2.5, (e) ST-TEFB50-2.5, and (f) ST-TMEFB-2.5**

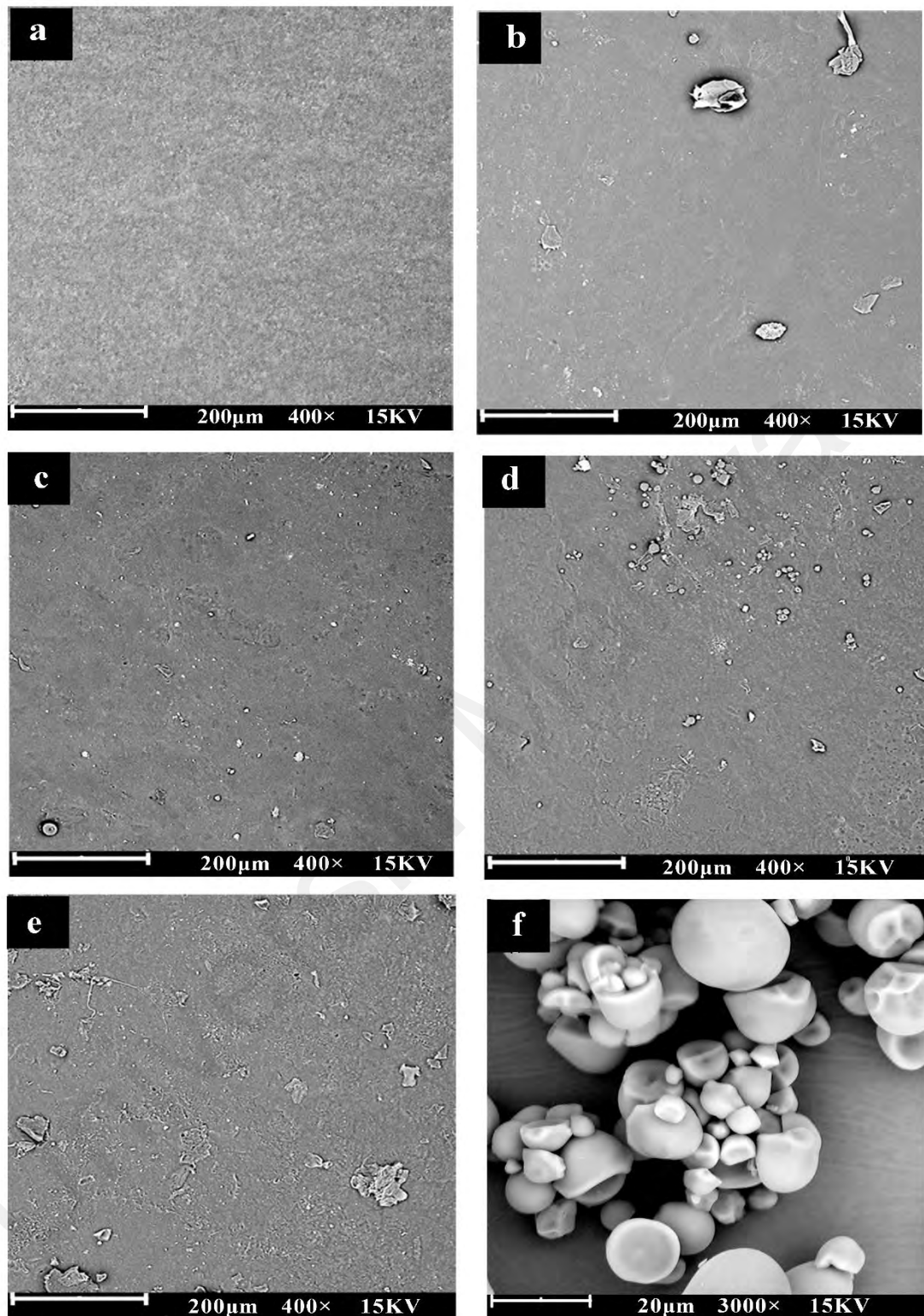


**Figure 4.9: Scanning electron microscopy images of starch-based bioplastics and native starch. (a) ST, (b) ST-TEFB10-2.5, (c) ST-TEFB10-5, (d) ST-TEFB10-10, (e) ST-TEFB10-20, and (f) starch granules**

The surface images of the bio-composites with different contents of TEFB10 fibers are shown in Figure 4.9. More white domains were found as higher contents of TEFB10

fibers were incorporated, which also demonstrated that the addition of TEFB10 fibers hampered the plasticization of starch. It could be seen that no fiber aggregate was formed in the composites with fiber contents of 2.5-5 wt%, which indicated the uniform dispersion of fibers. However, on the surfaces of the composites with 10 wt% TEFB fibers, many circular aggregates appeared, which might be the retrograded starch granules compared to the native starch. Many retrograded starch granules were also observed by Soni, Asoh, Hsu, Shimamura, and Uyama (2020) on the cross-section of cellulose nanofiber reinforced starch films and Agustin et al. (2014) who worked with the bioplastics based on starch and cellulose nanocrystals from rice straw. The craters on the fiber surfaces, created by the silica removal, can act as the reinforcing agents to induce the starch chains to organize into crystalline regions (Campos et al., 2018). In addition, the crystallization process would be enhanced in the temperature range between the glass transition temperature and melting temperature ( $T_m$ ) because nucleation and propagation involved the mobility of polymer chains (Shi & Gao, 2016; Xie, Hu, Jin, Xu, & Chen, 2014). The viscosity of starch was reduced by the thermal compression, allowing the starch chains to flow, align, and recrystallize after cooling (Gilfillan, Nguyen, Sopade, & Doherty, 2012). Most of all, the content of TEFB fibers (10 wt%) was critical to form the retrograded starch granules. For example, no such aggregate was found on the surfaces of the composites with other contents of fibers. It was reported that 10 wt% chitin can act as the nucleating agent to induce the development of poly(vinyl alcohol) crystals, while 20 wt% chitin retarded the formation of crystals (Mok et al., 2020). However, fiber aggregates appeared on the surfaces of the composites with 20 wt% fibers.

#### 4.1.2.3 Diffraction scanning calorimetry (DSC)

Figure 4.10 shows the DSC curves of starch-based bioplastics reinforced with types of fibers. The DSC technique was not sensible enough to measure  $T_g$  of the bioplastics. All curves except ST-TEFB5-2.5 had the small and broad endothermic peaks, which are

assigned to the melting peaks of the bioplastics. However, there were two peaks found on the curve of ST-TEFB5-2.5, which might be related with the water evaporation (as noted by the circle) and melting peaks, respectively (Muscat et al., 2012). As shown in Table 4.3, onset melting temperature ( $T_{onset}$ ) and  $T_m$  of neat starch-based bioplastics were 143.6 and 155.1 °C, respectively. They were all increased significantly to 154.3-204.4 and 181.8-215.1 °C after the addition of raw and treated fibers except TEFB0 fibers because the reinforcements hindered the mobility of starch molecular chains. Regarding ST-TEFB5-2.5, the separation of the water evaporation peak from the melting peak might lead to the highest  $T_{onset}$  (204.4 °C) and  $T_m$  (207.3 °C) among all the bioplastics reinforced with TEFB fibers because water can produce the plasticization effect. The bioplastic with TEFB0 fibers revealed the lowest  $T_m$  compared to the samples with the other types of fibers. Besides, this sample also showed the highest elongation at break. These outcomes might indicate the plasticization effect of TEFB0 fibers. Comparatively, the composites with TEFB fibers exhibited lower  $T_m$  than the composites with raw EFB fibers (215.1 °C). Thus, it can be seen that the TEFB fibers had better compatibility with starch than EFB fibers in the bioplastics due to the removal of impurities. The bioplastics with lower  $T_m$  can melt more easily and have better plasticization properties during the preparation process. The addition of TEFB fibers treated by different contents of alkali contributed to diverse melting behaviors of the starch matrix.

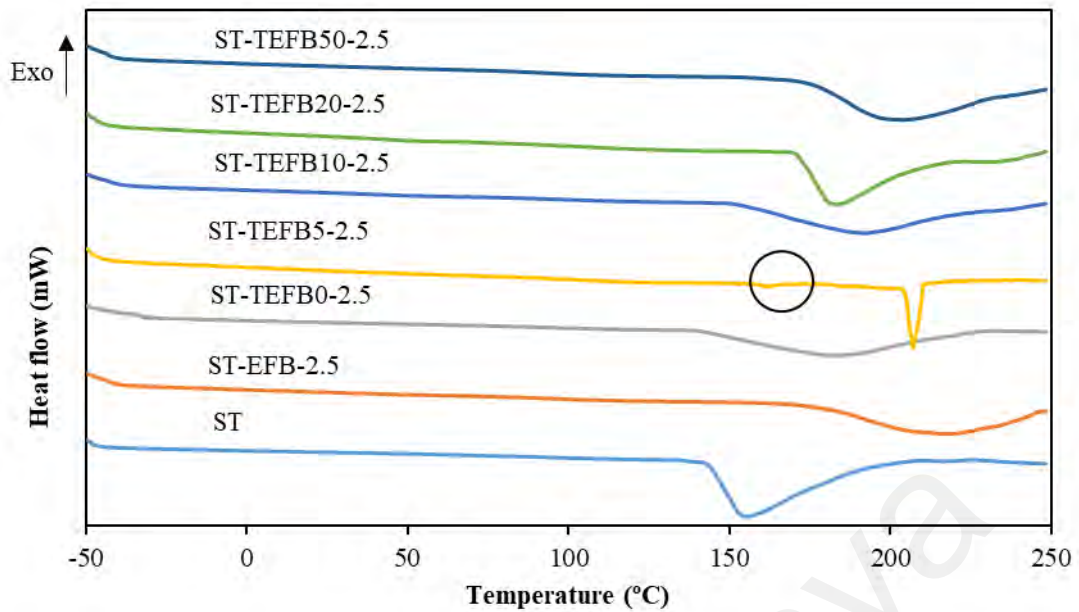


**Figure 4.10: DSC thermograms of starch-based bioplastics reinforced with different types of treated fibers. The circle indicates the water evaporation peak**

**Table 4.3: The melting temperature obtained from diffraction scanning calorimetry and thermal decomposition parameters from thermogravimetric analysis of the bioplastics incorporated with types of fibers**

Sample codes	$T_{onset}$ (°C) <sup>a</sup>	$T_m$ (°C) <sup>b</sup>	$T_{5\%WL}$ (°C) <sup>c</sup>	$T_{max1}$ (°C) <sup>d</sup>	$T_{max2}$ (°C) <sup>d</sup>
ST	143.6	155.1	143.4	-	308.2
ST-EFB-2.5	179.5	215.1	227.5	303.5	365.0
ST-TEFB0-2.5	140.6	181.8	177.5	320.0	378.7
ST-TEFB5-2.5	204.4	207.3	193.0	318.0	379.7
ST-TEFB10-2.5	154.3	192.2	226.3	325.2	371.1
ST-TEFB20-2.5	171.3	183.5	168.1	289.6	364.7
ST-TEFB50-2.5	176.4	200.9	159.4	303.3	367.6

<sup>a</sup>: Onset melting temperature. <sup>b</sup>: Melting temperature. <sup>c</sup>: Temperature at 5% weight loss. <sup>d</sup>: Temperature at maximum decomposition rate.  $T_{onset}$  and  $T_m$  were determined by DSC.  $T_{5\%WL}$  and  $T_{max}$  were from TGA.

DSC thermograms of the bioplastics reinforced with different contents of TEFB10 fibers are displayed in Figure 4.11 and the melting temperature of the composites is summarized in Table 4.4. The DSC thermogram of the bioplastics incorporated with 2.5 wt% TEFB10 fibers exhibited wider peak, decreased peak intensity and higher  $T_{onset}$  and  $T_m$  in comparison with the control sample. This result can be expected because the addition of fibers would promote the crystallization of the composites and hamper the

molecular mobility. As a result,  $T_{onset}$  and  $T_m$  of the bioplastics increased (Ma et al., 2017). However, after the addition of 5 wt% TEFB10 fibers, the melting peak became sharper and shifted to lower temperature. The thermal behavior of the bioplastics was due to the plasticization of 5 wt% TEFB10 fibers, as confirmed by increased elongation at break (Liu et al., 2013). Then, the shape of the peaks remained constant, and  $T_{onset}$  and  $T_m$  increased to higher temperatures when the contents of TEFB10 fibers increased from 5 to 20 wt%. 10-20 wt% TEFB10 fibers may only act as the reinforcing agents in the composites as shown by the significant increase of tensile strength, which formed intense interactions with starch and prevented the molecular mobility of the polymer chains, thus improving the  $T_{onset}$  and  $T_m$ . However, the composites with 10 wt% TEFB10 fibers showed higher  $T_m$  than those with 20 wt% TEFB10 fibers. This was consistent with the presence of huge amounts of retrograded starch for the composites with 10 wt% due to crystallization, as verified by the SEM analysis. The higher degree of crystallization usually results in higher  $T_m$  (Javidi, Hosseini, & Rezaei, 2016). These results demonstrated that TEFB10 fibers would affect the molecular mobility of starch matrix significantly, depending on their contents.

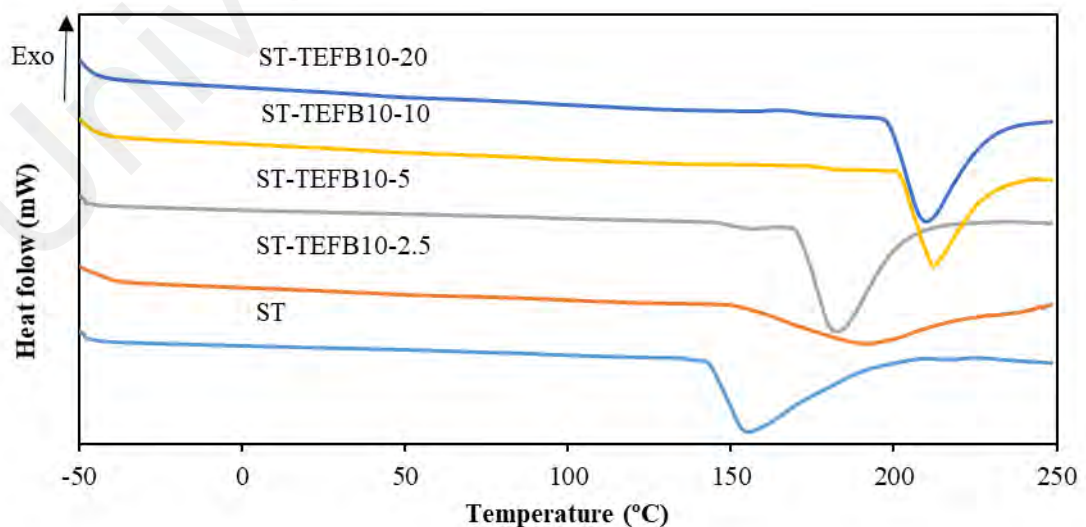


**Figure 4.11: Diffraction scanning calorimetry thermograms of starch-based bioplastics reinforced with different contents of TEFB10 fibers**

**Table 4.4: The melting temperature and thermal decomposition parameters of the bio-composites reinforced with various contents of TEFB10 fibers**

Formulations	$T_{onset}$ (°C) <sup>a</sup>	$T_m$ (°C) <sup>b</sup>	$T_{5\%WL}$ (°C) <sup>c</sup>	$T_{max1}$ (°C) <sup>d</sup>	$T_{max2}$ (°C) <sup>d</sup>
ST	143.6	155.1	143.4	-	308.2
ST-TEFB10-2.5	154.3	192.2	226.3	325.2	371.1
ST-TEFB10-5	171.0	182.3	189.4	276.0	346.6
ST-TEFB10-10	202.1	212.2	171.6	268.1	340.8
ST-TEFB10-20	198.8	210.0	-	-	-

<sup>a</sup>: Onset melting temperature. <sup>b</sup>: Melting temperature. <sup>c</sup>: Temperature at 5% weight loss. <sup>d</sup>: Temperature at maximum decomposition rate.  $T_{onset}$  and  $T_m$  were determined by DSC.  $T_{5\%WL}$  and  $T_{max}$  were from TGA.

#### 4.1.2.4 Thermogravimetric analysis (TGA)

The TG and DTG curves for neat ST and ST filled with types of fibers are shown in Figure 4.12. The results evidenced that the reinforcing fibers had a notable effect on the thermal decomposition of the bioplastics. The weight loss of the bioplastics primarily occurred in three steps. In the initial step, a weight loss of 10-20% was found from 30 to 300 °C, which is related to the loss of water and glycerol (Campos et al., 2018). The addition of all fibers, especially TEFB10 fibers, caused lower weight loss compared to the bioplastics without fibers in this stage. However, the bioplastics with TEFB20 or TEFB50 fibers started to decompose quickly after 280 °C. In the second stage of 300-440 °C, main decomposition of all the bioplastics took place, corresponding to the thermal decomposition of glycerol, starch, and fibers. After surpassing 360 °C, pure ST exhibited lower weight loss than the bioplastics reinforced with fibers, indicating that fibers reduced the ability of the bioplastics to resist high temperature (>360 °C). Finally, in the range of 440-600 °C, the degradation is mainly associated with carbonaceous residues (Edhirej et al., 2017).

$T_{5\%WL}$  for ST was measured at 143.4 °C. The introduction of fibers significantly improved  $T_{5\%WL}$  of the composites (Table 4.3). The composites with raw fibers and TEFB10 fibers showed the maximum values around the 226.3-227.5 °C. However, the composites reinforced with TEFB20 and TEFB50 fibers displayed remarkable reduction

of  $T_{5\%WL}$  compared to the other composites with fibers. By observing the weight loss in the whole heating process, TEFB10 fibers presented higher thermal stability to the bioplastics compared to other types of fibers.

DTG curves described that there was only one  $T_{max}$  for neat ST, while two  $T_{max}$ s were found for the bioplastics with the addition of fibers. It was found that  $T_{max2}$  of ST occurred at 308.2 °C, while  $T_{max2}$  of the bioplastics incorporated with fibers took place from 364.7 to 379.7 °C. This revealed that the thermal stability of the bioplastics was increased by the introduction of fibers, which can be ascribed to the inherent higher thermal stability of fibers than starch and good interactions between fibers and starch. It was noted that the bioplastic with raw fibers showed relatively lower  $T_{max1}$  and  $T_{max2}$  compared to the samples with treated fibers, although raw fibers had higher thermal stability than the treated fibers. This might demonstrate that raw EFB fiber showed lower compatibility in the bioplastic than treated fibers. The fibers treated by low alkali contents presented higher  $T_{max1}$  and  $T_{max2}$  to the bio-composites compared with fibers treated by high alkali contents, which was in accordance with the thermal stability of types of treated fibers. Specifically, the bioplastic with TEFB5 showed the highest  $T_{max2}$ , which was consistent with the highest  $T_{max}$  of TEFB5 fibers among all the treated fibers.

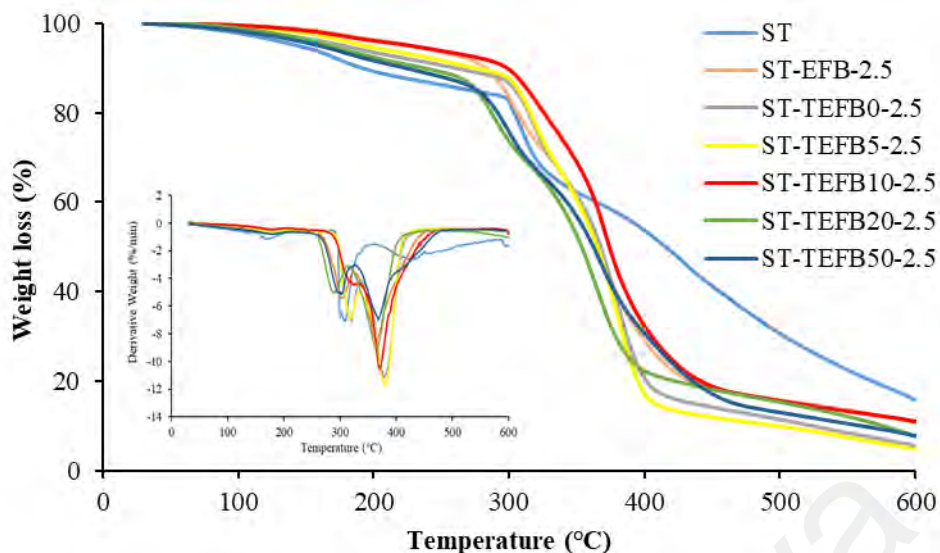


**Figure 4.12: Thermogravimetric and derivative thermogravimetric curves of starch-based bioplastics reinforced with types of fibers**

TG and DTG curves for the composites reinforced with various contents of TEFB10 fibers are shown in Figure 4.13. The plots evidenced that the contents of TEFB10 fibers showed a significant effect on the thermal decomposition of the bioplastics. The addition of fibers significantly improved the  $T_{5\%WL}$  from 143.4 °C of ST to 171.6-226.3 °C (Table 4.4).  $T_{5\%WL}$  presented lower values with the loadings of fibers increasing. After surpassing 360 °C, pure ST exhibited higher weight residue than the bioplastics with fibers, indicating that the addition of fibers reduced the thermal stability of the bioplastics to resist high temperature.

DTG curves described that  $T_{max1}$  reduced gradually as the increase of TEFB10 fiber contents.  $T_{max2}$  of the bioplastics incorporated with 2.5 wt% fibers was raised to 371.1 °C from 308.2 °C of ST. The composites with higher loadings of fibers revealed lower  $T_{max2}$ . Therefore, the loading levels of fibers showed negative effect on the thermal stability of the composites, which could be attributed to the poor dispersion of higher contents of fibers in the starch matrix, as confirmed by the SEM.

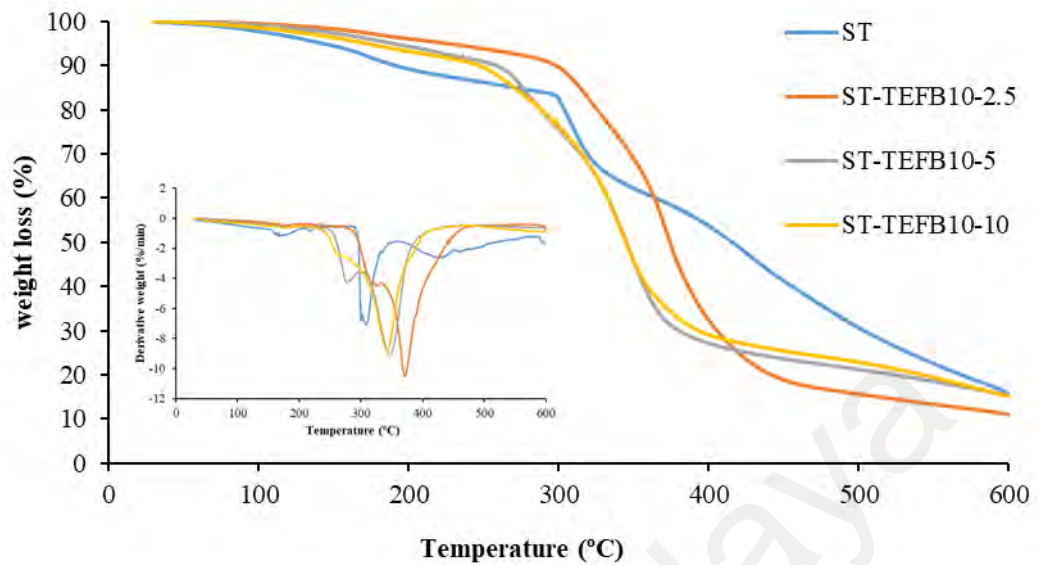


**Figure 4.13: Thermogravimetric and derivative thermogravimetric curves of starch-based bioplastics reinforced with various loadings of TEFB10 fibers**

#### 4.1.2.5 Mechanical properties

Tensile strength and elongation at break are extensively applied to reflect the tensile properties of the bioplastics (Shahbazi, Majzoobi, & Farahnaky, 2018; Teaca et al., 2013). Figure 4.14 clearly demonstrates the different reinforcing effects of raw and treated fibers on the mechanical properties of starch-based bioplastics. ST exhibited the low tensile strength of 0.45 MPa and elongation at break of 30.70%. When raw EFB fibers were blended with starch, the tensile strength was increased to 0.58 MPa ( $p > 0.05$ ), while the elongation at break was decreased significantly to 19.87% ( $p < 0.05$ ). This variation was assigned to high tensile strength and low elongation at break of EFB fibers. These data agreed with those observed by Sahari et al. (2013) and Agustin et al. (2014).

The bioplastics reinforced with TEFB0 fibers showed a similar tensile strength ( $p > 0.05$ ) but significantly higher elongation at break ( $p < 0.05$ ) when compared to the composites with raw EFB fibers. Then, the addition of fibers treated with 5-10 wt% NaOH improved the tensile strength statistically ( $p < 0.05$ ). The tensile strength for ST-TEFB10

bioplastics showed the maximum of 0.82 MPa which was increased by 82.22% in comparison with ST, while the elongation at break was decreased from 30.70% to 19.77%. This phenomenon was expected because tensile strength and elongation at break of the bioplastics usually changed oppositely after the incorporation of fibers according to previous studies (El Miri et al., 2015). The decreasing reinforcing ability of TEFB20 and TEFB50 fibers might be attributed to the serious disruption of fibers as confirmed by the SEM. Comparatively, the reinforcing effect of TMEFB fibers was close to TEFB50 fibers. In conclusion, the NaOH levels in the thermal treatment were much of importance to obtain starch-based bioplastics with high strength (Ma et al., 2017; Teaca et al., 2013). The results confirmed the hemicellulose and lignin-containing cellulose fibers can act as excellent reinforcements of starch-based bioplastics. It could be inferred that the treatments disrupted the recalcitrant interactions among cellulose, lignin, and hemicellulose and removed part of the amorphous materials which might hamper the reinforcing effect. Eventually, a good compatibility between treated fibers and starch was attained.

For starch-based bioplastics, TEFB10 fibers revealed the remarkable reinforcing effect, which was comparable to cellulose nanocrystals, nanoclay, and nanocellulose at the same loading level (Cheng et al., 2018; El Halal et al., 2015). If EFB fibers were utilized to extract cellulose nanocrystals, their yield based on previous results was supposed to be around 10 wt% of initial fibers (El Miri et al., 2015). In contrast, the yield of TEFB10 fibers would be nearly 5 times of cellulose nanocrystals. In addition, conventional alkaline treatment of fibers may approximately involve 0.5-2.5 g NaOH/g fibers (T. Liu et al., 2014; Liu, Mohanty, Askeland, Drzal, & Misra, 2004; Vandebossche et al., 2014), while the simple and environmentally benign treatment of TEFB10 fibers only used 0.1 g NaOH/g fibers. Therefore, this improvement required less use of chemicals and corrosion-resistant equipment and showed promising applications in the large-scale

operations (Baharuddin et al., 2013).

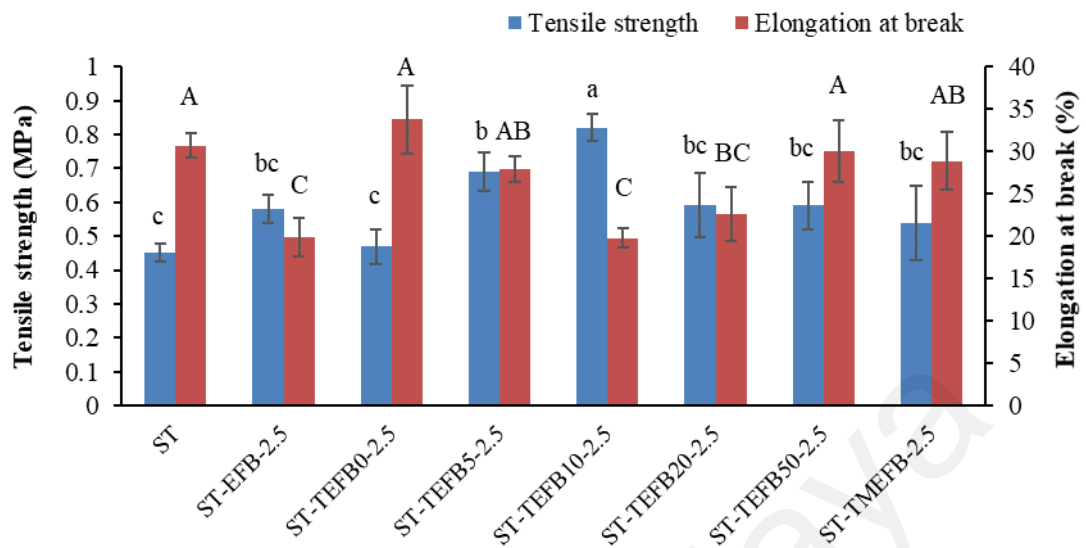


**Figure 4.14: Tensile strength and elongation at break of starch-based bioplastics reinforced with different types of treated empty fruit bunch fibers. a-c, A-C: Different letters with the uniform indicator show significant differences among the samples ( $p < 0.05$ )**

The tensile properties of the prepared bioplastics with various concentrations of TEFB10 fibers are presented in Figure 4.15. The TEFB10 fibers exhibited an obvious reinforcing effect on the mechanical properties of the composites. In general, the tensile strength increased significantly from 0.45 MPa to 1.99 MPa with TEFB10 fiber contents increasing from 0 to 20 wt% ( $p < 0.05$ ), while the elongation at break decreased except for the composites with 5 wt% fibers. The mechanical properties of the composites reinforced with fibers depend on factors such as fiber dispersion and interfacial adhesion in the matrix (Essabir et al., 2016). The treatment of EFB fibers made more hydroxyl groups exposed on the surface and enhanced the interactions with starch by hydrogen bonds. Additionally, uniform dispersion of TEFB10 fibers in the blends, which was verified by the SEM analysis, also accounted for better reinforcement.

Interestingly, 5 wt% TEFB10 fibers enhanced the tensile strength and elongation at break of the composites simultaneously. As for cellulose in TEFB10 fibers, it is well

acknowledged that cellulose improves the mechanical properties by the strong interfacial interactions with starch through hydrogen bonds (Popescu, Dogaru, & Popescu, 2017; Teaca et al., 2013). Lignin is characterized by diversity of chemical composition or molecular weight depending on the botanical origins and extraction conditions (Yang et al., 2019). Lignin would migrate to the fiber surface due to the thermal treatment. It was reported that lignin can act as a plasticizer or reinforcing agent of starch or a compatibilizer for cellulose and starch depending on its content and composition (Naseem et al., 2016; Tarasov et al., 2018). The presence of lignin might explain the unique impact of 5 wt% TEFB10 fibers on the mechanical properties of the composites. The resulted bio-composites with 5 wt% fibers presented superior tensile strength and elongation at break at the same time and were easy to cut for further characterization. Also, the thermal stability of the composites decreased significantly as the contents of TEFB10 fibers increased, as shown by the TGA result. Besides, TEFB10 fibers at contents above 10 wt% were likely to hamper the plasticization of starch seriously or form aggregates in the composites. The addition of 5-20 wt% TEFB10 fibers showed no obvious effect on the water resistance properties of the composites as shown below. Therefore, the composites containing 5 wt% TEFB10 fibers were chosen to perform the crosslinked composites with CA or EO further.

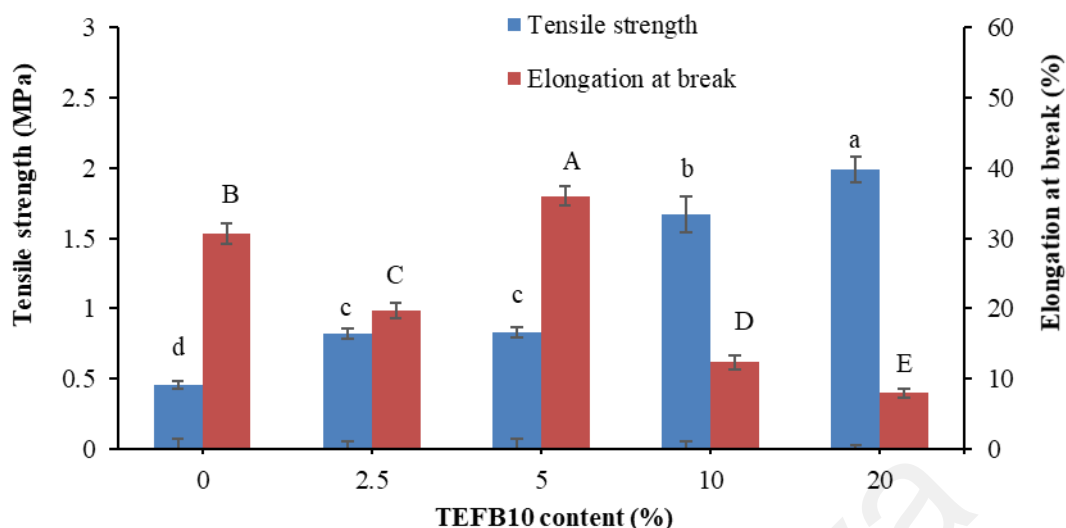


**Figure 4.15: Tensile strength and elongation at break of different concentrations of TEFB10 fiber reinforced bioplastics. a-d, A-E: Different letters within the same symbol show significant differences among the samples ( $p < 0.05$ )**

#### 4.1.2.6 Water uptake and solubility

Water uptake and solubility are very crucial for the application of the bioplastics at a high humidity (Popescu et al., 2017; Shahbazi et al., 2018). Sorption behavior imposes a significant effect on shelf life and mechanical properties of the thermoplastic starch products (Chaudhary et al., 2009). On account of the presence of hydroxyl and other polar groups, raw EFB fibers exhibited the moisture absorption at 8.35% as revealed in Table 4.1. Water uptake of treated EFB fibers all decreased slightly compared to that of EFB fibers. Hemicellulose pyrolysis and removal of water soluble matters lowered the hygroscopicity of TEFB fibers (C. Lee et al., 2018). Water uptake and solubility of the resulted bioplastics with fibers are presented in Figure 4.16. The addition of fibers showed no evident effect on the water uptake of the bioplastics which varied from 23.89% to 24.16% ( $p > 0.05$ ). These results were approximate to the values demonstrated by other studies (Abraal et al., 2019; Ghanbari et al., 2018). This might be explained by the low loading levels and the hydrophilic nature of TEFB fibers. The hydrogen bond interactions between fibers and starch cannot hinder the water molecules diffusing into the starch

matrix (Abral et al., 2019; Ghanbari et al., 2018).

ST exhibited high water solubility with a value of 34.27% because of its hydrophilic property, which was close to the values of starch-based films reported by other researchers (Hu et al., 2009). Bioplastics reinforced by raw EFB, TEFB0, TEFB5, and TMEFB fibers presented no obvious difference of water solubility ( $p > 0.05$ ), while the fibers treated by 10-50 wt% NaOH reduced the water solubility significantly ( $p < 0.05$ ). The thermal treatment with suitable alkaline concentrations could expose more hydroxyl groups on the fiber surface to form strong hydrogen bonds with the hydroxyl groups of starch, thus restricting the dissolution of the bioplastics in water (Popescu et al., 2017).

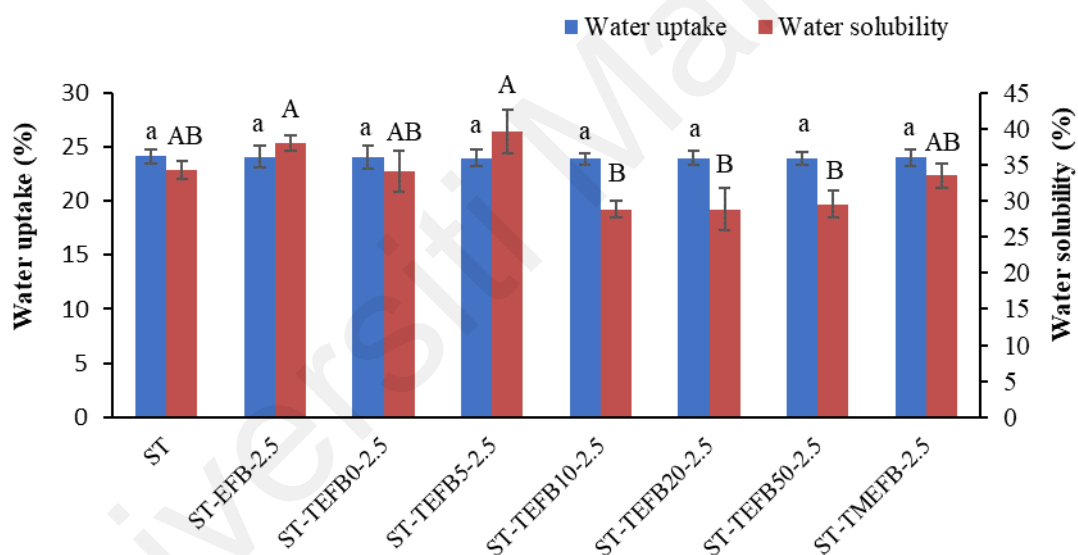


**Figure 4.16: Water uptake and solubility of starch-based bioplastics reinforced with different types of treated empty fruit bunch fibers. a, A-B: Various letters within the same indicator show remarkable differences among the samples ( $p < 0.05$ )**

As shown in Figure 4.17, reductions of water uptake from 24.16% to 19.95% and water solubility from 34.27% to 26.52% were observed with TEFB10 fiber amount up to 20%. This is expected because fibers are less hygroscopic than starch due to a higher degree of crystallinity (Rico et al., 2016). Moreover, hydrogen bond interactions between TEFB10 fibers and starch triggered the formation of a dense network structure, thereby preventing

water penetrating into the samples (Agustin et al., 2014; Ghanbari et al., 2018).

Starch and fibers are hydrophilic as a result of their numerous hydroxyl groups (Rico et al., 2016; Svagan, Hedenqvist, & Berglund, 2009). The reinforcing effects of TEFB fibers were weakened gradually at high water contents and storage time, because water would replace the interactions between starch and TEFB fibers by forming the interactions with them separately (Teaca et al., 2013). The addition of glycerol further deteriorated the properties because glycerol is a highly water-retaining material (Hu et al., 2009). Therefore, interfacial interaction among these molecules would be easily destroyed by water. Further improvement should be emphasized on the water resistance of the composites.

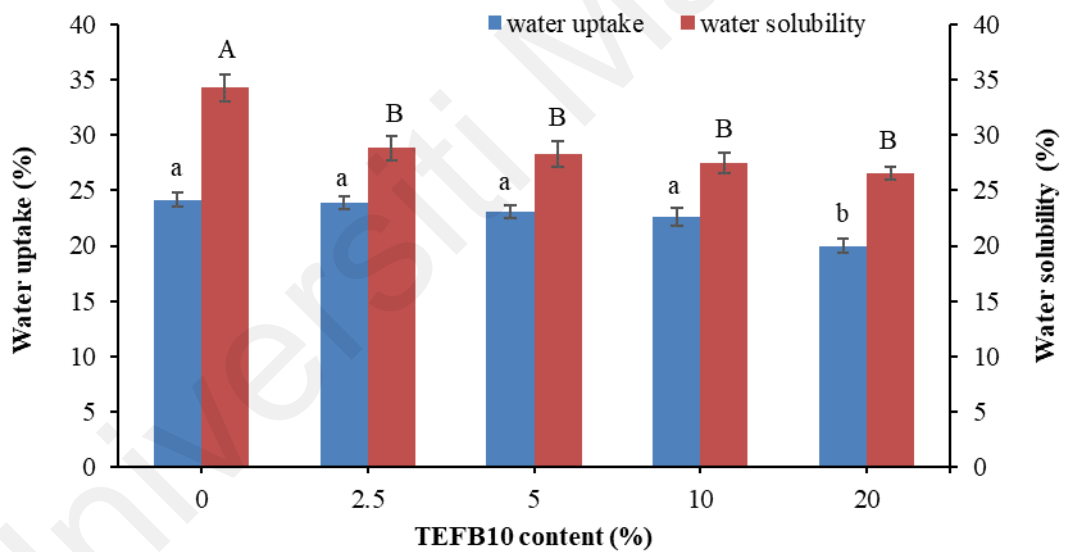


**Figure 4.17: Water uptake and solubility of starch-based bioplastics reinforced with different contents of TEFB10 fibers. a-b, A-B: Different letters with the identical indicator show significant differences among the samples ( $p < 0.05$ )**

#### 4.1.2.7 Opacity

Transparent bioplastics are characterized with low values of opacity. The opacity of starch-based bioplastics incorporated with fibers depends on the assembling pattern of starch and fibers in the bio-composites (El Miri et al., 2015; Li et al., 2015). The opacity

of the bioplastics was investigated with an UV-vis spectroscopy at a chosen wavelength of 600 nm. As shown in Figure 4.18, the opacity of ST was significantly improved from 0.073 to 0.11 by its blending with EFB fibers ( $p < 0.05$ ), in accordance with the outcomes of Gonzalez-Gutierrez, Partal, Garcia-Morales, and Gallegos (2010) for the starch-based films. This result was expected because the average size of EFB fibers was about 63  $\mu\text{m}$  and their presence would reflect and absorb the light, thus increasing the opacity of the bioplastics (Abral et al., 2019). All alkaline treated fibers except TEFB20 fibers decreased the opacity of the bioplastics significantly ( $p < 0.05$ ) which was comparable to the opacity of ST. The bioplastics with TEFB50 fibers showed the best transparency. In general, these results suggested that the treatment of EFB fibers led to a good compatibility with starch, thus reducing TEFB fiber aggregation and contributing to the penetration of visible light through the bioplastics (El Miri et al., 2015).

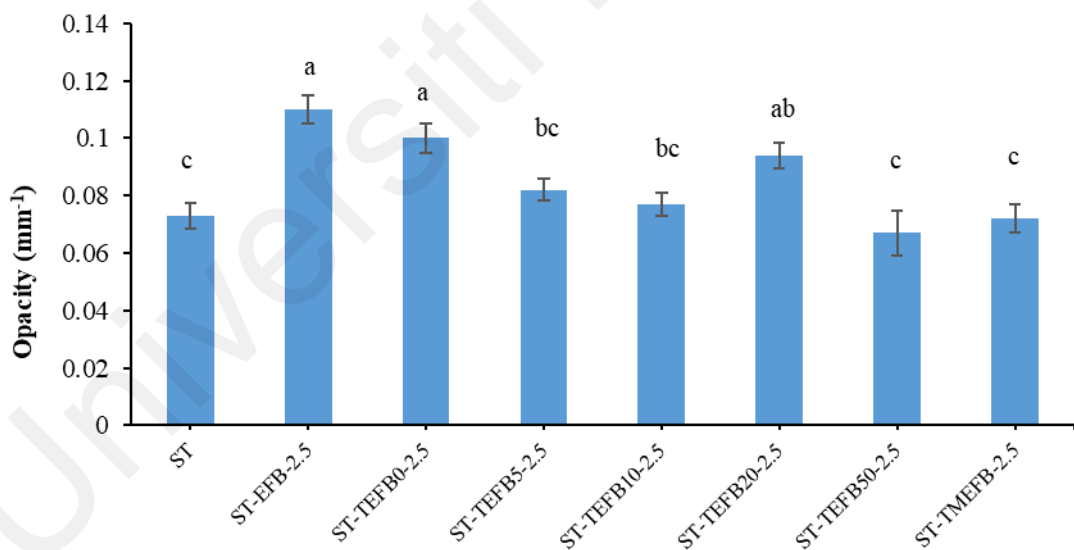


**Figure 4.18: The opacity of starch-based bioplastics reinforced with types of fibers. a-c: Significant differences among the samples ( $p < 0.05$ ) are shown by different letters within the same indicator**

Figure 4.19 depicts the opacity of the fabricated bioplastics with different concentrations of TEFB10 fibers. The opacity was slightly increased by TEFB fiber contents from 0 to 5 wt% ( $p > 0.05$ ). This was corresponding to the good dispersion and

compatibility of TEFB10 fibers in the composites, thus benefitting the transmittance of visible light through the bioplastics. However, higher fiber contents (10-20 wt%) increased the opacity of the bioplastics obviously ( $p < 0.05$ ) because the fibers formed aggregations, thus absorbing and scattering the light remarkably (Abral et al., 2019).

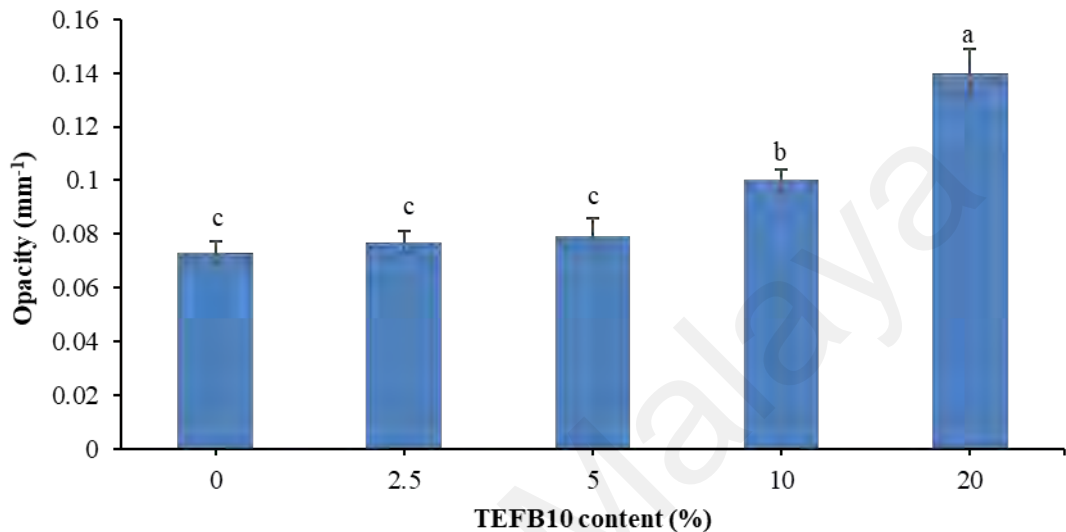


**Figure 4.19: The opacity of starch-based bioplastics reinforced with different contents of TEFB10 fibers. a-c: Significant differences among the samples ( $p < 0.05$ ) are demonstrated by different letters within the same indicator**

#### 4.1.2.8 Water vapor permeability (WVP)

The WVP is widely used to evaluate moisture transfer of the composites. The WVP of the studied bioplastics with different concentrations of TEFB10 fibers is shown in Figure 4.20. The WVP of ST was  $5.95 \times 10^{-5}$  g m/m<sup>2</sup> h Pa which was the same order of magnitude compared to other studies (Wang et al., 2009). The WVP of the composites decreased significantly with the TEFB10 fiber contents increasing ( $p < 0.05$ ) and was  $3.82 \times 10^{-5}$  g m/m<sup>2</sup> h Pa at 20 wt% TEFB fibers. This might be related to the formation of “tortuous path” structures due to the fibers, which blocked water molecules through the composites (Popescu et al., 2017). In addition, the enhanced hydrogen bond interactions between fibers and starch/glycerol could also prevent water vapor passing through the biocomposites.

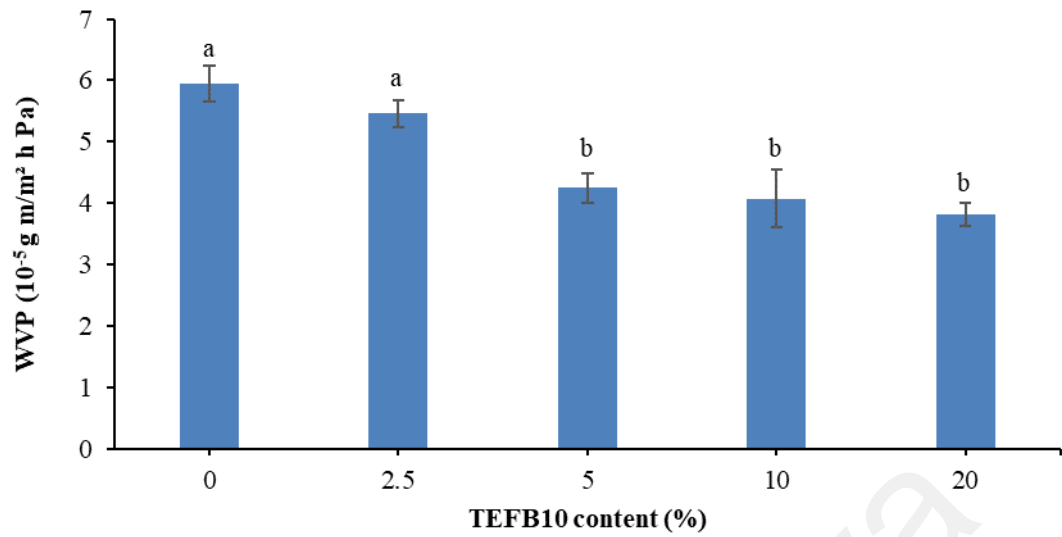


**Figure 4.20: Water vapor permeability of starch-based bioplastics reinforced with various contents of TEFB10 fibers. a-b: Significant differences among the samples ( $p < 0.05$ ) are illustrated by different letters within the same indicator**

Universiti Malaysia

## **4.2 PART 2: Preparation and characterization of crosslinked starch/fiber-based bioplastics with citric acid or epoxidized plant oils**

### **4.2.1 Characterization of epoxidized plant oils**

The FTIR spectra for PO, SO and EO are presented in Figure 4.21. The general spectra of PO and SO were similar. The bands displayed at  $3007\text{ cm}^{-1}$  are associated with C-H stretching vibrations of C=C-H (Tanrattanakul & Saithai, 2009). The terminal methyl groups of the triglyceride present strong C-H stretching vibrations in the  $2922\text{ cm}^{-1}$ , while the stretching vibrations of methylene groups in C-H show the bands at  $2853\text{ cm}^{-1}$ . Two strong characteristic ester groups arising from C=O and C-O stretching vibrations are situated at  $1742\text{ cm}^{-1}$  and  $1236\text{ cm}^{-1}$ , respectively. In the spectrum of PO, the band intensity for alkene group in the  $3007\text{ cm}^{-1}$  was lower compared to SO, which indicated there were more double bonds in SO (Tanrattanakul & Saithai, 2009).

Regarding EPO and ESO, the epoxidation reaction was apparent by observing the decreased intensity of the bands for the double bonds ( $3007\text{ cm}^{-1}$ ) and the appearance of bands at  $824\text{ cm}^{-1}$  attributed to the epoxide groups (C-O-C) (Belhassen et al., 2014). The remaining signals for double bonds revealed incomplete epoxidation conversion. The intensity of the bands for ESO at  $824\text{ cm}^{-1}$  was higher compared to that of EPO, which demonstrated higher degree of epoxidation of ESO. This was also confirmed by the oxirane oxygen contents of the prepared EPO and ESO which were 2.95% and 6.23%, respectively. Therefore, it was expected that ESO had a better chemical reactivity.

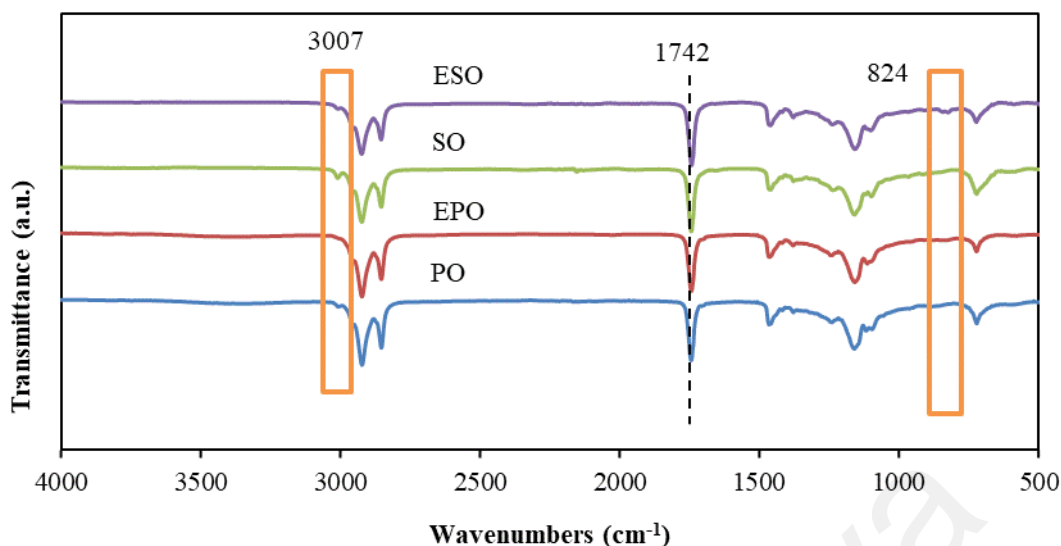


**Figure 4.21: FTIR spectra of raw plant oils and epoxidized plant oils. The rectangles indicate the bands at respective wavenumbers**

#### **4.2.2 Preparation and characterization of crosslinked starch/fiber-based bioplastics with CA or EO**

The resulted bio-composites with 5 wt% TEFB10 fibers presented superior tensile strength and elongation at break at the same time and were easy to cut for further characterization as discussed in the part 1 tensile strength section. Therefore, the composites containing 5 wt% TEFB10 fibers were chosen to perform the crosslinked composites with CA or EO further.

##### **4.2.2.1 Fourier transform infrared spectroscopy (FTIR)**

The FTIR spectra of the crosslinked bioplastics are shown in Figure 4.22-24. For the composites with CA, the characteristic bands in the 1724  $\text{cm}^{-1}$  regions for C=O stretching intensified and shifted to higher wavenumbers with the concentrations of CA increasing. This demonstrated the formation of ester bonds between starch and CA. Additionally, the new bands could also be assigned to the overlapping bands from CA, the ester bonds between glycerol and CA, and the characteristic bands of hemicellulose and lignin (Ma, Chang, Yu, & Stumborg, 2009). The lower bands in the 3289  $\text{cm}^{-1}$  regions with CA

contents increasing revealed the decreased number of free O-H due to the crosslinking interactions. The bands at approximately  $1636\text{ cm}^{-1}$ , representing the absorbed water in starch, decreased with increasing CA contents, which might confirm the enhanced water resistance of the bioplastics because of esterification reaction.

The wavenumbers for O-H stretching were all situated at higher wavenumbers after the addition of CA, which can be ascribed to the reduction of hydrogen bonds within starch molecules and the formation of hydrogen bonds among starch, fibers, and CA. It was found that CA could form intense hydrogen bond interactions with the hydroxyl groups of starch by plasticization (Wang et al., 2009).

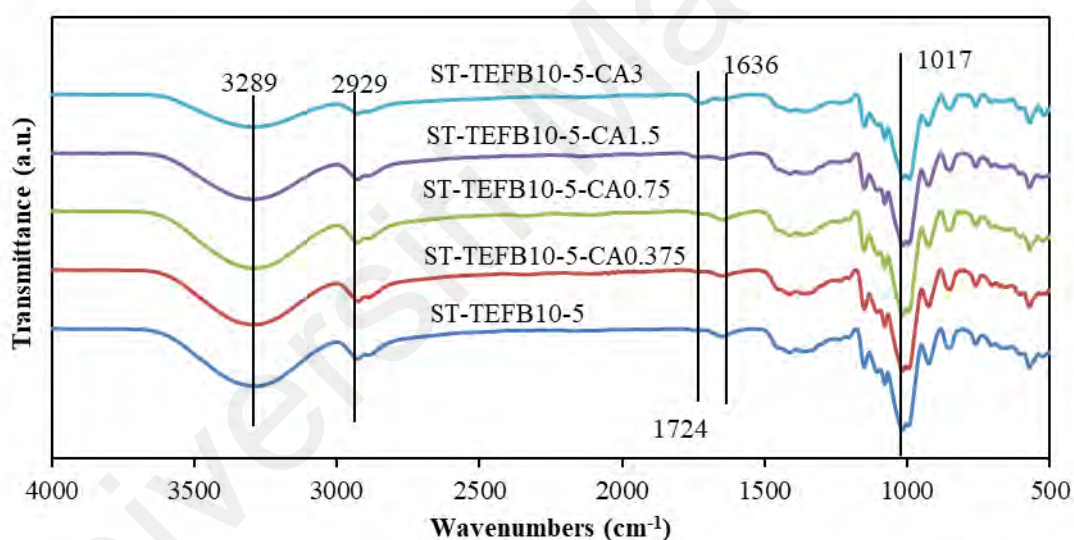


**Figure 4.22: Fourier transform infrared spectra of crosslinked bioplastics with citric acid. The solid lines indicate the bands at respective wavenumbers**

The FTIR spectra of the bioplastics with EO did not show much change due to the similar band characteristic of EPO and ESO and their low loading levels (Figure 4.23-24). The typical bands for C=O stretching vibration of oils at  $1742\text{ cm}^{-1}$  were only detected obviously in the bioplastics with high contents of ESO. It was found that the bands for O-H stretching changed to higher wavenumbers and became less intense after the introduction of EO. These results could reveal the interactions between EO and

starch/fibers (Tanrattanakul & Saithai, 2009). Belhassen et al. (2014) reported that oxirane groups of ESO were supposed to crosslink with the hydroxyl groups of starch. Moreover, partial oxirane moieties might be converted into hydroxyl groups by the ring opening reaction with H<sub>2</sub>O during the drying process of the casting solutions (Salih et al., 2015). The resulted oil-based bio-polyols would facilitate the interactions among the composites due to their hydroxyl groups. However, given the low content of EO and the interference of the bands of starch, the condensation reaction between EO and starch was not detected. The possible interaction or reaction mechanism between EO and starch/fibers is described in Figure 4.25.

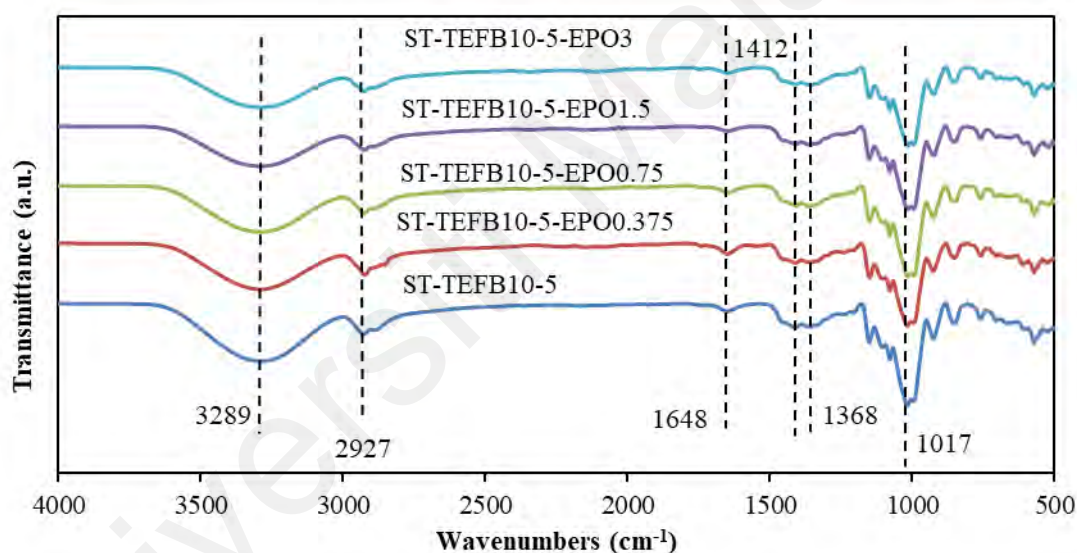


**Figure 4.23: Fourier transform infrared spectra of starch/fiber-based bioplastics incorporated with epoxidized palm oil. The dashed lines indicate the bands at respective wavenumbers**

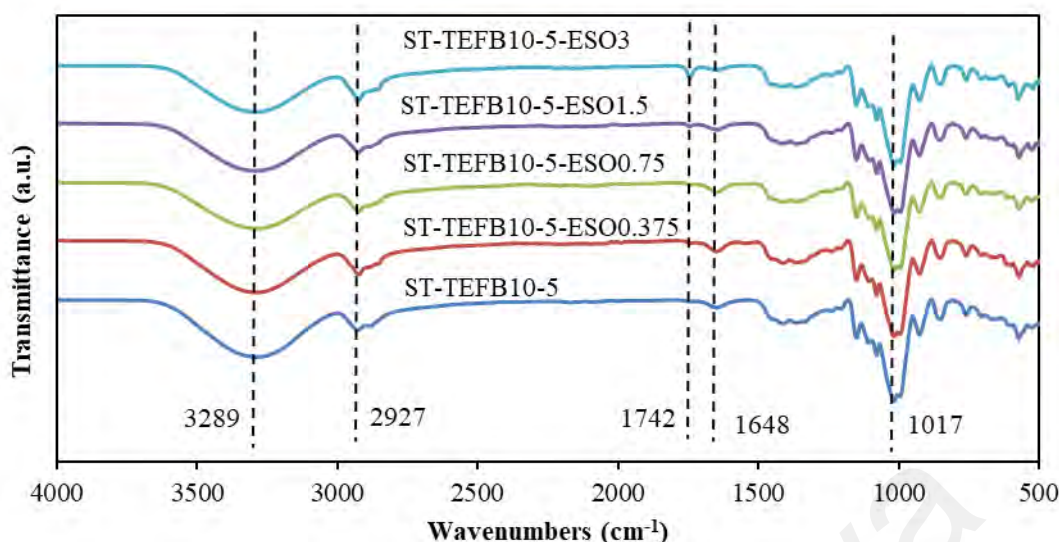


**Figure 4.24: Fourier transform infrared spectra of starch/fiber-based bioplastics incorporated with epoxidized soybean oil. The dashed lines indicate the bands at respective wavenumbers**

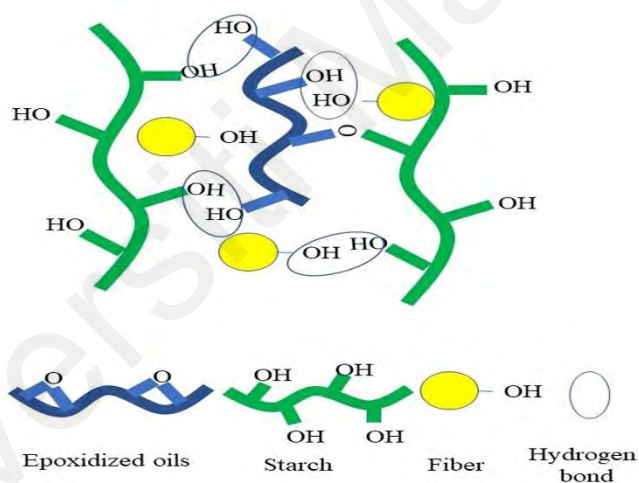


**Figure 4.25: Proposed interaction or reaction between epoxidized plant oils and starch/fibers**

#### 4.2.2.2 Scanning electron microscopy (SEM)

The surface micrographs of the prepared bioplastics are represented in Figure 4.26. The surface of ST-TEFB10-5 was smooth with fibers easily distinguished (Gironès et al., 2012; Rico et al., 2016). Because of considerable particle size of TEFB10 fibers, the interfacial adhesion between starch and TEFB10 fibers was compromised. Importantly, many white domains, which were supposed to be fibers or starch granules, were clearly

observed in the bioplastics (El Miri et al., 2015; Wang et al., 2009).

We selected the sample with 0.75 wt% crosslinkers to do SEM because the sample showed the highest reinforcing effect. Also, 3 wt% crosslinkers showed a reduction of tensile strength. Therefore, the sample can indicate the structure change sufficiently. When 0.75 wt% CA was incorporated into the composites (Figure 4.26b), the dissolution and fragmentation of starch granules were accelerated. The damaged starch granules can be penetrated by the plasticizers easily, thus the plasticization of starch was improved dramatically. So high compatibility of starch and fibers was realized with the introduction of CA (Li et al., 2015). The addition of 3 wt% CA caused the presence of many cavities on the surface which should be due to the decomposition of starch by CA as confirmed by the DSC and water solubility below.

Universiti Malaysia

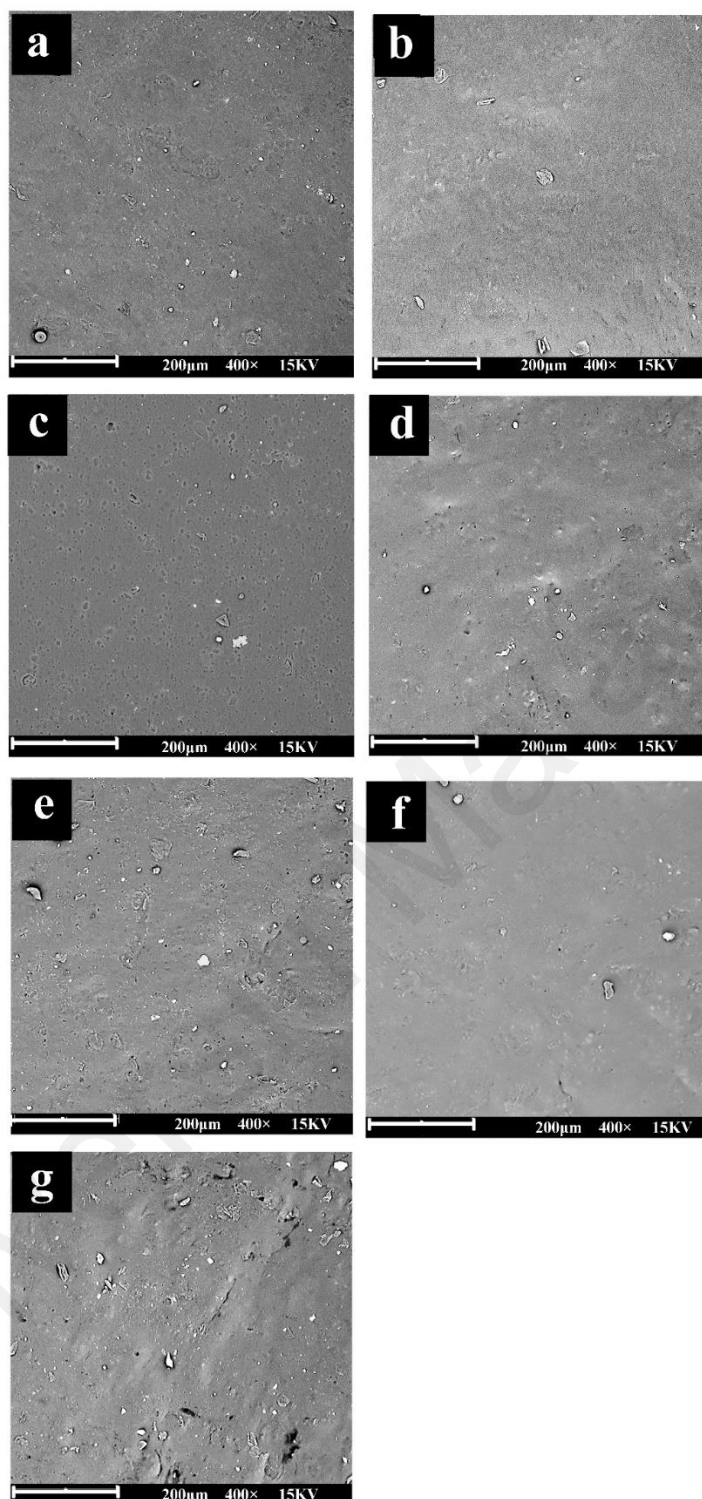


**Figure 4.26: Surface images of the crosslinked bioplastics. (a) ST-TEFB10-5, (b) ST-TEFB10-5-CA0.75, (c) ST-TEFB10-5-CA3, (d) ST-TEFB10-5-EPO0.75, (e) ST-TEFB10-5-EPO3, (f) ST-TEFB10-5-ESO0.75, and (g) ST-TEFB10-5-ESO3**

Both the EO types and contents contributed to significant effects on the surface morphology of the bioplastics (Figure 4.26d-g). When 0.75 wt% EO was blended, fewer

white domains were observed, indicating the improved compatibility of TEFB fibers and starch. The composites with ESO revealed smoother and more compact structure than those with EPO and CA. The epoxide group can establish physical or chemical interactions with the hydroxyl groups in starch and fibers at high temperature during compression molding (Balart et al., 2016; Belhassen et al., 2014). The higher oxirane oxygen content of ESO enabled more reaction points with starch through crosslinking compared to EPO (Orue et al., 2018). Thus, ESO provided a stronger effect on starch and TEFB fillers, resulting in a better starch-fiber adhesion.

Incorporating high concentrations of EO (3 wt%) generated remarkable changes of the composites' surface structures. Many cavities corresponding to oil rich phase were observed along with discontinuities, reflecting the poor compatibility of the components. Also, the composites with ESO showed more voids compared to the one with EPO. Extra EO would aggregate and migrate due to the phase separation during drying steps of films (Xiong et al., 2014). The interactions among EO, starch and fibers were insufficient to prevent phase separation during the solution evaporation (Javidi et al., 2016). This was in consistent with the poor mechanical properties as discussed below. Thus, 0.75 wt% EO was considered to be a good compatibilizer level for the bioplastics.

#### 4.2.2.3 Diffraction scanning calorimetry (DSC)

DSC thermograms and thermal parameters of starch-based bioplastics are displayed in Figure 4.27 and Table 4.5, respectively. On the DSC thermogram of ST-TEFB10-5 bioplastic, the broad endothermic peak is attributed to the melting peak.  $T_{onset}$  and  $T_m$  were 171.0 and 182.3 °C, respectively.

It can be noticed that  $T_{onset}$  of the composites crosslinked with CA was decreased to 146.4-165.1 °C. This confirmed the reduction of interfacial tension between the two polymers by CA (Khanoonkon, Yoksan, & Ogale, 2016). However, the composites with

0.375-0.75 wt% CA exhibited similar  $T_m$  with the control samples. These results might be attributed to the combined crosslinking and plasticization effect of CA. After the addition of 1.5 wt% CA, the DSC curves of the composites showed three peaks. There were several possible reasons for this behavior. Firstly, the appearance of several  $T_m$ s could be explained by the molecular weight reduction of starch due to hydrolysis (Menzel et al., 2013). When 1.5 wt% CA was introduced, the decomposition of starch by CA occurred according to the increased water solubility. The simultaneous occurrence of the decomposition and crosslinking of starch by CA has been reported by many studies (Shi et al., 2007).  $T_m$  of starch-based bioplastics was quite dependent on the molar mass of starch (Zhang et al., 2019). The reduction in molecular weight of starch would reduce the chain entanglement and result in higher mobility than the raw starch due to the decrease of the size of crystallite (lamella thickness) (Da Róz, Zambon, Curvelo, & Carvalho, 2011). The crystalline structure of unmodified starch-based bioplastics is mainly due to the amylopectin fraction. With the widespread chain breaking due to acid hydrolysis, the crystal structure was probably destroyed, leading to more linear polymers (Shi et al., 2007). The double endothermic peaks of neat PLA and its composites have been reported as a result of lamellar rearrangement of crystallization along with the reorganization of poor crystalline regions of PLA with different crystalline structures (Awale et al., 2018; Xiong et al., 2013b). In addition, the appearance of many  $T_m$ s peaks might be also ascribed to the different components in the composites, which showed low compatibility (Khanonkon et al., 2016; Ortega-Toro, Jimenez, Talens, & Chiralt, 2014). It was likely to have four types of starch in the composites with 1.5 wt% CA, including raw starch, un-crosslinked and decomposed starch, crosslinked and un-decomposed starch, and crosslinked and decomposed starch due to the decomposition and crosslinking effect of 1.5 wt% CA. Starch with high degree of crosslinking cannot be plasticized by glycerol properly because polymer chains of starch were usually decomposed, and their film-

forming ability has been destroyed. Some researchers have used them as the reinforcing agents or compatibilizers in starch-based bioplastics (Ma, Jian, Chang, & Yu, 2008b; Yildirim-Yalcin et al., 2019). The different degree of decomposition and crosslinking of starch might lead to the incompatibility of the components. This phenomenon was also demonstrated by the craters on the SEM graphs of ST-TEFB10-5-CA3. In the end, the presence of impurities (for example, solvent or fillers) and plasticization of CA would also exert an important influence on the melting behavior of starch-based bioplastics (Shi et al., 2007). Significant differences of  $T_m$  in starch-based bioplastics were observed, depending on the moisture contents of the specimens (Jiménez, Fabra, Talens, & Chiralt, 2013a). Thus, it was not surprising to observe irregular graphs for the composites. However, the addition of 3 wt% CA led to the presence of two peaks on the DSC curves. According to the high-water solubility of the composites with 3 wt% CA, most of starch might have been decomposed, including crosslinked and un-crosslinked starch, which could present better compatibility. The  $T_m$  peaks can be approached or emerged by the improved compatibility of the composites (Khanonkon et al., 2016).

Comparatively, the composites with EPO showed higher  $T_m$  and  $T_{onset}$  compared to those with ESO at the same EO concentration except 0.75 wt%. Based on FTIR and SEM analysis, ESO showed better chemical reactivity than EPO for higher oxirane oxygen content, which increased the crosslinking with starch and prevented the melting of the bioplastics. The  $T_m$  and  $T_{onset}$  of the composites were increased significantly after the incorporation of 0.375 wt% EPO or ESO. These results suggested lower molecular mobility of starch chains due to the strengthened interaction between starch and EO, which was also confirmed by the huge increase of tensile strength as shown below. However, 0.75 wt% EO reduced the  $T_m$  and  $T_{onset}$  of the composites remarkably. A possible explanation of the reduced  $T_m$  was that EO were excess slightly and cannot crosslink or interact sufficiently with starch/fibers considering the fact that the tensile

strength did not show double increase compared to the composites with 0.375 wt% EO. Also, the presence of few voids in the SEM images of the composites with 0.75 wt% EO verified the outcome. Therefore, excess EO might occupy intermolecular spaces among starch like glycerol and facilitated the reduction of hydrogen bonds of starch, thus increasing the mobility of biopolymer chains (Rodríguez, Osés, Ziani, & Maté, 2006). The dangling chains of unreacted EO in the composite would increase the free volume, subsequently lowering the  $T_m$ . Moreover, it was reported that  $T_m$  shifted to lower temperature due to the plasticization effect (Javidi et al., 2016; Sarwono et al., 2012). However, 1.5-3 wt% EO might deteriorate the phenomenon which might be due to the incompatibility of excess EO and starch/fibers, thus hampering the melting of the composites. This was consistent with the behavior of phase separation as shown by the SEM.

**Table 4.5: The melting temperature and decomposition parameters of the bioplastics crosslinked with citric acid or epoxidized plant oils**

Formulations	$T_{onset}$ (°C) <sup>a</sup>	$T_m$ (°C) <sup>b</sup>	$T_{5\%WL}$ (°C) <sup>c</sup>	$T_{max1}$ (°C) <sup>d</sup>	$T_{max2}$ (°C) <sup>d</sup>
ST-TEFB10-5	171.0	182.3	189.4	276.0	346.6
ST-TEFB10-5-CA0.375	161.8	184.1	176.7	291.1	358.1
ST-TEFB10-5-CA0.75	146.4	181.1	151.6	283.2	342.2
ST-TEFB10-5-CA1.5	163.0	190.2/217.7/223.2	176.1	294.4	348.6
ST-TEFB10-5-CA3	165.1	170.8/195.0	173.4	295.2	370.5
ST-TEFB10-5-EPO0.375	215.4	220.1	166.3	279.5	349.4
ST-TEFB10-5-EPO0.75	152.2	172.9	168.7	-	345.8
ST-TEFB10-5-EPO1.5	208.8	219.1	167.8	284.1	354.1
ST-TEFB10-5-EPO3	202.6	213.7	175.8	273.1	350.1
ST-TEFB10-5-ESO0.375	210.5	216.3	200.4	298.5	364.3
ST-TEFB10-5-ESO0.75	162.6	174.7	159.6	279.6	359.5
ST-TEFB10-5-ESO1.5	188.6	199.7	188.3	290.3	359.6
ST-TEFB10-5-ESO3	195.4	206.8	179.4	285.2	357.7

<sup>a</sup>: Onset melting temperature. <sup>b</sup>: Melting temperature. <sup>c</sup>: Temperature at 5% weight loss. <sup>d</sup>: Temperature at maximum decomposition rate.  $T_{onset}$  and  $T_m$  were determined by DSC.  $T_{5\%WL}$  and  $T_{max}$  were from TGA.

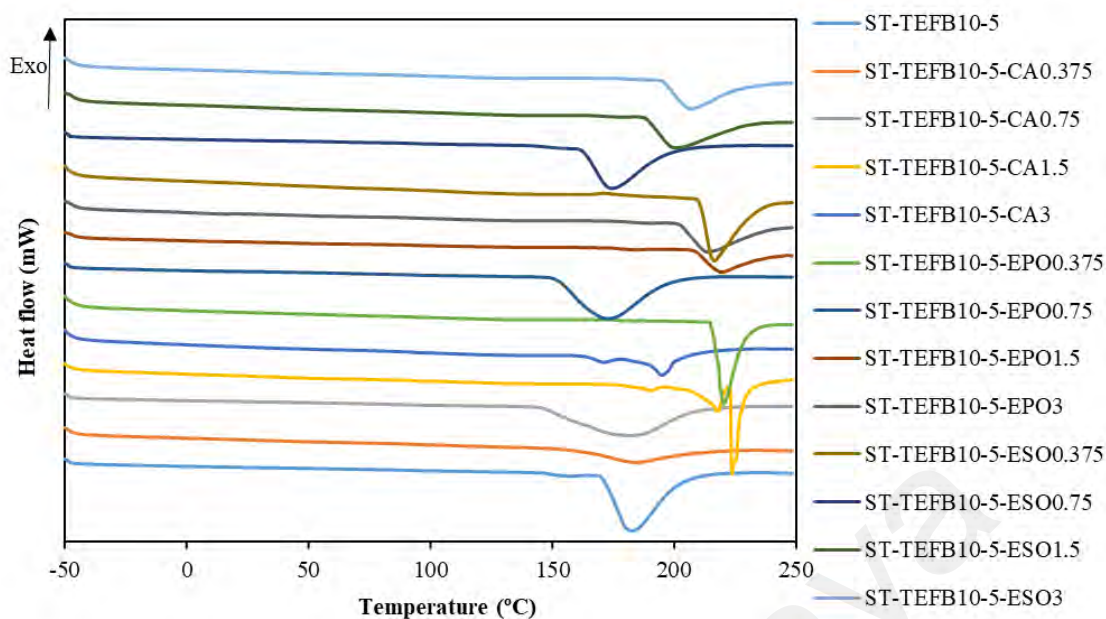


**Figure 4.27: Diffraction scanning calorimetry thermograms of the crosslinked bioplastics**

#### 4.2.2.4 Thermogravimetric analysis (TGA)

The TG and DTG curves for starch-based bioplastics with types of crosslinkers are shown in Figure 4.28-30. The thermal degradation behaviors of the composites incorporated with CA or EO were similar to the control samples. The weight loss of the bioplastics primarily occurred in three steps. In the initial step, a weight loss of 10-20% was found from 30 to 270 °C, which is related to the loss of water, CA, and glycerol (Campos et al., 2018). In the second stage of 270-420 °C, the weight loss of the bioplastics corresponds to the thermal decomposition of glycerol, starch, EO and fibers. Finally, in the scope of 420-600 °C, the degradation is mainly attributed to carbonaceous residues.

$T_{5\%WL}$  of ST-TEFB10-5 was 189.4 °C as shown in Table 4.5. After the addition of CA,  $T_{5\%WL}$  of the composites was reduced which might be ascribed to the decomposition of unreacted CA. The composites with 0.75 wt% CA revealed the lowest  $T_{5\%WL}$ . This might be due to that CA was excess for crosslinking based on that the tensile strength did not increase remarkably when the contents of CA increased from 0.375 to 0.75 wt%. The

excess CA was mainly used to dissolve the unplasticized starch granules and acted as the compatibilizer or plasticizer between starch and TEFB10 fibers, as shown by the SEM. These excess CA might decompose easily during the heating process and cause the decrease of  $T_{5\%WL}$ . However, the tensile strength increased significantly again when the CA content increased from 0.75 to 1.5 wt%, which might indicate that crosslinking of starch and CA was promoted due to the dissolution of starch granules by 0.75 wt% CA. The dissolution of starch would consume less CA due to the lower pH and more CA can participate in the crosslinking reaction. Therefore,  $T_{5\%WL}$  of the composites with 1.5-3 wt% CA increased. DTG curves described that two maximum decomposition rate peaks were observed.  $T_{max1}$  and  $T_{max2}$  of ST-TEFB10-5 occurred at 276.6 and 346.6 °C, respectively.  $T_{max1}$  and  $T_{max2}$  of the composites with CA showed similar changes to  $T_{5\%WL}$ , which might be also related to above reasons. Considering the changes of DSC and TGA in the composites with CA, the effect of various contents of CA on the thermal properties might be affected by crosslinking, plasticization, or decomposition effect of CA.

After the addition of EO,  $T_{5\%WL}$  was all reduced except 0.375 wt% ESO, which changed similar to the composites with CA. This can also be explained by crosslinking and plasticization effect of different contents of EO and the decomposition of unbounded EO components (Thakur et al., 2017). It was observed epoxidized oils showed lower thermal stability than that for non-epoxidized oils (Orue et al., 2018). No obvious difference of  $T_{max1}$  and  $T_{max2}$  was observed between the composites with and without EPO. However, the addition of ESO improved  $T_{max1}$  and  $T_{max2}$  of the bioplastics, which was in the range of 279.6-298.5 °C and 357.7-364.3 °C, respectively. ST-TEFB10-5-ESO0.375 presented the highest thermal stability among all the composites. This revealed that the thermal stability of the bioplastics was increased by the introduction of ESO, which can be ascribed to the stronger interaction of ESO with fibers and starch. The composites with 0.75 wt% CA or EO showed the lowest thermal stability compared to that with other

contents of CA or EO. This might show that the plasticization effect of CA or EO would reduce the thermal stability of the composites. It was observed the addition of plasticizers such as epoxidized oils reduced the thermal stability of PLA matrix (Orue et al., 2018). As a summary, the addition of three crosslinkers slightly improved the thermal stability of the bioplastics at various concentrations.

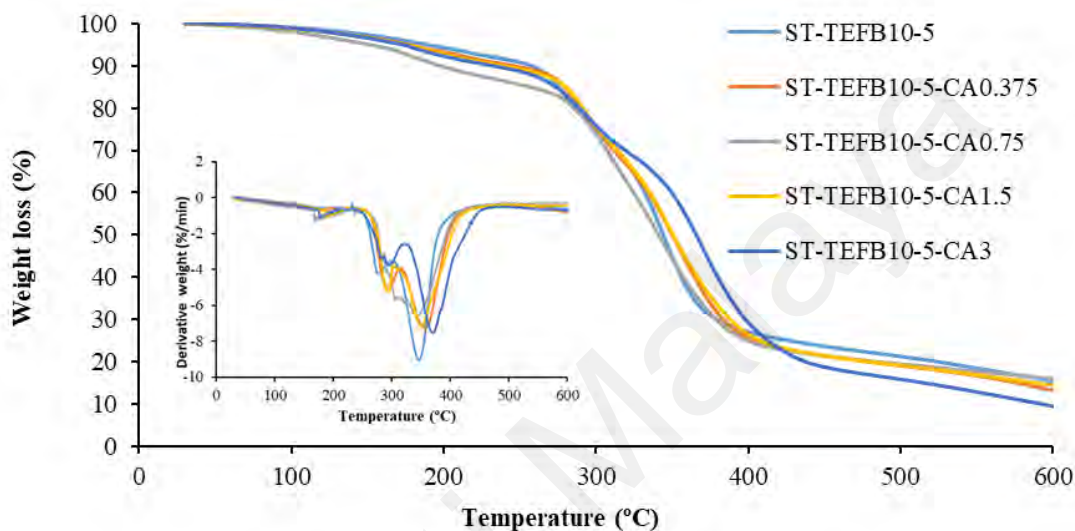


**Figure 4.28: Thermogravimetric and derivative thermogravimetric curves of starch/fiber-based bioplastics with citric acid**

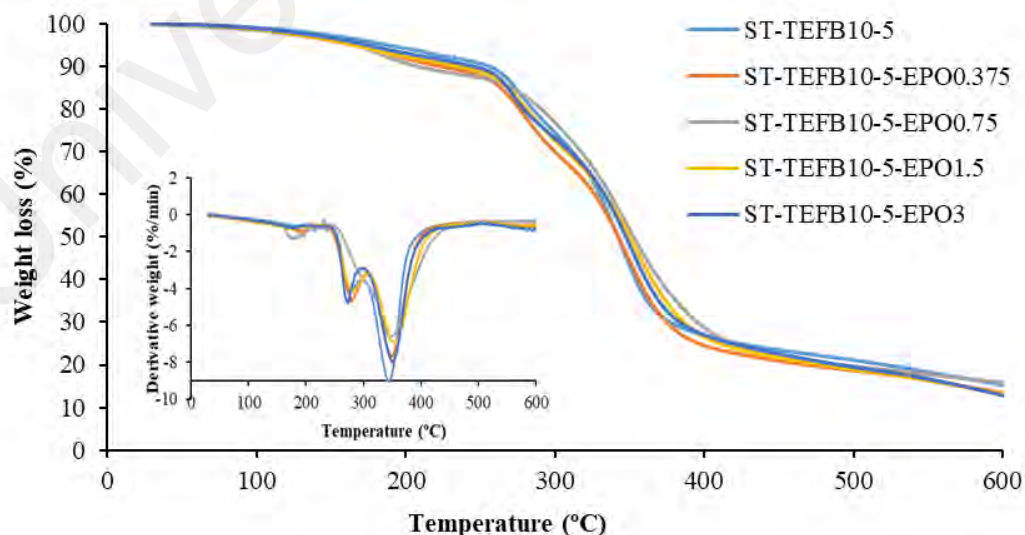


**Figure 4.29: Thermogravimetric and derivative thermogravimetric curves of starch/fiber-based bioplastics with epoxidized palm oil**

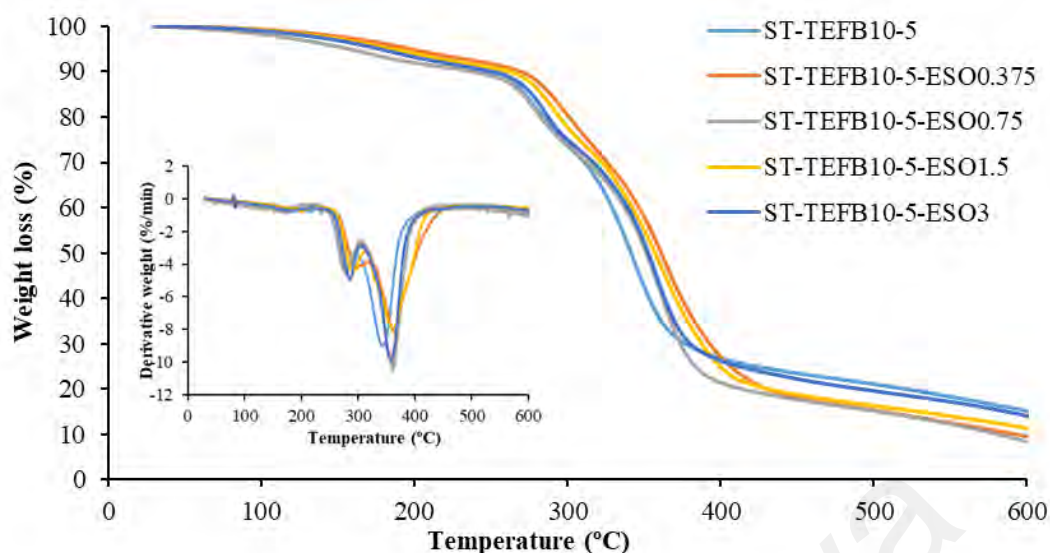


**Figure 4.30: Thermogravimetric and derivative thermogravimetric curves of starch/fiber-based bioplastics with epoxidized soybean oil**

#### 4.2.2.5 Mechanical properties

The tensile properties of the prepared bioplastics are presented in Figure 4.31 and 4.32. The composites without CA or EO were fairly flexible materials with the elongation at break of 36.01% and the tensile strength of 0.83 MPa. The addition of CA or EO exhibited an obvious reinforcing effect on the mechanical properties of the composites. It was clear the tensile strength of the crosslinked composites increased gradually with increasing CA contents, reached a maximum value 1.62 MPa at 1.5 wt% CA, and then decreased at 3 wt% CA. Elongation at break of the composites changed inversely to the trend of tensile strength. The reinforcing effect of CA could be attributed to crosslinking reaction between starch and CA and a compatibilization of CA between starch and TEFB fibers (Olsson et al., 2013; Seligra et al., 2016). Moreover, it has been reported that CA could form strong hydrogen bond interactions with starch when no esterification reaction was formed. These interactions contributed to the formation of a rigid network structure and strengthened the compatibility of starch and fibers (Olivato et al., 2012a).

On the other hand, the extra CA probably acted as a plasticizer which reduced the cohesiveness in the composites and led to consequent decrease of tensile strength (Das, Uppaluri, & Das, 2019; S. Sun et al., 2018). Accordingly, 3 wt% CA in the study emphasized the plasticization effect, which was similar to other reports (Da Róz et al., 2011; Olivato et al., 2012a). In addition, low molecular weight starch from the decomposition of starch by CA can act as the plasticizer of the composites (Da Róz et al., 2011; Olivato et al., 2012a).

The addition of a small number of EO induced a huge increase of the tensile strength ( $p < 0.05$ ). The tensile strength reached the maximum of 3.92 MPa with 1.5 wt% EPO and 5.42 MPa with 0.75 wt% ESO. The major reason for the increase of tensile strength was likely to be the consequence of the interaction between EO and starch/fiber (Belhassen et al., 2014). It was reported that EO could accumulate on the fiber surface by physical or chemical interactions. These interactions allowed load transfer from TEFB fibers to starch, which subsequently enhanced the reinforcing ability (Orue et al., 2018). The strengthened interactions led to a more brittle fracture as revealed by downward elongation at break ( $p < 0.05$ ). With the EO contents increasing from 1.5 to 3 wt%, the composites revealed the higher elongation at break and lower tensile strength. Similar results have been observed in starch-based films incorporated with various plant oils (Basiak et al., 2016; Volpe et al., 2018). The excess EO could not interact or crosslink sufficiently with starch/EFB and might contribute to the plasticization of the starch like the non-epoxidized oils (Basiak et al., 2016; Javidi et al., 2016). The decrease of tensile strength reflected the reduced interaction among starch molecules and might be caused by the formation of EO-EO interaction at higher oil contents due to their flexible properties. As a result, the looser structure of the composites was developed. This corresponded to the microvoids of EO rich phase as observed by the SEM micrographs.

Comparatively, EO showed higher reinforcing effect than CA which might be related to their better crosslinking or compatibilizer effect ( $p < 0.05$ ). ESO exhibited higher reinforcing effect on the composites than EPO ( $p < 0.05$ ) due to higher reactivity of epoxy groups (Balart et al., 2016). However, reinforced bioplastics with ESO were too brittle and would crack when cutting after conditioned. Belhassen et al. (2014) also came to the same conclusion and suggested increasing quantity of EO or using EO with lower reactivity. Considering the poor compatibility between starch and high content of EO, EPO was a suitable choice to alleviate the rigidification effect of ESO.

In conclusion, the results highlighted that the effect of CA or EO on the composites' tensile properties was determined by the types and concentrations. The introduction of CA or EO as a crosslinker can modify the tensile properties of the composites remarkably in the desired range, while excess CA or EO acted as a plasticizer to soften the composites. The reinforcing effect on tensile properties of the composites was ESO>EPO>CA. Moreover, palm oil is the most abundant commodity oil in Malaysia. Therefore, EPO was suggested to prepare the crosslinked EO in part 3.

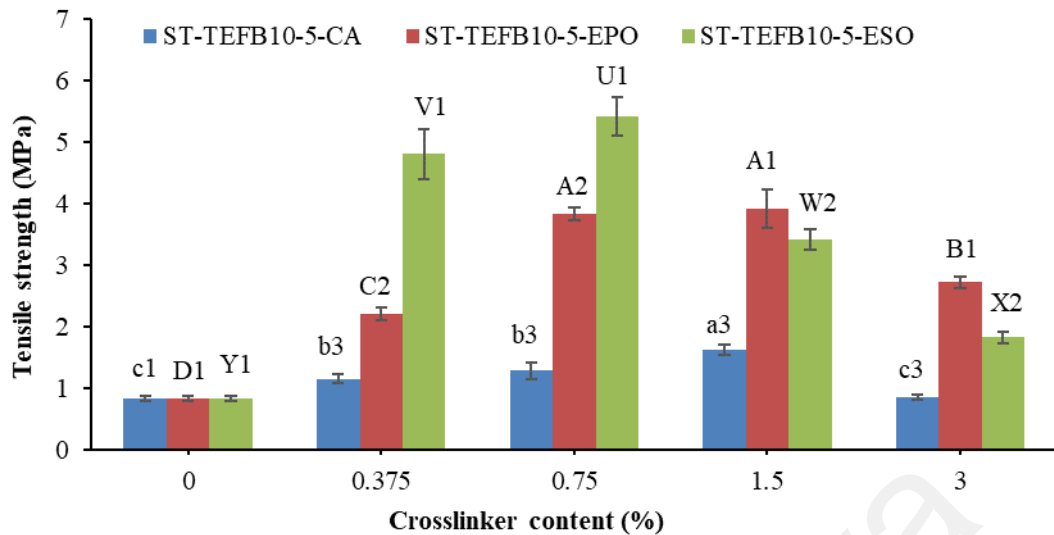


**Figure 4.31: Tensile strength of the crosslinked bioplastics. a-c, A-D, U-Y: Significant differences among the samples ( $p < 0.05$ ) are indicated by different letters within the same indicator. 1-3: Different numbers present significant differences among the formulations with different crosslinkers at the same concentration ( $p < 0.05$ )**

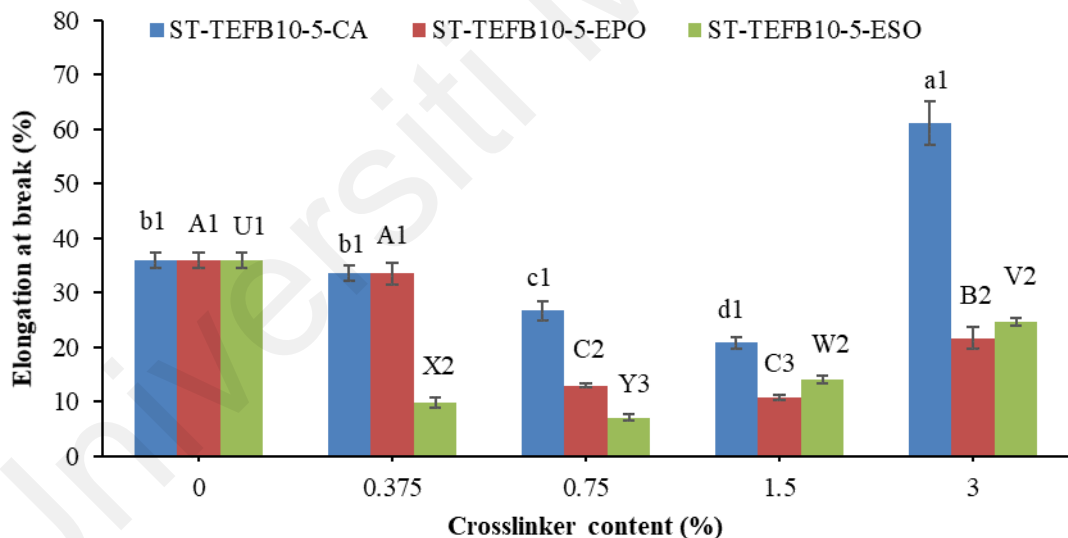


**Figure 4.32: Elongation at break of the crosslinked bioplastics. a-d, A-C, U-Y: Different letters within the same indicator present significant differences among the samples ( $p < 0.05$ ). 1-3: Different numbers indicate significant differences among the samples with different crosslinkers at the same concentration ( $p < 0.05$ )**

#### 4.2.2.6 Moisture content, water uptake and solubility

Water sensitivity is an important criterion of starch-based products for various applications. Moisture content, water uptake and solubility of the bioplastics with CA or

EO are investigated in Figure 4.33-4.35, respectively. ST-TEFB10-5 exhibited the moisture content of 8.24%. The moisture content of the composites showed no noticeable difference ( $p > 0.05$ ) after the incorporation of three modifiers. This demonstrated that all the samples were conditioned to constant weight and moisture content would not affect the mechanical properties of the composites.

ST-TEFB10-5 exhibited the water uptake of 23.06% and water solubility of 28.26%. Water uptake of the bioplastics modified with CA decreased slightly with CA contents increasing from 0.375 to 1.5 wt% ( $p > 0.05$ ) and then increased at 3 wt% CA. On the other hand, solubility of the bioplastics was not remarkably affected by CA contents from 0 to 1.5 wt%, but it increased significantly at 3 wt% CA concentrations ( $p < 0.05$ ). CA reinforced the composites with denser structure both chemically and physically, and thereby improved their water resistance (Seligra et al., 2016). Whereas, the numerous hydrophilic hydroxyl and carboxyl groups from extra CA tended to interact with water, thus increasing the water solubility (Owi et al., 2019). Furthermore, the addition of CA may cause a partial hydrolysis of starch chains due to the decrease of pH. Some researchers stated a positive relationship between starch degradation and water solubility (Reddy & Yang, 2010; Shi et al., 2008). Therefore, the decomposition and crosslinking of starch by CA would take place at the same time and starch degraded significantly at 3 wt% CA (Lee & Chang, 2019; Ortega-Toro et al., 2014; J. Zhou et al., 2016). Amounts of studies obtained same results with our research. Olivato et al. (2012a) studied the effect of CA on the performance of thermoplastic starch/polyester blown films. The inclusion of CA increased the weight loss of the films in water when the concentration of CA was 1.5 wt% due to the acid hydrolysis of starch. Corn starch films, containing CA (1 g/100 g starch), were obtained by compression (160 °C for 2 min). Films containing CA showed higher solubility (31%) than CA-free films (15%) (Ortega-Toro et al., 2014). The effects of eggshell powder and CA on the properties of thermoplastic starch were explored by

melt-blending. The introduction of 1% CA caused the formation of crosslinking structures and led to rapid biodegradation of starch due to hydrolysis (Praprudivongs & Wongpreedee, 2020).

Some studies observed lower solubility of the CA-crosslinked bioplastics because they added the catalysts to promote the crosslinking, used lower temperature for crosslinking, or applied modified starch as the materials. For example, Reddy and Yang (2010) prepared the crosslinked bioplastics with 5% CA and the catalyst sodium hypophosphite (50 wt% of CA) by compression molding at 160 °C for 5 min. After 3 days in water, both the crosslinked and non-crosslinked films lost about 25% of their weight. After 35 days, the non-crosslinked films lost 75% of their weight, whereas the crosslinked films had only 25% weight loss. Starch-based films with various contents of CA (0-20 wt% of starch) were obtained using solution casting. The water solubility was 26.64% for the control group and decreased notably to 23.76% for the sample containing 10% CA. The highest concentration of CA (20%) induced the highest solubility (36.56%) (Ghanbarzadeh et al., 2011). The influence of CA on hydroxyl-propylated and oxidized potato starch-based films has been examined by casting. The water solubility was decreased from 80% to 20% as the contents of CA increased from 0 to 30% (Menzel et al., 2013). However, the application of catalysts or modification of starch is usually not environmentally friendly, and the low crosslinking temperature cannot produce the samples with optimum strength.

In addition, there were some other studies which obtained the crosslinked starch particles with significantly lower water solubility. However, these particles were usually used as the reinforcements or compatibilizers in the bioplastics. Moreover, the modified starch was usually washed to remove unreacted CA or decomposed starch. Therefore, the solubility of the crosslinked starch decreased remarkably (Martins, Gutkoski, & Martins, 2018; J. Zhou et al., 2016).

Water uptake of the composites exhibited lower values owing to the incorporation of EO ( $p < 0.05$ ), while the solubility of the composites slightly decreased with the concentrations of EO increasing ( $p > 0.05$ ). There was no obvious difference of water uptake and solubility between the composites with EPO and ESO ( $p > 0.05$ ). The long fatty acid chains of EO can protect the hydroxyl groups of starch/fibers from moisture absorption and swelling due to their hydrophobicity (Schmidt, Porto, Laurindo, & Menegalli, 2013). Moreover, this may be explained by the enhanced interactions among EO, starch and EFB fibers, decreasing the availability of hydroxyl groups (Thakur et al., 2017; Xiong et al., 2014). Additionally, this could also be ascribed to the formation of tortuosity by EO, thus hampering water penetration (Chiumarelli & Hubinger, 2012).

The bioplastics with EO showed better reduction of water uptake and solubility compared to those with CA. The effect of three crosslinkers on water uptake and solubility did not show huge reduction. Starch, TEFB fibers and CA are hydrophilic as a result of their numerous hydroxyl or carboxyl groups (Rico et al., 2016; Svagan et al., 2009). Low reactivity between EO and starch cannot resist the water molecules greatly. At high water contents, water would replace the interactions among starch, TEFB fibers and modifiers by forming the interactions with them separately (Teaca et al., 2013). The addition of glycerol further deteriorated the properties because glycerol is a highly water-retaining material (Hu et al., 2009). Therefore, interactions among these molecules would be easily destroyed by water. Improvement of water resistance of the composites was under future research.

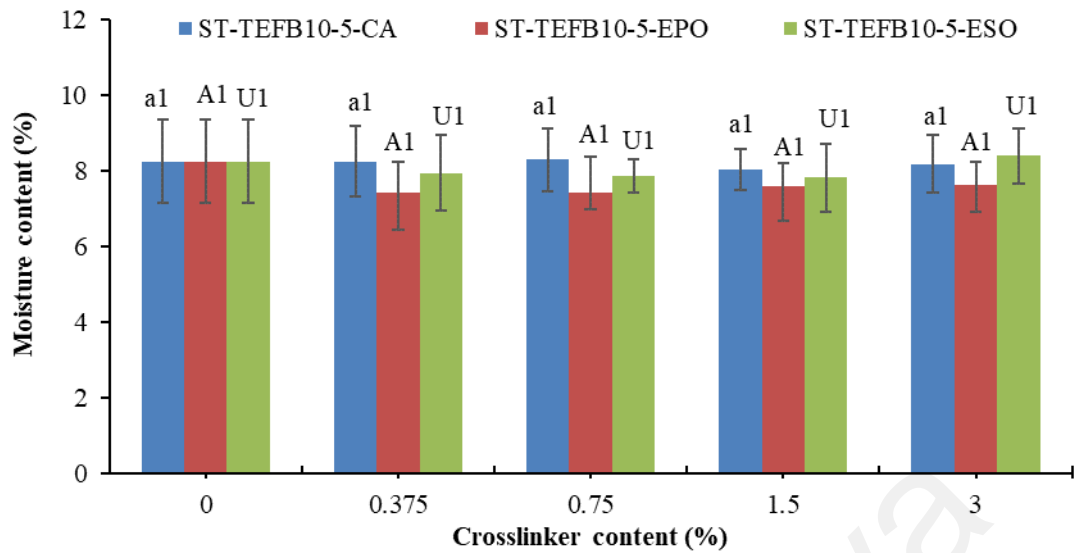


**Figure 4.33: Moisture content of the crosslinked bioplastics. a, A, U: Same letter within the same indicator indicates no significant difference among the samples ( $p > 0.05$ ). 1: Same number indicates no significant difference among the formulations with different crosslinkers at the same concentration ( $p > 0.05$ )**

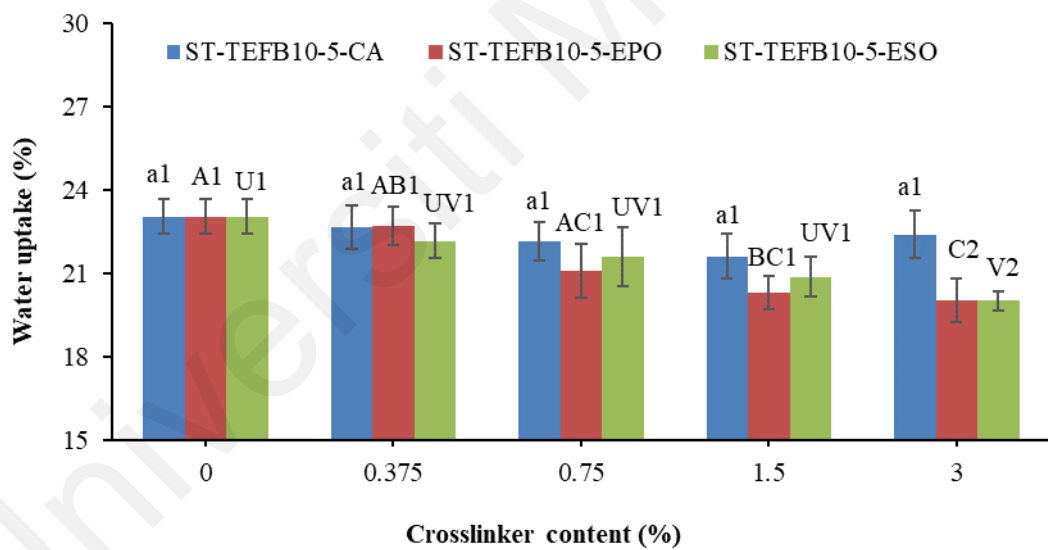


**Figure 4.34: Water uptake of the crosslinked bioplastics. a, A-C, U-V: In the same indicator, different letters represent significant differences among the specimens ( $p < 0.05$ ). 1-2: Different numbers means significant differences among the formulations with different crosslinkers at the same concentration ( $p < 0.05$ )**

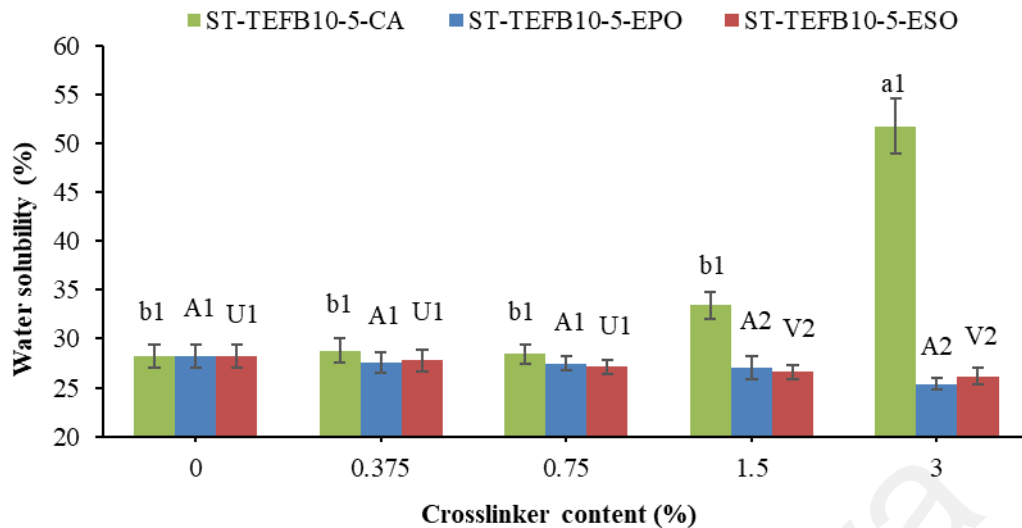


**Figure 4.35: Water solubility of the crosslinked bioplastics. a-b, A, U-V: Diverse letters within the same indicator demonstrate significant differences among the samples ( $p < 0.05$ ). 1-2: Different numbers indicate significant differences among the formulations with different crosslinkers at the same concentration ( $p < 0.05$ )**

#### 4.2.2.7 Water vapor permeability (WVP)

As is well known, the addition of crosslinking agents is one of two primary means to reduce the WVP of the bioplastics along with the addition of lipids (Brandelero, Grossmann, & Yamashita, 2012; P. Liu et al., 2016). The WVP of all studied composites with crosslinkers is shown in Figure 4.36. The WVP of ST-TEFB10-5 was  $4.25 \times 10^{-5}$  g m/m<sup>2</sup> h Pa. The addition of CA into the blends exhibited a significant reduction of the WVP. The WVP of the composites significantly decreased to  $3.47 \times 10^{-5}$  g m/m<sup>2</sup> h Pa at 1.5 wt% CA ( $p < 0.05$ ). This was due to the hydrophilic hydroxyl group substitution with hydrophobic ester groups. Furthermore, the crosslinking of CA formed a compact structure, which was also beneficial to reduce the WVP. However, the WVP increased again by the addition of 3 wt% CA. This can be probably illustrated by the decomposition of starch, which increased the starch chain mobility, hence triggering the polymeric network to become less dense and higher in water transmission (Owi et al., 2019).

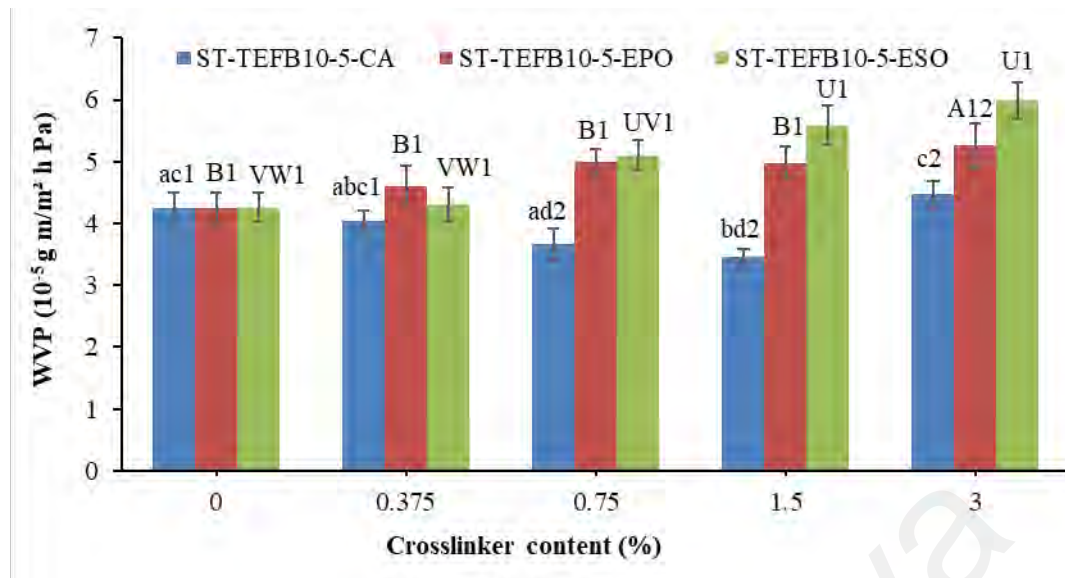


**Figure 4.36: Water vapor permeability of the crosslinked bioplastics. a-d, A-B, U-W: Different letters within the same indicator represent significant differences among the samples ( $p < 0.05$ ). 1-2: Different numbers demonstrate significant differences among the formulations with different crosslinkers at the same concentration ( $p < 0.05$ )**

Many factors, such as the composition and contents of oils added, interactions among components, drying process, and the final microstructure would affect the WVP of the bioplastics with oils. Moreover, the incorporation of oils could contribute to the tortuosity which increased the pathway length of water transfer (Basiak et al., 2016). However, the WVP increased gradually as EO were incorporated in the study. The similar behavior was also found in several studies (Atarés, De Jesús, Talens, & Chiralt, 2010; Javidi et al., 2016). The WVP of the composites with EPO and ESO showed no remarkable difference ( $p > 0.05$ ).

Firstly, this might be related with the number of microvoids on the surface of the composites which would facilitate the water transfer, as verified by the SEM graphs. Next, the interactions between lipid phase and biopolymer chains in o/w emulsion films might just increase the external tortuosity and take negligible effect on the moisture barrier of emulsified films (Phan The, Debeaufort, Voilley, & Luu, 2009). In the end, EO and Tween 80 might increase the free volume among starch chains due to their plasticization

effect, which facilitated the water transfer (Brandelero, Yamashita, & Grossmann, 2010). Overall, it can be concluded that the WVP would not be reduced by simply adding EO to the composites.

#### 4.2.2.8 Opacity

Good transparency of the materials used for packaging is an advantage because it allows consumers to see the products before buying (Acosta, Jiménez, Cháfer, González-Martínez, & Chiralt, 2015). Figure 4.37 depicts the opacity of the fabricated composites. It was clear that the ST-TEFB10-5 bioplastic exhibited the low opacity of 0.079. When CA was introduced into the composites, a slight increase of the opacity was observed. Many previous studies corroborated the above-mentioned changes (Wu et al., 2019). Crosslinking increased the polymeric chain compaction and hindered light to pass through the matrix, thus resulting in opaquer composites (Olivato et al., 2012b). However, the opacity of the composites did not change obviously under different concentrations of CA. The relatively low ratio and plasticization effect of CA, which gave rise to a less compact structure, can explain the phenomenon (Wu et al., 2019).

Optical properties of the biopolymer-based composites containing plant oils are directly related to their internal heterogeneity and surface morphology of the composites (Saber et al., 2017; Thakur et al., 2017). They are affected by the loading levels and distribution of oils, size of oil aggregates and drying process of the composites (Rodrigues et al., 2014). When various contents of EO were incorporated into starch-based biocomposites, the opacity was improved remarkably ( $p < 0.05$ ), revealing that the composites became less transparent. The results were similar to previous reports which demonstrated that the incorporation of oils or fatty acids reduced the transparency of biopolymer-based films (Basiak et al., 2016; Rodrigues et al., 2014). This could be explained in terms of the differences in the refractive index of EO and starch (Saber et al., 2017). Moreover, it has previously been reported that the reduction of transparency

might be related with the starch retrogradation or crystallinity phenomenon which increased the number of hydrogen bonds in the composites (Acosta et al., 2015; Jiménez et al., 2013a). Additionally, high contents of oils would hamper the plasticization of starch and lead to the presence of starch particles in the composites, which reduced the transmission of light (Jiménez, Fabra, Talens, & Chiralt, 2013b).

Comparatively, the composites with EO showed significantly higher opacity than those with CA ( $p < 0.05$ ). The concentration increments of both oils led to no obvious change of the opacity ( $p > 0.05$ ). The opacity of the composites containing EPO was slightly higher than ESO ( $p > 0.05$ ). Nevertheless, all the bioplastics still possessed good optical transparency and can be used as packaging materials.

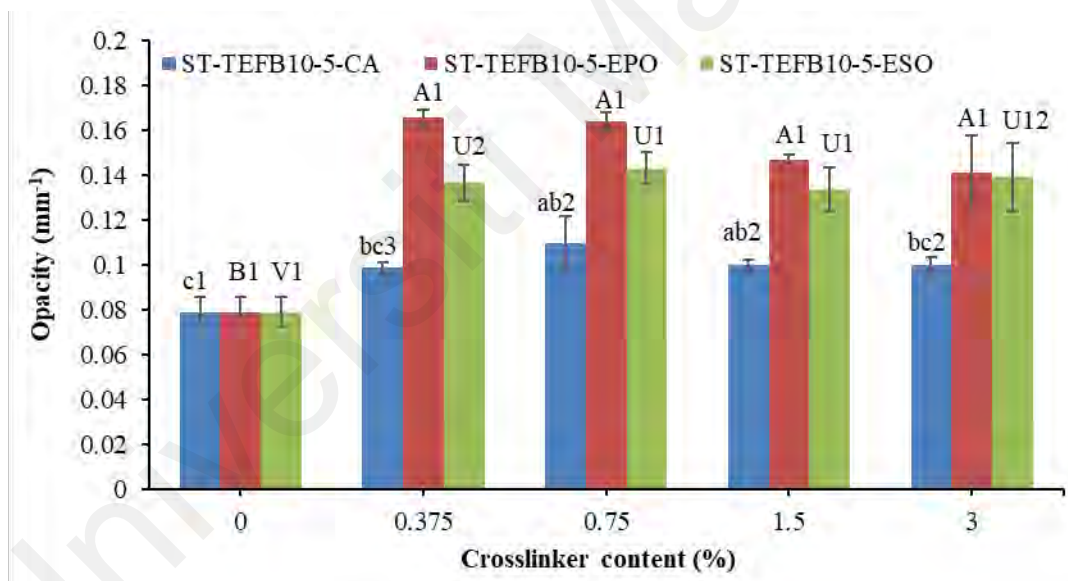


**Figure 4.37: The opacity of the crosslinked bioplastics. a-c, A-B, U-V: Different letters within the same indicator present significant differences among the samples ( $p < 0.05$ ). 1-2: Different numbers mean significant differences among the specimens with different crosslinkers at the same concentration ( $p < 0.05$ )**

#### 4.2.2.9 Biodegradability

Environmental impact of non-degradable plastic requires the use of renewable raw materials to develop the bioplastics that possess the integrity of petroleum-based plastics and show little or no negative impact on the environment at the same time (Oluwasina,

Olaleye, Olusegun, Oluwasina, & Mohallem, 2019). The biodegradation includes simultaneous hydrolysis and microbial attack. Starch is acknowledged to have a high biodegradation rate in the bioplastics (Hasan et al., 2020). The high degree of crystallinity and compact structure of fibers could restrict the enzymatic activity of microorganisms leading to a lower biodegradation rate (Fitch-Vargas et al., 2019). The weight loss of the composites with three crosslinkers are shown in Figure 4.38-40. For the composites without crosslinkers, the initial weight loss in day 0 was 29.02%, which might derive from the water-soluble glycerol because the analysis of weight loss was based on water solubility. The initial weight loss of the composites with different contents of crosslinkers ranged from 21.91 to 29.03% due to the formation of crosslinking, which were similar to the result of water solubility.

The weight loss for the composites with or without crosslinkers all increased significantly after 30 days ( $p < 0.05$ ). The weight loss of the composites with CA increased as the contents of CA increased from 0 to 3 wt%. This can be explained by that the addition of CA caused the decomposition of starch and facilitated the penetration of microorganism into the composites (Fitch-Vargas et al., 2019). These results were also reported by Praprudivongs and Wongpreedee (2020) in starch/eggshell powder/CA films, who observed that introducing CA led to unstable bioplastics in the soil.

Interestingly, the low water uptake and water solubility of bioplastics with EO did not retard the microbial degradation of the bioplastics (Oluwasina et al., 2019). The weight loss of the composites was improved by the addition of EO, while the contents of EO showed no obvious effect on the biodegradability of the composites. Especially, the addition of various contents of ESO resulted in significantly higher biodegradability of the composites from day 0 to day 30 compared to the control sample. The resulted composites presented high strength and good biodegradability. It can be concluded that the excellent biodegradability of starch blended bioplastics makes them promising

candidates for sustainable packaging applications in the near future.

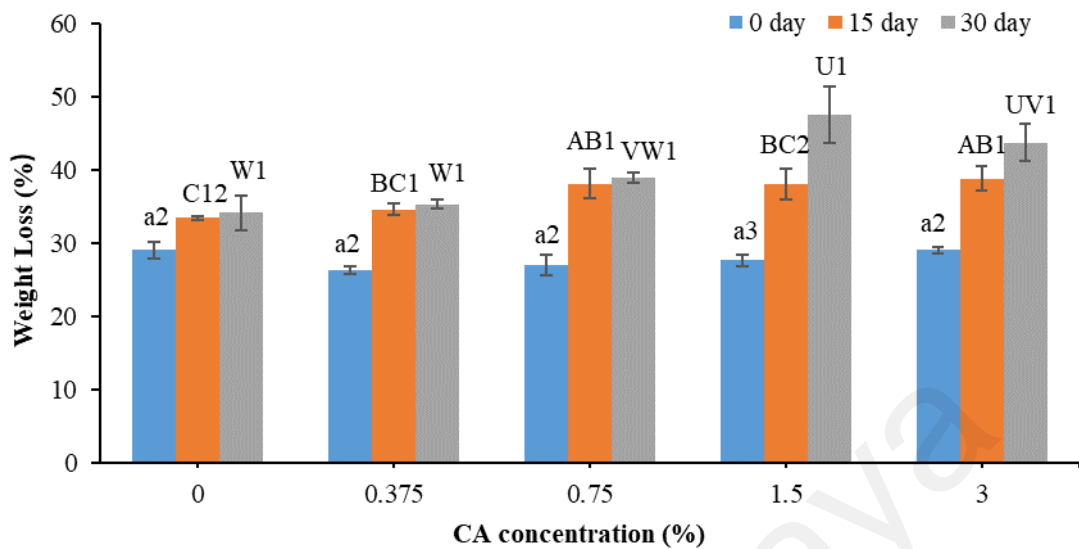


**Figure 4.38: The biodegradability of the crosslinked bioplastics with citric acid. a, A-C, U-W: Different letters within the same indicator present significant differences among the samples ( $p < 0.05$ ). 1-3: Different numbers mean significant differences among the specimens with different crosslinkers at the same concentration ( $p < 0.05$ )**

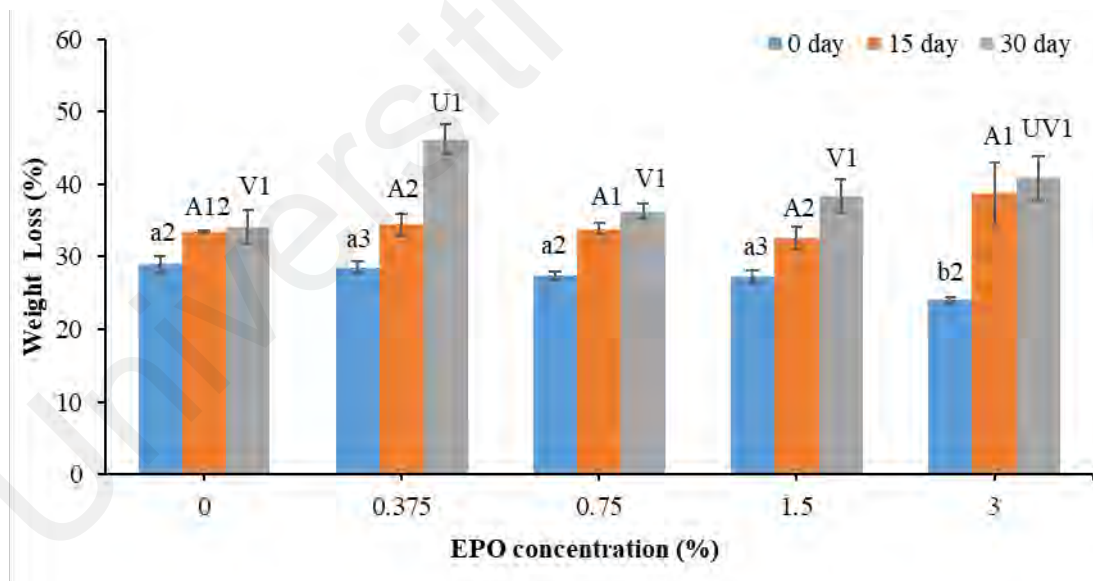


**Figure 4.39: The biodegradability of the crosslinked bioplastics with epoxidized palm oil. a-b, A, U-V: Different letters within the same indicator present significant differences among the samples ( $p < 0.05$ ). 1-3: Different numbers mean significant differences among the specimens with different crosslinkers at the same concentration ( $p < 0.05$ )**

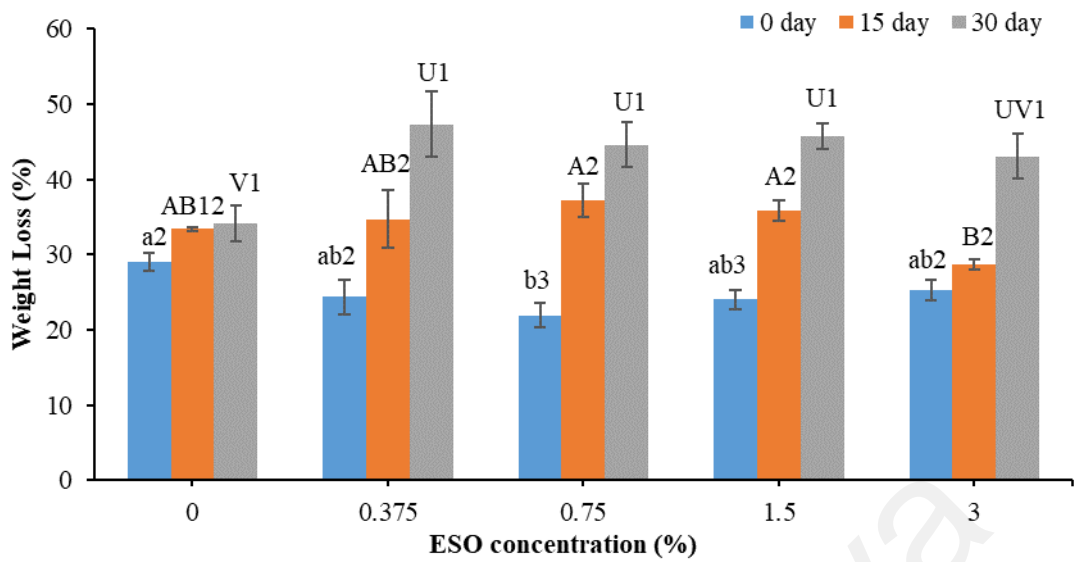


**Figure 4.40: The biodegradability of the crosslinked bioplastics with epoxidized soybean oil. a-b, A-B, U-V: Different letters within the same indicator present significant differences among the samples ( $p < 0.05$ ). 1-2: Different numbers mean significant differences among the specimens with different crosslinkers at the same concentration ( $p < 0.05$ )**

### **4.3 PART 3: Synthesis and characterization of starch/fiber-based bioplastics with citric acid-crosslinked epoxidized palm oil prepolymer (CEPO)**

#### **4.3.1 Fourier transform infrared spectroscopy (FTIR)**

ESO exhibited higher reinforcing effect on the composites than EPO (Balart et al., 2016). However, reinforced bioplastics with ESO were too brittle and would crack when cutting after conditioned. Moreover, EPO is the most abundant commodity oil in Malaysia. Therefore, EPO was chosen to conduct the experiment in this part.

The FTIR spectra for starch-based composites with EPO and CEPO are shown in Figure 4.41 and 4.42, respectively. In the spectra of the bioplastics, the bands in the 3287-3301  $\text{cm}^{-1}$ , 2923-2930  $\text{cm}^{-1}$ , 1743-1748  $\text{cm}^{-1}$ , and 993-1017  $\text{cm}^{-1}$  are characteristic of the vibrational stretching of O-H, C-H, C=O, and C-O-C (anhydroglucose ring), respectively (Wang et al., 2009). In comparison with the spectrum of the control bioplastic, the minor spectrum changes of the bio-composites containing EPO and CEPO were observed. After the addition of EPO or CEPO, the bands for O-H all shifted to lower wavenumbers. This indicated the hydrogen bond interactions were formed between oils and starch/glycerol/fibers. The bands around 2854-2856  $\text{cm}^{-1}$  corresponding to symmetric C-H stretching in methylene groups of EPO or CEPO intensified with EPO or CEPO contents increasing (Brandelero et al., 2012). Moreover, the composites with increasing contents of oils displayed more intense bands at wavenumbers of 1743-1748  $\text{cm}^{-1}$  (C=O). These characteristic bands of the bioplastics with CEPO were more intense than the bioplastics with EPO. This demonstrated the formation of ester groups between starch and CEPO. Additionally, the bands (C=O) could also be assigned to the overlapping bands from the ester bonds between glycerol and CA, unreacted CA, and the characteristic bands of lignin and hemicellulose.

The esterification reaction was further verified by the residual band of the washed starch/fibers/3%CEPO particles around 1744  $\text{cm}^{-1}$  as shown in Figure 4.43. It was

expected that the melt blending and compression molding process would further promote the esterification reaction (S. Sun et al., 2018; Ye et al., 2019). The previous studies showed that the epoxy groups of EO were consumed during the reaction with CA and subsequently the hydroxyl groups were introduced in the fatty acid chains (Pawar et al., 2016). The plausible mechanism about the epoxy ring opening reaction of EO with carboxyl groups in aqueous solution has been clearly presented in other studies (Gogoi et al., 2015b). This was also confirmed by disappearance of bands for epoxy groups ( $838\text{ cm}^{-1}$ ) in the spectrum of cured CEPO (Figure 4.44). This implied that complete reaction of EPO with CA has taken place. In the end, the possible reaction mechanism between starch/fibers and CEPO is summarized in Figure 4.45.

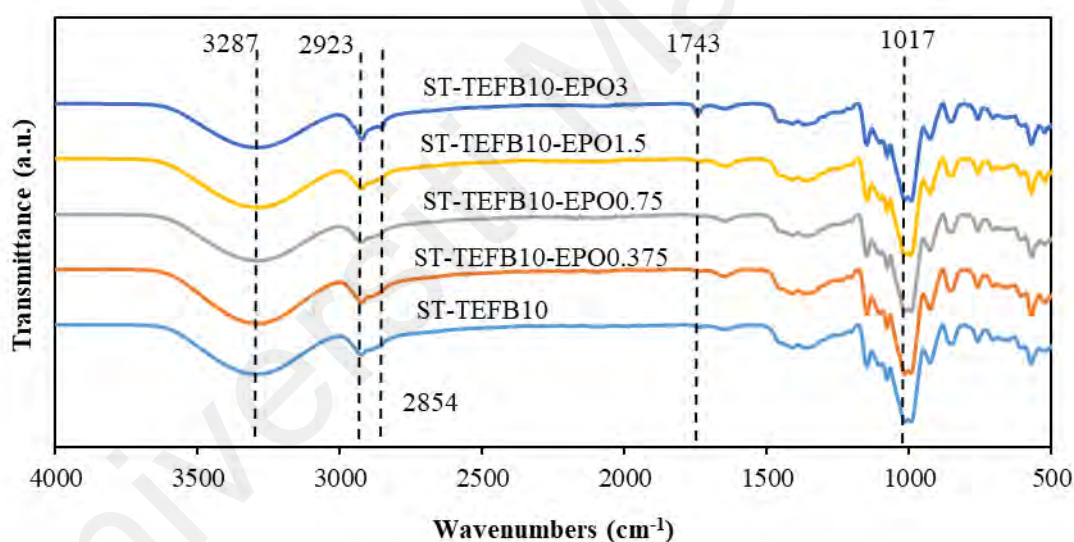


**Figure 4.41: Fourier transform infrared spectra of the bioplastics incorporated with epoxidized palm oil. The dashed lines indicate the bands at respective wavenumbers**

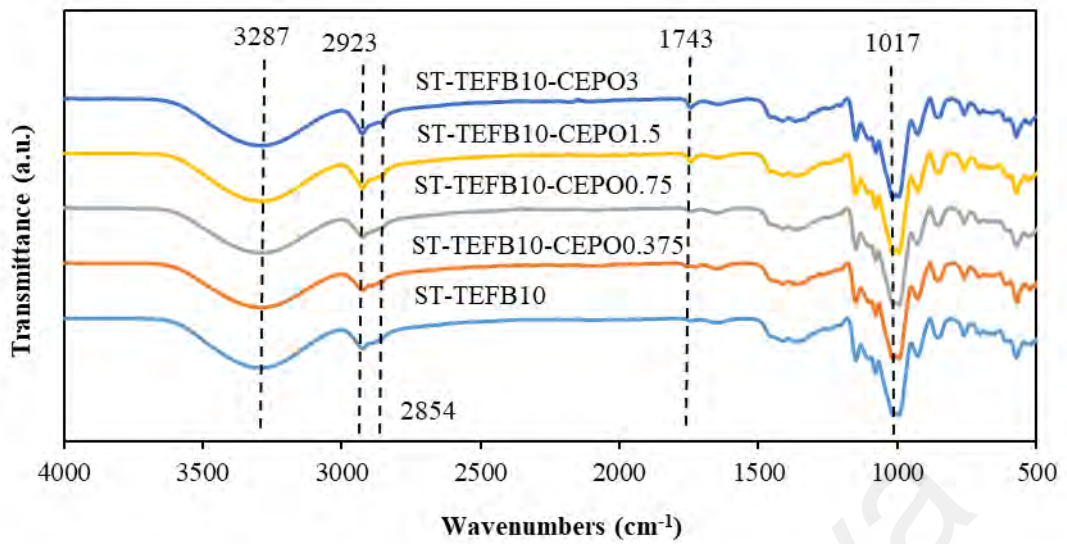


**Figure 4.42: Fourier transform infrared spectra of the bioplastics incorporated with citric acid-crosslinked epoxidized palm oil. The dashed lines indicate the bands at respective wavenumbers**

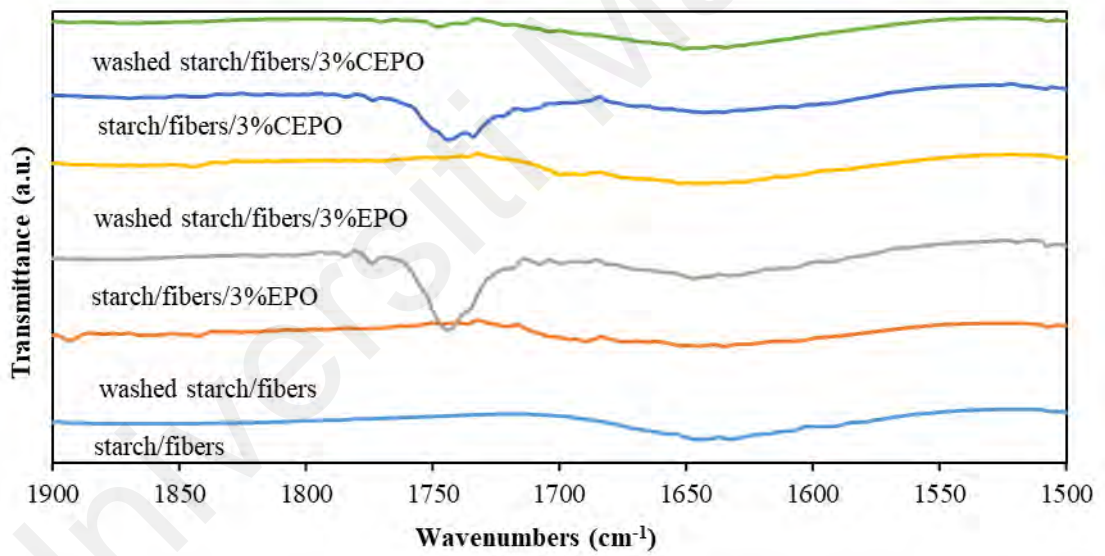


**Figure 4.43: Fourier transform infrared spectra of modified starch/fiber powders with epoxidized palm oil and citric acid-crosslinked epoxidized palm oil**

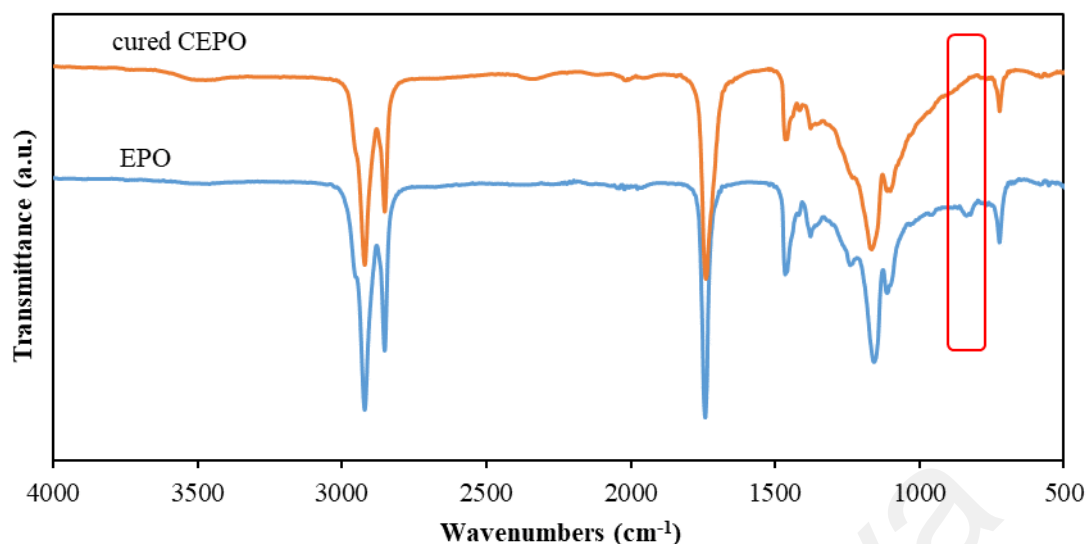


**Figure 4.44: Fourier transform infrared spectra of epoxidized palm oil and citric acid-crosslinked epoxidized palm oil. The red rectangle in the graph indicates the bands for epoxy group ( $838\text{ cm}^{-1}$ )**

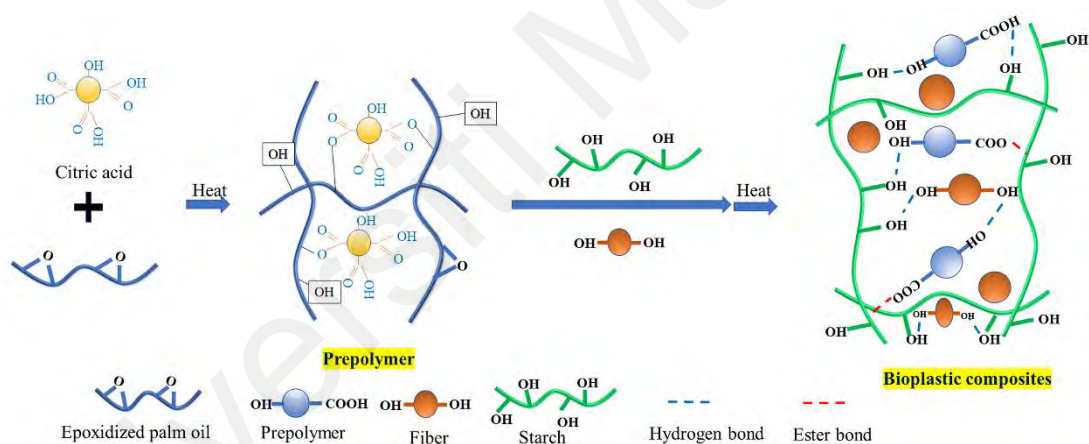


**Figure 4.45: Reaction mechanism between starch/fibers and citric acid-crosslinked epoxidized palm oil**

### 4.3.2 X-Ray diffraction (XRD)

XRD pattern can reflect the interactions of the components via the change in crystalline structure. The XRD patterns of starch and the prepared bio-composites are given in Figure 4.46. The raw starch exhibited the diffraction pattern of A-type with the typical peaks at  $2\theta$  of  $14.9$ ,  $17.3$ ,  $18.0$  and  $23.1^\circ$ . During the processing, the plasticizers penetrate into the starch granules, substitute intermolecular and intramolecular hydrogen bonds of starch with plasticizer-starch hydrogen bonds and alter the crystalline structure (Nguyen Vu &

Lumdubwong, 2016). For the studied bioplastics, the peaks for starch at 17.3, 18.0 and 23.1° were absent or less intense, indicating that the original crystalline structure of starch was disrupted completely by the processing (Belhassen et al., 2014). It was reported that the addition of lipids or other non-polar organic compounds hampered the presence of the B-type crystalline form of amylose, and the V-type single helical complex was the preferred form, which was mainly formed during melt extrusion (Jiménez et al., 2013a; Sartori & Menegalli, 2016). In the XRD patterns of the composites, a V-type pattern with typical diffraction peaks at  $2\theta$  equal to 13.5, 20.5 and 21.5° appeared (Kahvand & Fasihi, 2019; C. Zhang et al., 2018). The diffraction patterns of the composites were not apparently affected by the addition of EPO, which might indicate that the interaction between EPO and starch/fibers was weak (Zhao et al., 2018). However, the peaks at 21.5° became less intense on the diffraction curves of ST-TEFB10-CEPO with CEPO contents increasing. This could be attributed to that the carboxyl groups contributed to additional interactions with starch/fibers and the crosslinking reaction disrupted the ordered array of molecules (Wang et al., 2017). Crosslinking between CA and starch predominantly occurred in crystalline regions of the starch granules (S. Sun et al., 2018). The substitution of the hydroxyl groups of starch molecules with the ester groups prevented the inter- and intra-molecular hydrogen bindings, thus disrupting their crystal structures completely. It was also reported that the crosslinked starch molecules cannot reorganize in crystal structures (Ghosh Dastidar & Netravali, 2012). Other studies found that no obvious crystals in CA-crosslinked starch thermoplastics could be observed (Ning et al., 2007).

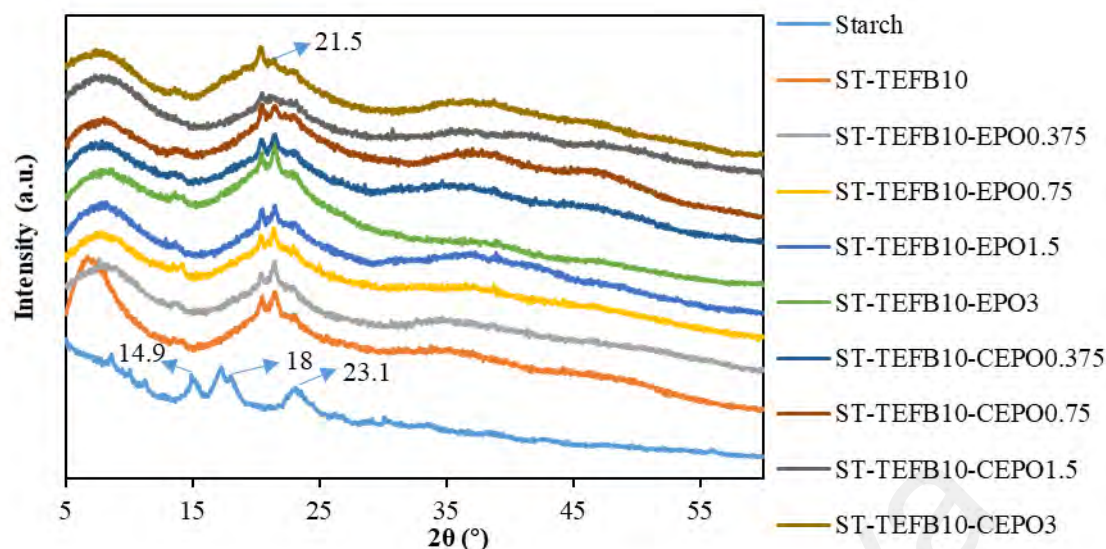


**Figure 4.46: X-ray diffraction patterns of starch and the bioplastics**

### 4.3.3 Scanning electron microscopy (SEM)

The surface photographs of all the fabricated bioplastics taken at magnifications of 400× and 1000× are shown in Figure 4.47a-j. The surface of ST-TEFB10 was homogeneous with few EFB fibers appearing sporadically. Some voids were observed which might be due to the presence of stearic acid (Jiménez et al., 2013b). Few white particles, which might be starch granules, were found clearly. After the addition of 0.75 wt% EPO or CEPO, the SEM images of the composites exhibited more micro-voids which were supposed to be oil micro-droplets (Orue et al., 2018). This indicated that EPO or CEPO was not well integrated in the bio-composites. Comparatively, the composites with EPO showed more micro-droplets than those with CEPO. However, fewer white particles were observed on the surface, which revealed that EPO or CEPO improved the plasticization of starch. When 3 wt% EPO was introduced, EPO was seen obviously as scattered micro-droplets on the surface of the composites. It was suggested that extra EPO might migrate to the films' surface during compression molding due to the phase separation, as previously described in starch-based films containing lipids (Acosta et al., 2015; Liu et al., 2019). When 3 wt% CEPO was incorporated into the blends, the oil

micro-droplets disappeared, and many cracks and holes were found. This indicated that the CEPO showed better compatibility with the matrix compared to EPO, but the compatibility was still weak. The esterification reaction between CEPO and starch was preferred to be performed at 130 °C for 2 h. But starch would decompose significantly at that condition (Olsson et al., 2013; Shi et al., 2007). Therefore, replacing CA with other more reactive compatibilizers such as silane coupling agents or maleic anhydride would help to accelerate the reaction (Dai, Xiong, Na, & Zhu, 2014; Xiong et al., 2013a).

Universiti Malaya

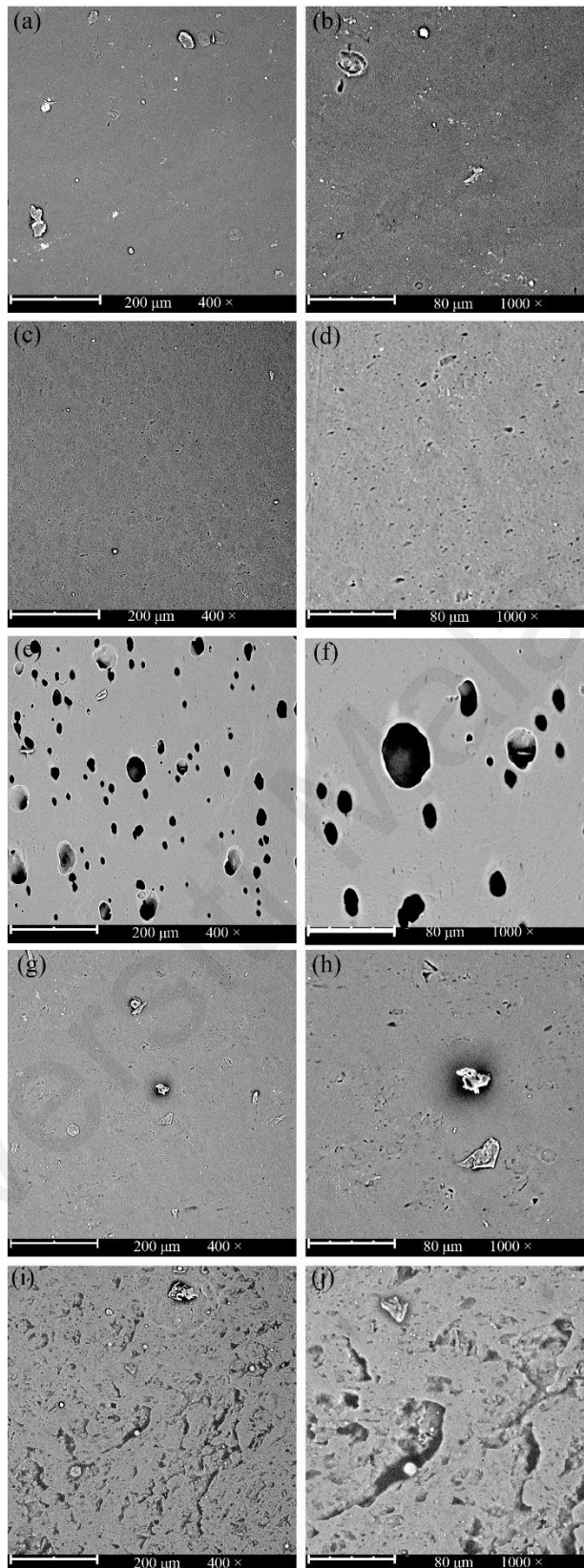


**Figure 4.47: The surface photographs of all the bioplastics. (a) ST-TEFB10, 400×, (b) ST-TEFB10, 1000×, (c) ST-TEFB10-EPO0.75, 400×, (d) ST-TEFB10-EPO0.75, 1000×, (e) ST-TEFB10-EPO3, 400×, (f) ST-TEFB10-EPO3, 1000×, (g) ST-TEFB10-CEPO0.75, 400×, (h) ST-TEFB10-CEPO0.75, 1000×, (i) ST-TEFB10-CEPO3, 400×, (j) ST-TEFB10-CEPO3, 1000×**

#### 4.3.4 Differential scanning calorimetry (DSC)

The DSC thermograms of the bio-composites are shown in Figure 4.48 and 4.49. The  $T_g$  was not detected because this transition is usually hard to be observed in starch-based bioplastics. Two endothermic peaks at 217.8 and 235.7 °C appeared in the curve of ST-TEFB10, which represented  $T_m$  of the composites. The separation of  $T_m$  might be attributed to the phase separation of the composites due to the addition of stearic acid (Khanonkon et al., 2016). The DSC curves of the composites with either EPO or CEPO all showed one melting peak, which indicated the enhanced miscibility of the composites. This could be ascribed to the partial crosslinking effect or strengthened interactions of EPO or CEPO with TEFB fibers and starch (Belhassen et al., 2014; Tee et al., 2014).

**Table 4.6: Thermal transition and decomposition parameters of all the prepared bioplastics crosslinked with epoxidized palm oil or citric acid-crosslinked epoxidized palm oil**

Sample codes	$T_{onset}$ (°C) <sup>a</sup>	$T_m$ (°C) <sup>b</sup>	$T_{5\%WL}$ (°C) <sup>c</sup>	$T_{max1}$ (°C) <sup>d</sup>	$T_{max2}$ (°C) <sup>d</sup>
ST-TEFB10	211.5	217.8/235.7	176.9	343.0	377.1
ST-TEFB10-EPO0.375	207.2	218.3	185.0	336.7	383.7
ST-TEFB10-EPO0.75	177.2	194.8	185.6	340.7	377.9
ST-TEFB10-EPO1.5	181.3	197.3	182.6	341.2	393.7
ST-TEFB10-EPO3	213.7	220.1	183.1	342.3	385.2
ST-TEFB10-CEPO0.375	212.5	218.8	184.6	339.2	373.9
ST-TEFB10-CEPO0.75	235.8	238.6	212.1	339.9	373.3
ST-TEFB10-CEPO1.5	224.8	229.8	160.3	337.2	375.9
ST-TEFB10-CEPO3	222.0	229.2	169.8	344.3	378.5

<sup>a</sup>: Onset melting temperature. <sup>b</sup>: Melting temperature. <sup>c</sup>: Temperature at 5% weight loss. <sup>d</sup>: Temperature at maximum decomposition rate.  $T_{onset}$  and  $T_m$  were determined by DSC.  $T_{5\%WL}$  and  $T_{max}$  were from TGA.

The melting temperatures for all the bioplastics are presented in Table 4.6. As the concentrations of EPO increased,  $T_{onset}$  and  $T_m$  of the composites reduced, attained the minimum  $T_{onset}$  at 177.2 °C and  $T_m$  at 194.8 °C for the ST-TEFB10-EPO0.75, and then increased again. The reduction of  $T_m$  might derive from the plasticizing effect of EPO toward the composites, which reduced the interfacial tension in the composites and facilitated the melting of the materials (Orue et al., 2018; Xiong et al., 2013a). Extra EPO caused the increase of  $T_m$ , which might be due to the incompatibility of excess EO and

starch/fibers, thus hampering the melting of the composites. This was consistent with the behavior of phase separation as shown by the SEM. However, the composites with various contents of CEPO showed an opposite trend of  $T_{onset}$  and  $T_m$  compared to those with EPO, with 0.75 wt% CEPO producing the highest  $T_m$  of 238.60 °C. This might be associated with the strong crosslinking effect between starch/fibers and CEPO (Javidi et al., 2016; Rodríguez et al., 2006). Crosslinking can reduce the molecular chain flexibility and restrain the molecular chain mobility (Zhang et al., 2019). However, 1.5-3 wt% CEPO contributed to the reduction of  $T_m$ . As discussed above, the incompatibility of excess CEPO and starch/fibers would hamper the melting of the composites and increase  $T_m$ . This reduction of  $T_m$  might be caused by the presence of CA. The melt temperatures ( $T_m$  and  $T_{onset}$ ) are quite dependent on the acid content and as a consequence on the molar mass of starch in the bio-composites (Da Róz et al., 2011). It was found that that carboxyl acids can promote the acid hydrolysis of starch molecular chains, causing the decrease in molecular weight of polymer and the chain entanglement. Therefore, during the extrusion process, the plasticizing effect of glycerol was favored and elevated by CA. Therefore, the free volume of starch chains increased, and the starch molecular movement was motivated (Zhang et al., 2019). This lowering of the melting temperature may be also explained by the decrease in the size of crystallite (lamella thickness), as revealed by the XRD analysis (Da Róz et al., 2011). As a result,  $T_m$  of the bioplastics decreased with increasing CEPO contents from 0.75 to 3 wt%.

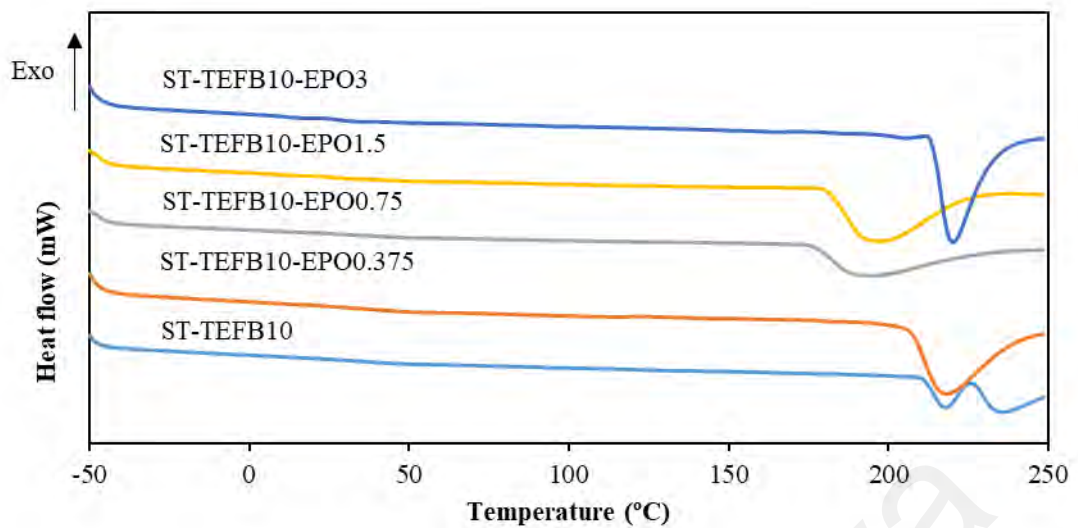


**Figure 4.48: Differential scanning calorimetry thermograms of the bioplastics incorporated with epoxidized palm oil**

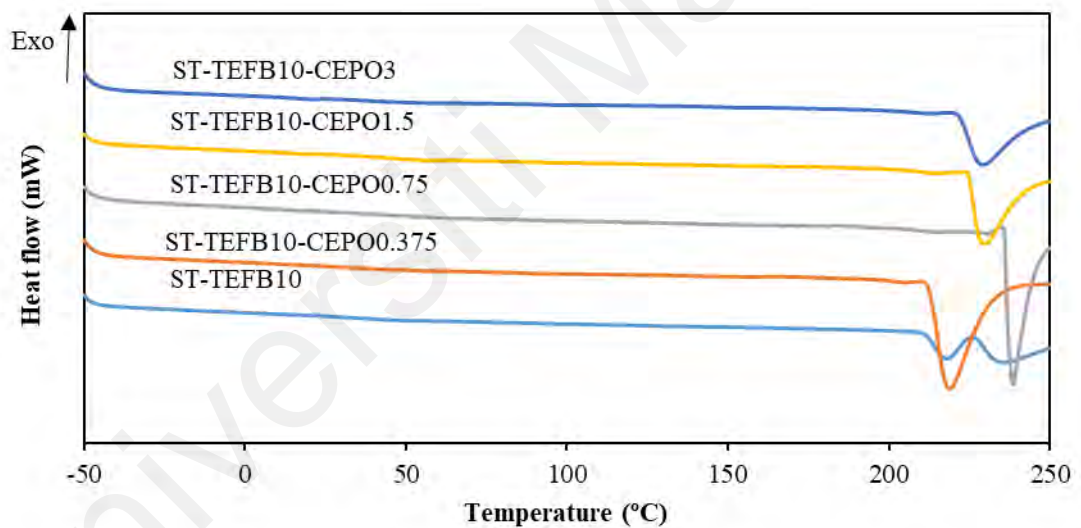


**Figure 4.49: Differential scanning calorimetry thermograms of the bioplastics incorporated with citric acid-crosslinked epoxidized palm oil**

#### 4.3.5 Thermogravimetric analysis (TGA)

Thermal stability of starch-based bioplastics was evaluated by TGA and the results are depicted in Figure 4.50 and 4.51. The thermal decomposition processes for all the bioplastics exhibited three-step weight loss at the temperature ranges of 30-270 °C, 270-430 °C and 430-600 °C, respectively. Initial mass loss is assigned to loss of moisture and

glycerol present in the bioplastics. The most significant weight loss occurred in the second step corresponding to decomposition of starch, glycerol, fibers, and oils (Harini et al., 2018). The plots suggested that the addition of various contents of EPO or CEPO caused less weight loss compared to the composites without oils during the decomposition process.

The  $T_{5\%WL}$  of ST-TEFB10 was 176.9 °C (Table 4.6). After the addition of EPO, it was increased to 182.6-185.6 °C. This phenomenon was opposite to the results in PART 2 for the composites with EPO prepared by solution casting. In the process of drying the solution, part of EPO might react with water to produce the polyols or other by-products, which might reduce the thermal stability of EPO (Orue et al., 2018). In contrast, the reaction was mainly conducted between EPO and starch/fibers when the samples were prepared by reactive blending. Therefore, the different preparation methods might lead to the opposite change of  $T_{5\%WL}$ . When CEPO was incorporated,  $T_{5\%WL}$  increased and reached the maximum of 212.1 °C at 0.75 wt% CEPO. The higher  $T_{5\%WL}$  of the samples should be due to the higher thermal stability after crosslinking. Then,  $T_{5\%WL}$  remarkably decreased to 160.3-169.8 °C as the contents of CEPO increased from 0.75 to 3 wt%. The decrease of  $T_{5\%WL}$  might be related to excessive CA which can not react sufficiently with EPO or starch/fibers and decomposed during heating process. It also might result in the decomposition of starch molecules.

The DTG curves of the composites showed two maximum decomposition rate peaks. The  $T_{max1}$  and  $T_{max2}$  for ST-TEFB10 were 343.0 and 377.1 °C, respectively. The addition of EPO or CEPO caused a slight reduction of  $T_{max1}$  except 3 wt% EPO.  $T_{max2}$  of the composites increased to 377.9-393.3 °C after the addition of EPO, while  $T_{max2}$  ranged from 373.3 to 378.5 °C with CEPO incorporated. It was investigated that starch plasticized with oil had a better thermal stability than starch plasticized only with glycerol (Balart et al., 2016). It is remarked that the main uses of epoxidized vegetable oils are as

plasticizers and thermal stabilizers for PVC. This stabilizing effect could be attributed to formation of hydrogen bonds between polymer chains and the plasticizers which can lead to improved thermal stability (Balart et al., 2016). Also, the presence of EPO can create a protective physical barrier on the surface of the bioplastics which prohibited the permeability of volatile decomposition products from the bioplastics and delayed the degradation process of the bioplastics eventually (Silverajah, Ibrahim, Zainuddin, Yunus, & Hassan, 2012). In addition, thermal stability of the bioplastics with oils was strictly dependent on the chemical structures of vegetable oils and the content of unsaturated fatty acid (Volpe et al., 2018). These results suggested that the composites with EPO revealed higher thermal stability than the samples with CEPO and control sample, and the thermal stability of the composites with CEPO was almost as good as that of control sample. This was probably due to the degradation of some of the starch molecules in the crosslinked bioplastics with CEPO when they were cured at high temperatures for the crosslinking reaction.

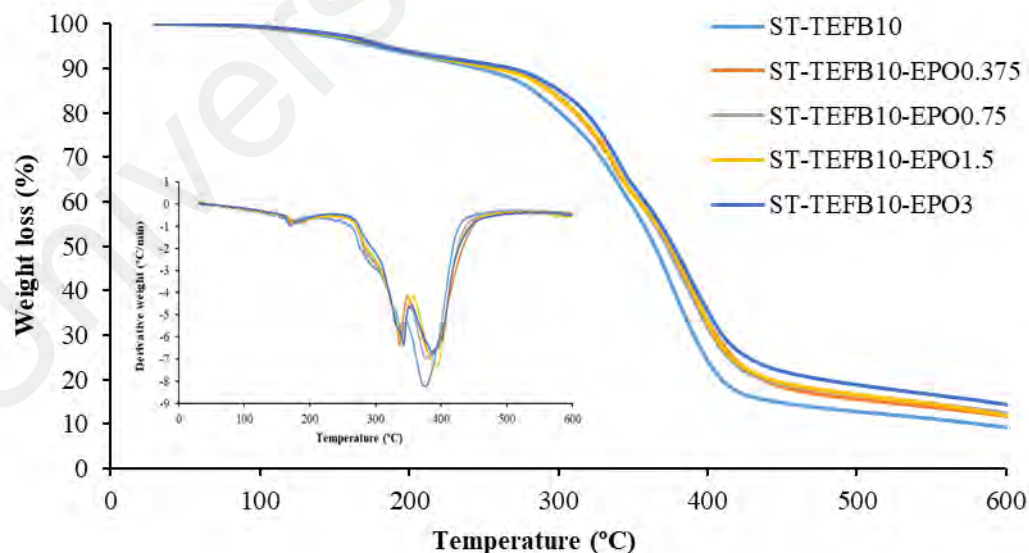


**Figure 4.50: Thermal behaviors of the bioplastics with epoxidized palm oil**

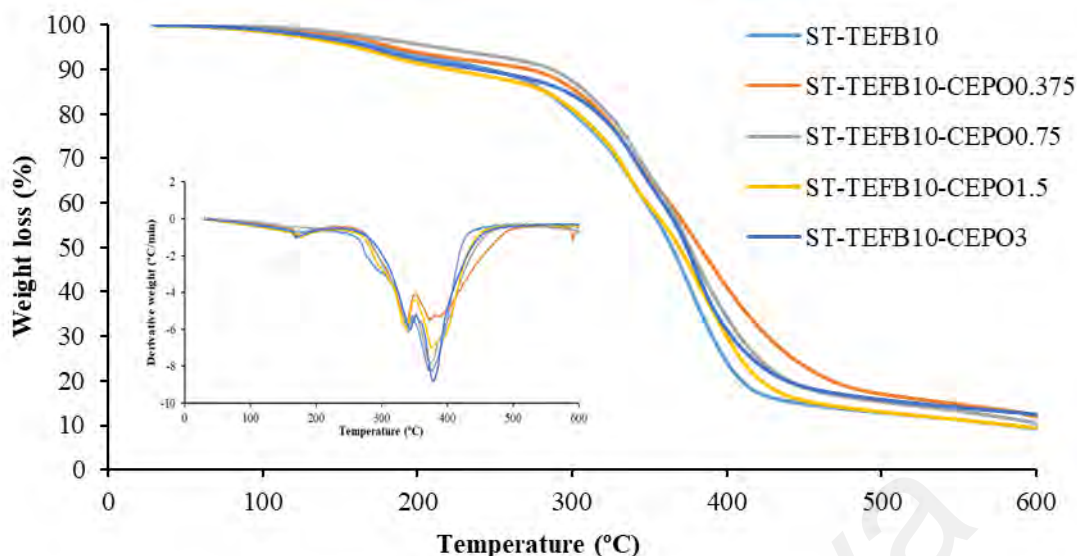


**Figure 4.51: Thermal behaviors of the bioplastics with citric acid-crosslinked epoxidized palm oil**

#### 4.3.6 Mechanical properties

The tensile strength and elongation at break of the prepared bioplastics were determined in Figure 4.52 and 4.53. The tensile strength and elongation at break of ST-TEFB10 was 3.67 MPa and 55.95%, respectively. The tensile strength increased significantly with 0.375-0.75 wt% EPO or CEPO added ( $p < 0.05$ ), and then sharply decreased when the contents of EPO or CEPO reached 1.5-3 wt% ( $p < 0.05$ ). Films incorporated with hydrophobic lipids generally led to the decrease in tensile strength with the concomitant increase in elongation at break due to the reduced interaction and incompatibility (Tongnuanchan et al., 2016). The major reason for the increased tensile strength confirmed the enhanced hydrogen bonds or crosslinking effect between starch/fibers and oils (Belhassen et al., 2014; Ortega-Toro et al., 2014). The decrease in the strength with up to 1.5 wt% EPO or CEPO might arise from phase separation. It was shown that the accumulation of the compatibilizers can possibly reduce the tensile strength of the bio-composites when their concentrations increased (Khanonkon et al., 2016). In addition, the oil-oil interactions derived from extra oils would replace the biopolymer-oil interactions, which was reported to reduce the strength of the composites

(Brandelero et al., 2012).

The blending of CEPO led to a higher evolution in the tensile strength of the composites than EPO ( $p < 0.05$ ). This effect was likely to be due to the stronger crosslinking of CEPO with starch. This results also confirmed that CA could act as a compatibilizer for EPO and starch (Ortega-Toro et al., 2014).

The elongation at break of the bioplastics decreased after the addition of both oils (0.375-0.75 wt%), which was expected owing to the strong reinforcing effect of EPO and CEPO. However, the addition of 3 wt% EPO or CEPO to the composites caused a significant increase in elongation at break, which might be caused by the formation of EO-EO interaction at higher oil contents due to their flexible properties. The excess oils could not crosslink sufficiently with starch/fibers and might contribute to the plasticization of the starch like the non-epoxidized oils (Basiak et al., 2016; Javidi et al., 2016). As a result, the looser structure of the composites was developed. This corresponded to the microvoids of oil rich phase in the SEM micrographs.

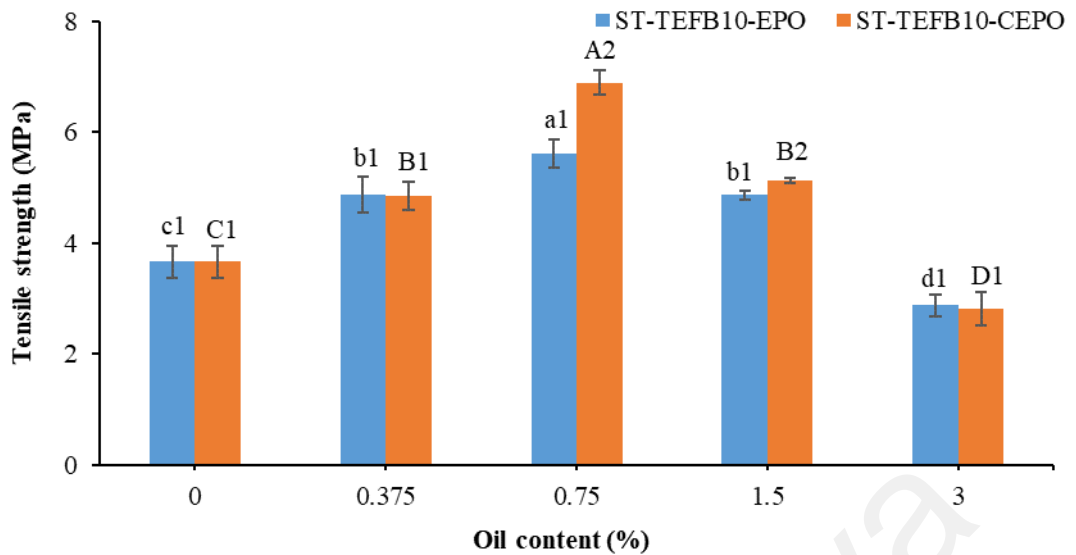


**Figure 4.52: Tensile strength of the prepared bioplastics. a-d, A-D: Significant differences among the specimens ( $p < 0.05$ ) are shown by diverse letters in the same indicator. 1-2: Different numbers demonstrate significant differences ( $p < 0.05$ ) between the samples with EPO and CEPO at the same loading**

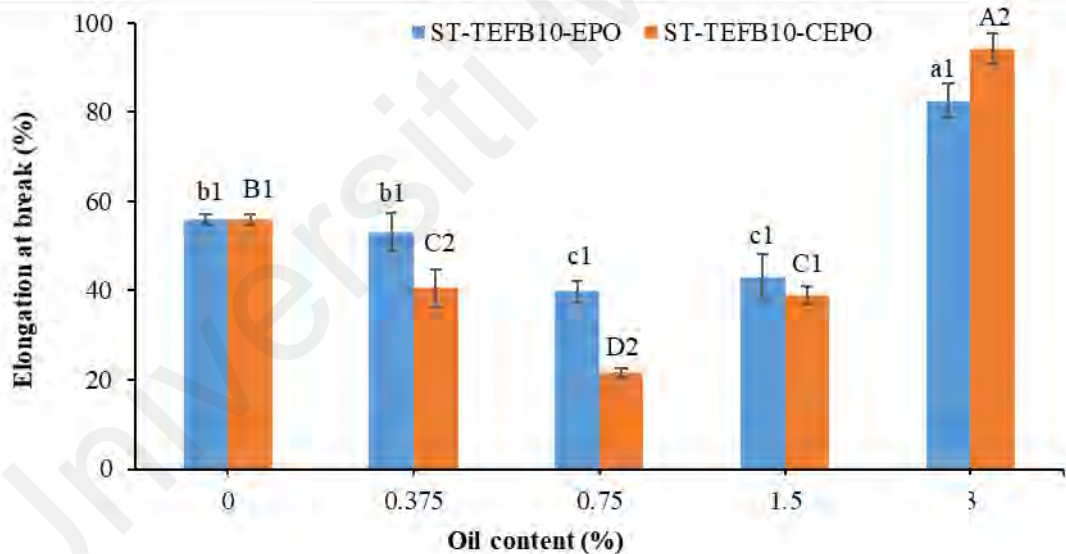


**Figure 4.53: Elongation at break of the prepared bioplastics. a-c, A-D: Significant differences among the formulations ( $p < 0.05$ ) are shown by different letters in the same indicator. 1-2: Different numbers demonstrate significant differences ( $p < 0.05$ ) between the samples with EPO and CEPO at the same loading**

#### 4.3.7 Water resistance properties

The effect of EPO and CEPO addition on the water resistance properties of the prepared bioplastics is analyzed in Figure 4.54-56. The moisture content, water uptake

and solubility of ST-TEFB10 were 8.76%, 24.14% and 38.99%, respectively, which were in agreement with previous reports (Chiumarelli & Hubinger, 2012). The results revealed that the addition of EPO or CEPO showed no remarkable effect on the moisture contents of the composites ( $p > 0.05$ ), which indicated that the samples were well-conditioned before characterization. Water solubility of the bio-composites was only slightly reduced by the introduction of various contents of EPO or CEPO ( $p > 0.05$ ), while the water uptake decreased significantly by the addition of various contents of both oils ( $p < 0.05$ ). The hydrogen bonds or crosslinking reaction between oils and starch/fibers could improve the interfacial adhesion of the composites and reduce the water sensitivity. In addition, the long fatty acid chains of oils would mask the surface hydroxyl groups of starch and EFB fibers, which might restrict the swelling of the bio-composites and cause lower water uptake and solubility of the composites (Belhassen et al., 2014). However, the oil concentrations and types had no remarkable effect on the water uptake ( $p > 0.05$ ). This might be attributed to serious phase separation and the micro-void structure with increasing contents of oils incorporated, as demonstrated by the SEM images.

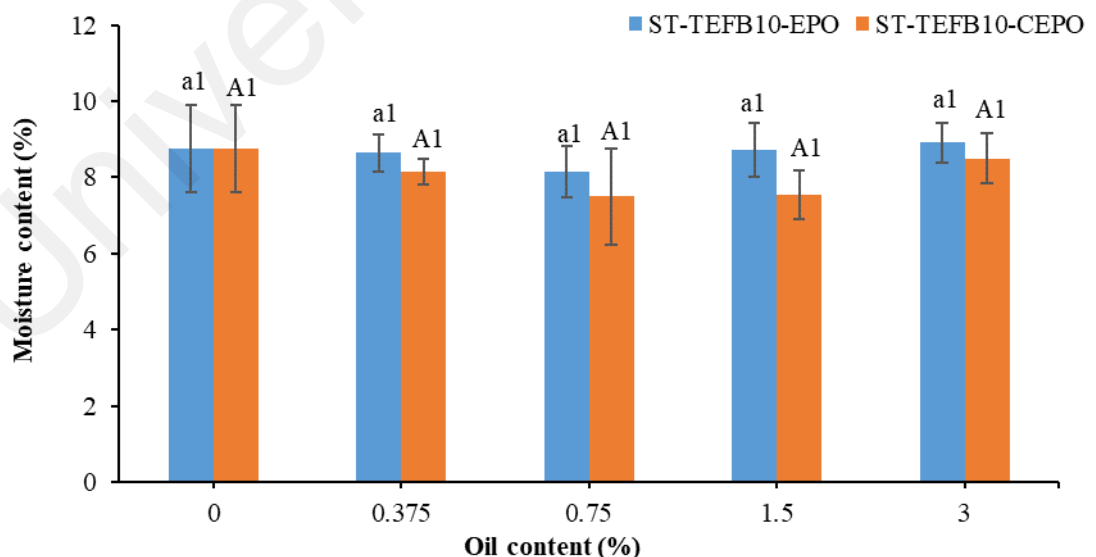


**Figure 4.54: Moisture content of starch-based bioplastics. a, A: Same letter within the same indicator indicates no significant difference among the samples ( $p > 0.05$ ). 1: Same number indicates no significant difference ( $p > 0.05$ ) between the formulations with EPO and CEPO at the same concentration**

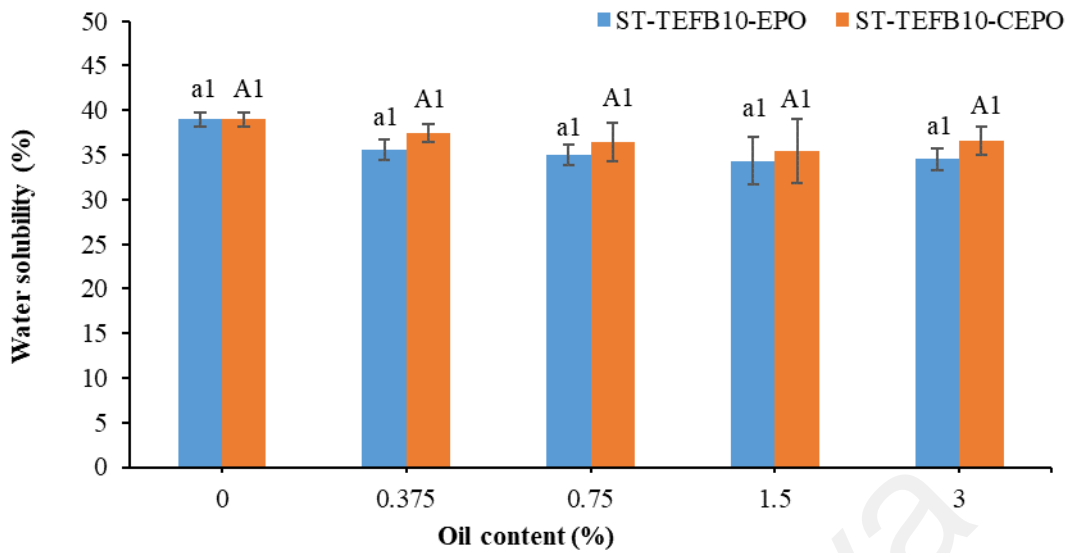


**Figure 4.55: Water solubility of starch-based bioplastics. a, A: No significant difference among the formulations ( $p > 0.05$ ) is shown by same letter within the same indicator. 1: Same number demonstrates no significant difference ( $p > 0.05$ ) between the samples with EPO and CEPO at the same concentration**

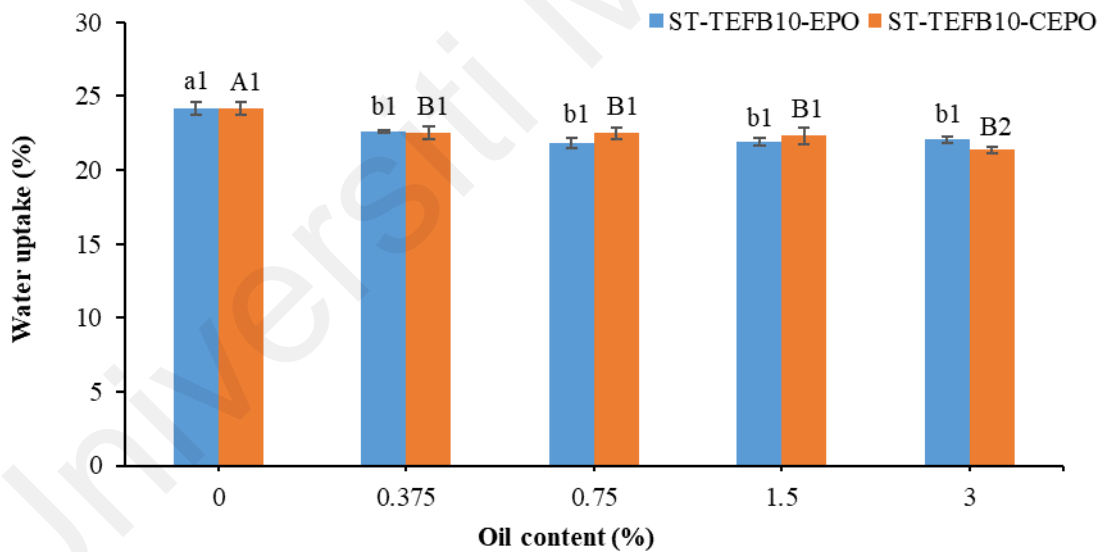


**Figure 4.56: Water uptake of starch-based bioplastics. a-b, A-B: Different letters within the same indicator denote significant differences among the samples ( $p < 0.05$ ). 1-2: Different numbers mean significant differences ( $p < 0.05$ ) between the formulations with EPO and CEPO at the same concentration**

#### 4.3.8 Opacity

The opacity of the bioplastics is a critical property in the application for food packaging. The opacity of the samples is directly related to the surface morphology and

internal heterogeneity (Jiménez et al., 2013b). Figure 4.57 describes the opacity of studied bioplastics with EPO or CEPO. The ST-TEFB10 recorded an opacity value of 0.16. The effect of oil addition contributed to the changes of opacity depending on the loadings of oils incorporated. The addition of 0.75 wt% EPO provided significantly higher opacity to the composites at 0.20 ( $p < 0.05$ ), while the opacity of the other composites was similar ( $p > 0.05$ ). This result has been reported previously in starch-based composites containing fatty acids (Jiménez et al., 2012; Thakur et al., 2017). This could be explained by the different refractive index of EO and starch (Saberri et al., 2017). Moreover, addition of oils prompted larger matrix disorder in the composites due to the coalescence of lipids on the bioplastics surface (Sartori & Menegalli, 2016). Lipids, which are not compatible with hydrophilic biopolymers, would remain in the form of dispersed phase in the bioplastics, thus promoting the light dispersion and causing a lower transparency (Acosta et al., 2015).

When CEPO was incorporated into the composites, it contributed to a significant increase of the opacity to 0.19 and 0.21 at 0.75 and 1.5 wt% CEPO, respectively ( $p < 0.05$ ). The decrease of transparency might be related to the appearance of new crystalline domains presenting a different refractive index from the amorphous phase. It was related that the crosslinking activity within the polymeric chain modified the refractive index of the composites and hindered the passage of the light (Acosta et al., 2015; Jiménez et al., 2012). The composites with 3 wt% CEPO showed no remarkable difference of the opacity compared to ST-TEFB10 ( $p > 0.05$ ). This might be due to that the incorporation of 3 wt% CEPO in the composites caused phase separation and promoted the penetration of light through these voids.

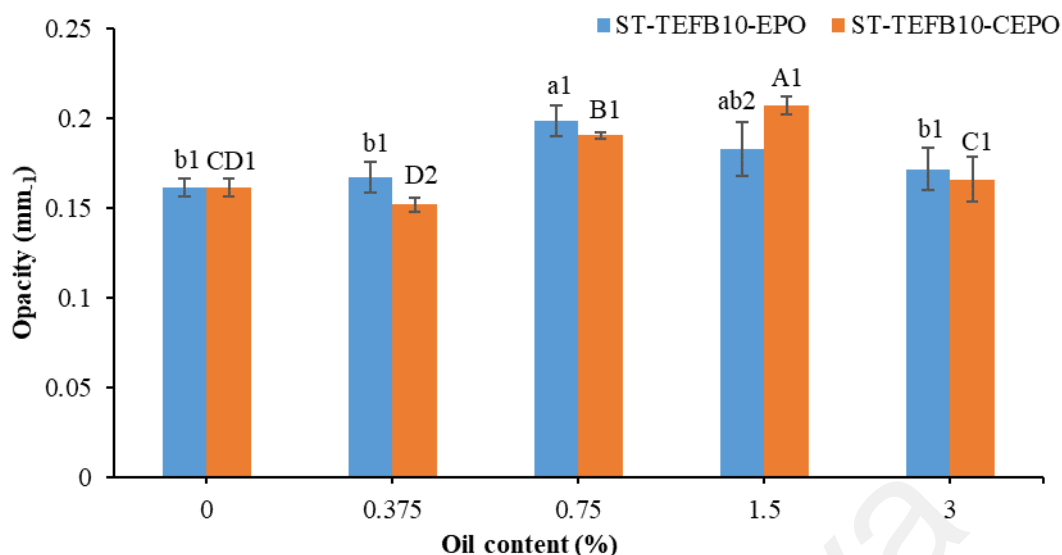


**Figure 4.57: The opacity of starch-based bioplastics. a-c, A-D: Significant differences among the samples ( $p < 0.05$ ) are indicated by different letters within the same indicator. 1-2: Different numbers present significant differences ( $p < 0.05$ ) between the formulations with EPO and CEPO at the same loading level**

#### 4.3.9 Water vapor permeability (WVP)

The WVP of the starch-based bioplastics with different concentrations of EPO or CEPO is presented in Figure 4.58. The WVP of the composites incorporated with lipids is highly dependent on the properties of lipids, chain length of the fatty acids and the interactions among the components (Thakur et al., 2017). It can be seen that the highest WVP ( $4.74 \times 10^{-5} \text{ g m/m}^2 \text{ h Pa}$ ) was the control specimen (ST-TEFB10). The high WVP of the composites derived from the hydrophilicity of starch, fibers, and glycerol. The addition of EPO significantly decreased the WVP ( $p < 0.05$ ) with 0.75 wt% EPO showing the minimum WVP ( $4.43 \times 10^{-5} \text{ g m/m}^2 \text{ h Pa}$ ). There was no notable difference of the WVP among the composites with different contents of EPO. This might be attributed to the serious oil aggregation behavior with higher contents of EPO introduced, as indicated by the SEM images of bioplastics with 3 wt% EPO. It was noticed that the WVP decreased markedly to  $4.08 \times 10^{-5} \text{ g m/m}^2 \text{ h Pa}$  with the increase of CEPO from 0 to 3 wt% ( $p < 0.05$ ). The addition of lipid generally decreased the WVP of the studied bio-composites as the hydrophobic lipid increased the hydrophobicity of the composites and made water

vapor penetration become more difficult, as observed in previous studies (Ge et al., 2019). Moreover, the shielded hydroxyl groups of starch by the hydrophobic layers also reduced the water sensitivity of the composites by acting as a barrier that blocked the incoming water vapors (Balakrishnan et al., 2019). In addition, the interactions among starch, fibers, and the crosslinking agents could have produced a tortuous path to prevent water vapor passing through (Ray & Okamoto, 2003).

The composites with CEPO showed lower WVP compared to those with EPO. This behavior might be ascribed to the fact that the esterification reaction between CEPO and starch grafted hydrophobic ester groups in the starch chains, which hampered the water molecules through the matrix (Garcia et al., 2014). Crosslinking formed a tight structure and restricted the movements of starch molecules, therefore reducing the WVP of the composites (Reddy & Yang, 2010; Yildirim-Yalcin et al., 2019). Also, it was found that the presence of CA gave rise to the decrease of WVP because the hydrophilic groups were replaced by the hydrophobic ester groups (Seligra et al., 2016). Additionally, this might also be due to the compatibilizing effect of CA, which provoked a more homogeneous and compact structure and decreased the phase separation of starch/fibers and oils (Garcia et al., 2014).

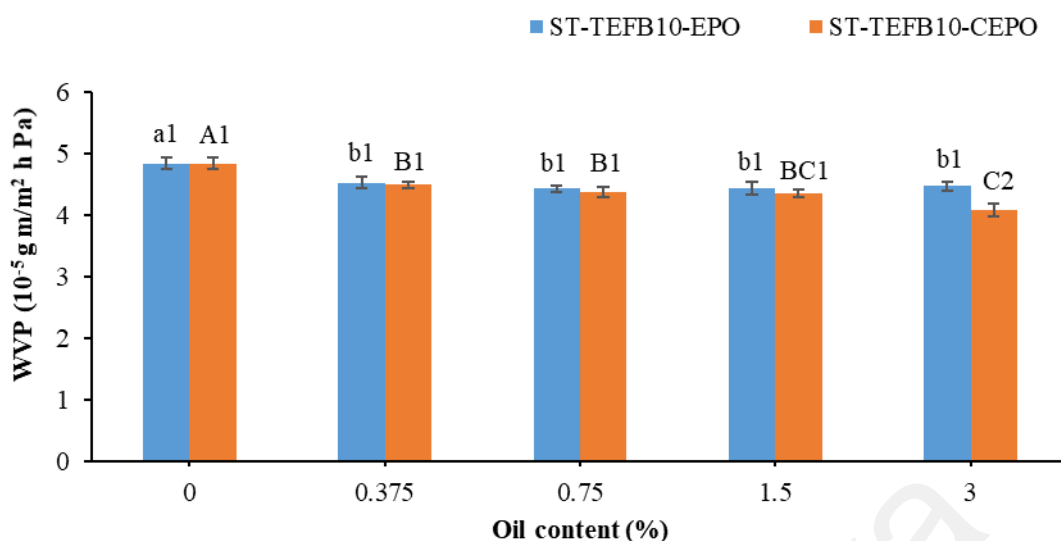


**Figure 4.58: Water vapor permeability of starch-based bioplastics with epoxidized palm oil and citric acid-crosslinked epoxidized palm oil. a-b, A-C: Significant differences among the samples ( $p < 0.05$ ) are indicated by different letters within the same indicator. 1-2: Different numbers present significant differences ( $p < 0.05$ ) between the formulations with EPO and CEPO at the same loading level**

#### 4.3.10 Biodegradability

Biodegradability of the bioplastics could be affected positively or negatively by the moisture content of the soil, nature microbe, and the properties of bioplastics such as density, moisture, and the presence of plant bioactive (Oluwasina et al., 2019). In soil, water diffuses into the bioplastics, causing swelling of the samples and enhancing biodegradation because of the increases of microbial growths. Figures 4.59 and 4.60 describe the weight loss of the composites with EPO and CEPO, respectively. The initial weight loss of the control sample was 27.92% based on the water solubility analysis and its weight loss increased to 44.7% after 30 days. The addition of EPO or CEPO showed no significant effect on the weight loss of the composites at day 0. The weight loss of the composites with various contents of EPO increased gradually as the degradation time increased and attained significant difference after 30 days ( $p < 0.05$ ). The loading levels of EPO presented no remarkable effect on the weight loss ( $p > 0.05$ ). These results confirmed that the biodegradability of the bioplastics was not affected by the

incorporation of EPO, which might be due to the weak interaction between EPO and starch matrix.

The biodegradability of the composites synthesized with CEPO was not affected by 0.375 wt% CEPO compared to that of the control group, but it was reduced significantly as the contents of CEPO increased from 0.75 to 3 wt% after 30 days. This was because EPO were tightly combined with starch by the crosslinking effect of CA, which decreased moisture absorption and prevented microorganisms from decomposing the materials (Oluwasina et al., 2019). These results agreed with the previous outcomes in starch-based films which showed that crosslinking slowed biodegradability (Seligra et al., 2016).

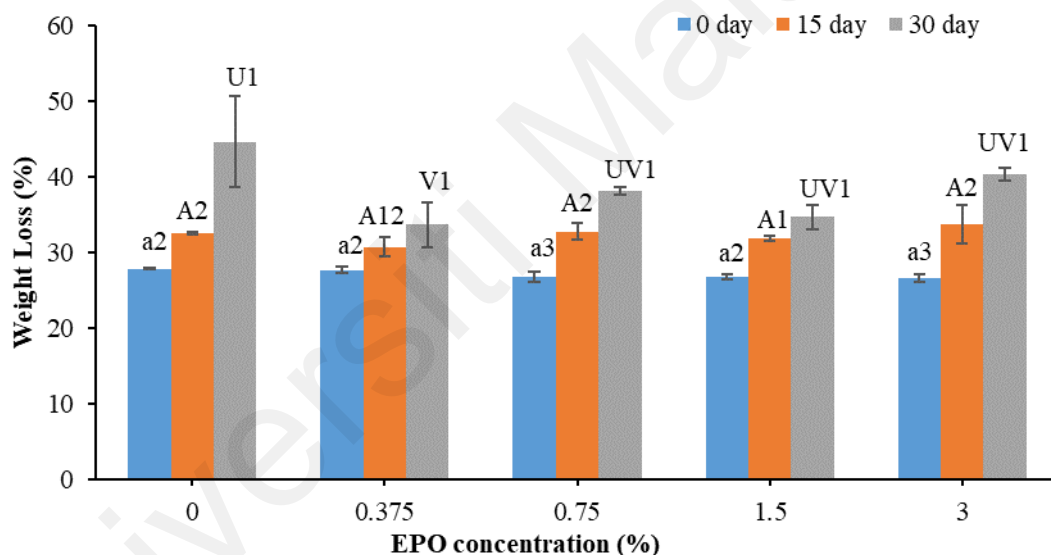


**Figure 4.59: The biodegradability of starch-based bioplastics with epoxidized palm oil. a, A, U-V: Significant differences among the samples ( $p < 0.05$ ) are indicated by different letters within the same indicator. 1-3: Different numbers present significant differences ( $p < 0.05$ ) of weight loss with time increasing at the same EPO level**

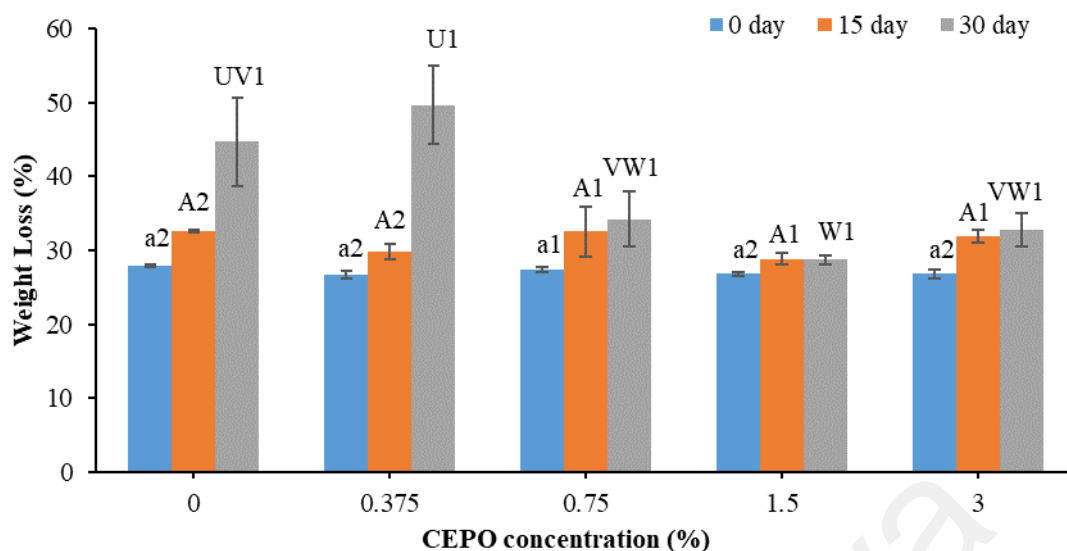


**Figure 4.60: The biodegradability of starch-based bioplastics with citric acid-crosslinked epoxidized palm oil. a, A, U-W: Significant differences among the samples ( $p < 0.05$ ) are indicated by different letters within the same indicator. 1-2: Different numbers present significant differences ( $p < 0.05$ ) of weight loss with time increasing at the same CEPO level**

#### 4.3.11 Comparison of the properties of starch-based bioplastics and low-density polyethylene (LDPE)

Piñeros-Hernandez, Medina-Jaramillo, López-Córdoba, and Goyanes (2017) reported that packaging application took up about 39.6% of total plastics and accounted for the largest market share. LDPE is one of the most widely used polymers for packaging in the world. However, LDPE is non-biodegradable and causes the plastic pollution (Li et al., 2015). Nowadays, the biodegradable starch-based bioplastics shows the interesting and promising potential to replace or minimize the use of petrochemical-based plastic such as LDPE (Owi et al., 2019).

Some properties of the prepared bioplastics (ST-TEFB10-CEPO0.75) in the study were compared to those of commercial LDPE (Table 4.7). Tensile strength of the bioplastics (6.90 MPa) was comparable to LDPE (7.42 MPa), while the elongation at break was very low (21.60%) in contrast with stretchable LDPE (279.21%). The bioplastics showed better transparency and biodegradability, but extremely higher water uptake and water

solubility compared to LDPE. Therefore, the water sensitivity of bioplastics is the key disadvantage compared to LDPE, which should be paid more attention in the future. In conclusion, these environmentally friendly starch-based bioplastics in this study have the potential to replace part of LDPE in the plastic industry.

**Table 4.7: Properties of the bioplastics prepared in the study and commercial low-density polyethylene in the market**

<b>Items of the samples</b>	<b>ST-TEFB10-CEPO0.75</b>	<b>LDPE</b>
Tensile strength (MPa)	6.90±0.22	7.42±0.44
Elongation at break (%)	21.60±1.05	279.21±25.48
Water uptake (%)	22.47±0.41	0
Water solubility (%)	36.39±2.18	0.53±0.069
Opacity (mm <sup>-1</sup> )	0.19±0.0020	0.27±0.0087
Biodegradability (%)	34.21%	0

## CHAPTER 5: CONCLUSIONS AND RECOMMENDATIONS

### 5.1 Conclusions

This study aimed to synthesize starch-based bioplastics with enhanced mechanical and water resistance properties using lignocellulosic fibers and crosslinking agents. EFB fibers were subjected to thermal and alkaline treatments in order to improve their adhesion with starch matrix. The treatments resulted in significant composition and structure changes of the fibers. The surface materials such as spherical particles (tyloses), fatty acid, lignin, or hemicellulose were partially removed, which led to cleaner surfaces as revealed by the FTIR and SEM. There was remarkable loss of fibers and deterioration of the fiber surface with alkali contents exceeding 10 wt% of fibers in the thermal treatment. XRD profiles showed that TEFB10 fibers showed the highest CrI. TGA results revealed that the treatments decreased the thermal stability of the fibers. These changes further affected the reinforcing performance of the fibers in the bioplastics. SEM analysis indicated a good fiber dispersion in the starch-based bioplastics. The composites with TEFB fibers exhibited lower  $T_m$  than the composites with raw EFB fibers. The addition of raw EFB and TEFB fibers enhanced the thermal stability of the bioplastics. EFB fibers treated with 10 wt% NaOH obtained the yield of 52.44% and produced the best reinforcing effect on the properties of the bioplastics. The tensile strength of the produced bioplastics was increased by 82.22% compared to neat ST and the water solubility showed the minimum value at 28.81%. At the same time, bioplastics with TEFB fibers presented similar opacity to pure starch-based bioplastics. These results obviously demonstrated that the simple and effective fiber treatment methodology could maximize the utility of hemicellulose and lignin-containing lignocellulosic fibers to reinforce the starch-based bioplastics with superior mechanical and water resistance properties.

Then, the effect of different concentrations of TEFB10 fibers on the properties of starch-based bioplastics was investigated. A good dispersion of 2.5-5 wt% TEFB10 fibers within the plasticized starch matrix was evidenced by the SEM analysis. Besides, TEFB10 fibers at contents above 10 wt% were likely to hamper the plasticization of starch seriously or form aggregates in the composites. The  $T_m$  and thermal stability of the composites were enhanced by the addition of TEFB10 fibers. However, the thermal stability of the bio-composites reduced as the contents of fibers increased. Mechanical properties were sharply enhanced by the incorporation of TEFB10 fibers. Particularly, the addition of 5 wt% TEFB10 fibers enhanced the tensile strength and elongation at break of the composites simultaneously. Water uptake, solubility, and WVP of starch-based bioplastics decreased moderately as the fiber contents increased. The opacity of the bio-composites was improved by the increasing contents of fibers. In conclusion, the formulation with 5 wt% TEFB10 fibers showed more favorable properties.

Subsequently, starch/TEFB-based bioplastics were crosslinked by various concentrations of CA, EPO or ESO to further reduce the disadvantages of the composites. The esterification of starch with CA was shown by the FTIR spectra. Given the low content of EO and the interference of the bands of starch, the condensation reaction between EO and starch was not detected by the FTIR. The SEM micrographs showed that low contents (0.75 wt%) of crosslinkers, especially ESO, improved the plasticization of starch and the compatibility of starch and fibers. The addition of 3 wt% CA caused the presence of many cavities on the surface of the bioplastics due to the decomposition of starch by CA. Incorporating high concentrations of EO (3 wt%) generated many cavities along with discontinuities on the surface, reflecting the poor compatibility of the components due to the phase separation. The DSC results confirmed that 0.75 wt% CA or EO contributed to the plasticization of starch with a noticeable decrease in  $T_m$ . The composites with 1.5-3 wt% CA showed the incompatibility of the components due to the

decomposition of starch. The composites with higher contents of EO revealed higher  $T_m$  due to the phase separation. The thermal stability of the composites was slightly improved by the incorporation of three modifiers. The composites with ESO presented higher thermal stability than the composites with EPO or CA. The tensile strength of the bioplastics was sharply enhanced by the incorporation of a small amount of CA or EO. EO showed higher reinforcing effect than CA which might be related to their better crosslinking or compatibilizer effect. ESO exhibited higher reinforcing effect on the composites than EPO due to higher degree of epoxidation. 3 wt% crosslinkers acted as the plasticizers and deteriorated these properties. The water uptake and solubility declined moderately after the introduction of the crosslinkers while overloading of CA caused the increase of water solubility due to the degradation of starch. The addition of CA decreased the WVP of the resulted bioplastics due to the formation of compact structure, while EO increased the WVP because of some microvoids from phase separation. The addition of three crosslinkers all increased the opacity of the composites. The biodegradability of the composites was not inhibited by the incorporation of the crosslinkers. These results suggested that EO should be better modifiers than CA to prepare starch/fiber-based bioplastics with enhanced properties. The formulation with 0.75 wt% CA or EO showed more superior properties than the composites with other contents of CA or EO.

In the end, in order to improve the compatibility and reactivity of EPO in the bio-composites and evaluate its industrial value, starch/TEFB-based bioplastics containing different concentrations of EPO or CEPO, i.e. 0.375, 0.75, 1.5, and 3 wt%, were synthesized by melt blending, followed by compression molding. The FTIR spectra for the bioplastics indicated the formation of new hydrogen bonds between starch/fibers and EPO or CEPO, and ester bonds between starch/fibers and CEPO. The X-ray diffraction patterns of the bioplastics were clearly affected by the incorporation of CEPO. The SEM images exhibited that CEPO showed better compatibility in the composites compared to

EPO due to the esterification reaction. The DSC curves of the bioplastics indicated that EPO contributed to the plasticization of starch with a notable decrease in  $T_m$ , while CEPO acted as a crosslinking agent and improved the  $T_m$  of the composites. The TGA results suggested that EPO provided higher thermal stability to the composites than CEPO. The addition of EPO or CEPO promoted the mechanical properties and decreased water uptake, WVP and transparency of the bioplastics. The biodegradability of the bioplastics was hampered remarkably by the introduction of high contents of CEPO. Comparatively, CEPO presented higher reinforcing effect on the composites than EPO due to the crosslinking effect. The results confirmed that EPO could be used as a reactive modifier for starch/fiber-based bioplastics. This effect could be enhanced by chemically grafting EPO with CA. The formulation with 0.75 wt% CEPO exhibited better properties. The low-cost and fully bio-based bioplastics with superior tensile and water resistance properties could be used as an alternative to LDPE for the application of packaging.

## 5.2 Recommendations

It was confirmed in the study that starch was decomposed by high contents of CA which would affect the water resistance properties of bioplastics. For further research, it can be recommended that starch can be modified on the surface by silane coupling agent or maleic anhydride to improve its reactivity with CEPO. Moreover, the stoichiometric ratio of epoxy equivalent weight for EPO and acid equivalent weight for CA is 1:1 when CEPO is prepared. In this case, the carboxyl groups of CA would be completely consumed by epoxy groups of EPO. Higher contents of CA might promote better compatibility in the composites by reacting with starch.

Secondly, other characterization techniques such as dynamic mechanical analysis (DMA) and field emission scanning electron microscopy (FESEM) can also be carried out to further study the structure and properties of the prepared bioplastics.

Also, due to the reactivity of EPO towards the carboxyl groups, we can try to use citrate starch as the materials to make the bioplastics.

Next, blending the enhanced bioplastics with other biodegradable polymers such as PLA, PBAT is also promising, which can reduce the production cost of the bioplastics.

In the end, glycerol is needed to be modified or replaced because of its hydrophilicity. Glycerol and sebacic acid can develop flexible materials after the condensation reaction. The flexible prepolymers might act as the secondary plasticizers of modified starch. Additionally, sebacic acid is also a curing agent of EO. Therefore, it can be a medium to link glycerol with EO. The addition of crosslinked EPO might hamper the plasticization of starch. This problem might be overcome by that starch can be plasticized firstly and then crosslinked EPO is introduced.

Universiti Malaysia

## REFERENCES

- Abdullah, M. A., Nazir, M. S., Raza, M. R., Wahjoedi, B. A., & Yussof, A. W. (2016). Autoclave and ultra-sonication treatments of oil palm empty fruit bunch fibers for cellulose extraction and its polypropylene composite properties. *Journal of Cleaner Production*, *126*, 686-697.
- Abral, H., Hartono, A., Hafizulhaq, F., Handayani, D., Sugiarti, E., & Pradipta, O. (2019). Characterization of PVA/cassava starch biocomposites fabricated with and without sonication using bacterial cellulose fiber loadings. *Carbohydr Polym*, *206*, 593-601.
- Abral, H., Putra, G. J., Asrofi, M., Park, J. W., & Kim, H. J. (2018). Effect of vibration duration of high ultrasound applied to bio-composite while gelatinized on its properties. *Ultrason Sonochem*, *40*, 697-702.
- Acosta, S., Jiménez, A., Cháfer, M., González-Martínez, C., & Chiralt, A. (2015). Physical properties and stability of starch-gelatin based films as affected by the addition of esters of fatty acids. *Food Hydrocolloids*, *49*, 135-143.
- Adamus, J., Szychaj, T., Zdanowicz, M., & Jędrzejewski, R. (2018). Thermoplastic starch with deep eutectic solvents and montmorillonite as a base for composite materials. *Industrial Crops and Products*, *123*, 278-284.
- Ago, M., Ferrer, A., & Rojas, O. J. (2016). Starch-Based Biofoams Reinforced with Lignocellulose Nanofibrils from Residual Palm Empty Fruit Bunches: Water Sorption and Mechanical Strength. *ACS Sustainable Chemistry & Engineering*, *4*(10), 5546-5552.
- Agrawal, A., Kaushik, Nirmala, & Biswas, Soumitra. (2014). Derivatives and Applications of Lignin - An Insight. *THE SCITECH JOURNAL*, *1*(7), 30-36.
- Agustin-Salazar, S., Cerruti, P., Medina-Juarez, L. A., Scarinzi, G., Malinconico, M., Soto-Valdez, H., & Gamez-Meza, N. (2018). Lignin and holocellulose from pecan nutshell as reinforcing fillers in poly (lactic acid) biocomposites. *Int J Biol Macromol*, *115*, 727-736.
- Agustin, M. B., Ahmmad, B., Alonzo, S. M. M., & Patriana, F. M. (2014). Bioplastic based on starch and cellulose nanocrystals from rice straw. *Journal of Reinforced Plastics and Composites*, *33*(24), 2205-2213.
- Alves, V. D., Mali, S., Beléia, A., & Grossmann, M. V. E. (2007). Effect of glycerol and amylose enrichment on cassava starch film properties. *Journal of Food Engineering*, *78*(3), 941-946.

- Andreuccetti, C., Carvalho, R. A., & Grosso, C. R. F. (2010). Gelatin-based films containing hydrophobic plasticizers and saponin from *Yucca schidigera* as the surfactant. *Food Research International*, 43(6), 1710-1718.
- Angelini, S., Cerruti, P., Immirzi, B., Santagata, G., Scarinzi, G., & Malinconico, M. (2014). From biowaste to bioresource: Effect of a lignocellulosic filler on the properties of poly(3-hydroxybutyrate). *Int J Biol Macromol*, 71, 163-173.
- Angelini, S., Cerruti, P., Immirzi, B., Scarinzi, G., & Malinconico, M. (2016). Acid-insoluble lignin and holocellulose from a lignocellulosic biowaste: Bio-fillers in poly(3-hydroxybutyrate). *European Polymer Journal*, 76, 63-76.
- Asrofi, M., Abrial, H., Putra, Y. K., Sapuan, S. M., & Kim, H. J. (2018). Effect of duration of sonication during gelatinization on properties of tapioca starch water hyacinth fiber biocomposite. *Int J Biol Macromol*, 108, 167-176.
- Atarés, L., De Jesús, C., Talens, P., & Chiralt, A. (2010). Characterization of SPI-based edible films incorporated with cinnamon or ginger essential oils. *Journal of Food Engineering*, 99(3), 384-391.
- Awale, R. J., Ali, F. B., Azmi, A. S., Puad, N. I. M., Anuar, H., & Hassan, A. (2018). Enhanced Flexibility of Biodegradable Polylactic Acid/Starch Blends Using Epoxidized Palm Oil as Plasticizer. *Polymers (Basel)*, 10(977), 1-12.
- Ayrilmis, N., Jarusombuti, S., Fueangvivat, V., & Bauchongkol, P. (2011). Effect of thermal-treatment of wood fibres on properties of flat-pressed wood plastic composites. *Polymer Degradation and Stability*, 96(5), 818-822.
- Badia, J. D., Kittikorn, T., Strömberg, E., Santonja-Blasco, L., Martínez-Felipe, A., Ribes-Greus, A., . . . Karlsson, S. (2014). Water absorption and hydrothermal performance of PHBV/sisal biocomposites. *Polymer Degradation and Stability*, 108, 166-174.
- Baharuddin, A. S., Sulaiman, A., Kim, D. H., Mokhtar, M. N., Hassan, M. A., Wakisaka, M., . . . Nishida, H. (2013). Selective component degradation of oil palm empty fruit bunches (OPEFB) using high-pressure steam. *Biomass and Bioenergy*, 55, 268-275.
- Balakrishnan, P., Sreekala, M. S., Geethamma, V. G., Kalarikkal, N., Kokol, V., Volova, T., & Thomas, S. (2019). Physicochemical, mechanical, barrier and antibacterial properties of starch nanocomposites crosslinked with pre-oxidised sucrose. *Industrial Crops and Products*, 130, 398-408.
- Balart, J. F., Fombuena, V., Fenollar, O., Boronat, T., & Sánchez-Nacher, L. (2016). Processing and characterization of high environmental efficiency composites

based on PLA and hazelnut shell flour (HSF) with biobased plasticizers derived from epoxidized linseed oil (ELO). *Composites Part B: Engineering*, 86, 168-177.

Basiak, E., Debeaufort, F., & Lenart, A. (2016). Effect of oil lamination between plasticized starch layers on film properties. *Food Chem*, 195, 56-63.

Baumberger, S., Abaecherli, A., Fasching, M., Gellerstedt, G., Gosselink, R., Hortling, B., . . . de Jong, E. (2007). Molar mass determination of lignins by size-exclusion chromatography: towards standardisation of the method. *Holzforschung*, 61(4), 459-468.

Baumberger, S., Lapiere, C., & Monties, B. (1998). Utilization of Pine Kraft Lignin in Starch Composites: Impact of Structural Heterogeneity. *Journal of Agricultural and Food Chemistry*, 46(6), 2234-2240.

Béguin, P., & P Aubert, J. (1994). The biological degradation of cellulose. *FEMS Microbiol Rev*, 13(1), 25-58.

Belhassen, R., Vilaseca, F., Mutjé, P., & Boufi, S. (2014). Thermoplasticized starch modified by reactive blending with epoxidized soybean oil. *Industrial Crops and Products*, 53, 261-267.

Bergel, B. F., Dias Osorio, S., da Luz, L. M., & Santana, R. M. C. (2018). Effects of hydrophobized starches on thermoplastic starch foams made from potato starch. *Carbohydr Polym*, 200, 106-114.

Berthet, M. A., Commandré, J. M., Rouau, X., Gontard, N., & Angellier-Coussy, H. (2016). Torrefaction treatment of lignocellulosic fibres for improving fibre/matrix adhesion in a biocomposite. *Materials & Design*, 92, 223-232.

Bhalla, A., Fasahati, P., Particka, C. A., Assad, A. E., Stoklosa, R. J., Bansal, N., . . . Hegg, E. L. (2018). Integrated experimental and technoeconomic evaluation of two-stage Cu-catalyzed alkaline-oxidative pretreatment of hybrid poplar. *Biotechnol Biofuels*, 11, 143-153.

Blennow, A., Jensen, S. L., Shaik, S. S., Skryhan, K., Carciofi, M., Holm, P. B., . . . Tanackovic, V. (2013). Future cereal starch bioengineering: cereal ancestors encounter gene technology and designer enzymes. *Cereal Chemistry*, 90(4), 274-287.

Bocz, K., Szolnoki, B., Marosi, A., Tábi, T., Wladyka-Przybylak, M., & Marosi, G. (2014). Flax fibre reinforced PLA/TPS biocomposites flame retarded with multifunctional additive system. *Polymer Degradation and Stability*, 106, 63-73.

- Bouza, R. J., Gu, Z., & Evans, J. H. (2016). Screening conditions for acid pretreatment and enzymatic hydrolysis of empty fruit bunches. *Industrial Crops and Products*, 84, 67-71.
- Brandelero, R. P., Grossmann, M. V., & Yamashita, F. (2012). Films of starch and poly(butylene adipate co-terephthalate) added of soybean oil (SO) and Tween 80. *Carbohydr Polym*, 90(4), 1452-1460.
- Brandelero, R. P. H., Yamashita, F., & Grossmann, M. V. E. (2010). The effect of surfactant Tween 80 on the hydrophilicity, water vapor permeation, and the mechanical properties of cassava starch and poly(butylene adipate-co-terephthalate) (PBAT) blend films. *Carbohydrate Polymers*, 82(4), 1102-1109.
- Brodin, M., Vallejos, M., Opedal, M. T., Area, M. C., & Chinga-Carrasco, G. (2017). Lignocellulosics as sustainable resources for production of bioplastics – A review. *Journal of Cleaner Production*, 162, 646-664.
- Campos, A., Sena Neto, A. R., Rodrigues, V. B., Luchesi, B. R., Mattoso, L. H. C., & Marconcini, J. M. (2018). Effect of raw and chemically treated oil palm mesocarp fibers on thermoplastic cassava starch properties. *Industrial Crops and Products*, 124, 149-154.
- Carbonell-Verdu, A., Bernardi, L., Garcia-Garcia, D., Sanchez-Nacher, L., & Balart, R. (2015). Development of environmentally friendly composite matrices from epoxidized cottonseed oil. *European Polymer Journal*, 63, 1-10.
- Chabrat, E., Abdillahi, H., Rouilly, A., & Rigal, L. (2012). Influence of citric acid and water on thermoplastic wheat flour/poly(lactic acid) blends. I: Thermal, mechanical and morphological properties. *Industrial Crops and Products*, 37(1), 238-246.
- Chaudhary, A. L., Torley, P. J., Halley, P. J., McCaffery, N., & Chaudhary, D. S. (2009). Amylose content and chemical modification effects on thermoplastic starch from maize - Processing and characterisation using conventional polymer equipment. *Carbohydrate Polymers*, 78(4), 917-925.
- Cheng, J., Zheng, P., Zhao, F., & Ma, X. (2013). The composites based on plasticized starch and carbon nanotubes. *Int J Biol Macromol*, 59, 13-19.
- Cheng, L., Zhang, D., Gu, Z., Li, Z., Hong, Y., & Li, C. (2018). Preparation of acetylated nanofibrillated cellulose from corn stalk microcrystalline cellulose and its reinforcing effect on starch films. *Int J Biol Macromol*, 111, 959-966.
- Chiesa, S., & Gnansounou, E. (2014). Use of Empty Fruit Bunches from the oil palm for bioethanol production: a thorough comparison between dilute acid and dilute

alkali pretreatment. *Bioresour Technol*, 159, 355-364.

- Chiew, Y. L., & Shimada, S. (2013). Current state and environmental impact assessment for utilizing oil palm empty fruit bunches for fuel, fiber and fertilizer - A case study of Malaysia. *Biomass and Bioenergy*, 51, 109-124.
- Chiumarelli, M., & Hubinger, M. D. (2012). Stability, solubility, mechanical and barrier properties of cassava starch - Carnauba wax edible coatings to preserve fresh-cut apples. *Food Hydrocolloids*, 28(1), 59-67.
- Chung, Y., Ansari, S., Estevez, L., Hayrapetyan, S., Giannelis, E. P., & Lai, H.-M. (2010). Preparation and properties of biodegradable starch-clay nanocomposites. *Carbohydrate Polymers*, 79(2), 391-396.
- Cieśla, K., & Sartowska, B. (2016). Modification of the microstructure of the films formed by gamma irradiated starch examined by SEM. *Radiation Physics and Chemistry*, 118, 87-95.
- Clasen, S. H., Muller, C. M. O., Parize, A. L., & Pires, A. T. N. (2018). Synthesis and characterization of cassava starch with maleic acid derivatives by etherification reaction. *Carbohydr Polym*, 180, 348-353.
- Coral Medina, J. D., Woiciechowski, A. L., Filho, A. Z., Brar, S. K., Magalhães Júnior, A. I., & Soccol, C. R. (2018). Energetic and economic analysis of ethanol, xylitol and lignin production using oil palm empty fruit bunches from a Brazilian factory. *Journal of Cleaner Production*, 195, 44-55.
- Cova, A., Sandoval, A. J., Balsamo, V., & Müller, A. J. (2010). The effect of hydrophobic modifications on the adsorption isotherms of cassava starch. *Carbohydrate Polymers*, 81(3), 660-667.
- Da Róz, A. L., Zambon, M. D., Curvelo, A. A. S., & Carvalho, A. J. F. (2011). Thermoplastic starch modified during melt processing with organic acids: The effect of molar mass on thermal and mechanical properties. *Industrial Crops and Products*, 33(1), 152-157.
- Dai, L., Zhang, J., & Cheng, F. (2019). Effects of starches from different botanical sources and modification methods on physicochemical properties of starch-based edible films. *Int J Biol Macromol*, 132, 897-905.
- Dai, X., Xiong, Z., Na, H., & Zhu, J. (2014). How does epoxidized soybean oil improve the toughness of microcrystalline cellulose filled polylactide acid composites? *Composites Science and Technology*, 90, 9-15.

- Das, A., Uppaluri, R., & Das, C. (2019). Feasibility of poly-vinyl alcohol/starch/glycerol/citric acid composite films for wound dressing applications. *Int J Biol Macromol*, *131*, 998-1007.
- de Mesquita, J. P., Donnici, C. L., Teixeira, I. F., & Pereira, F. V. (2012). Bio-based nanocomposites obtained through covalent linkage between chitosan and cellulose nanocrystals. *Carbohydr Polym*, *90*(1), 210-217.
- Dhakai, H. N., Ismail, S. O., Zhang, Z., Barber, A., Welsh, E., Maigret, J.-E., & Beaugrand, J. (2018). Development of sustainable biodegradable lignocellulosic hemp fiber/polycaprolactone biocomposites for light weight applications. *Composites Part A: Applied Science and Manufacturing*, *113*, 350-358.
- Doherty, W. O. S., Mousavioun, P., & Fellows, C. M. (2011). Value-adding to cellulosic ethanol: Lignin polymers. *Industrial Crops and Products*, *33*(2), 259-276.
- Duval, A., & Lawoko, M. (2014). A review on lignin-based polymeric, micro- and nano-structured materials. *Reactive and Functional Polymers*, *85*, 78-96.
- Duval, A., Molina-Boisseau, S., & Chirat, C. (2013). Comparison of Kraft lignin and lignosulfonates addition to wheat gluten-based materials: Mechanical and thermal properties. *Industrial Crops and Products*, *49*, 66-74.
- Edhirej, A., Sapuan, S. M., Jawaid, M., & Zahari, N. I. (2017). Cassava/sugar palm fiber reinforced cassava starch hybrid composites: Physical, thermal and structural properties. *Int J Biol Macromol*, *101*, 75-83.
- El Halal, S. L., Colussi, R., Deon, V. G., Pinto, V. Z., Villanova, F. A., Carreno, N. L., . . . Zavareze Eda, R. (2015). Films based on oxidized starch and cellulose from barley. *Carbohydr Polym*, *133*, 644-653.
- El Miri, N., Abdelouahdi, K., Barakat, A., Zahouily, M., Fihri, A., Solhy, A., & El Achaby, M. (2015). Bio-nanocomposite films reinforced with cellulose nanocrystals: Rheology of film-forming solutions, transparency, water vapor barrier and tensile properties of films. *Carbohydr Polym*, *129*, 156-167.
- Elfehri Borchani, K., Carrot, C., & Jaziri, M. (2015). Biocomposites of Alfa fibers dispersed in the Mater-Bi® type bioplastic: Morphology, mechanical and thermal properties. *Composites Part A: Applied Science and Manufacturing*, *78*, 371-379.
- Essabir, H., Bensalah, M. O., Rodrigue, D., Bouhfid, R., & Qaiss Ael, K. (2016). Biocomposites based on Argan nut shell and a polymer matrix: Effect of filler content and coupling agent. *Carbohydr Polym*, *143*, 70-83.

- European-bioplastics. (2020). Bioplastics market data. Retrieved from <https://www.european-bioplastics.org/market/>
- Fahma, F., Hori, N., Iwata, T., & Takemura, A. (2017). PVA nanocomposites reinforced with cellulose nanofibers from oil palm empty fruit bunches (OPEFBs). *Emirates Journal of Food and Agriculture*, 29(5), 323-329.
- Fahma, F., Iwamoto, S., Hori, N., Iwata, T., & Takemura, A. (2010). Isolation, preparation, and characterization of nanofibers from oil palm empty-fruit-bunch (OPEFB). *Cellulose*, 17(5), 977-985.
- Fakhouri, F. M., Costa, D., Yamashita, F., Martelli, S. M., Jesus, R. C., Alganer, K., . . . Innocentini-Mei, L. H. (2013). Comparative study of processing methods for starch/gelatin films. *Carbohydr Polym*, 95(2), 681-689.
- Faruk, O., Bledzki, A. K., Fink, H.-P., & Sain, M. (2012). Biocomposites reinforced with natural fibers: 2000-2010. *Progress in Polymer Science*, 37(11), 1552-1596.
- Feldman, D., Banu, D., Campanelli, J., & Zhu, H. (2001). Blends of vinylic copolymer with plasticized lignin- Thermal and Mechanical Properties. *Journal of Applied Polymer Science*, 81, 861-874.
- Feofilova, E. P., & Mysyakina, I. S. (2016). Lignin: Chemical structure, biodegradation, and practical application (a review). *Applied Biochemistry and Microbiology*, 52(6), 573-581.
- Fialho, E. M. A. R., Pola, C. C., Bilck, A. P., Yamashita, F., Tronto, J., Medeiros, E. A. A., & Soares, N. F. F. (2017). Starch, cellulose acetate and polyester biodegradable sheets: Effect of composition and processing conditions. *Mater Sci Eng C Mater Biol Appl*, 78, 932-941.
- Fitch-Vargas, P. R., Camacho-Hernandez, I. L., Martinez-Bustos, F., Islas-Rubio, A. R., Carrillo-Canedo, K. I., Calderon-Castro, A., . . . Aguilar-Palazuelos, E. (2019). Mechanical, physical and microstructural properties of acetylated starch-based biocomposites reinforced with acetylated sugarcane fiber. *Carbohydr Polym*, 219, 378-386.
- French, A. D. (2013). Idealized powder diffraction patterns for cellulose polymorphs. *Cellulose*, 21(2), 885-896.
- Frollini, E., Bartolucci, N., Sisti, L., & Celli, A. (2015). Biocomposites based on poly(butylene succinate) and curaua: Mechanical and morphological properties. *Polymer Testing*, 45, 168-173.

- Gallos, A., Paës, G., Allais, F., & Beaugrand, J. (2017). Lignocellulosic fibers: a critical review of the extrusion process for enhancement of the properties of natural fiber composites. *RSC Advances*, 7(55), 34638-34654.
- Galus, S., & Kadzińska, J. (2015). Food applications of emulsion-based edible films and coatings. *Trends in Food Science & Technology*, 45(2), 273-283.
- Gao, W., Liu, P., Li, X., Qiu, L., Hou, H., & Cui, B. (2019). The co-plasticization effects of glycerol and small molecular sugars on starch-based nanocomposite films prepared by extrusion blowing. *Int J Biol Macromol*, 133, 1175-1181.
- Garavand, F., Rouhi, M., Razavi, S. H., Cacciotti, I., & Mohammadi, R. (2017). Improving the integrity of natural biopolymer films used in food packaging by crosslinking approach: A review. *Int J Biol Macromol*, 104(Pt A), 687-707.
- García, N. L., Lamanna, M., D'Accorso, N., Dufresne, A., Aranguren, M., & Goyanes, S. (2012). Biodegradable materials from grafting of modified PLA onto starch nanocrystals. *Polymer Degradation and Stability*, 97(10), 2021-2026.
- Garcia, P. S., Grossmann, M. V. E., Shirai, M. A., Lazaretti, M. M., Yamashita, F., Muller, C. M. O., & Mali, S. (2014). Improving action of citric acid as compatibiliser in starch/polyester blown films. *Industrial Crops and Products*, 52, 305-312.
- Ge, X., Yu, L., Liu, Z., Liu, H., Chen, Y., & Chen, L. (2019). Developing acrylated epoxidized soybean oil coating for improving moisture sensitivity and permeability of starch-based film. *Int J Biol Macromol*, 125, 370-375.
- Ghanbari, A., Tabarsa, T., Ashori, A., Shakeri, A., & Mashkour, M. (2018). Preparation and characterization of thermoplastic starch and cellulose nanofibers as green nanocomposites: Extrusion processing. *Int J Biol Macromol*, 112, 442-447.
- Ghanbarzadeh, B., Almasi, H., & Entezami, A. A. (2011). Improving the barrier and mechanical properties of corn starch-based edible films: Effect of citric acid and carboxymethyl cellulose. *Industrial Crops and Products*, 33(1), 229-235.
- Ghosh Dastidar, T., & Netravali, A. N. (2012). 'Green' crosslinking of native starches with malonic acid and their properties. *Carbohydr Polym*, 90(4), 1620-1628.
- Gibson, L. J. (2012). The hierarchical structure and mechanics of plant materials. *JR Soc Interface*, 9(76), 2749-2766.
- Gilfillan, W. N., Nguyen, D. M. T., Sopade, P. A., & Doherty, W. O. S. (2012). Preparation and characterisation of composites from starch and sugar cane fibre. *Industrial Crops and Products*, 40, 45-54.

- Gironès, J., López, J. P., Mutjé, P., Carvalho, A. J. F., Curvelo, A. A. S., & Vilaseca, F. (2012). Natural fiber-reinforced thermoplastic starch composites obtained by melt processing. *Composites Science and Technology*, 72(7), 858-863.
- Glasser, W. G. (1999). Classification of lignin according to chemical and molecular structure. In *Lignin: Historical, Biological, and Materials Perspectives* (Vol. 742, pp. 216-238): American Chemical Society.
- Gogoi, P., Boruah, M., Sharma, S., & Dolui, S. K. (2015a). Blends of epoxidized alkyd resins based on Jatropha oil and the epoxidized oil cured with aqueous citric acid solution: a green technology approach. *ACS Sustainable Chemistry & Engineering*, 3(2), 261-268.
- Gogoi, P., Horo, H., Khannam, M., & Dolui, S. K. (2015b). In situ synthesis of green bionanocomposites based on aqueous citric acid cured epoxidized soybean oil-carboxylic acid functionalized multiwalled carbon nanotubes. *Industrial Crops and Products*, 76, 346-354.
- Goh, K. Y., Ching, Y. C., Chuah, C. H., Abdullah, L. C., & Liou, N.-S. (2015). Individualization of microfibrillated celluloses from oil palm empty fruit bunch: comparative studies between acid hydrolysis and ammonium persulfate oxidation. *Cellulose*, 23(1), 379-390.
- Goncalves, K. M., Sutili, F. K., Leite, S. G., de Souza, R. O., & Leal, I. C. (2012). Palm oil hydrolysis catalyzed by lipases under ultrasound irradiation--the use of experimental design as a tool for variables evaluation. *Ultrason Sonochem*, 19(2), 232-236.
- Gonzalez-Gutierrez, J., Partal, P., Garcia-Morales, M., & Gallegos, C. (2010). Development of highly-transparent protein/starch-based bioplastics. *Bioresour Technol*, 101(6), 2007-2013.
- González, D., Santos, V., & Parajó, J. C. (2011). Silane-treated lignocellulosic fibers as reinforcement material in polylactic acid biocomposites. *Journal of Thermoplastic Composite Materials*, 25(8), 1005-1022.
- Graupner, N. (2008). Application of lignin as natural adhesion promoter in cotton fibre-reinforced poly(lactic acid) (PLA) composites. *Journal of Materials Science*, 43(15), 5222-5229.
- Gupta, A., Simmons, W., Schueneman, G. T., Hylton, D., & Mintz, E. A. (2017). Rheological and Thermo-Mechanical Properties of Poly(lactic acid)/Lignin-Coated Cellulose Nanocrystal Composites. *ACS Sustainable Chemistry & Engineering*, 5(2), 1711-1720.

- Haafiz, M. K., Hassan, A., Khalil, H. P., Fazita, M. R., Islam, M. S., Inuwa, I. M., . . . Hussin, M. H. (2016). Exploring the effect of cellulose nanowhiskers isolated from oil palm biomass on polylactic acid properties. *Int J Biol Macromol*, *85*, 370-378.
- Hajiha, H., & Sain, M. (2015). High toughness hybrid biocomposite process optimization. *Composites Science and Technology*, *111*, 44-49.
- Harini, K., Chandra Mohan, C., Ramya, K., Karthikeyan, S., & Sukumar, M. (2018). Effect of Punica granatum peel extracts on antimicrobial properties in Walnut shell cellulose reinforced Bio-thermoplastic starch films from cashew nut shells. *Carbohydr Polym*, *184*, 231-242.
- Hasan, M., Gopakumar, D. A., Olaiya, N. G., Zarlaida, F., Alfian, A., Aprinasari, C., . . . Khalil, H. (2020). Evaluation of the thermomechanical properties and biodegradation of brown rice starch-based chitosan biodegradable composite films. *Int J Biol Macromol*, *156*, 896-905.
- Hassan, M. M., Tucker, N., & Le Guen, M. J. (2020). Thermal, mechanical and viscoelastic properties of citric acid-crosslinked starch/cellulose composite foams. *Carbohydr Polym*, *230*, 115675-115686.
- Hassan, O., Ling, T. P., Maskat, M. Y., Ilias, R. M., Badri, K., Jahim, J., & Mahadi, N. M. (2013). Optimization of pretreatments for the hydrolysis of oil palm empty fruit bunch fiber (EFBF) using enzyme mixtures. *Biomass and Bioenergy*, *56*, 137-146.
- Holmgren, A., Brunow, G., Henriksson, G., Zhang, L., & Ralph, J. (2006). Non-enzymatic reduction of quinone methides during oxidative coupling of monolignols: implications for the origin of benzyl structures in lignins. *Org Biomol Chem*, *4*(18), 3456-3461.
- Hosseini, S. E., & Wahid, M. A. (2014). Utilization of palm solid residue as a source of renewable and sustainable energy in Malaysia. *Renewable and Sustainable Energy Reviews*, *40*, 621-632.
- Hou, X., Sun, F., Yan, D., Xu, H., Dong, Z., Li, Q., & Yang, Y. (2014). Preparation of lightweight polypropylene composites reinforced by cotton stalk fibers from combined steam flash-explosion and alkaline treatment. *Journal of Cleaner Production*, *83*, 454-462.
- Hu, G., Chen, J., & Gao, J. (2009). Preparation and characteristics of oxidized potato starch films. *Carbohydrate Polymers*, *76*(2), 291-298.

- Irvine, G. M. (1985). The significance of the glass-transition of lignin in thermomechanical pulping. *Wood Science and Technology*, 19(2), 139-149.
- Javidi, Z., Hosseini, S. F., & Rezaei, M. (2016). Development of flexible bactericidal films based on poly(lactic acid) and essential oil and its effectiveness to reduce microbial growth of refrigerated rainbow trout. *LWT - Food Science and Technology*, 72, 251-260.
- Jiménez, A., Fabra, M. J., Talens, P., & Chiralt, A. (2012). Effect of re-crystallization on tensile, optical and water vapour barrier properties of corn starch films containing fatty acids. *Food Hydrocolloids*, 26(1), 302-310.
- Jiménez, A., Fabra, M. J., Talens, P., & Chiralt, A. (2013a). Phase transitions in starch based films containing fatty acids. Effect on water sorption and mechanical behaviour. *Food Hydrocolloids*, 30(1), 408-418.
- Jiménez, A., Fabra, M. J., Talens, P., & Chiralt, A. (2013b). Physical properties and antioxidant capacity of starch-sodium caseinate films containing lipids. *Journal of Food Engineering*, 116(3), 695-702.
- John, M. J., & Anandjiwala, R. D. (2008a). Recent developments in chemical modification and characterization of natural fiber-reinforced composites. *Polymer Composites*, 29(2), 187-207.
- John, M. J., & Anandjiwala, R. D. (2008b). Recent developments in chemical modification and characterization of natural fiber-reinforced composites. 29(2), 187-207.
- Kadam, A., Pawar, M., Yemul, O., Thamke, V., & Kodam, K. (2015). Biodegradable biobased epoxy resin from karanja oil. *Polymer*, 72, 82-92.
- Kahvand, F., & Fasihi, M. (2019). Plasticizing and anti-plasticizing effects of polyvinyl alcohol in blend with thermoplastic starch. *Int J Biol Macromol*, 140, 775-781.
- Khanoonkon, N., Yoksan, R., & Ogale, A. A. (2016). Effect of stearic acid-grafted starch compatibilizer on properties of linear low density polyethylene/thermoplastic starch blown film. *Carbohydrate Polymers*, 137, 165-173.
- Kim, H., Jane, J., & Lamsal, B. (2017). Hydroxypropylation improves film properties of high amylose corn starch. *Industrial Crops and Products*, 95, 175-183.
- Kim, J. R., & Sharma, S. (2012). The development and comparison of bio-thermoset plastics from epoxidized plant oils. *Industrial Crops and Products*, 36(1), 485-499.

- Koda, K., Gaspar, A. R., Yu, L., & Argyropoulos, D. S. (2005). Molecular weight-functional group relations in softwood residual kraft lignins. *Holzforschung*, 59(6), 612-619.
- Kovačević, Z., Bischof, S., Vujasinović, E., & Fan, M. (2016). The influence of pre-treatment of *Spartium junceum* L. fibres on the structure and mechanical properties of PLA biocomposites. *Arabian Journal of Chemistry*, 12(4), 449-463.
- Kowalczyk, D., & Baraniak, B. (2014). Effect of candelilla wax on functional properties of biopolymer emulsion films - A comparative study. *Food Hydrocolloids*, 41, 195-209.
- Krogars, K., Heinämäki, J., Karjalainen, M., Rantanen, J., Luukkonen, P., & Yliruusi, J. (2003). Development and characterization of aqueous amylose-rich maize starch dispersion for film formation. *European Journal of Pharmaceutics and Biopharmaceutics*, 56(2), 215-221.
- Kulma, A., Skórkowska-Telichowska, K., Kostyn, K., Szatkowski, M., Skała, J., Drulis-Kawa, Z., . . . Szopa, J. (2015). New flax producing bioplastic fibers for medical purposes. *Industrial Crops and Products*, 68, 80-89.
- Kun, D., & Pukánszky, B. (2017). Polymer/lignin blends: Interactions, properties, applications. *European Polymer Journal*, 93, 618-641.
- Laurichesse, S., & Avérous, L. (2014). Chemical modification of lignins: Towards biobased polymers. *Progress in Polymer Science*, 39(7), 1266-1290.
- Lebreton, L., & Andrady, A. (2019). Future scenarios of global plastic waste generation and disposal. *Nature-Palgrave Communications*, 5(1), 1-11.
- Lee, C., Yang, T., Cheng, Y., & Lee, C. (2018). Effects of thermal modification on the surface and chemical properties of moso bamboo. *Construction and Building Materials*, 178, 59-71.
- Lee, S., Ashaari, Z., Ang, A. F., Abdul Halip, J., Lum, W., Dahali, R., & Halis, R. (2018). Effects of two-step post heat-treatment in palm oil on the properties of oil palm trunk particleboard. *Industrial Crops and Products*, 116, 249-258.
- Lee, Y. K., & Chang, Y. H. (2019). Structural and in vitro digestibility properties of esterified maca starch with citric acid and its application as an oil-in-water (O/W) pickering emulsion stabilizer. *Int J Biol Macromol*, 134, 798-806.
- Lei, B., Liang, Y., Feng, Y., He, H., & Yang, Z. (2018). Preparation and characteristics of biocomposites based on steam exploded Sisal fiber modified with amphipathic

epoxidized soybean oil resin. *Materials*, 11(9), 1731-1744.

- Lennartsson, P. R., Niklasson, C., & Taherzadeh, M. J. (2011). A pilot study on lignocelluloses to ethanol and fish feed using NMMO pretreatment and cultivation with zygomycetes in an air-lift reactor. *Bioresour Technol*, 102(6), 4425-4432.
- Lewis, A., Waters, J. C., Stanton, J., Hess, J., & Salas-de la Cruz, D. (2016). Macromolecular Interactions Control Structural and Thermal Properties of Regenerated Tri-Component Blended Films. *Int J Mol Sci*, 17(12), 1989-2003.
- Li, A., & Li, K. (2014). Pressure-sensitive adhesives based on epoxidized soybean oil and dicarboxylic acids. *ACS Sustainable Chemistry & Engineering*, 2(8), 2090-2096.
- Li, J., Ye, F., Liu, J., & Zhao, G. (2015). Effects of octenylsuccination on physical, mechanical and moisture-proof properties of stretchable sweet potato starch film. *Food Hydrocolloids*, 46, 226-232.
- Li, M., Pu, Y., & Ragauskas, A. J. (2016). Current understanding of the correlation of lignin structure with biomass recalcitrance. *Front Chem*, 4, 1-8.
- Li, S.-X., Zou, J.-Y., Li, M.-F., Wu, X.-F., Bian, J., & Xue, Z.-M. (2017). Structural and thermal properties of *Populus tomentosa* during carbon dioxide torrefaction. *Energy*, 124, 321-329.
- Li, X., Tabil, L. G., & Panigrahi, S. (2007). Chemical Treatments of Natural Fiber for Use in Natural Fiber-Reinforced Composites: A Review. *Journal of Polymers and the Environment*, 15(1), 25-33.
- Lim, W. S., Ock, S. Y., Park, G. D., Lee, I. W., Lee, M. H., & Park, H. J. (2020). Heat-sealing property of cassava starch film plasticized with glycerol and sorbitol. *Food Packaging and Shelf Life*, 26, 100556-100563.
- Lin, Y., Xia, X., Shang, K., Elia, R., Huang, W., Cebe, P., . . . Kaplan, D. L. (2013). Tuning Chemical and Physical Cross-Links in Silk Electrogels for Morphological Analysis and Mechanical Reinforcement. *Biomacromolecules*, 14(8), 2629-2635.
- Liu, H., Adhikari, R., Guo, Q., & Adhikari, B. (2013). Preparation and characterization of glycerol plasticized (high-amylose) starch-chitosan films. *Journal of Food Engineering*, 116(2), 588-597.
- Liu, P., Sun, S., Hou, H., & Dong, H. (2016). Effects of fatty acids with different degree of unsaturation on properties of sweet potato starch-based films. *Food Hydrocolloids*, 61, 351-357.

- Liu, R., Peng, Y., Cao, J., & Chen, Y. (2014). Comparison on properties of lignocellulosic flour/polymer composites by using wood, cellulose, and lignin flours as fillers. *Composites Science and Technology*, *103*, 1-7.
- Liu, T., Williams, D. L., Pattathil, S., Li, M., Hahn, M. G., & Hodge, D. B. (2014). Coupling alkaline pre-extraction with alkaline-oxidative post-treatment of corn stover to enhance enzymatic hydrolysis and fermentability. *Biotechnol Biofuels*, *7*(1), 48-59.
- Liu, W., Chen, T., Xie, T., & Qiu, R. (2016). Soybean oil-based thermosets with N -vinyl-2-pyrrolidone as crosslinking agent for hemp fiber composites. *Composites Part A: Applied Science and Manufacturing*, *82*, 1-7.
- Liu, W., Drzal, L. T., Mohanty, A. K., & Misra, M. (2007). Influence of processing methods and fiber length on physical properties of kenaf fiber reinforced soy based biocomposites. *Composites Part B: Engineering*, *38*(3), 352-359.
- Liu, W., Misra, M., Askeland, P., Drzal, L. T., & Mohanty, A. K. (2005). 'Green' composites from soy based plastic and pineapple leaf fiber: fabrication and properties evaluation. *Polymer*, *46*(8), 2710-2721.
- Liu, W., Mohanty, A. K., Askeland, P., Drzal, L. T., & Misra, M. (2004). Influence of fiber surface treatment on properties of Indian grass fiber reinforced soy protein based biocomposites. *Polymer*, *45*(22), 7589-7596.
- Liu, W., Qiu, J., Chen, T., Fei, M., Qiu, R., & Sakai, E. (2019). Regulating tannic acid-crosslinked epoxidized soybean oil oligomers for strengthening and toughening bamboo fibers-reinforced poly(lactic acid) biocomposites. *Composites Science and Technology*, *181*, 107709-107718.
- Lomeli-Ramirez, M. G., Kestur, S. G., Manriquez-Gonzalez, R., Iwakiri, S., de Muniz, G. B., & Flores-Sahagun, T. S. (2014). Bio-composites of cassava starch-green coconut fiber: part II-Structure and properties. *Carbohydr Polym*, *102*, 576-583.
- López, J. P., Mutjé, P., Carvalho, A. J. F., Curvelo, A. A. S., & Gironès, J. (2013). Newspaper fiber-reinforced thermoplastic starch biocomposites obtained by melt processing: Evaluation of the mechanical, thermal and water sorption properties. *Industrial Crops and Products*, *44*, 300-305.
- López, O. V., Zaritzky, N. E., Grossmann, M. V. E., & García, M. A. (2013). Acetylated and native corn starch blend films produced by blown extrusion. *Journal of Food Engineering*, *116*(2), 286-297.
- Lu, D. R., Xiao, C. M., & Xu, S. J. (2009). Starch-based completely biodegradable polymer materials. *Express Polymer Letters*, *3*(6), 366-375.

- Ma, X., Chang, P. R., & Yu, J. (2008a). Properties of biodegradable thermoplastic pea starch/carboxymethyl cellulose and pea starch/microcrystalline cellulose composites. *Carbohydrate Polymers*, 72(3), 369-375.
- Ma, X., Cheng, Y., Qin, X., Guo, T., Deng, J., & Liu, X. (2017). Hydrophilic modification of cellulose nanocrystals improves the physicochemical properties of cassava starch-based nanocomposite films. *Food Science and Technology*, 86, 318-326.
- Ma, X., Jian, R., Chang, P. R., & Yu, J. (2008b). Fabrication and Characterization of Citric Acid-Modified Starch Nanoparticles/Plasticized-Starch Composites. *Biomacromolecules*, 9, 3314-3320.
- Ma, X. F., Chang, P. R., Yu, J. g., & Stumborg, M. (2009). Properties of biodegradable citric acid-modified granular starch/thermoplastic pea starch composites. *Carbohydrate Polymers*, 75(1), 1-8.
- Ma, Y., Asaadi, S., Johansson, L.-S., Ahvenainen, P., Reza, M., Alekhina, M., . . . Sixta, H. (2015). High-Strength Composite Fibers from Cellulose-Lignin Blends Regenerated from Ionic Liquid Solution. *Chemistry sustainability energy materials*, 8(23), 4030-4039.
- Mahjoub, R., Bin Mohamad Yatim, J., & Mohd Sam, A. R. (2013). A review of structural performance of oil palm empty fruit bunch fiber in polymer composites. *Advances in Materials Science and Engineering*, 2013, 1-9.
- Maier, C., Ensenberger, S., Irmscher, S. B., & Weiss, J. (2016). Glutaraldehyde induced cross-linking of oppositely charged oil-in-water emulsions. *Food Hydrocolloids*, 57, 221-228.
- Malaysian-Palm-Oil-Board (2020). Re: Malaysian Palm Oil Board [<http://bepi.mpob.gov.my/index.php/en/>]. Message posted to <http://bepi.mpob.gov.my/index.php/en/>
- Maniglia, B. C., & Tapia-Blacido, D. R. (2019). Structural modification of fiber and starch in turmeric residue by chemical and mechanical treatment for production of biodegradable films. *Int J Biol Macromol*, 126, 507-516.
- Martins, P. C., Gutkoski, L. C., & Martins, V. G. (2018). Impact of acid hydrolysis and esterification process in rice and potato starch properties. *Int J Biol Macromol*, 120(Pt A), 959-965.
- Medina, J. D., Woiciechowski, A., Zandona Filho, A., Nosedá, M. D., Kaur, B. S., & Soccol, C. R. (2015). Lignin preparation from oil palm empty fruit bunches by sequential acid/alkaline treatment--A biorefinery approach. *Bioresour Technol*, 194, 172-178.

- Medina, J. D. C., Woiciechowski, A., Filho, A. Z., Nigam, P. S., Ramos, L. P., & Soccol, C. R. (2016). Steam explosion pretreatment of oil palm empty fruit bunches (EFB) using autocatalytic hydrolysis: A biorefinery approach. *Bioresour Technol*, *199*, 173-180.
- Meng, L. P., Li, S., Yang, W. D., Simons, R. Y., Yu, L., Liu, H. S., & Chen, L. (2019). Improvement of Interfacial Interaction between Hydrophilic Starch Film and Hydrophobic Biodegradable Coating. *ACS Sustainable Chemistry & Engineering*, *7*(10), 9506-9514.
- Meng, X. T., Bocharova, V., Tekinalp, H., Cheng, S. W., Kisliuk, A., Sokolov, A. P., . . . Ozcan, S. (2018). Toughening of nanocellulose/PLA composites via bio-epoxy interaction: Mechanistic study. *Materials & Design*, *139*, 188-197.
- Menzel, C., Olsson, E., Plivelic, T. S., Andersson, R., Johansson, C., Kuktaite, R., . . . Koch, K. (2013). Molecular structure of citric acid cross-linked starch films. *Carbohydr Polym*, *96*(1), 270-276.
- Miranda, C. S., Ferreira, M. S., Magalhães, M. T., Bispo, A. P. G., Oliveira, J. C., Silva, J. B. A., & José, N. M. (2015). Starch-based Films Plasticized with Glycerol and Lignin from Piassava Fiber Reinforced with Nanocrystals from Eucalyptus. *Materials Today: Proceedings*, *2*(1), 134-140.
- Mistri, E., Routh, S., Ray, D., Sahoo, S., & Misra, M. (2011). Green composites from maleated castor oil and jute fibres. *Industrial Crops and Products*, *34*(1), 900-906.
- Miyata, Y., Yamazaki, Y., Hirano, Y., & Kita, Y. (2018). Quantitative analysis of the aqueous fraction from the Fe-assisted hydrothermal liquefaction of oil palm empty fruit bunches. *Journal of Analytical and Applied Pyrolysis*, *132*, 72-81.
- Mohamad Yazid, N. S., Abdullah, N., Muhammad, N., & Matias-Peralta, H. M. (2018). Application of starch and starch-based products in food industry. *Journal of Science and Technology*, *10*(2), 144-174.
- Mohammed, L., Ansari, M. N. M., Pua, G., Jawaid, M., & Islam, M. S. (2015). A Review on Natural Fiber Reinforced Polymer Composite and Its Applications. *International Journal of Polymer Science*, *2015*, 1-15.
- Mok, C. F., Ching, Y. C., Abu Osman, N. A., Muhamad, F., Mohd Junaidi, M. U., & Choo, J. H. (2020). Preparation and characterization study on maleic acid cross-linked poly(vinyl alcohol)/chitin/nanocellulose composites. *Journal of Applied Polymer Science*, *137*(35), 49044-49059.
- Montero, B., Rico, M., Rodriguez-Llamazares, S., Barral, L., & Bouza, R. (2017). Effect of nanocellulose as a filler on biodegradable thermoplastic starch films from tuber,

cereal and legume. *Carbohydr Polym*, 157, 1094-1104.

- Moreno, O., Cardenas, J., Atares, L., & Chiralt, A. (2017). Influence of starch oxidation on the functionality of starch-gelatin based active films. *Carbohydr Polym*, 178, 147-158.
- Mościcki, L., Mitrus, M., Wójtowicz, A., Oniszczyk, T., Rejak, A., & Janssen, L. (2012). Application of extrusion-cooking for processing of thermoplastic starch (TPS). *Food Research International*, 47(2), 291-299.
- Moshiul Alam, A. K. M., Beg, M. D. H., Reddy Prasad, D. M., Khan, M. R., & Mina, M. F. (2012). Structures and performances of simultaneous ultrasound and alkali treated oil palm empty fruit bunch fiber reinforced poly(lactic acid) composites. *Composites Part A: Applied Science and Manufacturing*, 43(11), 1921-1929.
- Mousavioun, P., Doherty, W. O. S., & George, G. (2010). Thermal stability and miscibility of poly(hydroxybutyrate) and soda lignin blends. *Industrial Crops and Products*, 32(3), 656-661.
- Mukherjee, T., Sani, M., Kao, N., Gupta, R. K., Quazi, N., & Bhattacharya, S. (2013). Improved dispersion of cellulose microcrystals in polylactic acid (PLA) based composites applying surface acetylation. *Chemical Engineering Science*, 101, 655-662.
- Muller, J., Gonzalez-Martinez, C., & Chiralt, A. (2017). Combination of Poly(lactic) Acid and Starch for Biodegradable Food Packaging. *Materials (Basel)*, 10(8), 952-974.
- Muscat, D., Adhikari, B., Adhikari, R., & Chaudhary, D. S. (2012). Comparative study of film forming behaviour of low and high amylose starches using glycerol and xylitol as plasticizers. *Journal of Food Engineering*, 109(2), 189-201.
- Nair, S. S., Chen, H., Peng, Y., Huang, Y., & Yan, N. (2018). Polylactic Acid Biocomposites Reinforced with Nanocellulose Fibrils with High Lignin Content for Improved Mechanical, Thermal, and Barrier Properties. *ACS Sustainable Chemistry & Engineering*, 6(8), 10058-10068.
- Nanda, S., Maley, J., Kozinski, J. A., & Dalai, A. K. (2015). Physico-Chemical Evolution in Lignocellulosic Feedstocks During Hydrothermal Pretreatment and Delignification. *Journal of Biobased Materials and Bioenergy*, 9(3), 295-308.
- Narkchamnan, S., & Sakdaronnarong, C. (2013). Thermo-molded biocomposite from cassava starch, natural fibers and lignin associated by laccase-mediator system. *Carbohydr Polym*, 96(1), 109-117.

- Naseem, A., Tabasum, S., Zia, K. M., Zuber, M., Ali, M., & Noreen, A. (2016). Lignin-derivatives based polymers, blends and composites: A review. *Int J Biol Macromol*, 93(Pt A), 296-313.
- Ng, F., Yew, F., Basiron, Y., & Sundram, K. (2011). A renewable future driven with Malaysian palm oil-based green technology. *Journal of Oil Palm & The Environment*, 2, 1-7.
- Nguyen Vu, H. P., & Lumdubwong, N. (2016). Starch behaviors and mechanical properties of starch blend films with different plasticizers. *Carbohydr Polym*, 154, 112-120.
- Ni, S., Zhang, H., Godwin, P. M., Dai, H., & Xiao, H. (2018). ZnO nanoparticles enhanced hydrophobicity for starch film and paper. *Materials Letters*, 230, 207-210.
- Ning, W., Jiugao, Y., Xiaofei, M., & Ying, W. (2007). The influence of citric acid on the properties of thermoplastic starch/linear low-density polyethylene blends. *Carbohydrate Polymers*, 67(3), 446-453.
- Niu, Y., Zhang, X., He, X., Zhao, J., Zhang, W., & Lu, C. (2015). Effective dispersion and crosslinking in PVA/cellulose fiber biocomposites via solid-state mechanochemistry. *Int J Biol Macromol*, 72, 855-861.
- Nor Amalini, A., Noor Haida, M. K., Imran, K., & Mohamad Haafiz, M. K. (2019). Relationship between dissolution temperature and properties of oil palm biomass based-regenerated cellulose films prepared via ionic liquid. *Materials Chemistry and Physics*, 221, 382-389.
- Norul Izani, M. A., Paridah, M. T., Anwar, U. M. K., Mohd Nor, M. Y., & H'ng, P. S. (2013). Effects of fiber treatment on morphology, tensile and thermogravimetric analysis of oil palm empty fruit bunches fibers. *Composites Part B: Engineering*, 45(1), 1251-1257.
- Novo, L. P., Gurgel, L. V., Marabezi, K., & Curvelo, A. A. (2011). Delignification of sugarcane bagasse using glycerol-water mixtures to produce pulps for saccharification. *Bioresour Technol*, 102(21), 10040-10046.
- Nurmi, J. (1993). *Heating values of the above ground biomass of small-sized trees* (Vol. 236): Acta Forestalia Fennica.
- Nurul Suraya Rosli, Shuhaida Harun, Jamaliah Md Jahim , & Othaman, , R. (2017). Chemical and Physical Characterization of Oil Palm Empty Fruit Bunch. *Malaysian Journal of Analytical Science*, 21(1), 188-196.

- Ochi, S. (2006). Development of high strength biodegradable composites using Manila hemp fiber and starch-based biodegradable resin. *Composites Part A: Applied Science and Manufacturing*, 37(11), 1879-1883.
- Olivato, J. B., Grossmann, M. V., Bilck, A. P., & Yamashita, F. (2012a). Effect of organic acids as additives on the performance of thermoplastic starch/polyester blown films. *Carbohydr Polym*, 90(1), 159-164.
- Olivato, J. B., Grossmann, M. V. E., Yamashita, F., Eiras, D., & Pessan, L. A. (2012b). Citric acid and maleic anhydride as compatibilizers in starch/poly(butylene adipate-co-terephthalate) blends by one-step reactive extrusion. *Carbohydrate Polymers*, 87(4), 2614-2618.
- Olsson, E., Hedenqvist, M. S., Johansson, C., & Jarnstrom, L. (2013). Influence of citric acid and curing on moisture sorption, diffusion and permeability of starch films. *Carbohydr Polym*, 94(2), 765-772.
- Oluwasina, O. O., Olaleye, F. K., Olusegun, S. J., Oluwasina, O. O., & Mohallem, N. D. S. (2019). Influence of oxidized starch on physicomechanical, thermal properties, and atomic force micrographs of cassava starch bioplastic film. *Int J Biol Macromol*, 135, 282-293.
- Ortega-Toro, R., Jimenez, A., Talens, P., & Chiralt, A. (2014). Properties of starch-hydroxypropyl methylcellulose based films obtained by compression molding. *Carbohydr Polym*, 109, 155-165.
- Orue, A., Eceiza, A., & Arbelaz, A. (2018). Preparation and characterization of poly(lactic acid) plasticized with vegetable oils and reinforced with sisal fibers. *Industrial Crops and Products*, 112, 170-180.
- Owi, W. T., Ong, H. L., Sam, S. T., Villagrancia, A. R., Tsai, C., & Akil, H. M. (2019). Unveiling the physicochemical properties of natural Citrus aurantifolia crosslinked tapioca starch/nanocellulose bionanocomposites. *Industrial Crops and Products*, 139, 111548-111561.
- Parshetti, G. K., Kent Hoekman, S., & Balasubramanian, R. (2013). Chemical, structural and combustion characteristics of carbonaceous products obtained by hydrothermal carbonization of palm empty fruit bunches. *Bioresour Technol*, 135, 683-689.
- Pawar, M., Kadam, A., Yemul, O., Thamke, V., & Kodam, K. (2016). Biodegradable bioepoxy resins based on epoxidized natural oil (cottonseed & algae) cured with citric and tartaric acids through solution polymerization: A renewable approach. *Industrial Crops and Products*, 89, 434-447.

- Perez, J., Munoz-Dorado, J., de la Rubia, T., & Martinez, J. (2002). Biodegradation and biological treatments of cellulose, hemicellulose and lignin: an overview. *Int Microbiol*, 5(2), 53-63.
- Phan The, D., Debeaufort, F., Voilley, A., & Luu, D. (2009). Influence of hydrocolloid nature on the structure and functional properties of emulsified edible films. *Food Hydrocolloids*, 23(3), 691-699.
- Piñeros-Hernandez, D., Medina-Jaramillo, C., López-Córdoba, A., & Goyanes, S. (2017). Edible cassava starch films carrying rosemary antioxidant extracts for potential use as active food packaging. *Food Hydrocolloids*, 63, 488-495.
- Polat, Y., Stojanovska, E., Negawo, T. A., Doner, E., & Kilic, A. (2017). Lignin as an Additive for Advanced Composites. In *Green Biocomposites* (pp. 71-89).
- Popescu, M., Dogaru, B., & Popescu, C. (2017). The influence of cellulose nanocrystals content on the water sorption properties of bio-based composite films. *Materials & Design*, 132, 170-177.
- Praprudivongs, C., & Wongpreedee, T. (2020). Use of eggshell powder as a potential hydrolytic retardant for citric acid-filled thermoplastic starch. *Powder Technology*, 370, 259-267.
- Qiao, X., Tang, Z., & Sun, K. (2011). Plasticization of corn starch by polyol mixtures. *Carbohydrate Polymers*, 83(2), 659-664.
- Quiles-Carrillo, L., Montanes, N., Sammon, C., Balart, R., & Torres-Giner, S. (2018). Compatibilization of highly sustainable polylactide/almond shell flour composites by reactive extrusion with maleinized linseed oil. *Industrial Crops and Products*, 111, 878-888.
- Rahimi, A., Ulbrich, A., Coon, J. J., & Stahl, S. S. (2014). Formic-acid-induced depolymerization of oxidized lignin to aromatics. *Nature*, 515(7526), 249-252.
- Rahman, M. M., & Netravali, A. N. (2018). Advanced green composites using liquid crystalline cellulose fibers and waxy maize starch based resin. *Composites Science and Technology*, 162, 110-116.
- Raman, J. K., & Gnansounou, E. (2014). Ethanol and lignin production from Brazilian empty fruit bunch biomass. *Bioresour Technol*, 172, 241-248.
- Ray, S. S., & Okamoto, M. (2003). Biodegradable Polylactide and its nanocomposites: opening a new dimension for plastics and composites. *Macromol Rapid Commun*, 24(14), 815-840.

- Reddy, N., & Yang, Y. (2010). Citric acid cross-linking of starch films. *Food Chemistry*, *118*(3), 702-711.
- Remón, J., Matharu, A. S., & Clark, J. H. (2018). Simultaneous production of lignin and polysaccharide rich aqueous solutions by microwave-assisted hydrothermal treatment of rapeseed meal. *Energy Conversion and Management*, *165*, 634-648.
- Rico, M., Rodriguez-Llamazares, S., Barral, L., Bouza, R., & Montero, B. (2016). Processing and characterization of polyols plasticized-starch reinforced with microcrystalline cellulose. *Carbohydr Polym*, *149*, 83-93.
- Rodrigues, D. C., Caceres, C. A., Ribeiro, H. L., de Abreu, R. F. A., Cunha, A. P., & Azeredo, H. M. C. (2014). Influence of cassava starch and carnauba wax on physical properties of cashew tree gum-based films. *Food Hydrocolloids*, *38*, 147-151.
- Rodríguez, M., Osés, J., Ziani, K., & Maté, J. I. (2006). Combined effect of plasticizers and surfactants on the physical properties of starch based edible films. *Food Research International*, *39*(8), 840-846.
- Rosa, M. F., Chiou, B. S., Medeiros, E. S., Wood, D. F., Williams, T. G., Mattoso, L. H., . . . Imam, S. H. (2009). Effect of fiber treatments on tensile and thermal properties of starch/ethylene vinyl alcohol copolymers/coir biocomposites. *Bioresour Technol*, *100*(21), 5196-5202.
- S. Bailey, R., & Kraft, H. (1987). A Study of Fibre Attrition in the Processing of Long Fibre Reinforced Thermoplastics. *Journal of the Polymer Processing Society*, *2*(2), 94-101.
- Saberi, B., Chockchaisawasdee, S., Golding, J. B., Scarlett, C. J., & Stathopoulos, C. E. (2017). Development of biocomposite films incorporated with different amounts of shellac, emulsifier, and surfactant. *Food Hydrocolloids*, *72*, 174-184.
- Sagnelli, D., Hebelstrup, K. H., Leroy, E., Rolland-Sabate, A., Guilois, S., Kirkensgaard, J. J. K., . . . Blennow, A. (2016). Plant-crafted starches for bioplastics production. *Carbohydr Polym*, *152*, 398-408.
- Sagnelli, D., Kirkensgaard, J. J. K., Giosafatto, C. V. L., Ogrodowicz, N., Kruczala, K., Mikkelsen, M. S., . . . Blennow, A. (2017). All-natural bio-plastics using starch-beta-glucan composites. *Carbohydr Polym*, *172*, 237-245.
- Sahari, J., Sapuan, S. M., Zainudin, E. S., & Maleque, M. A. (2013). Thermo-mechanical behaviors of thermoplastic starch derived from sugar palm tree (*Arenga pinnata*). *Carbohydr Polym*, *92*(2), 1711-1716.

- Salih, A. M., Ahmad, M. B., Ibrahim, N. A., Dahlan, K. Z., Tajau, R., Mahmood, M. H., & Yunus, W. M. (2015). Synthesis of radiation curable palm oil-based epoxy acrylate: NMR and FTIR spectroscopic investigations. *Molecules*, *20*(8), 14191-14211.
- Sartori, T., & Menegalli, F. C. (2016). Development and characterization of unripe banana starch films incorporated with solid lipid microparticles containing ascorbic acid. *Food Hydrocolloids*, *55*, 210-219.
- Sarwono, A., Man, Z., & Bustam, M. A. (2012). Blending of epoxidised palm oil with epoxy resin: the effect on morphology, thermal and mechanical properties. *Journal of Polymers and the Environment*, *20*(2), 540-549.
- Schmidt, V. C. R., Porto, L. M., Laurindo, J. B., & Menegalli, F. C. (2013). Water vapor barrier and mechanical properties of starch films containing stearic acid. *Industrial Crops and Products*, *41*, 227-234.
- Segal, L., Creely, J. J., Martin, A. E., & Conrad, C. M. (1959). An empirical method for estimating the degree of crystallinity of native cellulose using the X-ray diffractometer. *Textile research journal*, *29*(10), 786-794.
- Seligra, P. G., Medina Jaramillo, C., Fama, L., & Goyanes, S. (2016). Biodegradable and non-retrogradable eco-films based on starch-glycerol with citric acid as crosslinking agent. *Carbohydr Polym*, *138*, 66-74.
- Shahbazi, M., Majzoobi, M., & Farahnaky, A. (2018). Physical modification of starch by high-pressure homogenization for improving functional properties of  $\kappa$ -carrageenan/starch blend film. *Food Hydrocolloids*, *85*, 204-214.
- Shen, L., Haufe, J. I., & Patel, M. (2009). Product Overview and Market Projection of Emerging Bio-Based Plastics-PRO-BIP 2009-Final Report. *Report, Utrecht University, The Netherlands*.
- Shi, M., & Gao, Q. (2016). Recrystallization and in vitro digestibility of wrinkled pea starch gel by temperature cycling. *Food Hydrocolloids*, *61*, 712-719.
- Shi, R., Bi, J., Zhang, Z., Zhu, A., Chen, D., Zhou, X., . . . Tian, W. (2008). The effect of citric acid on the structural properties and cytotoxicity of the polyvinyl alcohol/starch films when molding at high temperature. *Carbohydrate Polymers*, *74*(4), 763-770.
- Shi, R., Zhang, Z., Liu, Q., Han, Y., Zhang, L., Chen, D., & Tian, W. (2007). Characterization of citric acid/glycerol co-plasticized thermoplastic starch prepared by melt blending. *Carbohydrate Polymers*, *69*(4), 748-755.

- Silva, D. W., Scatolino, M. V., Pereira, T. G. T., Vilela, A. P., Eugenio, T. M. C., Martins, M. A., . . . Mendes, L. M. (2020). Influence of thermal treatment of eucalyptus fibers on the physical-mechanical properties of extruded fiber-cement composites. *Materials Today: Proceedings*, 31, S348-S352.
- Silverajah, V. S., Ibrahim, N. A., Zainuddin, N., Yunus, W. M., & Hassan, H. A. (2012). Mechanical, thermal and morphological properties of poly(lactic acid)/epoxidized palm olein blend. *Molecules*, 17(10), 11729-11747.
- Sohni, S., Norulaini, N. A. N., Hashim, R., Khan, S. B., Fadhullah, W., & Mohd Omar, A. K. (2018). Physicochemical characterization of Malaysian crop and agro-industrial biomass residues as renewable energy resources. *Industrial Crops and Products*, 111, 642-650.
- Soni, R., Asoh, T.-A., Hsu, Y.-I., Shimamura, M., & Uyama, H. (2020). Effect of starch retrogradation on wet strength and durability of cellulose nanofiber reinforced starch film. *Polymer Degradation and Stability*, 177, 109165-109171.
- Staroszczyk, H., & Janas, P. (2010). Microwave-assisted preparation of potato starch silicated with silicic acid. *Carbohydrate Polymers*, 81(3), 599-606.
- Sukiran, M. A., Abnisa, F., Syafiie, S., Wan Daud, W. M. A., Nasrin, A. B., Abdul Aziz, A., & Loh, S. K. (2020). Experimental and modelling study of the torrefaction of empty fruit bunches as a potential fuel for palm oil mill boilers. *Biomass and Bioenergy*, 136.
- Sun, R., Lawther, J. M., & Banks, W. B. (1996). Effects of pretreatment temperature and alkali concentration on the composition of alkali-soluble lignins from wheat straw. *Journal of Applied Polymer Science*, 62(9), 1473-1481.
- Sun, S., Liu, P., Ji, N., Hou, H., & Dong, H. (2018). Effects of various cross-linking agents on the physicochemical properties of starch/PHA composite films produced by extrusion blowing. *Food Hydrocolloids*, 77, 964-975.
- Sun, X. (2004). Isolation and characterisation of cellulose obtained by a two-stage treatment with organosolv and cyanamide activated hydrogen peroxide from wheat straw. *Carbohydrate Polymers*, 55(4), 379-391.
- Sun, Y., Hu, Q., Qian, J., Li, T., Ma, P., Shi, D., . . . Chen, M. (2016). Preparation and properties of thermoplastic poly(caprolactone) composites containing high amount of esterified starch without plasticizer. *Carbohydr Polym*, 139, 28-34.
- Sun, Y., Yang, L. p., Lu, X. h., & He, C. b. (2015). Biodegradable and renewable poly(lactide)-lignin composites: synthesis, interface and toughening mechanism. *Journal of Materials Chemistry A*, 3(7), 3699-3709.

- Sun, Z., Fridrich, B., de Santi, A., Elangovan, S., & Barta, K. (2018). Bright side of lignin depolymerization: toward new platform chemicals. *Chem Rev*, *118*(2), 614-678.
- Suzuki, A. H., Botelho, B. G., Oliveira, L. S., & Franca, A. S. (2018). Sustainable synthesis of epoxidized waste cooking oil and its application as a plasticizer for polyvinyl chloride films. *European Polymer Journal*, *99*, 142-149.
- Svagan, A. J., Hedenqvist, M. S., & Berglund, L. (2009). Reduced water vapour sorption in cellulose nanocomposites with starch matrix. *Composites Science and Technology*, *69*(3-4), 500-506.
- Taghizadeh, A., & Favis, B. D. (2013). Effect of high molecular weight plasticizers on the gelatinization of starch under static and shear conditions. *Carbohydr Polym*, *92*(2), 1799-1808.
- Taguet, A., Bureau, M. N., Huneault, M. A., & Favis, B. D. (2014). Toughening mechanisms in interfacially modified HDPE/thermoplastic starch blends. *Carbohydr Polym*, *114*, 222-229.
- Tan, C., Saritpongteeraka, K., Kungsanant, S., Charnnok, B., & Chaiprapat, S. (2018). Low temperature hydrothermal treatment of palm fiber fuel for simultaneous potassium removal, enhanced oil recovery and biogas production. *Fuel*, *234*, 1055-1063.
- Tan, L., Yu, Y., Li, X., Zhao, J., Qu, Y., Choo, Y. M., & Loh, S. K. (2013). Pretreatment of empty fruit bunch from oil palm for fuel ethanol production and proposed biorefinery process. *Bioresour Technol*, *135*, 275-282.
- Tan, S. G., Ahmad, Z., & Chow, W. S. (2014). Reinforcing ability and co-catalytic effects of organo-montmorillonite clay on the epoxidized soybean oil bio-thermoset. *Applied Clay Science*, *90*, 11-17.
- Tan, Y. T., Ngoh, G. C., & Chua, A. S. M. (2018). Evaluation of fractionation and delignification efficiencies of deep eutectic solvents on oil palm empty fruit bunch. *Industrial Crops and Products*, *123*, 271-277.
- Tanrattanakul, V., & Saithai, P. (2009). Mechanical properties of bioplastics and bioplastic-organoclay nanocomposites prepared from epoxidized soybean oil with different epoxide contents. *Journal of Applied Polymer Science*, *114*(5), 3057-3067.
- Tarasov, D., Leitch, M., & Fatehi, P. (2018). Lignin-carbohydrate complexes: properties, applications, analyses, and methods of extraction: a review. *Biotechnol Biofuels*, *11*, 269-297.

- Teaca, C. A., Bodirlau, R., & Spiridon, I. (2013). Effect of cellulose reinforcement on the properties of organic acid modified starch microparticles/plasticized starch bio-composite films. *Carbohydr Polym*, 93(1), 307-315.
- Tee, Y. B., Talib, R. A., Abdan, K., Chin, N. L., Basha, R. K., & Yunos, K. F. M. (2014). Toughening Poly(Lactic Acid) and aiding the melt-compounding with bio-sourced plasticizers. *Agriculture and Agricultural Science Procedia*, 2, 289-295.
- Teixeira, E. d. M., Curvelo, A. A. S., Corrêa, A. C., Marconcini, J. M., Glenn, G. M., & Mattoso, L. H. C. (2012). Properties of thermoplastic starch from cassava bagasse and cassava starch and their blends with poly (lactic acid). *Industrial Crops and Products*, 37(1), 61-68.
- Terzopoulou, Z. N., Papageorgiou, G. Z., Papadopoulou, E., Athanassiadou, E., Alexopoulou, E., & Bikiaris, D. N. (2015). Green composites prepared from aliphatic polyesters and bast fibers. *Industrial Crops and Products*, 68, 60-79.
- Thakur, R., Pristijono, P., Golding, J. B., Stathopoulos, C. E., Scarlett, C. J., Bowyer, M., . . . Vuong, Q. V. (2017). Amylose-lipid complex as a measure of variations in physical, mechanical and barrier attributes of rice starch- $\kappa$ -carrageenan biodegradable edible film. *Food Packaging and Shelf Life*, 14, 108-115.
- Thakur, V. K., & Thakur, M. K. (2015). Recent advances in green hydrogels from lignin: a review. *Int J Biol Macromol*, 72, 834-847.
- Thakur, V. K., Thakur, M. K., Raghavan, P., & Kessler, M. R. (2014). Progress in green polymer composites from lignin for multifunctional applications: a review. *ACS Sustainable Chemistry & Engineering*, 2(5), 1072-1092.
- Thielemans, W., Can, E., Morye, S. S., & Wool, R. P. (2002). Novel applications of lignin in composite materials. *Journal of Applied Polymer Science*, 83(2), 323-331.
- Tolbert, A., Akinosho, H., Khunsupat, R., Naskar, A. K., & Ragauskas, A. J. (2014). Characterization and analysis of the molecular weight of lignin for biorefining studies. *Biofuels, Bioproducts and Biorefining*, 8(6), 836-856.
- Tongnuanchan, P., Benjakul, S., Prodpran, T., Pisuchpen, S., & Osako, K. (2016). Mechanical, thermal and heat sealing properties of fish skin gelatin film containing palm oil and basil essential oil with different surfactants. *Food Hydrocolloids*, 56, 93-107.
- Umar, S., Kamarudin, M. S., & Ramezani-Fard, E. (2013). Physical properties of extruded aquafeed with a combination of sago and tapioca starches at different moisture contents. *Animal Feed Science and Technology*, 183(1-2), 51-55.

- Uzoh, C. F., Onukwuli, O. D., Odera, R. S., & Ofochebe, S. (2013). Optimization of polyesterification process for production of palm oil modified alkyd resin using response surface methodology. *Journal of Environmental Chemical Engineering*, 1(4), 777-785.
- Vandenbossche, V., Brault, J., Vilarem, G., Hernández-Meléndez, O., Vivaldo-Lima, E., Hernández-Luna, M., . . . Rigal, L. (2014). A new lignocellulosic biomass deconstruction process combining thermo-mechano chemical action and biocatalytic enzymatic hydrolysis in a twin-screw extruder. *Industrial Crops and Products*, 55, 258-266.
- Villalobos, K., Rojas, H., González-Paz, R., Granados, D. B., González-Masís, J., Baudrit, J. V., & Corrales-Ureña, Y. R. (2017). Production of Starch Films Using Propolis Nanoparticles as Novel Bioplasticizer. *Journal of Renewable Materials*, 5(3), 189-198.
- Volpe, V., De Feo, G., De Marco, I., & Pantani, R. (2018). Use of sunflower seed fried oil as an ecofriendly plasticizer for starch and application of this thermoplastic starch as a filler for PLA. *Industrial Crops and Products*, 122, 545-552.
- Wang, N., Zhang, X., Han, N., & Bai, S. (2009). Effect of citric acid and processing on the performance of thermoplastic starch/montmorillonite nanocomposites. *Carbohydrate Polymers*, 76(1), 68-73.
- Wang, R., Liu, P., Cui, B., Kang, X., & Yu, B. (2019). Effects of different treatment methods on properties of potato starch-lauric acid complex and potato starch-based films. *Int J Biol Macromol*, 124, 34-40.
- Wang, Z., Zhao, S., Song, R., Zhang, W., Zhang, S., & Li, J. (2017). The synergy between natural polyphenol-inspired catechol moieties and plant protein-derived bioadhesive enhances the wet bonding strength. *Sci Rep*, 7(1), 9664-1674.
- Witteck, T., & Tanimoto, T. (2008). Mechanical properties and fire retardancy of bidirectional reinforced composite based on biodegradable starch resin and basalt fibres. *Express Polymer Letters*, 2(11), 810-822.
- Woggum, T., Sirivongpaisal, P., & Wittaya, T. (2015). Characteristics and properties of hydroxypropylated rice starch based biodegradable films. *Food Hydrocolloids*, 50, 54-64.
- World-Economic-Forum. (2016). The new plastics economy. Rethinking the future of plastics. *World Economic Forum*
- Wu, H., Lei, Y., Lu, J., Zhu, R., Xiao, D., Jiao, C., . . . Li, M. (2019). Effect of citric acid induced crosslinking on the structure and properties of potato starch/chitosan

composite films. *Food Hydrocolloids*, 97, 105208-105218.

- Wu, Q., Rabu, J., Goulin, K., Sainlaud, C., Chen, F., Johansson, E., . . . Hedenqvist, M. S. (2017). Flexible strength-improved and crack-resistant biocomposites based on plasticised wheat gluten reinforced with a flax-fibre-weave. *Composites Part A: Applied Science and Manufacturing*, 94, 61-69.
- Wu, R. L., Wang, X. L., Li, F., Li, H. Z., & Wang, Y. Z. (2009). Green composite films prepared from cellulose, starch and lignin in room-temperature ionic liquid. *Bioresour Technol*, 100(9), 2569-2574.
- Xie, F., Pollet, E., Halley, P. J., & Avérous, L. (2013). Starch-based nano-biocomposites. *Progress in Polymer Science*, 38(10-11), 1590-1628.
- Xie, Y. Y., Hu, X. P., Jin, Z. Y., Xu, X. M., & Chen, H. Q. (2014). Effect of temperature-cycled retrogradation on in vitro digestibility and structural characteristics of waxy potato starch. *Int J Biol Macromol*, 67, 79-84.
- Xiong, Z., Ma, S. Q., Fan, L. B., Tang, Z. B., Zhang, R. Y., Na, H. N., & Zhu, J. (2014). Surface hydrophobic modification of starch with bio-based epoxy resins to fabricate high-performance polylactide composite materials. *Composites Science and Technology*, 94, 16-22.
- Xiong, Z., Yang, Y., Feng, J., Zhang, X., Zhang, C., Tang, Z., & Zhu, J. (2013a). Preparation and characterization of poly(lactic acid)/starch composites toughened with epoxidized soybean oil. *Carbohydr Polym*, 92(1), 810-816.
- Xiong, Z., Zhang, L., Ma, S., Yang, Y., Zhang, C., Tang, Z., & Zhu, J. (2013b). Effect of castor oil enrichment layer produced by reaction on the properties of PLA/HDI-g-starch blends. *Carbohydr Polym*, 94(1), 235-243.
- Yan, Q., Hou, H., Guo, P., & Dong, H. (2012). Effects of extrusion and glycerol content on properties of oxidized and acetylated corn starch-based films. *Carbohydrate Polymers*, 87(1), 707-712.
- Yang, J., Ching, Y. C., & Chuah, C. H. (2019). Applications of lignocellulosic fibers and lignin in bioplastics: a review. *Polymers*, 11, 751-777.
- Yang, W., Fortunati, E., Dominici, F., Giovanale, G., Mazzaglia, A., Balestra, G. M., . . . Puglia, D. (2016). Effect of cellulose and lignin on disintegration, antimicrobial and antioxidant properties of PLA active films. *Int J Biol Macromol*, 89, 360-368.
- Yao, K., Cai, J., Liu, M., Yu, Y., Xiong, H., Tang, S., & Ding, S. (2011). Structure and properties of starch/PVA/nano-SiO<sub>2</sub> hybrid films. *Carbohydrate Polymers*, 86(4),

- Yarahmadi, E., Didehban, K., Sari, M. G., Saeb, M. R., Shabaniyan, M., Aryanasab, F., . . . Puglia, D. (2018). Development and curing potential of epoxy/starch-functionalized graphene oxide nanocomposite coatings. *Progress in Organic Coatings*, *119*, 194-202.
- Yatigala, N. S., Bajwa, D. S., & Bajwa, S. G. (2018). Compatibilization improves physico-mechanical properties of biodegradable biobased polymer composites. *Composites Part A: Applied Science and Manufacturing*, *107*, 315-325.
- Ye, J., Luo, S., Huang, A., Chen, J., Liu, C., & McClements, D. J. (2019). Synthesis and characterization of citric acid esterified rice starch by reactive extrusion: A new method of producing resistant starch. *Food Hydrocolloids*, *92*, 135-142.
- Yildirim-Yalcin, M., Seker, M., & Sadikoglu, H. (2019). Development and characterization of edible films based on modified corn starch and grape juice. *Food Chem*, *292*, 6-13.
- Yoshida, H., Mörck, R., Kringstad, K. P., & Hatakeyama, H. (1987). Kraft lignin in polyurethanes I. Mechanical properties of polyurethanes from a kraft lignin-polyether triol-polymeric MDI system. *Journal of Applied Polymer Science*, *34*(3), 1187-1198.
- Yunus, R., Salleh, S. F., Abdullah, N., & Biak, D. R. (2010). Effect of ultrasonic pre-treatment on low temperature acid hydrolysis of oil palm empty fruit bunch. *Bioresour Technol*, *101*(24), 9792-9796.
- Zaini, I. N., Novianti, S., Nurdiawati, A., Irhamna, A. R., Aziz, M., & Yoshikawa, K. (2017). Investigation of the physical characteristics of washed hydrochar pellets made from empty fruit bunch. *Fuel Processing Technology*, *160*, 109-120.
- Zeng, R., Wu, Y., Li, Y., Wang, M., & Zeng, J. (2017). Curing behavior of epoxidized soybean oil with biobased dicarboxylic acids. *Polymer Testing*, *57*, 281-287.
- Zhang, C., Li, F. Y., Li, J. F., Li, Y. L., Xu, J., Xie, Q., . . . Guo, A. F. (2018). Novel treatments for compatibility of plant fiber and starch by forming new hydrogen bonds. *Journal of Cleaner Production*, *185*, 357-365.
- Zhang, L., Wang, X. F., Liu, H., Yu, L., Wang, Y., Simon, G. P., & Qian, J. (2018). Effect of plasticizers on microstructure, compatibility and mechanical property of hydroxypropyl methylcellulose/hydroxypropyl starch blends. *Int J Biol Macromol*, *119*, 141-148.

- Zhang, S., He, Y., Yin, Y., & Jiang, G. (2019). Fabrication of innovative thermoplastic starch bio-elastomer to achieve high toughness poly(butylene succinate) composites. *Carbohydr Polym*, 206, 827-836.
- Zhang, Y. R., Zhang, S. D., Wang, X. L., Chen, R. Y., & Wang, Y. Z. (2009). Effect of carbonyl content on the properties of thermoplastic oxidized starch. *Carbohydrate Polymers*, 78(1), 157-161.
- Zhao, S., Wang, Z., Kang, H., Li, J., Zhang, S., Han, C., & Huang, A. (2018). Fully bio-based soybean adhesive in situ cross-linked by interactive network skeleton from plant oil-anchored fiber. *Industrial Crops and Products*, 122, 366-374.
- Zhao, T., Wu, Y., Li, Y., Wang, M., & Zeng, J. (2017). High performance and thermal processable dicarboxylic acid cured epoxidized plant oil resins through dynamic vulcanization with Poly(lactic acid). *ACS Sustainable Chemistry & Engineering*, 5(2), 1938-1947.
- Zhou, J., Tong, J., Su, X., & Ren, L. (2016). Hydrophobic starch nanocrystals preparations through crosslinking modification using citric acid. *Int J Biol Macromol*, 91, 1186-1193.
- Zhou, X., Sain, M. M., & Oksman, K. (2016). Semi-rigid biopolyurethane foams based on palm-oil polyol and reinforced with cellulose nanocrystals. *Composites Part A: Applied Science and Manufacturing*, 83, 56-62.
- Zianor Azrina, Z. A., Beg, M. D. H., Rosli, M. Y., Ramli, R., Junadi, N., & Alam, A. (2017). Spherical nanocrystalline cellulose (NCC) from oil palm empty fruit bunch pulp via ultrasound assisted hydrolysis. *Carbohydr Polym*, 162, 115-120.